# SOME MORPHOLOGICAL ASPECTS OF PVC PROCESSING

by

ADANGO MIADONYE, BSc, LPRI

A Doctoral Thesis submitted in partial fulfilment
of the requirements for the award of
Doctor of Philosophy of the
Loughborough University of Technology

July 1983

Supervisor: D A Hemsley, BSc, Dip.RMS

Institute of Polymer Technology.

*DEDICATION*

*Dedicated with great affection to Mrs J S LongJohn, a mother of rare breed, and to Mr R D LongJohn*

*QUOTATION*

*"Philosophy, as I understand the word, is something intermediate between theology and science. Like theology, it consists of speculations on matters as to which definite knowledge has, so far, been unascertainable; but like science it appeals to human reason rather than to authority, whether that of tradition or that of revelation. All definite knowledge - so I shall contend - belongs to science; all dogma as to what surpasses definite knowledge to theology. But between theology and science there is a No Man's Land, exposed to attack from both sides; this No Man's Land is philosophy".*

*Bertrand Russell (1872-1970)*

## ACKNOWLEDGEMENTS

I would like to express my very profound gratitude to my supervisor Mr D A Hemsley for responding to the pressures imposed on him during the creation of this thesis, and for his guidance. He enriched me with useful suggestions and provocative ideas which largely helped to shape the entire work. I also thank Professor A W Birley for his administrative skill which not only brought me into this programme but also through which I was able to accomplish it.

My appreciation is expressed to the following for their help: Dr M Gilbert and Dr D E Marshall for organising series of PVC group meetings for cross-fertilization of ideas; the IPT technicians for their kind cooperation; Messrs R Lees and J Bates for their assistance in electron microscopy without visible rancour; Dr R P Higgs and Mr S C Jones (formerly with BP Chemicals, Barry) for their help in producing the extrudates and extruder core samples; Mr B Salville and Mr G A R Matthews of South Bank Polytechnic for providing me with some useful reading materials. Gratitude also to my friends and colleagues in IPT Loughborough University, for their various useful suggestions.

I am grateful for the bursary from Rivers State and later the Federal Government of Nigeria which enabled me to complete this research. I gratefully acknowledge the grant provided by the Polymer Engineering Directorate of the SERC in support of the programme of which this is a part. I also thank BP Chemicals, Barry, Glamorgan for their support.

I am indebted to Dady and Mother, Dr O R LongJohn, Mr S J Bikikoro, my mother-in-law Madam B Johnson-Hart, Mr M Hart and Mr and Mrs U C Okirie for their encouragement, fervent prayers and occasional financial assistance.

I am particularly grateful to my wife and family who have endured my absence from home with insuperable fortitude. Special thanks to Mr and Mrs B M Mutagahywa for their kind cooperation and generosity shown to me while I was staying with them. I owe special gratitude to Dr and Mrs R U Ononogbo, and Justice and Mrs R Jacks who assisted my wife during her numerous trips between London and Lagos in making sure my bursary was extended to cater for the final period of this work. My thanks to Mrs Janet Smith for her immaculate typing and kindness.

Finally, my gratitude to the Almighty God for giving me the health, strength and courage to pull through.

## ABSTRACT

The efficiency of unplasticised polyvinylchloride (UPVC) extrusion from dry blends of high-attrition mixers largely depends on powder characteristics of the dry blends. Better understanding of the morphological features of the powder blend and its processed form would therefore underlie the optimisation of the efficiency of the overall process. This is the theme, and therefore the *'raison d'être'*, for the present study.

The programme has included the study of morphological changes in dry blends, extrudates, extruder core samples and compression mouldings. Effective evaluations of their properties have required the integral use of microscopy methods with conventional instrumentation. Microscopy methods were the primary techniques employed in this study. Qualitative and quantitative application of UV fluorescence microscopy techniques were developed and used to obtain results in agreement with conventional methods.

Fluorescence microscopy has been used to study the changes in particle morphology and additive distribution during blending. Powder densities were found to increase with blending conditions, and fluorescence work showed the occurrence of 'breakdown' and 'adhesion' of particles during blending. Also differential interference contrast (DIC) technique was used to examine additives distribution. Solid additives were found to coat the surfaces of PVC grains. No significant change in distribution was observed at different blending speeds, but grain shape, not size, affects additives distribution. Cast-film method showed that a single stabilizer particle can only protect the area it is occupying from thermal degradation.

Blends were extruded into strips and compression moulded into sheets. Electron and light microscopy were used to study additives distribution and fusion. Samples prepared by petrological

techniques showed marked differences in morphological features of samples extruded at different conditions. Similar observations were made with UV fluorescence, DIC and electron microscopy. The results obtained by impact strength, solvent absorption, shrinkage and 'surface skin' thickness measurements were not all correlated. However, additives distribution strongly depended on changes in morphological features, and both were found to affect physical properties significantly.

Fluorescence and DIC microscopy demonstrated that fusion increases along the screw length, but varies slightly within the same screw zone. Solvent tests gave misleading results due to particle-compaction effect, but results of differential scanning calorimeter broadly agreed with microscopy observations. Relative fluorescence intensity, as a measure of degradation, was found to decrease along the screw (from feed to metering zones), the values apparently depending on the prevailing extrusion temperature.

CONTENTS

## FIGURES

## TABLES

# CHAPTER 1

# INTRODUCTION AND GENERAL BACKGROUND OF PROJECT

## 1.1 INTRODUCTION

### 1.1.1 Vinylchloride Polymers

The homopolymer of vinylchloride contains the repeat unit $\{CH_2\text{-}CHCl\}_n$, where 'n' denotes the degree of polymerization. The repeat unit is introduced by addition polymerization of the monomer (see Section 1.4.2) and, in commercial polymers averages 100 repeat units per chain. The homopolymer produced is structurally very unstable and has not been successfully processed alone at normal processing temperature, but this problem is vastly overcome when adequate amounts of modifying agents such as stabilizers, plasticisers and lubricants are incorporated into the polymer before processing. Since polymerization is mainly by free radical addition mechanism the structure is essentially atatic, with some syndiotactic sequences. Therefore the polymer is amorphous with up to 10% short range crystallinity introduced by the presence of syndiotacticity[1,32].

There are various polyvinylchloride homopolymers and, copolymers with such monomers as vinylacetate, propylene, vinylidene chloride etc. In petrochemical and plastic industries the term 'polyvinylchloride' is used to call virtually any polymer in which vinylchloride accounts for at least 60% by weight of the resin composition. This situation seems justified since in the extreme case, the copolymer could contain vinylchloride contents of 50% by weight of the composition (for example, vinylchloride/asbestos floor tiles).

In many cases, plasticiser is incorporated into vinylchloride polymer with higher molecular weight. This reduces processing difficulties and, most important, imparts flexibility to the product, hence the product is identified as 'flexible' PVC.

Where PVC product contains no plasticiser the word 'unplasticised' PVC has been used, but if very little amount of plasticiser is used to aid processing the product is called 'rigid' PVC. Both terms have also been used indiscriminately by writers to mean PVC products without any plasticiser content. In this thesis the word 'unplasti cised' PVC is preferred, and the abbreviation 'UPVC' will be used wherever it is more convenient.

### 1.1.2 Historical Survey

The formation of vinylchloride was first observed by Liebig, but the preparation was first reported in a paper by Regnault in 1835[2]. The same year, two later publications[3,4] showed that the preparation was essentially the by-product of a free radical reaction. The method used was to expose 1,2-dichloroethane in an alcoholic solution of potassium hydroxide in sunlight for several days. The reaction yielded a white precipitate which, after repeated careful analysis of the product, was assigned the formula $C_2H_3Cl$.

Despite these earlier works, the first mention of vinyl polymerization was in 1860 by Hofmann[5], who described the metamorphosis of an ethylene bromide. But an intensive investigation was further carried out by Baumann which was reported in 1872. Baumann, in his investigation confirmed Hofmann's observations and, repeated Hofmann's experiment using vinylchloride in place of ethylene bromide[6]. After Baumann's successful polymerization of vinylchloride, he also correctly determined the density of the product as $1.406 g\ cm^{-3}$.

Apart from these references, there was no further interest in vinylchloride for almost forty years. Many present day writers have associated these barren years with the period when our early investigators probably did not recognise the polymeric nature or commercial importance of the material. However, renewed interest was brought about by the overcapacity in the production of calcium carbide in Europe in 1928. The over-estimation of acetylene as a

potential elluminant in early 1900s led to the unnecessary construction of many new acetylene plants. Therefore, there was a substantial drop in the price of calcium carbide by nearly £20 per ton within five years. In Germany the position was particularly acute, and hence they set up an extensive research programme to investigate possible chemical uses of acetylene.

In 1912, Klatte of Griesheim-Elektron[7] filed a patent claiming the manufacture of vinylchloride monomer by reaction between acetylene and hydrogen chloride in the presence of mercuric chloride catalyst. He also described in his patent, the applications of polyvinylchloride as film, fibre and lacquer. At about the same period, work on vinyl-halides was being carried out by Ostromislensky et al[8] in Russia. Ostromislensky's work was mainly regarded as an extension of reaction mechanisms in vinylchloride polymerization.

Subsequently, the technique of copolymerization to improve processing characteristics and the use of peroxides as polymerization initiators was introduced[9]. Wide areas of non-rigid applications were opened up through the discovery of the plasticising effect by Semon[10] of B F Goodrich. Susich et al[11] also discovered the important principles of heat stabilisation.

Industrial production of PVC sprang up from the 1930s. In Europe its production was started in Germany in 1931 (Badische Anilin-Undsad a Fabrik, I G Farbenindustrie A.G); in the United States in 1933 (Union Carbide Corporation); in Japan in 1939 (Shin Nippon Chisso Hiryo); in Great Britain and France in 1940 (Imperial Chemical Industries Ltd and Pechiney-Saint-Gobain respectively) and in Italy in 1951 (Montecatin S.G). The outbreak of the Second World War was a boost to the polyvinylchloride industries. It was during this period that PVC made its landslide, when the highly costly rubber was effectively substituted with plasticised polyvinylchloride in some applications (particularly in cable insulations and sheathing for marine applications).

Polyvinylchloride is now one of the three major plastics, between polyethylene and polystyrene. World production has increased with new areas of application since after the war. The annual growth rate was consistently at 10% in the late 1970s (see Section 1.1.3), most probably due to the economic recession.

### 1.1.3 Commercial and Economic Aspects

Polyvinylchloride is the first commercially available synthetic thermoplastic[12] and the most versatile of all plastics in terms of the number and variety of end uses. However, the present day economic recession and the awareness of the toxicity of the monomer have placed polyvinylchloride (PVC) second to the polyolefins. The amount produced is about 25% of the total production of all plastics and about 40% of thermoplastics.

The commercial and economic review of the problems and anticipation of future prospects reveals several milestones in its historical background, which has been adequately discussed by several authors[13-15]. A brief discussion of this issue has already been made in the last two paragraphs of Section 1.2. The landmark discovery of effect of plasticising agents on PVC in the USA in 1933 increased the production level of the polymer. Table 1.1 shows the growth history of PVC in the United States from 1945 to 1980[16,17]. The long term growth rate has been within 16%, but this has fallen in the 1970s to within 10%.

The real progress in world production occurred within the last two decades. Before then, progress had been relatively slow, so that between 1945 and 1960 production increased by a mere one million tons (i.e. 50,000 tons to 1.5 million tons). Table 1.2 shows the average annual world growth rate of polyvinylchloride from 1960 to 1980. Detailed figures for the consumption of PVC since 1958 in most Western European countries are also shown in Table 1.3. West Germany with an outstanding economy and commerce first substituted rubber for plasticised PVC in 1937 and since then, has maintained the highest annual consumption in Europe.

TABLE 1.1
Average growth rates of PVC consumption in the United States[16,17]

| Year | PVC Consumption (million lbs) | 5-year Growth Rate (%) |
|---|---|---|
| 1945 | 79 | - |
| 1950 | 315 | 38 |
| 1955 | 506 | 10 |
| 1960 | 900 | 12 |
| 1965 | 1854 | 16 |
| 1970 | 3000 | 10 |
| 1975 | 3500 | 11 |
| 1980 | 9748 | 10 |

TABLE 1.2
World PVC-Consumption[18]: average growth rates (percent per annum)

| World | 1960-1970 | 1970-1980 |
|---|---|---|
| Western Europe | 16 | 10 |
| Japan | 16 | 12 |
| USA | 13 | 10 |

*'World' excludes the Eastern Europe and China countries

TABLE 1.3
PVC Consumption in Western Europe** (in $10^3$ metric tons)[19]

| Countries | 1958 | 1960 | 1965 | 1970 | 1976 |
|---|---|---|---|---|---|
| Austria | 6 | 12 | 20 | - | - |
| France | 61 | 87 | 182 | 340 | - |
| Italy | 35 | 70 | 163 | 300 | - |
| Netherlands | 18 | 28 | 60 | 103 | - |
| Sweden | 11 | 17 | 40 | 69 | - |
| United Kingdom | 67 | 98 | 201 | 345 | 422 |
| West Germany | 88 | 157 | 416 | 700 | - |

** Selected Western European countries

In the Eastern European countries, Soviet Union started production in 1940 using suspension techniques for polymerization[30]. Between 1950 and 1960 production increased by 200% and then by 300% during the period from 1960 to 1965. The record of production is indicated below in Table 1.4.

TABLE 1.4
Production of SPVC in the USSR

| Years | 1965 | 1966 | 1967 | 1968 | 1969 | 1970 |
|---|---|---|---|---|---|---|
| Production (in tons) | 100 | 127 | 142 | 250 | 290 | 450 |

Interested readers on the progress of PVC production in Eastern European countries are referred to references 21-23.

The majority of the countries which have invested in development have erected plants for the manufacture of PVC during recent

years. In the Third World especially, these plants have been designed with the use of imported technology. Japan has been very active in this field besides having a sizeable export of manufactured PVC.

Generally, as with all plastic materials the price of PVC has fallen drastically. This has in the past contributed considerably to its high rate of growth. During the same period there has been a steady increase in the price of nearly all basic raw materials, so that PVC is now able to compete in a number of large-scale applications[92].

It would be ambiguous to make any conceptual forecast on the commercial and economic future of PVC for the next decade. Rather, it is certain that PVC will progress alongside with innovation and technological changes in the plastic industry.

### 1.1.4 Industrialization of Polyvinylchloride

Little was realised on the importance of this versatile thermoplastic at the early stage. It was the need to replace the costly rubber goods with less expensive material of almost identical properties that accelerated the industrialization of polyvinylchloride. This brought a change in the long term running academic curiosity (see Section 1.2) and, in 1935 the first large-scale production of polyvinylchloride began.

The production of the monomer and its subsequent polymerization are discussed in the following sub-sections.

#### 1.1.4.1 Production and toxicity of vinylchloride monomer

There are two major routes for the production of vinylchloride monomer (VCM):

i) the acetylene route
ii) the ethylene route.

The acetylene route involves the addition of hydrogen chloride to acetylene in the presence of mercuric chloride catalyst via

$$\underset{\text{acetylene}}{CH{\equiv}CH} + HCl \xrightarrow{Hg\ CL_2} \underset{\text{vinylchloride}}{CH_2{=}CHCl} + 22.8\ Kcal\ mol^{-1}$$

This route has limited use due to the high energy required in the production of calcium carbide used for acetylene. Another setback is that the monomer made by this process can contain such impurities as very small amounts of acetylene; methylacetylene; 1,1-dichloroethane; allene or acetaldehyde.

The second route involves the dehydrochlorination of dichloroethane. This is the ethylene route as shown below:

$$CH_2{=}CH_2 + Cl_2 \rightarrow Cl\ CH_2 - CH_2Cl \quad \text{(dichloroethane)}$$

$$\downarrow\ 1000^{o}C$$

$$\underset{\text{vinylchloride}}{CH_2{=}CHCl} + HCl$$

Unlike the acetylene route, this process is about 95% efficient and yields from 55 to 60% monomer. It has undergone considerable development with the need to use cheaper starting materials and, hence, reducing the price of the monomer.

Its early disadvantage is the production of hydrogen chloride, but this has been overcome by oxychlorination process[24]. A typical process involves the equation:

$$\underset{\text{ethylene}}{CH_2{=}CH_2} + HCl + \tfrac{1}{2}\ O_2 \xrightarrow{CuCl_2} \underset{\text{vinylchloride}}{CH_2{=}CHCl} + H_2O$$

Interested readers are referred to references 25 and 26.

One major setback in the production of vinylchloride monomer (VCM) is the toxicity of the monomer. The monomer has been associated with the cause of angiosarcoma (liver cancer) and possibly other diseases[27]. In the United States many employees involved with vinylchloride conversion were reported dead in the late 1960s[28,29]. This had led to the Governments of many countries imposing very high safety limits on exposure of workers to VCM. The regulation also affects the quantity of residual monomer allowed in polymers intended for food applications.

Although the allowable limits for eight hours had been dropped from 500 parts per million (previous limit) to 1 ppm, governments and customers are still calling for very strict safety measures. Therefore, anyone contemplating the use of VCM is advised to consult the latest information on the governmental regulations and safety measures. The latest development in this matter is well discussed in references 92 and 93.

### 1.1.4.2 Manufacture of polyvinylchloride

Vinylchloride monomer is polymerized commercially by four main methods:

i) Bulk (mass) polymerization
ii) Suspension polymerization
iii) Emulsion polymerization
iv) Solution polymerization

But the major processes are Suspension and Emulsion methods, and are sometimes referred to as traditional methods. These methods help to dissipate heat of polymerization ($\Delta Hp$) which is about 110 kJ $mol^{-1}$. Suspension polymerization is by far the most extensively used, but a few large Bulk polymerization plants are also operated. The Bulk method was developed in France by Pechiney Company. It has been used world-wide, and has been reported to

give polymers similar to suspension polymers. The growth rates of Bulk polymers since 1965 is also higher than for its counterparts. Solution polymerization is rarely used for the manufacture of vinylchloride homopolymers. It is only used for polymerization involving speciality copolymers. This is attributed to the high heat of polymerization of solution polymers.

With reference to this work, an account of Suspension polymerization methods only will be considered. In Suspension polymerization the initiator must be water soluble. Therefore this method consists of dispersion of the monomer as droplets ($\sim$100$\mu$) in water by agitation and the use of a Suspension agent. The Suspension agent is usually a water soluble polymer (examples: polyvinyl alcohol; acrylics; cellulose derivatives), and largely controls the particle size, porosity and size distribution. The stirring is slow speed, about 30 rpm and also has a slight effect on particle size. At the end of polymerization the product is a slurry of polymer particles in water.

Temperature control in Suspension polymerization is aided by an aqueous phase. Therefore the kinetic rate equation is given as:

$$\text{Rate} \propto [I]^{\frac{1}{2}}$$

where Rate = rate of polymerization
[I] = initiator concentration

Hence, polymer molecular weight is independent of [I] and is varied by varying polymerization temperature[30].

Many types of polyvinylchloride are produced by these three main methods. In most cases, different types of PVC are produced from the same method. This is because of the emphasis laid on improving the properties of the polymer. (In all the techniques,

TABLE 1.5: Types of Vinylchloride Polymer

| Properties | EMULSION | | SUSPENSION | | | MASS | |
|---|---|---|---|---|---|---|---|
| | I Spray Dried | II Coagulated washed and dried | I Original type | II Easy-processing (EP) | III Non-porous | I Original type | II Easy-processing (EP) |
| Particle size (app. microns) | 70% less than 75μ (e.g. mainly 30-50μ) | less than 100μ | 90% less than 75μ (e.g. mainly 30-50μ) | 60-95% greater than 75μ (e.g. mainly 75-200μ) | 95% greater than 75μ | 90% less than 75μ | 60-95% greater than 75μ |
| Type of particle | cenospheres or fragments | fine particles | glossy and porous spheres | irregular shaped and porous | irregular shaped and spheres | fine particles | irregular shaped and porous |
| Purity | least pure | purer than spray-dried | Purer than Emulsion | | | Purest | |
| Potential clarity and freedom from colour | least | better than spray-dried | Better than emulsion | | | Best | |
| Electrical resistivity | lowest | almost as high as suspension | Much higher than emulsion | | | Highest | |
| Reaction to plasticiser (cold) | wet, sticky mixture or paste | wet, sticky mixture or paste | wet mixture | damp mixture | very wet mixture | wet, sticky mixture | damp mixture |

/Continued...

TABLE 1.5 ... continued

| | | | | | | | |
|---|---|---|---|---|---|---|---|
| Reaction to plasticiser on heating | gels | gels | gels | dry plasticised powder | ? | gels | dry plasticised powder |
| Heat stability (general, not invariable trend) | usually poorest | better than syray-dried | Usually better than emulsion but depends on recipte to plant conditions | | | Best | |

the polymer produced is structurally unstable). Some of these types of PVC available commercially are given in Table 1.5.

### 1.1.5 Additives for Polyvinylchloride

All thermoplastics, possibly including all polymers, on prolonged storage suffer from ageing and degradation effects. In some plastics, these effects are observed during processing. For polyvinylchloride a successful minimization of these phenomena during processing and storage somehow depend on the incorporation of additives mostly during processing. Additives, hence are a very important entity in the polyvinylchloride industry. A prime formulation achievement involves the possible combination of polyvinylchloride resin with the following additives: fillers; stabilizers; lubricants; plasticisers; extenders; waxes and pigments. These additives (and many others) are not all used in a single formulation and, choice depends on the required properties of the fibricated, article. Few of these additives listed above will be discussed, with more attention to stabilizers and lubricants.

#### 1.1.5.1 Plasticisers[31,32]

Plasticisers are used in polyvinylchloride products where softness and flexibility are required. They convert the hard and brittle polymer to soft and flexible materials which have an entirely different spectrum of end uses than the parent product. The extent of flexibility depends on the quantity of plasticiser being used and sparingly affects the properties of PVC up to an optimum limit. Suitable plasticisers are high molecular weight liquids which are:

a) non-volatile and difficult to extract with solvent;
b) relatively easy to mix with PVC polymers (which should be an easy processing type (EP) to give free flowing dry blend).

Plasticisers are classified according to their compatibility with PVC via:

i) Primary plasticisers
ii) Secondary plasticisers

Primary plasticisers are those capable of forming one phase-system when mixed in any proportion with PVC. They are phthalates (examples: dioctyl phthalate (DOP); diisooctyl phthalate) and phosphites (TXP; TTP)[+] and, used mainly for high temperature and good weathering resistance applications. Secondary plasticisers are also compatible with PVC but only for a limited composition range. They are mostly esters of aliphatic acids (DOZ; DAZ)[+] and ester alcohols known as polymeric plasticisers (example is: polypropylene adipate (PPA)) and retain flexibility at low temperature.

### 1.1.5.2 Fillers[32,33]

Fillers are additivesused with PVC to reduce cost where mechanical and other properties (e.g. opacity) can tolerate their inclusion. There are two different forms: fibrous (for mechanical applications) and particulate (for electrical and heat applications). The coarse grade of chalk and whitening of particulatefillers are the cheapest, but yield rough or at best matt surfaces. The finer grades of particulate filler yield smoother products provided agglomeration is avoided. Different fillers are used depending on the application of the end-uses.

The quantity of fillers which can be incorporated without adversely affecting the polymer properties vary from 5 parts per hundred of resin (phr) to 40 phr. Some of these fillers include calcium carbonate (natural and synthetic), china clay, carbon black, antimony trioxide and 'asbestos'.

+ TXP trixylyl phosphate
TTP tritolyl Phosphate
DOZ dioctyl azelate
DAZ dialphanyl azelate

1.1.5.3 Stabilizers

Whether plasticised or as in this case unplasticised - polyvinylchloride, stabiliser is always incorporated. Stabilizers are additives which contain acid acceptors[34] capable of reacting with and neutralizing the hydrogen chloride (HCl) evolved during high temperature processing and outdoor exposure. When unstabilized PVC is processed at high temperature, by the time as little as 0.1% of HCl is evolved, an intense discolo ration is observed. Many investigators[35,36] have inferred that the colour change (from white, yellow, brown to black) is due to the formulation of conjugated polyene structures arising from elimination of HCl from consecutive vinylchloride units.

Little is known about the reaction mechanism for the thermal degradation, but a free radical mechanism has generally been accepted[37,38]. A generalised equation showing the formation of short chain polyeneswhen PVC degrades is as shown below:

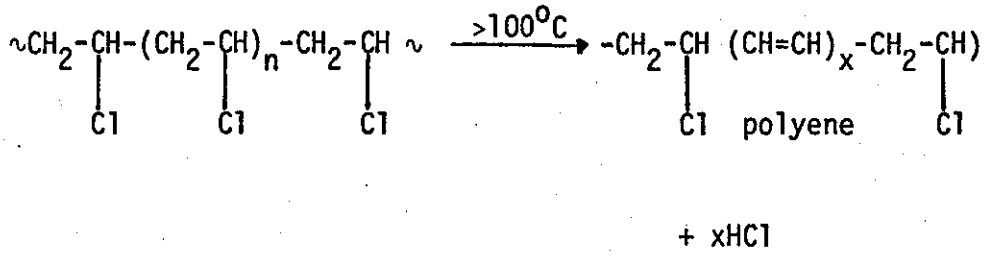


(where x > 5 and usually n is from 1 to 30 x $10^3$).

The various reaction mechanisms which have been proposed for thermal decomposition of PVC are classified as follows:

i) Unimolecular elimination
ii) Free-radical chain
iii) Ionic mechanism

Since little is known about the reaction mechanism of thermal decomposition of PVC, it is understandable that there is no satisfactory explanation to the reaction mechanism of stabilization. However, two

TABLE 1.6: Stabilizer Class and Typical Examples

| Class | Typical Products | Possible problem areas |
|---|---|---|
| Basic lead compounds | Dibasic lead stearate; tribasic lead sulphate | Ecology |
| Metal soaps | Stearate of barium, cadmium, zinc, magnesium | Toxicity |
| Organotin compounds | Dibutyl tin maleate | Cost |
| Oxivane compounds | Epoxidized soya bean oil | Compatibility and storage |

end results are apparent: the formation of polyene which imparts colour on the unstabilized PVC; and the generation of HCl during degradation. Therefore a substance could contribute effective stabilizing activity in PVC if

1. It can prevent discolouration.
2. Absorb the hydrogen chloride (HCl) evolved.

Stabilizers are normally classified according to their chemical type and Table 1.6 lists the main groups of stabilizers, together with typical examples. All of these react with the HCl formed to give $LCl_2$; $MX_2$ and $R_2SnX_2$ (for lead compounds, metal soaps and organotins) respectively. The structural aspects of polyvinyl-chloride stabilization depend on the technique of polymerization. Products produced at low polymerization temperatures tend to be more heat stable than those at high temperatures. The occurrence of branching phenomena in PVC has been reported to be one of the factors leading to instability points. Few other factors which have been observed are the presence of short chain polymers and free radical sites resulting from HCl elimination during processing. Therefore the basic lead compounds, such as white lead, basic lead carbonate, are very effective stabilisers. They are hydrogen chloride acceptors and hence minimise its autocatalytic effect on dehydro-chlorination. These basic lead stabilizers are used at 3-10 phr and are well known heat stabilizers.

Metal soaps and phenolates such as cadmium, zinc stearates are effective at 1-3 phr. Mixtures of these stabilizers most times give better results due to their effect of 'synergism'. For all metal soap stabilizers, an induction period is observed after which hydrogen chloride evolution proceeds at the rate markedly greater than that of unstabilized PVC. This defect is more prominent with group $II^B$ than group $II^A$ metal soaps. The commercial metal soaps are most often compounded with secondary and organic stabilisers - for low-toxic formulations. This also helps to improve the performance of the stabilizers[39,40].

Another set of effective stabilizers are the organotin compounds. These have very effective groups of substances for protecting vinylchloride based polymers. They could be used also in conjunction with small amounts of other stabilisers such as oxirane compounds and metal soaps. The $R_2SnX_2$ and $RSnX_3$ structures normally have 'R' as dibutyl or n-octyl and 'X' as carboxylate; unsaturated carboxylate; tin-sulphur or bonded organic sulphur compounds[41]. The amounts of organotin stabilizer added are usually from 0.2 to 2 phr, and mainly for applications where high transparency is required.

### 1.1.5.4 Lubricants[33,42-44]

Lubricant is incorporated to modify the processing behaviour of PVC, by reducing friction during fabrication. Hence there are two types of lubricants:

1. External lubricants
2. Internal lubricants

The external lubricants are those which reduce friction between PVC melt and metal surfaces of processing equipment. This type of lubricant is used for both plasticised and unplasticised PVC and is relatively incompatible with PVC. At processing temperature they migrate to surfaces of products and prevent sticking of the hot material to the metal surfaces. Examples of these lubricants are stearic acids, lead; zinc ; and other metal stearates. Others are paraffin wax and low molecular weight polyethene. Typical quantities used are 0.25 to 1 phr and the only problem is fear of 'plate-out'.

Another type of lubricant used is the internal lubricant. This is added to reduce friction within the PVC melt. Therefore they are not needed in plasticised, but are extensively used in unplasticised PVC fabrications. It is far more compatible with PVC than the external lubricant, and hence migration to the surface is

not possible. For this reason, the substance is usually non-polar; examples are amide, waxes, montan waxes, esters, ester of stearic acid.

The additives discussed above, including a few more, when they are properly formulated, mixed and blended with PVC produce inherently stable polymers and environmentally adequate products. Their discovery greatly enhanced the consumption of PVC in domestic and industrial applications.

### 1.1.6 Applications

Plastics have replaced most of the traditional materials in many applications due to its characteristics (processability, availability and cost) and polyvinylchloride (PVC) accounts for 25% of these applications. Its versatility, non-flammability and cheapness have made PVC one of the widely used synthetic polymers. Its broad spectrum of end uses include: curtains; furnishings; upholstery; fabrics; women's and children's nightwear; blankets; mattresses; rugs and industrial fire-protective clothings. Blends with wool or nylon are also used in various clothing applications. This is because of non-flammability properties of PVC and to impart sufficient non-flammability at least 75% of PVC is required in blends. Table 1.7 shows industrial applications of PVC and the reasons for their use.

TABLE 1.7
Industrial areas of application of PVC

| INDUSTRY | REASONS FOR USE |
|---|---|
| Building | Flame resistance, cheap, abrasion resistance, chemical resistance (including weathering) |
| Packaging | Clarity, products readily made, resistance to liquids |
| Electrical | Good electrical properties, flame resistance, cheap, flexible |
| Clothing/footwear | Abrasion resistance, flexibility, chemical and solvent resistance |

The major areas of industrial and domestic applications are better discussed under two extreme types of PVC:

1. Flexible (plasticised) PVC
2. Rigid (unplasticised) PVC.

Plasticised PVC has successfully replaced natural rubber in many applications. It is used for calendered sheet and film, for food and packaging industries; cable and wire; coatings; flooring; belting; footwear; automotive and aircraft upholstery, dipping and slush mouldings and many miscellaneous articles including foams.

Rigid polyvinylchloride is supplied both as powder and as finished compounds in granular form. Rigid vinyls are designed to take maximum advantage of the chemical inertness of polyvinylchloride. Rigid pipes, fittings; valves; ducts and hoods in chemical plants to carry salt water and crude oil, are all areas of rigid PVC application. Other uses also include profiles; filter frames; rigid sheet and film; bottles and records. Generally speaking, consumption of rigid PVC at present is higher than that of flexible polyvinylchloride. Table 1.8 summarises the various areas of PVC application.

It is certain that the non-flammable property and cheapness of polyvinylchloride will continuously provide new areas of application.

TABLE 1.8

PVC processing and areas of applications

| Processing Method | Applications | |
|---|---|---|
| | Plasticised | Unplasticised |
| Calendering | Film and sheet for example; packaging; floor covering; rainwear; protective clothing. | |
| Extrusion | tubes, hosepipe, wire covering, cable sheathing | pressure pipe; effluent pipe; profiles (examples: shuttering, drain-pipes, monofilaments) |
| Extrusion/Blow moulding | Bottles and containers | Bottles and containers |
| Injection moulding | Footwear | Solid mouldings (examples: fittings for pipes) |
| Rotational mouldings | Playballs, dolls; | toys |
| Spreading | Coated substrates (examples: leather-cloth; carpet backing) | |

## 1.2 Previous Work and Project Objectives

### 1.2.1 Previous Work

Polyvinylchloride is utilised in many applications and currently in terms of tonnage consumption, it is one of the three leading plastic materials in the world. Despite its versatility, PVC is difficult to process at normal processing temperatures due to the irregularity of its structure. To process PVC free from degradation and discolouration the incorporation of primary ingredients such as stabilizer and/or plasticiser, lubricants and perhaps processing aid are necessary. The structure of the polymer proves to be thermally unstable and therefore processing it without additives - especially a stabilizer - has been unsuccessful.

In this programme the formulation contains only a lead stabilizer and lubricants, which give a simple formulation to enable the study of the effect of processing conditions on stabilizer distribution and morphological changes in powder blend and its processed form. Stabilizers have been reported by several authors[38,45-47] to prevent dehydrochlorination, excessive degradation and discolouration during processing at normal processing temperature, but very few published works exist on distribution of these stabilizers - especially in the processed materials.

Previous work based on distribution of additives and morphological changes in unplasticised PVC blend and its processed form has been reported by Hemsley et al[48]. It was thought that these factors (distribution of additives and morphological changes) were the major cause of characteristic changes of powder blends during high speed blending. By employing light and electron microscopy in conjunction with other physical property methods, solid additives were found to coat the surfaces of the PVC grains, and to distribute sporadically in the processed material.

Investigations on morphological changes in materials along extruder screws and in the final extrudate when powder blends are extruded had been carried out with little attention on distribution of stabilizers. Gale's[49] investigation on twin screw extrusion of UPVC dry blends were based mainly on the effect of lubricants on additive dispersion in a high attrition mixer and on fusion rate in extrusion. He blended lubricants of various types and concentrations with UPVC suspension polymer and extruded some of the blends through a twin screw extruder. On characterizing the powder blends, Gale found that solid additives coat the surfaces of the UPVC grains, and that discharge temperature influences bulk density and flow properties of the polymer. Using common light microscopy methods to examine the samples along the twin screws and the final extrudates, Gale was able to conclude that different lubricants affect the fusion mechanism of extruded UPVC in different ways.

Unlike Gale, the investigation carried out by Allsopp[50] was closer to explaining the distribution of stabilizer in extruded materials. Allsopp used UV fluorescence light and differential interference contrast microscopy methods in addition to common light microscopy methods to study the fusion of UPVC samples along extruder screws and of the final product of a twin screw extruder. He observed the distribution of tribasic lead sulphate stabilizer in the stripped samples with UV fluorescence microscope, but commented there was little or no fluorescence observed in the final extrudate. However, there is apparently no detailed study on the distribution of stabilizer in the extrudate nor on the stabilizer distribution affected by any processing conditions.

### 1.2.2 Project Objectives

This work forms part of a large programme being undertaken in the Institute of Polymer Technology, aimed at studying the relationships between PVC powder morphology, processing conditions, structure and properties of products.

In direct powder processing the granulation stage is completely omitted thus providing, among other things, enormous savings in equipment costs and material handling[51,52,53]. Therefore many processors are turning to direct powder processing, but if these benefits are to be derived consistency of powder blends must be ensured to avoid erratic and surging output.

With this view, the present work is based on studying the relationships between additives distribution, morphological changes and processing conditions of three different, but interconnected fabricating methods - blending, extrusion and compression moulding. The objectives of this research are therefore as follows:

i) Investigate the effect of different blenders on the dry blend characteristics;

ii) Evaluate the effect of operating conditions, within a single blender, on powder blend characteristics;

iii) Examination of the effects of processing parameters on the additives distribution and morphological changes along extruder screws and in final extrudates of a twin-screw extruder;

iv) Study of the influence of relatively low shear-rate on additives distribution and morphological changes in compression moulding.

In order to meet these objectives however, the appropriate sample preparation techniques for the assessment of the relationships between stabilizer distribution, morphological changes and processing conditions must be developed.

## 1.3 Background of Project

### 1.3.1 Morphology and Particulate Structure of Polyvinylchloride

Morphology of polyvinylchloride (PVC) normally comprises of the composite nature of the polymer bead which is readily visible by microscopy before or/and after processing. PVC morphology could be studied either at low percentage of conversion during polymerization, before processing or after fabrication processes. Many workers[54-56] have studied the morphology of PVC grains before processing and found that there are three types of PVC polymers as a result of polymerization techniques. During the commercial polymerization either by bulk, suspension or emulsion method the primary particles cluster and to some extent fuse together to form grains of varying porosity and sizes. Table 1.5 illustrates the order of sizes for particles of each polymerization method. They have different particles morphology for bulk, suspension and emulsion polymer grains. The illustrated micrograph of these grain types from publication by Tragen and Bonnemayne[57] is shown in Figure 1.1.

Bulk polymer grains retain their agglomerated particle structure from the interior to the surface which is rounded and slightly compacted. Suspension polymer grains are being covered by a membrane (skin) of about 0.2 μm thick (although it is possible to produce skin-free SPVC). Although both bulk and suspension polymers contain interstitial voids, suspension PVC has larger skin-covered voids. Emulsion polymer grains are cenospherical due to latex-drying conditions, and consist of loosely agglomerated primary particles.

#### 1.3.1.1 Morphology of PVC particle

The morphology of a single PVC resin particle, whether of bulk, suspension or emulsion, is built up of grain, sub-grains, agglomerates, primary particles, domains and micro-domains as has been described and demonstrated by several workers[1,59-61]. This was not actually discovered until late 1960s[97,64], before then

FIGURE 1.1: Classification of Polyvinylchloride Grains[57]

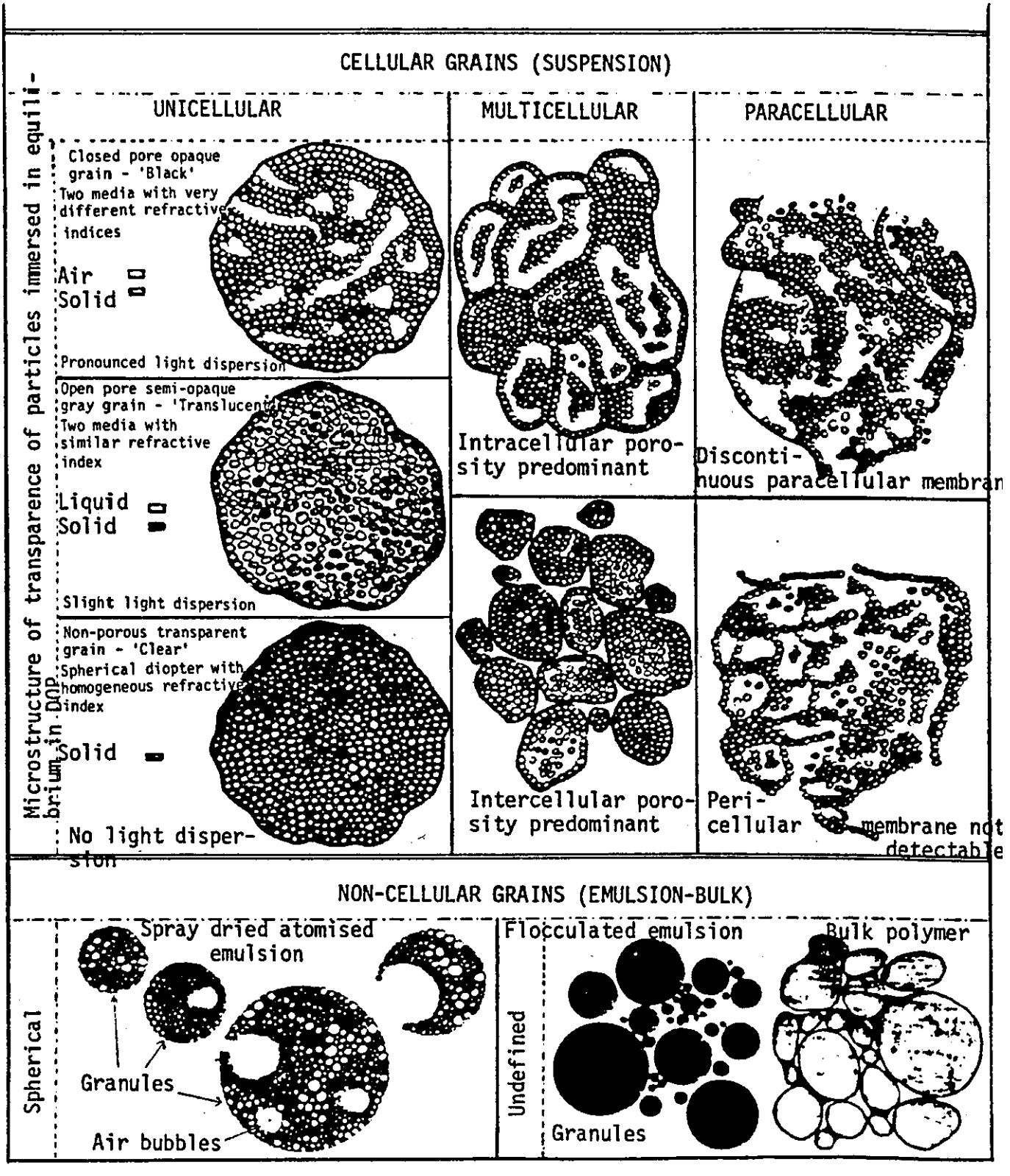

emphasis was laid only on grain types resulting from different polymerization processes. Table 1.9 shows the terminology recommended for the classification of these PVC morphologies, as issued in the 2nd International Symposium on PVC held in July 1976.

Allsopp[60] examined the PVC grains during polymerization and reported that microdomains are formed and precipitated from the monomer phase at the very early stage of polymerization and, consist of coiled macromolecules of about 0.02 μm size. At less than 2% conversion, these nascent particles aggregate to form the domains (0.2 μm size) and thereafter become primary particles. Work[63] also reported the existence of primary particles at this stage of polymerization with average size of about 0.7 μm. The primary particles are stable and form a feature of PVC morphology. At more than 2% conversion the formed primary particles flocculate, and growth proceeds in these flocs until a macrosize (of 100 μm average size) is attained. The arrangement of these grains morphology has been portrayed by many authors[65-67] and is illustrated in the sketches in Figure 1.2.

1.3.1.2 Morphology of processed PVC

The morphology of processed PVC has been of considerable concern to the processors. The heterogeneous nature of the grain imposes processing difficulties, therefore attempts have been made by investigators to find the relationship between PVC morphology and processing history[68-70]. It has been shown that during processing the 100-120 μm PVC grains are broken down to 10 μm agglomerates and then to 1 μm primary particles which is the flow unit in most conditions[71,72]. Terselius et al[69] had reported that neither the 200°A microdomain nor the 0.2 μm domain structure is deformable but that the connective tissue between the 0.2 μm domain is highly deformable. This evidence is found to be consistent with the flow unit of unplasticised PVC being an approximately spherical domain of about 0.2 μm diameter which is not deformable itself during

TABLE 1.9:
Morphological characterization of terminology[60]

| Recommended Term | Approx. Size | | Origin or Description | Previous Terminology |
|---|---|---|---|---|
| | Range (μm) | Average (μm) | | |
| Grain | 50-250 | 130 | Visible constituent of free flowing powders, made up of more than one monomer droplet | Granule; powder particle. Cellular grain |
| Sub-grain | 10-150 | 40 | Polymerised monomer droplet | Sub-grainule; nodule Unicell |
| Agglomerate | 1- 10 | 5 | Formed during early stage of polymerization by coalescence of primary particles (1-2 μm). Grows with conversion to size shown | Aggregates. Primary particle. Cluster; Macro-globule |
| Domain | 0.1-0.2 | 0.2 (200 nm/ 2000°A) | Primary particle nucleus. Contains about $10^3$ micro-domains. Only observed at low conversion (less than 2%) or after mechanical working. Term only used to describe 0.1 μm species, becomes primary particle as soon as growth starts | Primary nucleus; Granule |
| Micro-domain | 0.01-0.02 | 0.02 | Smallest species so far identified. Aggregate of polymer chains - probably about 50 in number | Basic particle. Particle. |

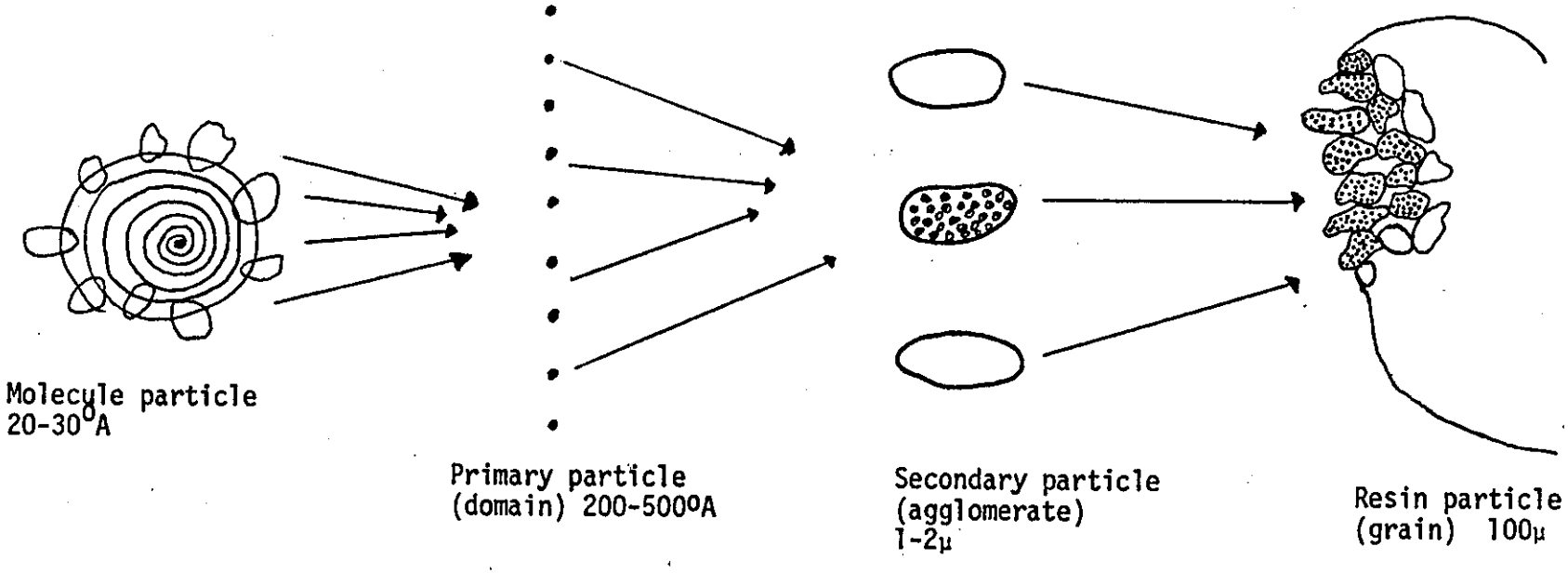


FIGURE 1.2: Microstructure of Polyvinylchloride[70]

processing. Munstedt[68] also reported that the 200°A micro-domain is held together internally by 'crystallinity' acting as crosslinks but the connective tissue between the 0.1 μm domains is far less ordered and easily deformable.

Although the various levels of morphology that are generated during polymerization and processing have been considered in detail by many authors, the morphology of the internal structures are still under investigation. Generally, morphology exerts a major influence on all stages of manufacture and processing, and on all subsequent steps from bulk handling, through mixing and shaping.

### 1.3.2 Principles of High-speed Blender

Dry blending is normally considered as the intimate combination of liquid or dry additives with PVC to produce a homogeneous free-flowing powder. This process is suitable for the easy-processing type polymer (see Section 1.4.2). In the late 1940s the commercially developed equipment, referred to in many literatures as premixers, for this process were low-speed mixers such as ribbon blenders, tumble blenders, sigma-type mixers and mullar-type mixers[73]. Where homogeneity is essential their end-products are homogenized in a compounding machine[74].

These premixers develop little or no frictional heat during blending operation and heating is supplied mainly by external sources. Their application to blending rigid formulations was not a total success and there was a need to develop a high-speed mixer. In the late 1960s high-speed mixers such as Fielder blender, Henschel blender and Papenmeier blender were introduced[74,75]. The high shear associated with the high speed blender makes it possible for the generation of frictional heat during blending. The blends produced with them are normally free-flowing and comparatively more homogeneous. The high-speed blenders (intensive mixers) can be operated over a wide range of conditions so that powder blends can be extruded or moulded directly without the need for granulation.

Basically, intensive mixers utilise a specifically designed propeller-like impeller mounted in the bottom of a stationary chamber. An adjustable baffle blade deflects slow moving material from the top of the vortex down to the correct working area. The temperature sensoring device consists of an iron/constantan thermocouple which protrudes either through the baffle or wall of the mixing chamber. Intensive mixing is jacketed for heating, and cooling system which utilises either oil or steam. Typical intensive mixer is diagrammatically represented in Figure 1.3.

The 8 litre Fielder blender used in this project has a working capacity of 2 to 3 kg and the impeller rotates at a high speed ranging from 500 to 4500 rpm that creates a vortex mixing action. The mixing bowl is made of highly polished stainless steel which facilitates cleaning and greatly reduces cross-contamination (tending to zero). It also reduces wall friction and hence is less prone to wear. Charging hatches are provided in the lid so that the mixer top need not be removed for the introduction of solids or liquids. After attaining the required temperature the batch is in many cases discharged into a low-speed cooler mixer.

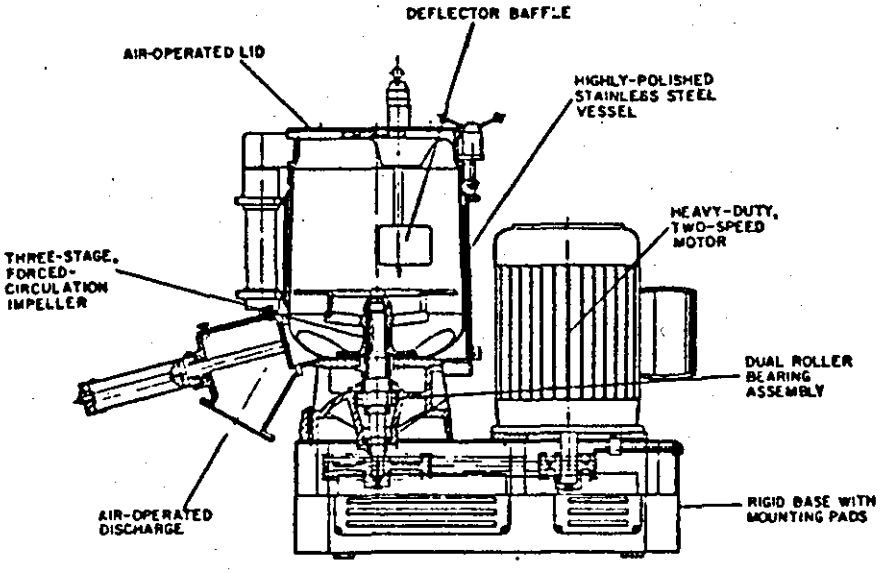


FIGURE 1.3: High Intensity Mixer for Dry Blending[76]

The cooler unit consists of a rather larger chamber and slow-impeller speed. The surface area of the cooler unit is about three times larger than that of the mixing chamber and with rotor speeds ranging from 100 to 1000 rpm. This cooler chamber is adjacently placed below the mixing bowl and has a water cooling inner jacket and is also made of highly polished stainless steel.

### 1.3.3 Principles of Twin-Screw Extruder[77-81]

The principle of a twin-screw extruder is known to be based on 'positive pumping' action. The extruder was invented and used extensively in Europe in the early 1940s. It was designed to be used mainly for compounding of plastics (i.e. plastics with pigments, pelletization of regrind etc), but was readily adapted for processing of dry blends. For many years dry blend extrusion of rigid polyvinylchloride has imposed problems with single screw extruders. Little was achieved by redesigning the screws of the single screw extruders because of high residence time associated with it. PVC being very sensitive to excessive heating was found to extrude with little or no difficulties in the twin-screw machine.

The successful direct extrusion of rigid PVC in the twin-screw extruder is generally associated with its working principles. The arrangements of the screws can be either counter-rotating or co-rotating as shown in Figure 1.4. The screw can also be designed to be either intermeshing or non-intermeshing. Regardless of the arrangements of the screws the extruder has been found to have a positive conveying action and mixing effectiveness. In twin-screw extrusion once the screws pick up the polymer (whether it is powder, flakes, pellets or regrind) at the feed throat, it is moved forward along the barrel regardless of its condition (solid, semi-fluxed or fluxed), pressure and/or feed rate. This is because there is no back pressure flow in the barrel due to the absence of a continuous channel. Therefore all particles are pushed forward continuously

FIGURE 1.4:
Rotation of screws in twin-screw extruder

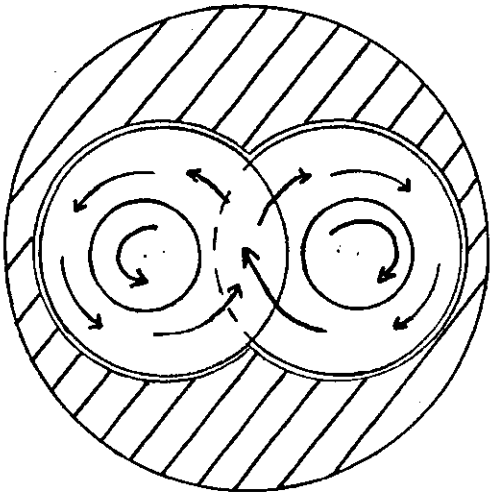

(a) Counter-rotating screws.

Very high shear rates are generated because material gets milled in between the screws

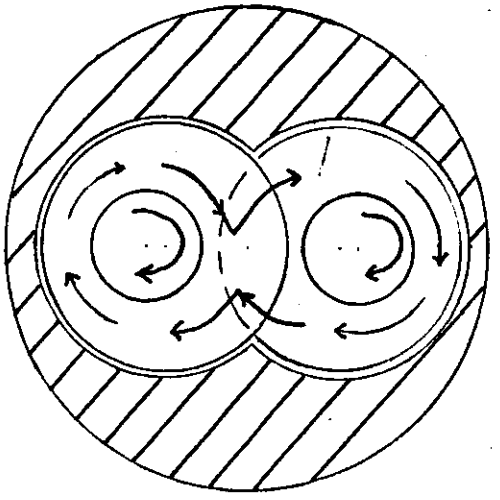

(b) Co-rotating screws.

Low shear rates are observed because material is transferred from one screw to the other.

and uniformly into two definite C-shaped sections.

Effective mixing is obtained mainly from a well designed screw clearance ranging in the order of 0.335 to 0.22 cms and which vary with different screw and extruder designs. Additional mixing action occurs at this region of the extruder where the material encounters highest shear rates. Also at this intermeshing point one screw wipes off the other and prevents the plastic melt from sticking onto the screws. In comparison with the single screw extruder however, the forward travel of the plastic material depends entirely upon the coefficient of friction developed between the plastic melt and the barrel wall being greater than that between the plastic melt and the screw. Despite this, the single screw extrusion output is also affected seriously by back pressure flow and heat flow.

In this programme the twin-screw extruder used is the Leistritz LS3034 with an optimum throughput of about 35 kg per hour. The screws are counter-rotating and intermeshing. Figure 1.5 shows a schematic representation of the extruder.

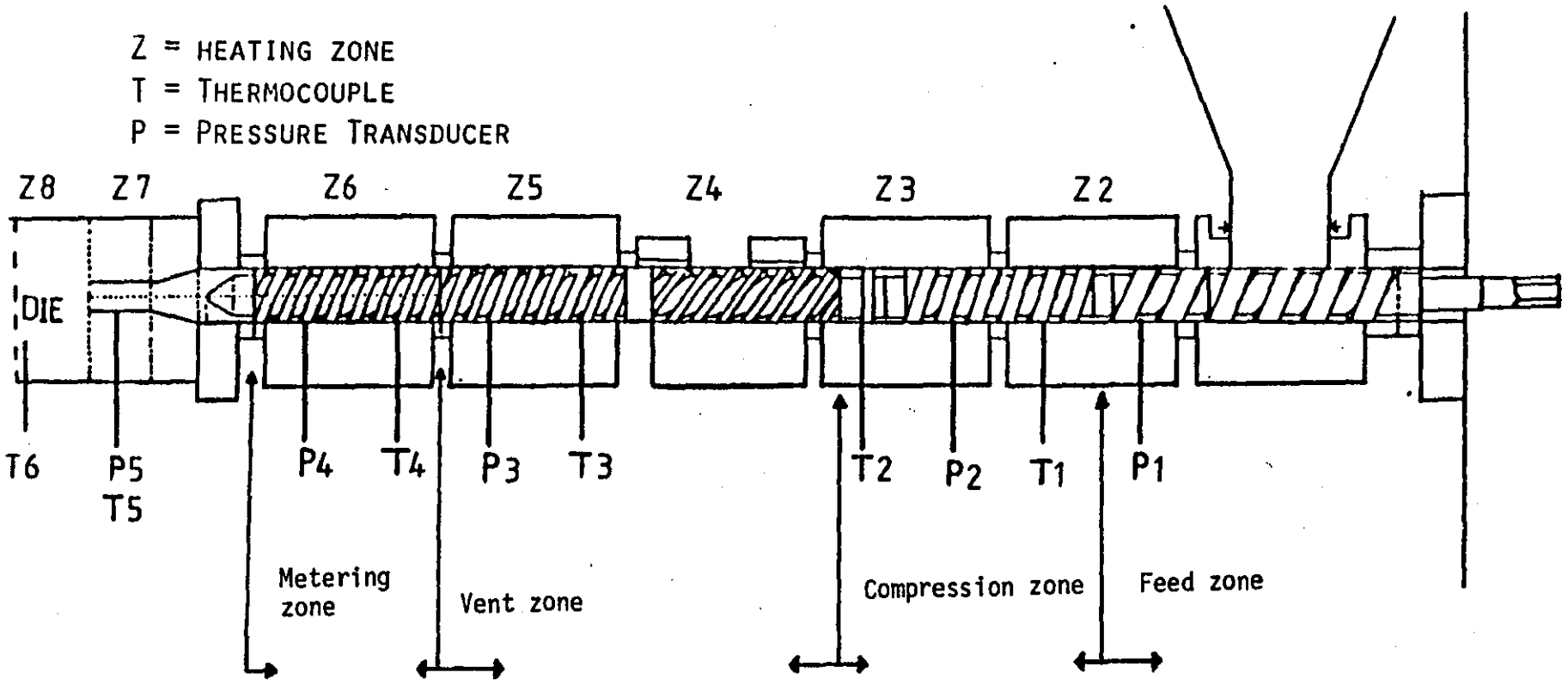


FIGURE 1.5: Schematic representation of the Leistritz LS.30.34twin screw extruder

### 1.3.4 Microscopy of Polymers

The past forty years has seen various fields of studies, such as microbiology, medicine, anatomy, metallurgy, zoology, geology, bacteriology, etc. benefitting from the advent of vastly improved microscopical techniques. The examination of plastic materials with these techniques, although in its infancy, has proved very successful. The areas of such investigation include the study of surfaces of plastic materials; examination of the mixing of various plastics such as plastics with rubbers; examining the homogeneous dispersion of additives e.g. fillers, stabilizers and pigments; investigation of stress and fractured surface topography; and the crystalline structure and particles morphology.

The low power optical microscopes and stereoscopes are not only used for the examination of tensile and impact specimens for edge notches or other stress raisers, but also for the observation of the surfaces of an electric strength specimen for voids and bubbles before test.

Microscopical examinations could be carried out with intact specimens, and many methods may be used simultaneously with microscopy, thereby making best use of small samples. Many authors have discussed extensively on the application of microscopes in testing and/or examination of plastic materials. Interested readers are referred to references 94-96.

There are two specific types of microscope:

1. Light microscope.
2. Electron microscope.

Both have been extensively employed in the study of the physical and chemical nature of polymeric materials. In PVC for instance, light microscopical methods have been used to study the process of polymerization[60] but with the advantages of higher magnification, the electron microscopy techniques have been found useful for

examining the morphology of the particles and microdomains[66,67,82,83].

The two important factors mostly considered in microscopy are 'resolution' and 'contrast'. The former depends essentially on the type of instrument, and on the wavelength of the illuminating radiation. Therefore considering the proper use of the microscope resolution is largely beyond the control of the observer. 'Contrast' relies mainly on the ability to assess the probable optical properties of the specimen and in selecting methods most likely to reveal these properties. Therefore the choice of microscope type and technique is vastly governed by these two conditions. Obviously if 'resolution' beyond the limits of the optical microscope is of primary importance the electron microscope must be used, but if the aim is to learn something about the chemical nature and degree of orientation of the specimens or about their dry mass or concentration, then the choice is invariably for the optical method.

Therefore the optical and electron microscopical methods were designed to complement each other and as long as microscopists are aware of the importance of 'resolution' and 'contrast', both methods will continue to exist in conjunction with each other.

### 1.3.4.1 Light microscope

The use of lenses to aid vision was discovered as far back as 60 AD[84,85], but the combination of concave and convex lenses by a Dutch instrumentalist - Hans Hansen in 1590 - led to invention of the microscope. Puzzled by its ability to reveal microorganisms and structures, J Faber of Bamberg[85] in 1625 designated the name 'microscope' meaning 'seer of little things' to the instrument. Since then optical microscopes have been continually modified to meet with scientific developments.

The modern microscopes could be attributed to a great work of Ernst Abbe[86] whose contribution in this field led to vast discoveries and improvements in microscopical techniques. Abbe's discoveries

quickened interests in microscope and a phase of rapid progress in microscopes occured within a short period.

In that process of innovation many microscopical techniques relevant to polymer studies were discovered. Some of these optical methods which have found application in the polymer field are as listed below:

1. Common light microscopy[a]
2. Dark-ground microscopy[a]
3. Phase-contrast microscopy[b]
4. Polarised-light microscopy[b]
5. Interference microscopy[a]
6. Ultraviolet and fluorescence microscopy[a]

a = transmitted and reflected light; b = transmitted light.

All microscopes have the same basic principles of image formation but vary with additional type of optical elements used for specific investigation. Figure 1.6 shows the diagrams of the types of optical microscope listed above.

The working principle of an elementary microscope has been adequately discussed by several authors[87-91]. It involves the fundamental principles of optical physics. The elements required in a basic compound microscope to produce a magnified image of an object are objective, eyepiece(s) and perhaps condenser lens, lamp and mirror. The objective produces a magnified image of the object, but the eyepiece examines and enlarges this real image formed by the objective. Hence magnification takes place in two stages and, theoretically, optimum total magnification is enhanced by employing short eyepiece and objective focal lengths - in conjunction with a long optical tube length. The image produced is always inverted and as a result when the object is moved, the image moves in an opposite direction. However, the introduction of a prism system as in Greenough stereoscopic microscope, has been found to alter this relationship. Many elementary microscopes also

FIGURE 1.6: Types of Light Microscope

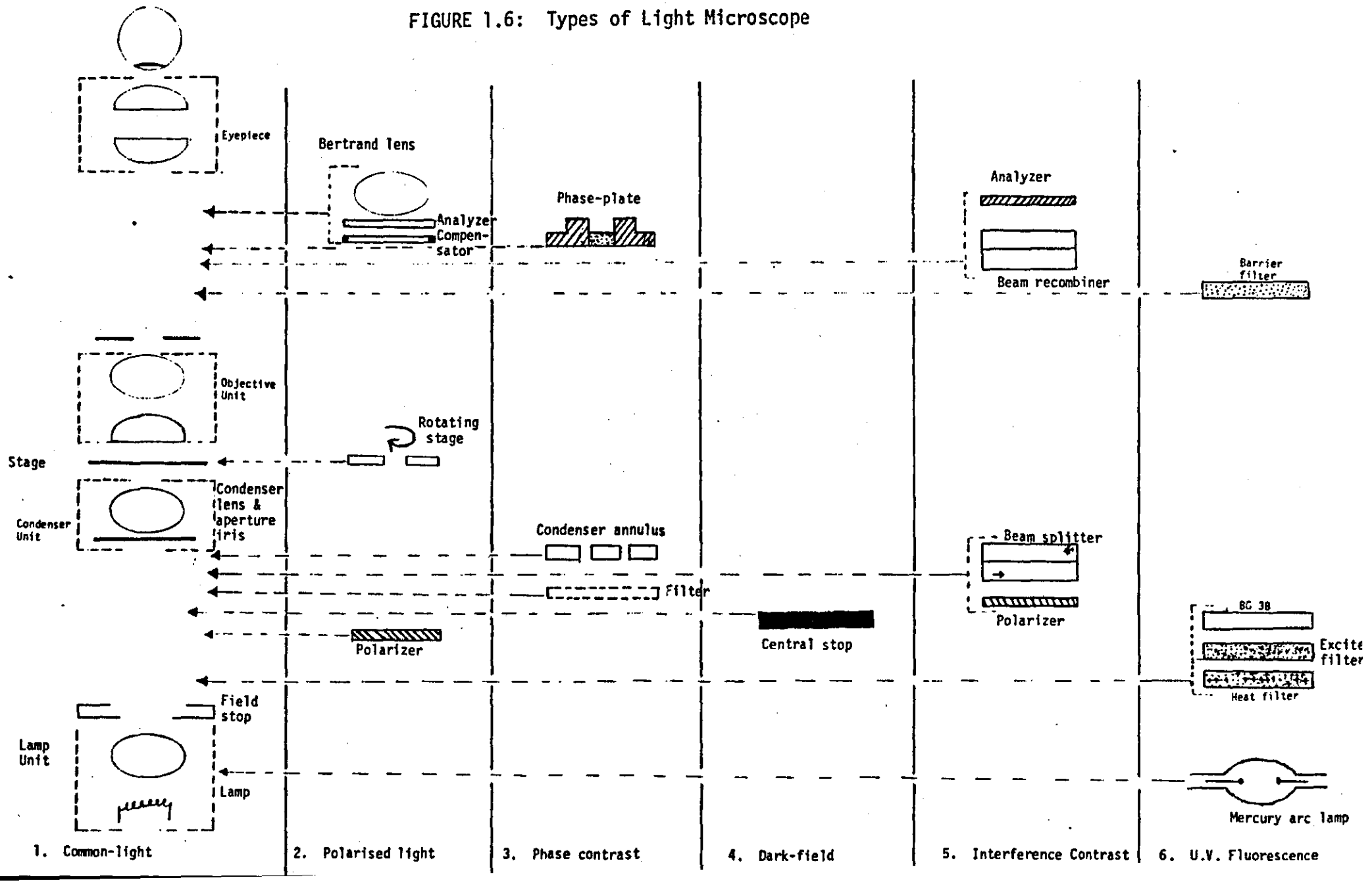

contain a light source and a condenser lens. The function of the condenser lens is to concentrate the light rays entering the objective, and hence is placed between the lamp and the object.

Other vital points in the implementation of light microscopy are its advantages and limitations. The disadvantages are well known to surround the optical elements: objectives and condenser lenses. Although enormous improvements have occurred in recent times, the problems may not have been completely eradicated. Some of these limitations are:

a) It is only useable over magnification range of up to x1600.
b) Lateral resolution is limited to a half wavelength of the light used.
c) Sometimes the specimen requires sufficient degree of transparency for transmitted light mode.

The main advantages apparently outweigh the disadvantages. Some of these advantages are as summarised below:

a) There are no beam damage problems.
b) Some methods (for example; interference light methods) have a greater sensitivity to surface slope than scanning electron microscopy, so that comparatively large areas of gently sloping surface can be successfully imaged.
c) The specimen is readily accessible and problems such as the rapid removal of volatiles are not encountered.
d) Modern interference light techniques allow quantitative assessments of surface roughness to a high degree of accuracy.

In this programme the differential interference contrast (DIC) and UV fluorescence microscopical methods are the optical techniques vastly employed and 'brief' accounts of these techniques are given in Chapter 3.

1.3.4.2 Electron microscopy

The effective use of electron microscopes started in about the late 1930s[89,98,99], when it was discovered that electrons exhibited a wavelength which could be less than one angstrom. Since then the developments that followed were rapid compared with that of optical microscopy and now it is one of the most useful instruments for the examination of plastics and other polymeric materials. The operating principles, unlike the optical microscope, is based on the use of electron wavelength to form the image of an object. This has been elaborately discussed in numerous literatures[99-103] and the operating instructions are well enumerated in the manufacturers manuals. Nevertheless a brief account of the image formation will be considered here.

To produce an image of a correctly prepared sample (see Section 3.3.3) electrons are emitted from sufficiently heated tungsten filaments. These electrons are accelerated by voltages of between 50 to 500 KV through a vacuum column onto the specimen. Focussing on this electron beam onto the specimen is accomplished by one or two condenser lenses, while the image is formed by two or more additional electromagnetic lenses. The image produced is either observed on a fluorescent screen and/or recorded photographically.

There are many models of electron microscope, and more new types of instruments and attachments arebeing developed rapidly. Some of these conventional electron microscopes include:

a) Scanning electron microscope (SEM)
b) Scanning transmission electron microscope (STEM), and
c) Transmission electron microscope (TEM).

Electron microscopes have numerous advantages over the optical microscope. Despite its broad spectrum of applications it has higher resolution; greater depth of focus - up to 1000 times; and it is possible to observe both the image of the sample and its diffraction pattern by changing the power of the intermediate lens.

In spite of these advantages, the electron microscope has some limitations. Sample preparation is more difficult and time consuming, and also far less characterization information is obtained as summarised in Table 1.10. This latter disadvantage of electron microscopes is minimized for TEM by using selected area diffraction (SAED) and for both TEM and SEM by adding a solid state, non-dispersive X-ray analyser (EDXRA) in order to determine elemental composition. But unfortunately, EDXRA cannot detect any elements below sodium in atomic number.

TABLE 1.10
Adapted morphological analysis of microscopes[104]

| Microscope Type | Identifying Characteristics | Applicable size range |
|---|---|---|
| SEM | Size, shape, surface, EDXRA | >0.1 μm |
| TEM | Size, shape, surface, EDXRA, SAED | 0.001- 1.0 |
| Optical | Size, shape, surface, homogeneity, transparency, refractive indices, colour, birefringence | >1.0 μm |

Generally speaking, focussing on the attractions and limitations of electron and optical microscopes, it could be seen that both methods complement each other.

# CHAPTER 2

# MATERIALS, FORMULATIONS AND PREPARATION OF SAMPLES

## 2.1 Materials

The materials used for this programme were:

Suspension polyvinylchloride
Dibasic lead stearate
Calcium stearate
Cr S 2411P wax
Normal lead stearate
Oxidized polyethylene wax (AC629A)
Glyceryl mono-stearate
Acrylic processing aid (Paraloid K120N)

The last four additives were used as 'secondary' ingredients for assessing the distribution of dibasic lead stearate in processed materials. The technical data and physical characteristics of some of these materials are discussed below.

### 1. Suspension polyvinylchloride

Polyvinylchloride suspension resin was supplied by BP Chemicals Ltd. It is the extrusion type resin with the technical name Breon S110/11. The technical data for the resin is given in Table 2.1.

TABLE 2.1
Technical data of Breon S110/11 suspension PVC[105]

| | |
|---|---|
| Viscosity No (ISO method IS 174:1974) | 111 |
| K-value (0.5% solution in cyclohexane) | 66 |
| Bulk density $Kgm^{-3}$ | 550 |
| Particle size (%) - less than 250 μm | 99.5 |
| - less than 75 μm | 2.0 |
| Wt loss (1 hr at 105°C) % max | 0.5 |

Breon S110/11 is homopolymer of a medium/high bulk density with a narrow particle distribution which gels quickly during processing. It also has excellent heat stability, and exceptional colour retention properties at high temperatures. Breon S110/11 is specially designed for the production of rigid pipes and corrugated clear sheet, and its excellent powder mixing properties makes it an ideal polymer for use when processing from powder compound especially in lead stabilized rigid formulations.

2. Dibasic lead stearate

Dibasic lead stearate (DBLS) is an organic lead stabilizer with a lubricating effect. Lead compound stabilizers are effective stabilizers for polyvinylchloride, but they fail to gain substantial commercial recognition to match their efficiency. This was mainly due to the toxic nature of lead which resulted in many government organisations passing strict regulations on the use of lead compounds. Therefore lead compound stabilizers are recommended only (i.e. in countries where they are not banned) for non-food and toy applications. The properties of the lead compounds used in this project are given in Table 2.2.

TABLE 2.2
Typical properties of lead compound stabilizers

| Properties | Dibasic lead stearate | Tribasic lead sulphate | Normal lead stearate |
|---|---|---|---|
| Formulation | $2PbO.Pb(C_{17}H_{35}CO_2)_2$ | $3PbO.PbSO_4.H_2O$ | $Pb(C_{17}H_{35}CO_2)_2$ |
| Form | Powder | Powder | Powder |
| Colour | White | White | White |
| Specific gravity | 2.0 | 6.4-7.2 | 1.4 |
| Lead content (%) | 55.6 | 83.4 | - |
| Refractive index ($n_D^{20}$) | 1.60 | 2.10 | 1.59 |

Dibasic lead stearate (the primary additive in this project) is a high temperature stabilizer and used mainly for electrical applications. It has a high compatibility with PVC and less lubricating effect, therefore it is used extensively in rigid PVC formulations. Dibasic lead stearate is usually used in small quantity in formulations (i.e. from 1 to 3 parts per hundred of resin).

Normal lead stabilizer is mostly employed as a lubricant stabilizer rather than as a primary stabilizer. The compatibility with polymer is low and in acting as a hydrogen chloride acceptor, liberates stearic acid which sprues or exudes. Hence normal lead stearate is usually employed at relatively low quantity, and mostly in conjunction with dibasic lead stearate.

Tribasic lead sulphate is a highly reactive good heat stabilizer with exceptional electrical properties. It is employed in many electrical applications including building cable compounds. The high reactivity has one big advantage, that is it could be used with polyester plasticisers to meet the ageing requirements of high temperature (90-120$^{o}$C) insulation.

The activities of these lead stabilisers, as enumerated above, refer to their applications in European countries only. In the United States and Japan the use of lead stabilizers is very limited officially.

3. Calcium stearate

Calcium stearate has a good lubricating property and is normally used as an internal lubricant. It can also be used for PVC stabilization when combined with other metal salts. The lubricant is employed extensively in rigid PVC in combination with lead stabilizers.

Calcium stearate has inferior electrical properties but equivalent heat stability to lead stearates. Comparatively it has

a better compatibility with PVC than normal lead stearate. The melting point is 120°C as determined with DSC measurement, the formula is $Ca(C_{18}H_{35}O_2)_2$ and refractive index is 1.50.

4. Wax GS 2411P

This is a very low molecular weight compound with a melting point of ~98°C. It is an external lubricant and has poor compatibility with polyvinylchloride. During processing it migrates to the surface and prevents adhering of the hot plastic melt onto the processing equipment.

5. Paraloid K120N

'Paraloid' (a trademark of Rohm and Haas Co) is a range of modifiers which fall within 4 different categories of chemical structures, each used for various specialised purposes in PVC. The categories are: acrylic processing aid, methacrylate terpolymer (MBS) impact modifier, acrylic impact modifier and acrylic copolymer gloss control agents.

K120N belongs to the acrylic processing aid category. It is a white, free-flowing dusty powder. It has a bulk density of 0.46 g/ml, specific gravity of 1.18. It offers faster, more controlled fusion and homogenization of PVC.

## 2.2 Formulations

Formulation is one of the most important factors in PVC processing industry. With the end-use borne in mind, the formulation is selected wherever possible in order to obtain the required properties (mechanical properties being primary factor) commensurate with processing behaviour and cost. These latter conditions may impose themselves on the selection of some ingredients.

The possible combinations of polymer with additives such as stabilizers, lubricants, plasticisers, fillers and pigments in PVC

formulations are almost without limits. The reason is that PVC is thermally unstable (see Chapter 3). For any single application, even having quite narrowly defined property and performance requirements, a considerable number of alternative formulations are usually possible.

In this project, a single formulation was developed to meet with the programme requirements and was referred to as the 'standard formulation'. Slight variations were then made on this 'standard formulation' while maintaining its 'structure'. This standard formulation, and the variable formulation (altogether add up to a total of 8 formulations) were supplied by B P Chemicals Ltd, Barry, Glamorgan.

In order to closely understand the relationship between stabilizer distribution and morphological changes it was even found ncessary to vary the stabilizer concentration. This led to an additional 6 formulations making a total of 14 formulations. These 14 formulations were divided into two conveniently workable groups as listed in Tables 2.3 and 2.4. Table 2.3 contains formulations 1 to 9, while Table 2.4 contains formulations 10 to 14. It is important to note that formulation 1 is the 'standard formulation', and that the rest of the formulations were developed from it.

TABLE 2.3: Suspension PVC Formulation (Group A)

| Quantity of ingredient (pph) / Ingredients | FORMULATION NUMBER | | | | | | | | |
|---|---|---|---|---|---|---|---|---|---|
| | 1* | 2 | 3 | 4 | 5 | 6 | 7 | 8 | 9 |
| Breon S110/11 | 100 | 100 | 100 | 100 | 100 | 100 | 100 | 100 | 100 |
| Dibasic lead stearate | 2.5 | 2.5 | 2.5 | 2.5 | 2.5 | 2.5 | 2.5 | 1.5 | - |
| Calcium stearate | 0.4 | 0.4 | 0.8 | 0.8 | 0.4 | 0.4 | 0.4 | 0.4 | 0.4 |
| G.S. 2411P wax | 0.3 | 0.15 | 0.3 | 0.15 | 0.3 | 0.3 | 0.3 | 0.3 | 0.3 |
| Oxidised PE wax | - | - | - | - | 0.2 | - | - | - | - |
| Glycerol monostearate | - | - | - | - | - | 0.4 | - | - | - |
| Paraloid K120N | - | - | - | - | - | - | 1.5 | - | - |
| Normal lead stearate | - | - | - | - | - | - | - | 1.5 | - |
| Tribasic lead sulphate | - | - | - | - | - | - | - | - | 2.5 |

* Standard formulation

TABLE 2.4: Suspension PVC formulation (Group B)

| Quantity of Ingredient (phr) / Ingredients | FORMULATION NUMBER | | | | |
|---|---|---|---|---|---|
| | 10 | 11 | 12 | 13 | 14 |
| Breon S110/11 | 100 | 100 | 100 | 100 | 100 |
| Calcium stearate | 0.4 | 0.4 | 0.4 | 0.4 | 0.4 |
| G.S. 2411P wax | 0.3 | 0.3 | 0.3 | 0.3 | 0.3 |
| Dibasic lead stearate | - | 1.0 | 2.0 | 3.0 | 4.0 |

## 2.3 Preparation of Samples

### 2.3.1 Preparation of Dry-blends

Two types of high speed mixers were used to prepare the dry blends of formulations described in Section 2.2. These intensive mixers were the 8-litre T K Fielder blender at IPT and the 10-litre Henschel blender at B P Chemicals Ltd. The general construction and principle of a high speed mixer is the same and has already been discussed in Section 1.3.2. The optimum blending conditions were determined by carrying out a series of tentative blending experiments.

The blend (thoroughly hand-mixed) was charged into the treated mixing chamber at a temperature of 75°C. When the required blending temperature (or time) was attained, the blend was discharged through a pneumatic valve into a low speed cooler mixer. The blend was left in the cooler mixer for about 5 minutes for a 2 kg-charge blend before discharging (the cooling time of blends in the cooler mixer being influenced by quantity and capacity of blend and cooler unit respectively).

During this period the cooler mixer dissipates the heat within the PVC powder mainly by conduction. Its low impeller speed and water cooled large surface area facilitates the removal of heat generated during blending. The cooling of the powder blend under this processing condition is very essential. For instance, there was a case when the hot blend was discharged into a plastic bucket of narrow surface-area, and left overnight. The following morning the blended powder was discarded because the colour turned brown and the powder had formed a hard and brittle disc. Therefore to avoid this incident the hot powder had to be agitated during cooling. Again, where the blend is stored in an ambient temperature prior to proper cooling to at least 40°C in the cooler chamber, some pebbles and lumps of powder are formed. This affects the flow-rate, and bulk density of the blend, and greatly impedes the feeding operation during processing.

The rest of the blends were prepared in the same manner and the blending conditions are listed in Table 2.5.

TABLE 2.5
Dry-blending conditions in high-speed mixers

A) Blends prepared in a Fielder Dry Blender

| | |
|---|---|
| Jacket temperature | 75°C |
| Blending speed | 3600 rpm |
| Blend discharge temperature | 120°C |
| Cooling speed | 150 rpm |
| Cooling time | 5 mins |
| Blender heating system | Steam |

B) Blends prepared in an Henschel Dry Blender

| | |
|---|---|
| Jacket temperature | 150°C |
| Blending speed | 2600 rpm |
| Blend discharge temperature | 120°C |
| Blender heating system | Oil |

### 2.3.2 Preparation of Extrudates

Each formulation was dry-blended in an 8 litre T K Fielder laboratory blender. Sufficient quantity of the homogeneous blend was passed through a twin screw extruder to produce strips. The Leistritz twin screw extruder was set at the standard extrusion conditions listed in Table 2.6. When an equilibrium condition was attained the powder blend was fed to the hopper and extruded through a 2 mm size die to form a strip. The strip was then passed through a sizing die placed 10 cm away from the extruder and through a vacuum water trough into a haul-off system. The length of the water trough is approximately 1.98m and allowed a complete solidification of the extrudate before the haul-off belt. When equilibrium condition was reached a flow of colour lines were displayed on one of the computer screens. Representative samples were taken at this point.

For the preparation of core samples, the machine was stopped and stripped down for an average of 10 minutes to obtain samples of the whole extruder profile. The design of the barrel allows for the screws to be retrieved only from the die end (i.e. unlike conventional barrels, this one cannot be opened). After turning all heating zones to 100°C the extruder was stopped, the die piece removed (there was no breaker plate and gauge) and a screw retrieval mechanism (see Figure 2.1) attached at the die end. Figures 2.2 and 2.3 show where the screws were pulled out with the mechanism, and where they were separated from the mechanism respectively. The sample was then carefully stripped from the twin screws. The entire process was timed to average 15 minutes from the time the extruder was stopped to when the sample was completely stripped from the screws.

But we also encountered some difficulties. The first thing we noticed was that if the screws were not withdrawn before a maximum time of 10 minutes, the unplasticised PVC degrades extensively to beyond the experimental interest. Secondly if the UPVC degrades and solidifies it becomes difficult to extract the screws and the PVC from the barrel with the screw retrieval mechanism. The reason is that the retrieval mechanism works by 'contact-gripping' of about 2 cm of the screw tip. Therefore if material is left within this 2 cm of the screw tip (due to difficulties in removal caused by either/both degradation or/and solidification) the gripping may not be strong enough to permit screw pulling. These problems were encountered on several occasions.

The material in each screw turn was numbered from the screw tips to the powder end and collected so that a complete profile of material from the feed to the die was retained for microscopy examination and physical property evaluations.

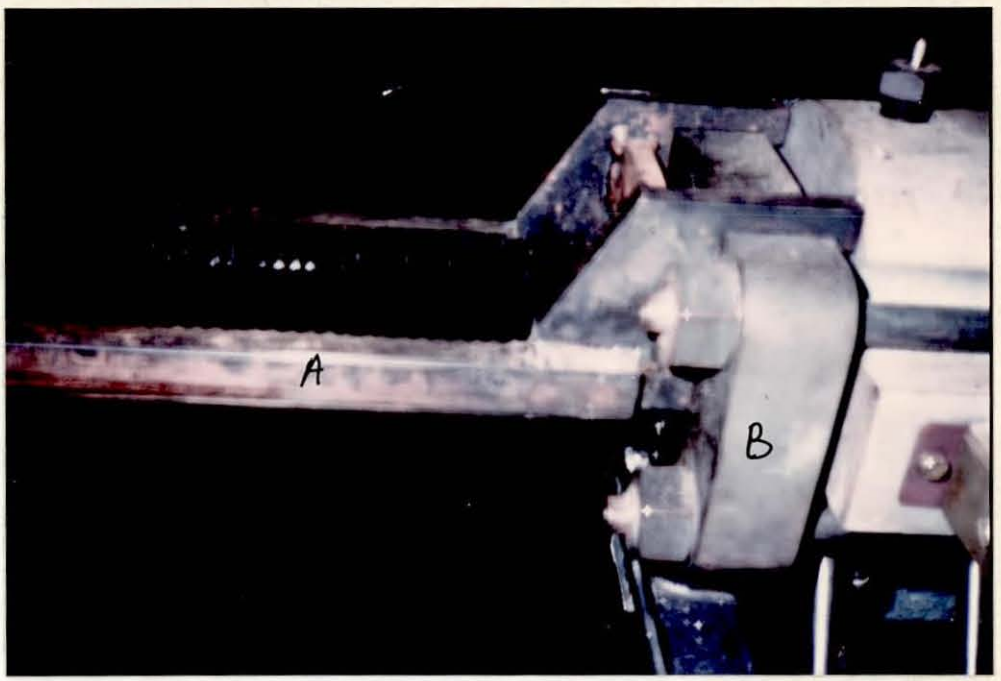


FIGURE 2.1: Photograph of screw extraction mechanism attached to end of extruder before extraction process. 'A' = extraction mechanism; 'B' = end-region of the twin screw extruder

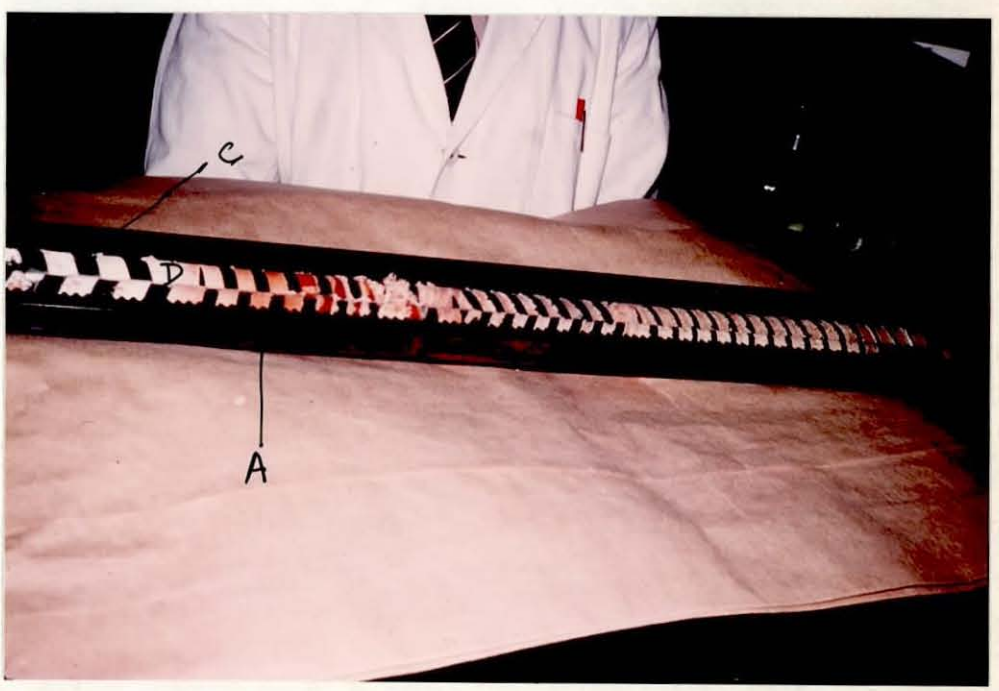


FIGURE 2.2: Photograph of screws and core sample between screw extraction mechanism after extraction process. 'A' = extraction mechanism; 'C' = extruder screws; 'D' = core sample

TABLE 2.7:

Zone control temperature variation of standard formulation extruded at various temperatures

| Zone control Temp. (°C) / Extrusion Temp (°C) | Extruder Zones | | | | | | |
|---|---|---|---|---|---|---|---|
| | 2 | 3 | 4 | 5 | 6 | 7 | 8* |
| 170 | 161 | 160 | 161 | 157 | 155 | 161 | 170 |
| 188 | 169 | 173 | 171 | 171 | 171 | 178 | 188 |
| 194 | 177 | 180 | 180 | 169 | 169 | 183 | 194 |
| 202 | 168 | 190 | 190 | 184 | 184 | 193 | 202 |
| 218 | 168 | 208 | 208 | 202 | 202 | 207 | 218 |
| 224 | 173 | 217 | 216 | 212 | 211 | 215 | 224 |

TABLE 2.8:

Zone control temperature variation of standard formulation extruded at various screw speeds

| Zone control temp (°C) / Screw speed (rpm) | Extruder Zones | | | | | | |
|---|---|---|---|---|---|---|---|
| | 2 | 3 | 4 | 5 | 6 | 7 | 8* |
| 20 | 177 | 180 | 180 | 169 | 169 | 183 | 194 |
| 25 | 177 | 181 | 180 | 170 | 170 | 183.5 | 194 |
| 30 | 173 | 180 | 180 | 170 | 170 | 183.5 | 194.5 |
| 40 | 172 | 180 | 180 | 170 | 170 | 183.5 | 195 |
| 50 | 167 | 180 | 180 | 169 | 170 | 184 | 194 |

* = Control die temperature representing the extrusion temperature

TABLE 2.6
Standard extrusion condition used

| Extruder zone | Zone Control Temperature ($^{o}C$) | Zone Control Pressure ($KN\ m^{-2}$) |
|---|---|---|
| 2 | 177 | 138 |
| 3 | 180 | 5138 |
| 4 | 180 | - |
| 5 | 169 | -55 |
| 6 | 169 | 7496 |
| 7 | 183 | 7614 |
| 8* | 194 | 9734 |

* Extrusion speed = 20 rpm; extrusion temperature = $194^{o}C$

### 2.3.3 Preparation of Compression Mouldings

The dry blends were compression moulded into rigid-PVC sheets of approximately 20 x 20 $cm^2$, with an average thickness of 0.3 cm, depending on the response of the formulation to processing temperature and pressure. The compression moulding machine used is a 40-ton manually operated platen with electric heating and water cooling systems.

The blends were moulded at the same processing conditions in a 3-plate mould. These processing conditions are listed in Table 2.9. After moulding, the samples were conditioned at a room temperature of $20^{o}C$ for 48 hours prior to further evaluations.

TABLE 2.9
Compression moulding conditions used.

| | |
|---|---|
| Moulding temperature | $190^{o}C$ |
| Moulding pressure | 35 kg $cm^{-2}$ |
| Induction time | 5 mins |
| Charge temperature | $190^{o}C$ |
| Discharge temperature | $50^{o}C$ |
| Quantity of charged powder | 230g |

# CHAPTER 3

# THE ESTABLISHMENT OF MICROSCOPICAL METHODS FOR CHARACTERIZING THE PROPERTIES OF UPVC POWDERS AND EXTRUDATES

## 3.1 Microscopical Methods Exploited

Light microscopy has been used as the principal method in evaluating the properties of the materials. From previous investigations on the morphology, structure and properties relationships in UPVC (see Section 1.7.1) it was thought prudent to exploit many microscopy methods. Tentative experiments were hence carried out with the following methods:

a) Polarised light
b) Common light
c) Differential interference contrast
d) Ultraviolet fluorescence light
e) Microradiography

Among these microscopical methods exploited differential interference contrast (DIC) and UV fluorescence light were found to be the most promising and, therefore, have been employed in evaluating the UPVC powder blends and processed materials. In a few cases, common light and electron microscopy methods have been used to substantiate the observations made with DIC and fluorescence methods.

The use of microradiography to study the distribution of stabilizers in processed materials, using X-rays in the 29-32 KV range, was largely unsuccessful. Its advantages over light microscopy include the fact that thicker microtomed/petrologically prepared sections can be examined (20-50 μm). The method relies on the absorption differential of X-rays in the specified range between stabilizer and polymer. When the sample is backed by the recording film and exposure is made, the contact negative will bear areas of varying optical density, as a result of the differences in absorption.

Very few particles were observed, mainly due to the size of the stabilizer particles being small. Since the resolution of this method is not as good as light microscopy in resolving small stabilizer particles the method was discarded.

The principles of DIC and fluorescence light microscopy methods will now be discussed. The fluorescence microscopy technique developed for studying the properties of the powder blends will also be described.

## 3.2 Differential Interference Contrast Microscopy[62,87,91,107,108]

The differential interference contrast (DIC) microscope is a two-beam qualitative instrument belonging to a shearing interference microscope using polarized light. It is not quantitative because there is no visible separation of the 'image beam' from the 'reference beam' as found with other interference microscopes. The shearing effect of the Savart crystal prisms provides an apparent 3-dimensional image of the object, and hence the technique is suitable for studying polymers – such as PVC powders.

The technique can be operated in either reflected or transmitted light mode. The latter mode of operation was used throughout this work. Basically, the working principle of the transmitted light differential interference contrast microscope, as illustrated in Figure 3.1 involves the passage of polarized light through the first Wollaston prism placed beneath the microscope condenser. Here the beam is sheared into two wavefronts (beam) before passing through the condenser and the specimen under investigation. (It is important to emphasise that the distance between the two beams is small compared with the resolution of the light microscope). The beams then pass through the objective and a second Wollaston prism (inverse of the first prism) where recombination takes place. Along the way through the analyser to the eye

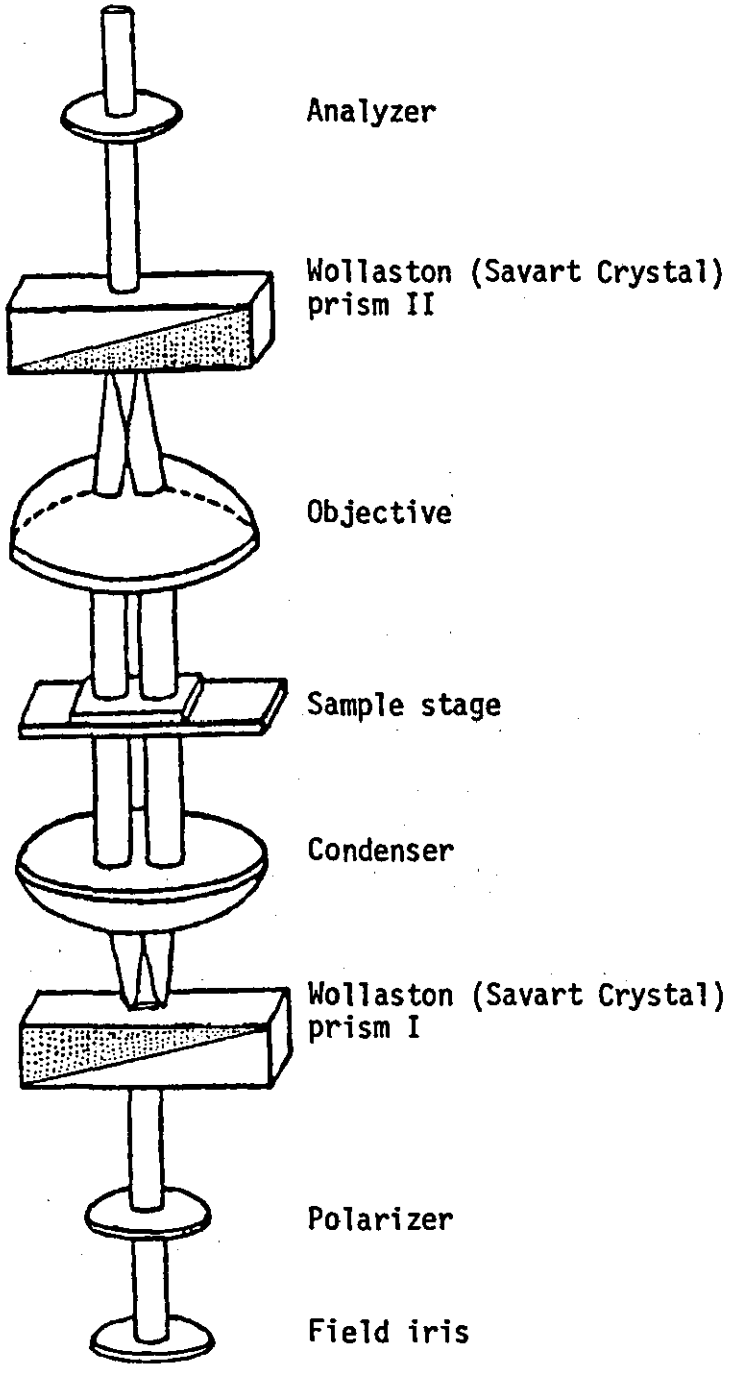


FIGURE 3.1: Diagram of a typical DIC microscopy set-up

piece (or screen) the beams interfere with each other to produce interference fringes depicting the specimen's image. By this means, contrast is gained without loss in resolution or optical section - ality. The theory and principles are well described in the manufacturers' manual[91].

Phase specimens which possess little contrast with ordinary bright-fields are more visible in the DIC. Both transmitted and reflected light DIC microscopy generally make use of the same interference principle, the major differences between them are as a result of different techniques in recombining the beams. The recombination of beams is by image formation in the reflected mode by an anlyser in polarized-light and by a Savart crystal prism in the DIC microscope. The advantages associated with using DIC are that:

1. the image is free from certain artefacts (the 'phase-contrast halo') and therefore a distinct relief effect and shallow depth of field are obtainable. This is entirely an artefact of the contrasting system which arises when the optical path is 'biased' by adjustment of the equipment so that the background colour is dark-grey.
2. the nature of the contrast can usually be altered to obtain the best conditions for the detail being studied; and
3. measurements of path difference can be made with precision.

Nevertheless, the DIC microscopy does not render phase-contrast obsolete. The latter is suitable for phase specimens with optical path differences of up to $\lambda/2$ retardation, while DIC is best with specimens of path difference between $\lambda/10$ and a full wavelength. Thus, it is intermediate between phase-contrast and conventional bright field.

## 3.3 Fluorescence Microscope

Fluorescence analysis is amongst the oldest and most established analytical techniques. It has been prevalent in biomedical researches for nearly a century[109-111], but little interest has been shown in the application of fluorescence microscopy to the study of polymers. This is because in the past microscopists have laid much emphasis on structural characterisation.

With the UV fluorescence microscope some polymers that fluoresce or which can be made to fluoresce can be observed while they are illuminating with light of the spectral region of their excitation spectra. The fluorescent properties of the polymers can then be analysed either qualitatively or quantitatively. Some of the analysis carried out in qualitative methods are:

i) The presence or absence of primary fluorescence
ii) The effect of fluorochromes on the object (presence or absence of secondary fluorescence)
iii) The true colour of fluorescence of the object
iv) The difference between the colour of fluorescence emitted by the fluorochrome and by the object through secondary fluorescence.
v) The approximate relative intensity of the light emitted by the object through fluorescence
vi) The approximate regions of excitation and emission spectra.

For quantitative methods the following analyses are mostly carried out:

i) The exact spectrophotometric curve of the excitation spectrum of the polymer
ii) The exact spectrophotometric curve of the emission spectrum of the polymer
iii) The fluorescence decay half life of the polymer.

The identification of polymers with any of the above information obtained with the fluorescence microscope is on the basis of their fluorescing characteristics, rather than revelation of minute structural details.

Fluorescence microscopes could be either transmitted or reflected light, and are very capable of housing many of the 'extras' available to common light microscopy as shown in Figure 1.6. By so doing variable techniques could be successfully administered. The most common (as used for this project) is the use of conventional microscopes, with little alteration for fluorescence work. Also fluorescence microscopy examination can be made in either bright or dark field for both the transmittance and reflectance modes. True phase-contrast observation is impossible and polarized light is rare except for some natural fibres (via difluorescence). These techniques have been widely discussed in literatures[112-114].

Fluorescence in reflectance mode has been widely employed for the investigation of opaque specimens, for example rocks, minerals and polymers. The major disadvantage is the presence of a beam splitter which reduces both exciting and fluorescent light. But these have now been modified to incorporate a dichromatic mirror which simultaneously functions partly as a combined exciter and barrier filter. Also the reflectance mode is preferred to the transmittance mode for studying transparent or translucent specimens, especially when a thickish specimen absorbs much of the exciting light as with the UV fluorescence. The effect of sample thickness on fluorescence intensity is shown in Figure 3.2. If transmitted light is employed on a thick specimen the only particles which fluoresce are those situated deep in the specimen, while particles on the surface fluoresce and can be more distinctly observed if reflected light is used.

FIGURE 3.2: Effect of specimen thickness on fluorescence intensity

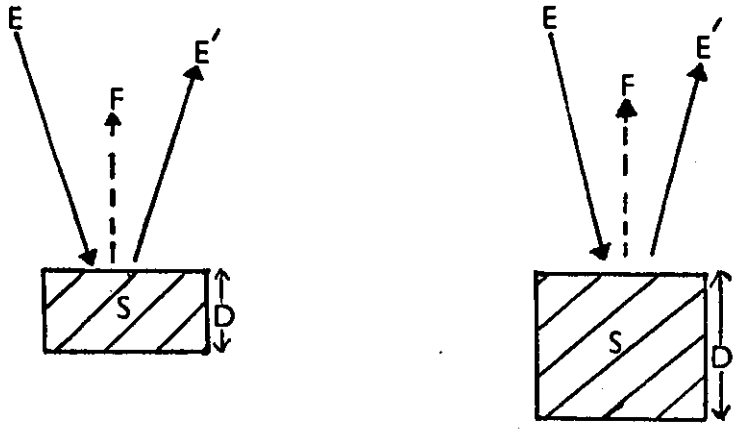


A) For incident-light fluorescence

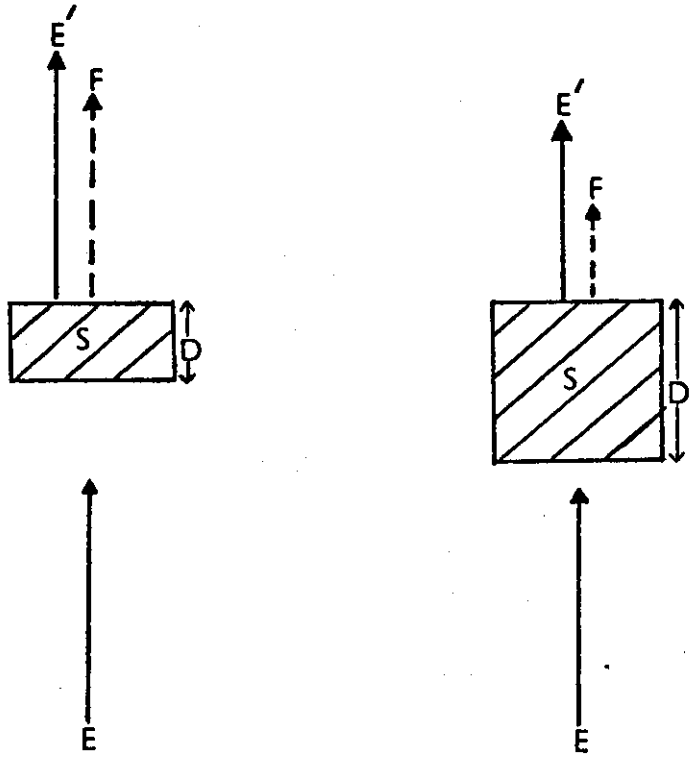


B) For transmitted-light fluorescence

E = exciting light; E' = exciting light transmitted or reflected;
F = fluorescence light; S = specimen; D = specimen thickness

### 3.3.1 Fluorescence Equipment[90,115]

The complete assemblies for fluorescence microscopy can be obtained from common-light microscope with 'extra' basic attachments such as high pressure mercury lamp, exciter filter, barrier filter and sometimes high NA objectives. The set-up of these attachments is shown in Figure 1.6.

For UV fluorescence light the high pressure mercury vapour lamps are most frequently used. They are found to radiate very strongly at about 365 nm and show reduced but strong and varying intensity at longer wavelength. In general, they are not suitable for the objects whose emission spectra occur in the longer wavelength region. Fluorescence outfits must at least contain one exciting filter and one barrier filter. To function satisfactorily, the exciter filtermust produce the same wavelength radiation of 365 nm as the light source. Its main purpose is to transmit all the excitation spectrum from the light source. To ensure that only the UV radiation is transmitted, in most cases additional filters such as 'heat' filters (which removes heat) and BG38 (which removes excess red-light) are used.

Barrier filters specific purpose is to absorb all ranges (scattered or residual) of excitation spectrum transmitted by the exciter filter. They are placed between the objective and primary image plane. If the barrier filter fails by the use of a wrong filter or otherwise, to filter out the UV light there is a risk of damage to the eye and photomicrographs will show a fogged instead of a black background (or mostly blue with colour film). Different microscope manufacturers have different types of filters. Some examples of exciter filters are UG1 and UG5 and barrier filters are K430, K530 and K490.

For this study, the fluorescence equipment consists of a Zeiss Universal microscope fitted with a UV lamp, Zeiss III RS fluorescence attachment and a Plan-Neufluor X16/0.50 objective, and used in the incident light mode.

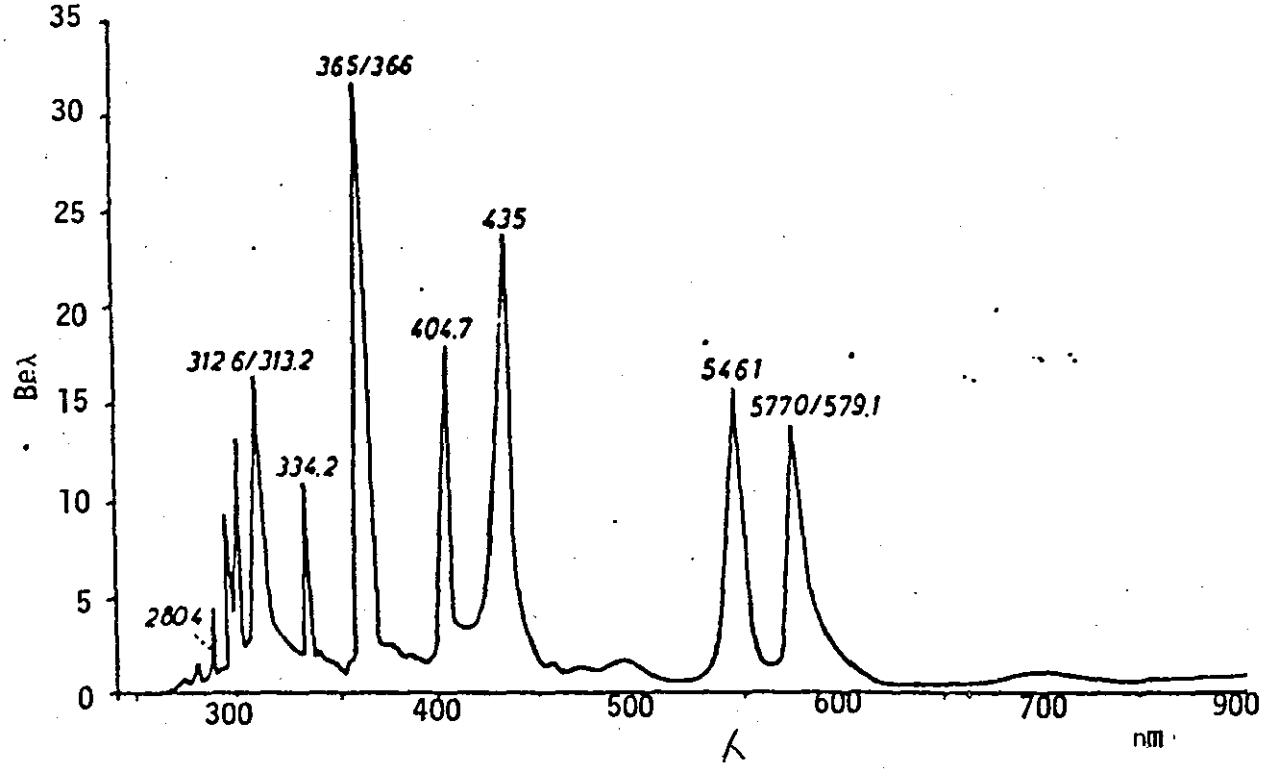


FIGURE 3.3: Emission spectrum of a typical mercury lamp(90)

The UV light source employed was a 50 watt HBO high pressure mercury vapour lamp. A monochromator placed between the lamp and the specimen illumination optics aids the emission wavelength from this lamp to irradiate closer to the 365 nm excitation wavelength. The adapted[90] emission peaks of a high pressure mercury lamp showing a strong emission peak at 365 nm wavelength is shown in Figure 3.3. The presence of high intensity after 300 nm shows that the mercury lamp is ideal for fluorescence microscopy of a specimen whose excitation spectra is in the longer wavelength. The filters used were the Standard G365 exciter filter and LP420 barrier filter. The transmission curves for these filters are shown in Figure 3.4.

Figure 3.4 reveals that the exciter filter G365 has maximum transmission also at 365 nm. Since the best suited filters are those with maximum transmission at 365 nm, therefore the G365 filter is an ideal exciter filter. The barrier filter (LP420) is inexpensive and absorbs wavelength shorter than 420 nm. Both filtration systems were housed in the Zeiss III RS fluorescence attachment.

The objectives used were Plan-Neofluor X16/0.50 and Neofluor X6.3/0.20. The former was used for much of the work but where greater depth of field is needed the lower numerical aperture objectives X6.3 (0.20 NA) and X10 (0.20 NA) were used.

### 3.3.2 Theory of Fluorescence Light Microscopy

With increasing requirements for the detailed examination of many substances, fluorescence microscopy is becoming one of the widely employed methods in fundamental studies and in the research of routine procedures. The theory underlying this method is based on the electronic and structural states of the substances. By successfully illuminating the substance, detailed analysis can be obtained from its fluorescence nature.

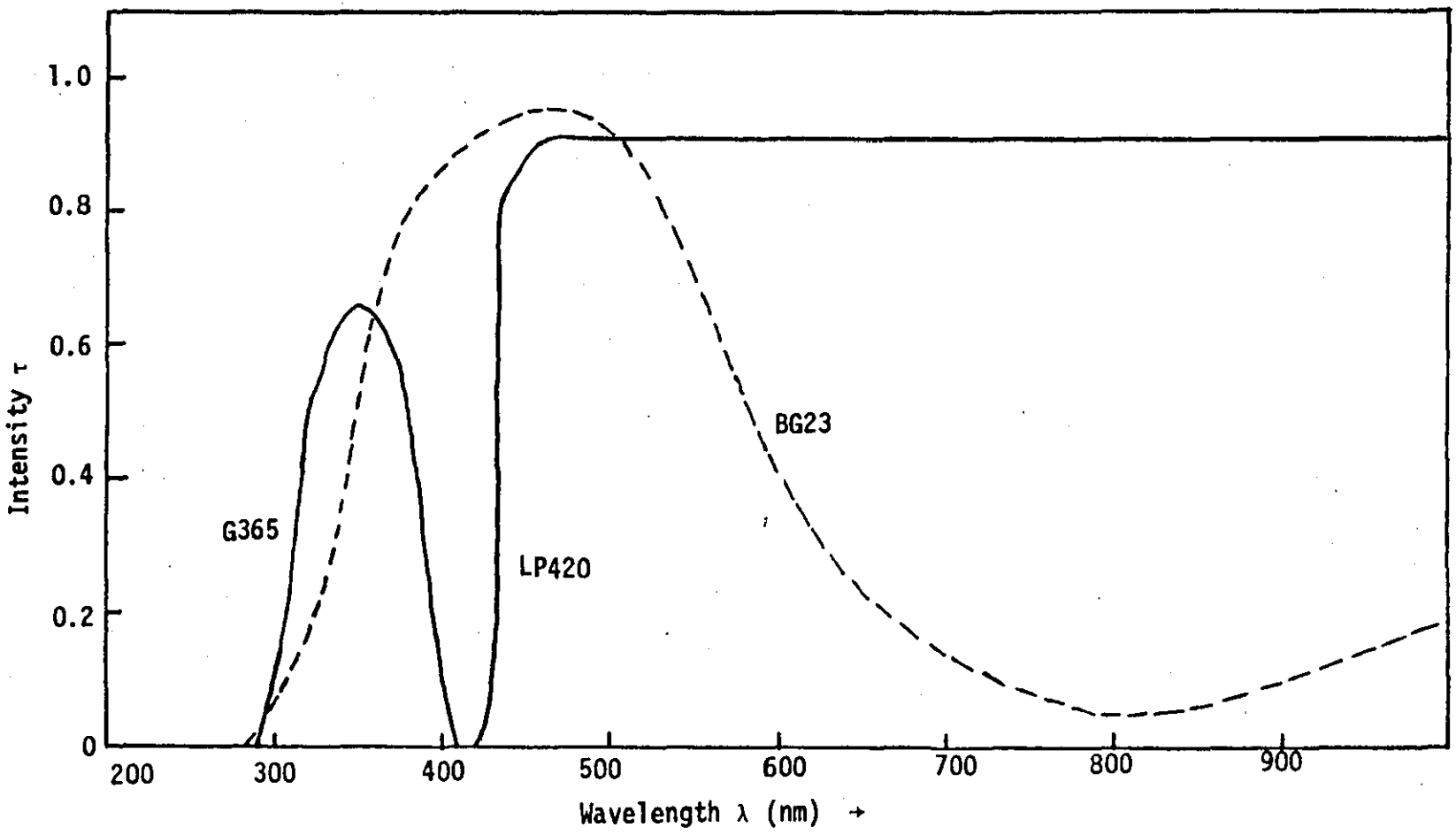


FIGURE 3.4: Transmission curves for the UV fluorescence filters.
G365 = exciting filter; LP420 = barrier filter; BG23 = red-absorbing filter

Considering the electronic state of a substance, when a compound is irradiated with short wavelengths the absorption of this energy results in the transposition of electrons from the ground state to higher energy states. Depending on the nature of the molecule, each energy state may contain several vibrational energy levels increasing in energy ($V_0 - V_\infty$). When the electrons eventually return to the vibrational level of the ground state from the lowest vibrational level of the excited state, the energy released may be dissipated in one of several ways. It may be emitted as light of longer wavelength. The emission of this light of longer wavelength ~~than that observed~~ is called fluorescence when it is in the visible region. Photodecomposition may also take place before the electron reaches the lowest vibrational level of the first excited state. Thus the transition from the unstable excited states to the stable ground state may occur by a number of routes other than fluorescence emission as represented on the Jablonski diagram in Figure 3.5. The electronic state of molecules falls into two categories: singlet and triplet states. Singlet state is an excited state in which the electron spin is conserved resulting in a total spin of zero. But if the spin of the excited electron is no longer opposed to that of the odd electron left in the previous orbital the total spin is unity, and that excited state is called triplet state. Fluorescence occurs only between the singlet states, usually from the lowest vibrational level of the first excited electronic state. The time interval between the acts of excitation and emission is short, of the order of $10^{-9}$ - $10^{-6}$ secs. Thus fluorescence occurs only while the object is illuminated.

The structure of molecules is also important in carrying out fluorescence studies. The molecules that have chromophores and hence can absorb ultraviolet light may have the potential to exhibit fluorescence. In order to effectively utilise fluorescence microscopes for quantitative and/or qualitative works it is necessary to know the basic effects of structure on the emission process.

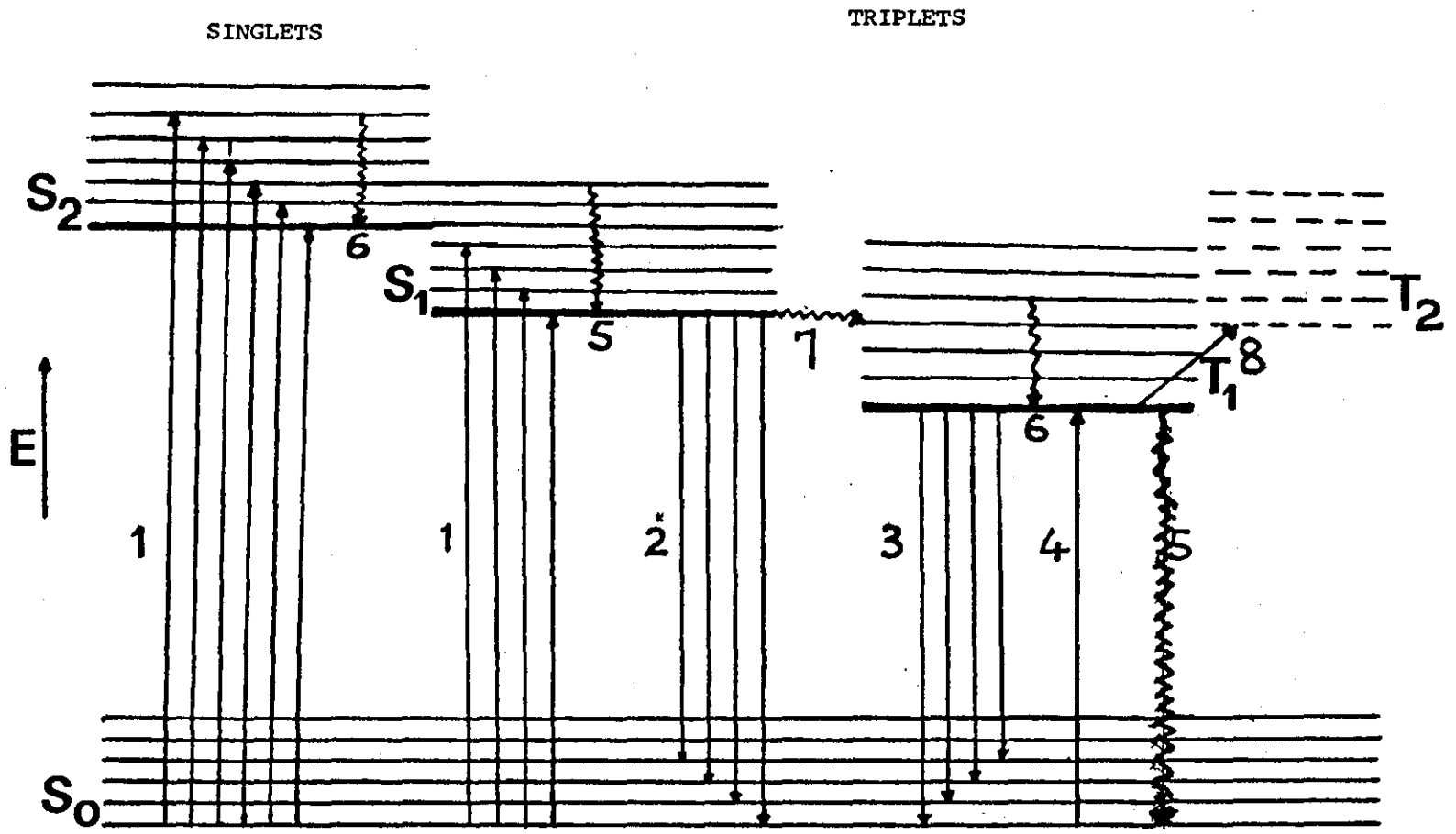


FIGURE 3.5: Diagramatic representation of molecular energy levels and transitions. $S_o$, ground state; $S_1$, first excited state; $S_2$; second excited state; $T_1$; first triplet state; $T_2$, second triplet state; 1, absorption; 2, fluorescence; 3, phosphorescence, 4, singlet → triplet states absorption (forbidden); 5, internal conversion; 6, vibrational relaxation; 7, intersystem crossing; 8, triplet → transition.

It may then become possible to convert a non-fluorescent material into a fluorescent species in most cases. Objects that do not possess the inherent property of fluorescence can be made to fluoresce by inducing certain fluorescent stains into the structures. The term 'secondary' fluorescence is used to describe this type produced by fluorochromes. But where fluorescence is an inherent property of the object the term 'primary' fluorescence is employed.

The increase in degree of conjugation often increases the intensity of fluorescence[116,117]. This is because fluorescence is observed mainly when electrons are promoted from $\pi$-bonding orbitals to the $\pi^*$-antibonding orbitals, and both orbital types are present only in unsaturated compounds. In addition to the requirements of a conjugated system of double bonds, certain geometrical considerations are also important. Thus planarity of the conjugated system is also essential for maximum fluorescence. This is well portrayed by the evidence that unsubstituted aromatic compounds exhibit a more intense fluorescence in the UV or visible region than the linear polyene compounds. When the planarity of a system is destroyed through steric hindrance, the free mobility of the $\pi$-electron will be partially inhibited resulting in a loss of fluorescence. The nature of substituted group plays an important role in the nature and extent of a molecule's fluorescence[118,119]. Groups that generally increase fluorescence are OH; $OCH_3$; $NH_2$; $NCH_3$ and $N(CH_3)_2$ while those that tend to diminish fluorescence include groups like CHO; $^{+}NH_3$; $NHCOCH_3$; COOH, halides and a host of others[120,121]. The latter are electron withdrawing groups, while the former are electron donating groups. In comparison saturated hydrocarbons such as PVC which contains $\sigma$-bonding orbitals and chlorine molecules, exhibition of fluorescence light is very remote. However $\pi$-bonding orbitals can be introduced by degrading the polymer to introduce short chain conjugated systems. Since this involves the elumination of hydrogen chloride, the chlorine molecules which diminish fluorescence are removed, and

through this way PVC can be made to fluoresce.

Therefore with proper utilization of fluorescence microscopy, assessment of PVC powder characteristics, topography of processed material, distribution of certain additives, level of degradation etc, which are related to the processing and thermal history of the polymer could be evaluated.

### 3.3.3. Proposed New Technique

It has been explained, in a previous section, that material will only fluoresce if it has a $\pi$-orbital system or contains a fluorochrome. For saturated organic polymers such as PVC it will be difficult and uneconomical to induce into the structure any fluorescing die. However, since the polymer is thermally unstable, fluorescence can be introduced by slight degradation to introduce short chain conjugated double-bond systems. This is the basis for the proposed new technique.

The advantages that were thought should accrue from this technique are as follows:

i) A sieved portion of the polymer resin can be slightly degraded, and returned to a blending batch. Since this portion fluoresces, after blending in the normal manner, morphological changes (agglomeration/breakdown of grains), as a result of blending conditions can be studied effectively.

ii) The degree of stabilizer distribution (as the relative thermal protection given to the polymer blend while heated) due to blending conditions can be readily determined. The effect of additives on degree of stabilizer distribution can also be determined readily.

The innovations of this proposed new technique are that:

i) With a Universal light microscopy equipment already available, the UV fluorescence attachment and optics used are inexpensive. The barrier filter and exciter (Section 4.2) used are inexpensive and quite efficient. For this particular work on powder blend, any objective of low numerical aperture (0.2 NA) and high magnification (X10) can be used.

ii) Sample preparation is quick, cheap and simple.

iii) Overall set-up is uncomplicated and hence minimum dependence on operator skill.

While it is possible to purchase dry blend in ready-mixed form from a number of suppliers, this method - fluorescence analysis - will prove useful to both producers and users on checking the 'quality' of their dry blends.

3.3.3.1 Description of the technique

In fluorescence analysis a 'reference' graph is made, from which the relative fluorescence intensity of the samples under study can be readily obtained. To produce a 'reference' graph, the PVC powder was blended without additive in the normal manner. Specimens were then prepared at different temperatures (from 150$^{o}$C to 210$^{o}$C) by heating approximately 1g of the resin in an oven for 5, 10 and 15 minutes. The fluorescence intensities of these heat treated resin grains were measured as described in Section4.1.2., and plotted against temperatures for different heating times. It is evident from the 'reference' graph (Figure 3.6) that the maximum fluorescence intensity occurs at 190$^{o}$C for 10 minutes heating time. Figure 3.6 is the plot of average of six readings tabulated in Appendix 1.

The powder blends under investigation were then heat-treated in the same manner at 190$^{o}$C for 10 minutes. Their fluorescence intensities were measured in % relative to the maximum point in the 'reference' graph.

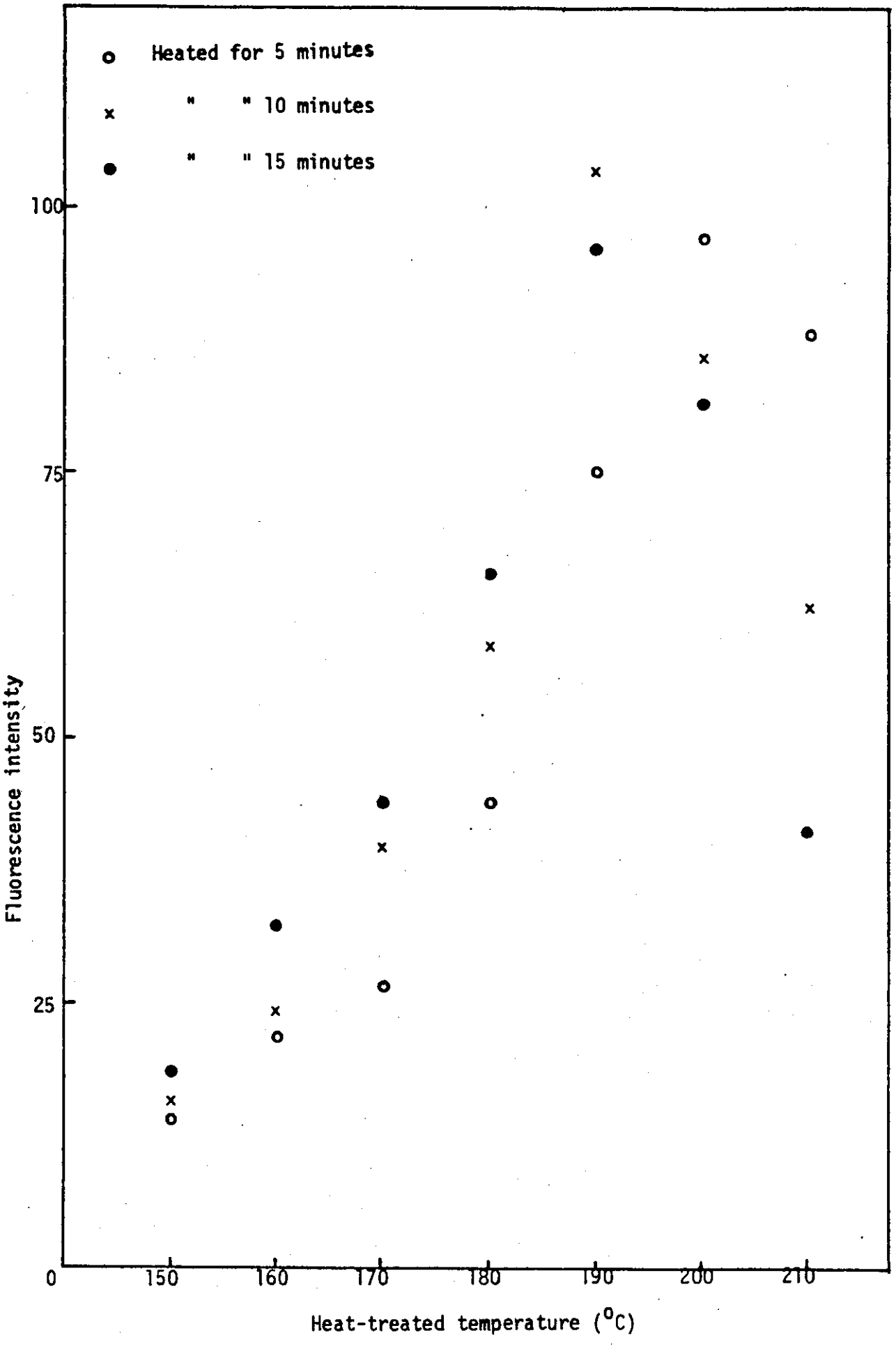


FIGURE 3.6:Fluorescence intensity of powder resin of different thermal treatments. 'Reference chart'.

Since the accuracy of fluorescence analysis chiefly depends on the amount of heat-treatment given to the powder specimens, the possible sources of error are as described below.

If the blends are less-heated weak fluorescence intensity is observed when they are viewed under a UV fluorescence microscope. High-speed blends most times contain grains of such fluorescence intensity, and in the analysis of particle size of the heated grains will introduce high discrepancies in the results. Conversely, PVC loses fluorecence intensity when it is overheated. This has been explained as the result of a shift in the absorption bands after a sequence length of about ten conjugated double bonds of varying length. This sequence length absorbs in the UV region and in the visible spectrum from 365 to about 450 nm. As the sequence length increases, due to further heat treatment, the absorption bands move to longer wavelengths. This leads to a change in the wavelength of the emitting radiation beyond 450 nm. This phenomenon occurs mainly at high degradation (from about 0.5% of the conjugated double bonds), and has been used (in some cases) to determine the extent of degradation in PVC.

The maximum fluorescence intensity observed in the 'reference' chart is in good agreement with the observations made by Gerrard et al[122] and De Coste[123]. Although the colour of the powder grains changed from white to reddish brown by heating at 190$^{o}$C for 10 minutes, the amounts of conjugated double bonds introduced into the polymer are less than 0.1%[122,123]. Figure 3.7 shows that when PVC is heated at 190$^{o}$C for 50 minutes only about 0.15% loss of HCl occurred.

The intense fluorescence observed at low levels of conjugated polyene sequence (e.g. when heated at 190$^{o}$C for 10 minutes) has been observed to be due to the result of resonance enhancement[124]. Preparing the specimens under the conditions described in this section, therefore, does not significantly affect their properties.

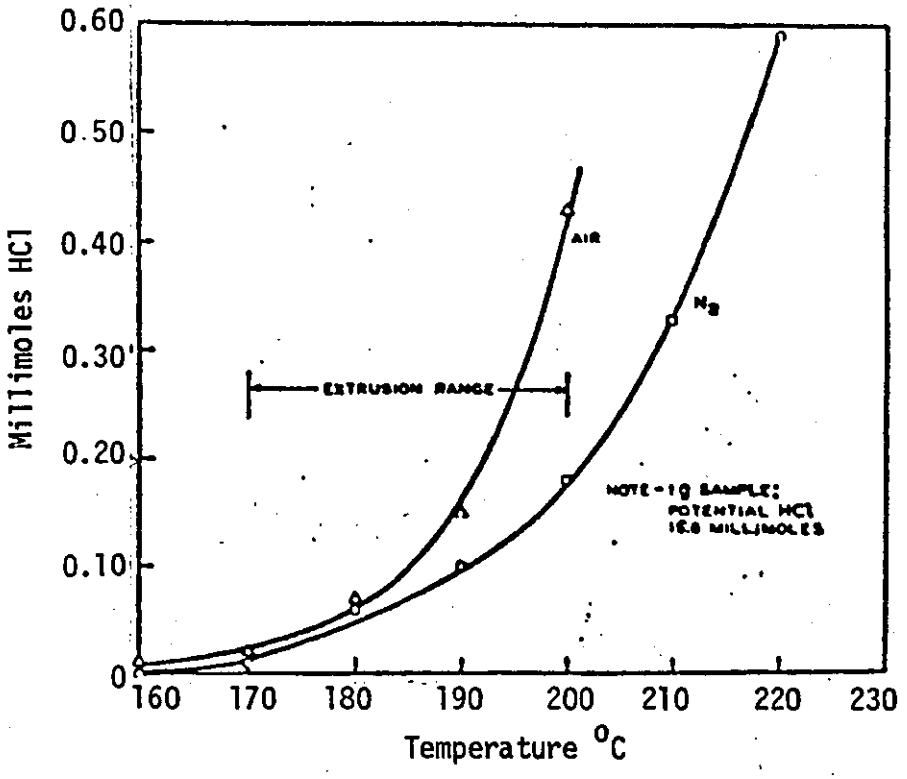


FIGURE 3.7: Thermal degradation of PVC resin in air and nitrogen[123]

In some quantitative fluorescence methods a different analysis which involves the measurement of fluorescence decay half-life of the polymer is usually carried out. The polymer is exposed to fluorescent light for several minutes while an attached chart recorder monitors the simultaneous decrease in fluorescence intensity with time. A typical example of this curve is shown in Figure 3.8 for samples heat-treated at two different temperatures. The fluorescence intensity decreases rapidly at first, before reaching a near-constant value.

This method was considered unsuitable for this work since the relative fluorescence intensity of the blends can be readily measured from the 'reference' graph.

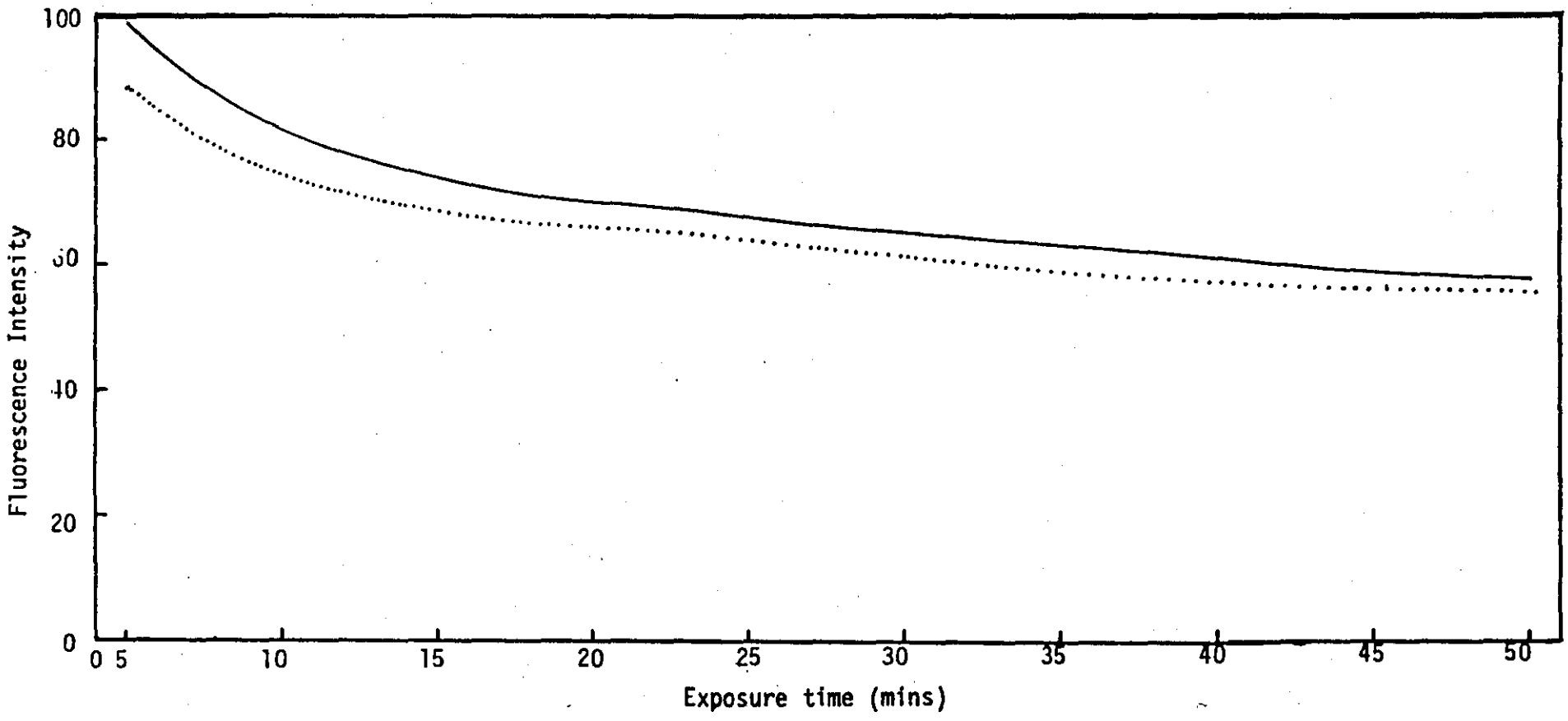


FIGURE 3.8:Relationship between fluorescence intensity and exposure time for blends heated for 10 minutes.
(-) 190°C heated temperature; (.....) 200°C heated temperature.

# CHAPTER 4

# EXPERIMENTAL METHODS

For convenience, the experimental techniques will be described under two distinct sections, viz Section 4.1 and Section 4.2. The first (Section 4.1) will describe exclusively all the experiments on powder blending studies. The second section (Section 4.2) will concentrate on the experiments carried out on subsequent processed materials.

## Section 4.1 POWDER BLENDING STUDIES:

### 4.1.1 Distribution of additives

#### 4.1.1.1 Differential interference contrast (DIC) microscopy

To study the distribution of additive, dry-blends prepared in the T K Fielder and Henschel laboratory mixers (Section 2.3 ) were examined with a differential interference contrast (DIC) microscope. Generally in microscopy discrepancy in results - quantitative or otherwise - is virtually inevitable mainly due to the analysis of insufficient sample size of the entire bulk. By using sampling techniques to obtain a representative specimen of the entire material, error in results has been kept to a minimum in this powder blending study.

The cone and quartering sampling technique was used in accordance with ASTM D1898-68. It consists of heaping the powder blend into a cone and then dividing into four parts. One part was then combined with the opposite part and the process repeated until a final 30-50g was left from which random samples were taken to study the properties of the powder blends.

For DIC microscopy, a representative sample was immersed in tricresyl phosphate immersion liquid and heated for 5 minutes at 98$^{o}$C. This is to eliminate or reduce the number of interstitial

voids present in the grains which scatter the incident light during microscopy. Observations were made and photomicrographs obtained in the transmitted light mode.

4.1.1.2 Fluorescence analysis

With a UV fluorescence microscope, the distribution of additive was measured in the form of relative fluorescence intensity on heat-treated grains. In this experiment it was found convenient to examine the powder blends 'dry' by carefully distributing the grains on a microscope slide.

A representative sample of each blend was heated for 10 minutes at 190°C in an oven. Prior to the start of the experiment, the oven was switched on and left for an hour to attain thermal equilibrium. The powder samples (approximately 3g), contained in an opened specimen bottle, were quickly placed in the oven. After 10 minutes the samples were removed from the oven and allowed to cool to room temperature. To avoid or minimize the errors that might be introduced through sample preparation the following precautions were taken:

1. To maintain a minimum drop in the oven temperature the specimen bottles were first placed in a hard non-heat conducting material which was quickly placed in the oven. The period taken in opening and closing the oven was timed to be 15 seconds.
2. All samples for close comparison - for instance samples of different blending speeds - were heat-treated in a single batch.

To measure the extent of stabilizer protection, the fluorescence intensity of these heated blends were measured relative to unstabilized blend with a Leitz MPU compact microscope photometer. Since the operating techniques of this instrument are well described in the manufacturer's manual[126], only the experimental

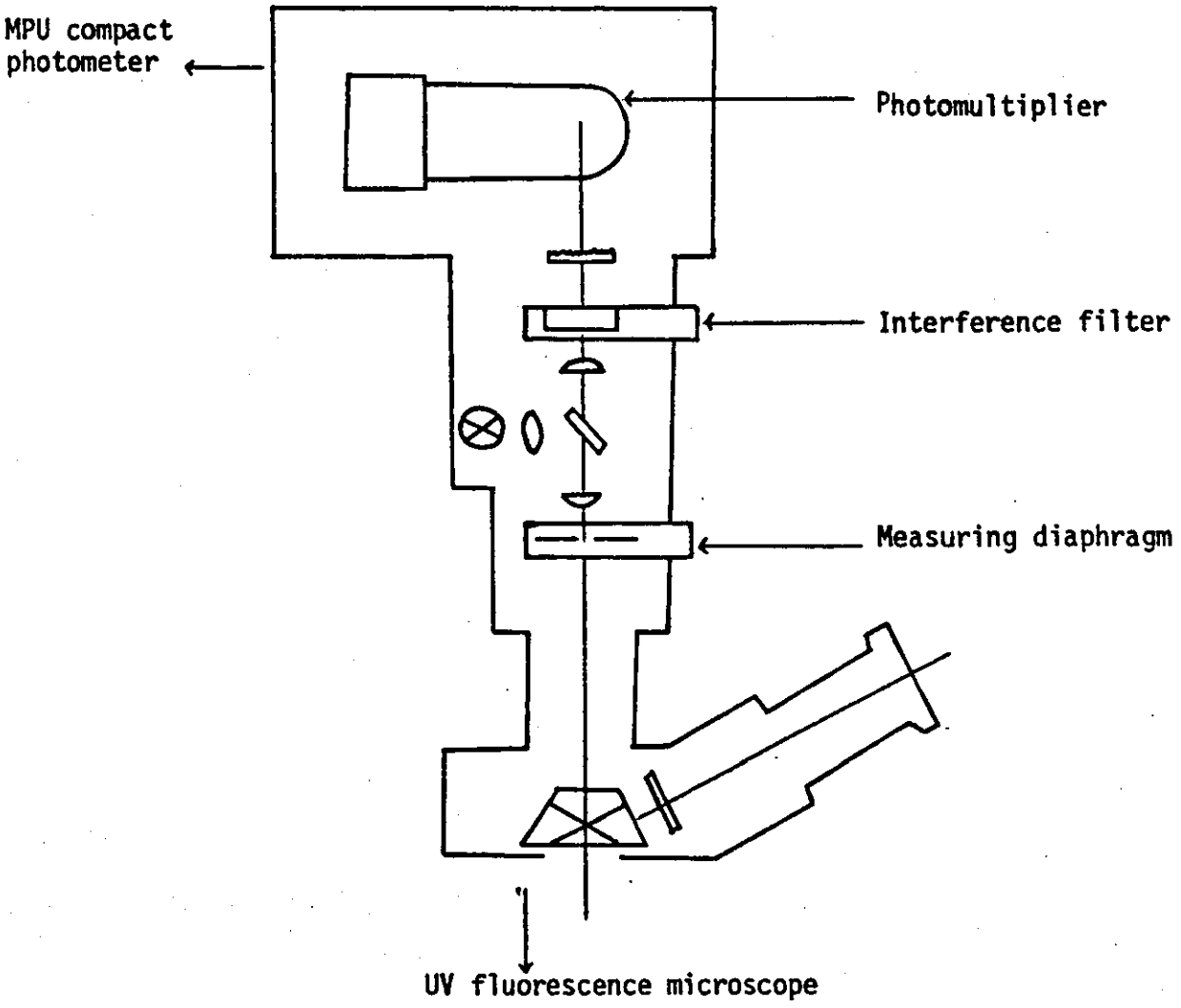


FIGURE 4.1: Diagram of the photometer attachment (beam)

procedure will be described here. The following operating parameters were used:

| | |
|---|---|
| Measured-value integration | (nX) continuous measurement and display |
| Sensitivity | X10 |
| Type of measuring diaphragm | Square diaphragm (type 620.532) |
| Type of filter | Green (broad band) |
| Voltage | 795V |

The photometer attachment which houses a photomultiplier, square diaphragm and green interference filter (see Figure 4.1) is mounted on the UV fluorescence microscope, and the grains are then brought to focus. By manually adjusting the lever of the square measuring diaphragm, a square of size nearly to the size of the measuring grains is chosen and, to be maintained throughout the experiment. This is because different square-sizes were found to given different intensity values.

When a fluorescing grain is brought under the measuring square (which is illuminated with an ordinary light housed on the photomultiplier) a recording button on the compact photometer is immediately pressed - to minimize the effect of fluorescence decay. The measured-value of relative fluorescence intensity is displayed on the built-in digital voltmeter. Six measurements were made for each specimen and their average determined. The obtained results were interpreted and related to the distribution of stabilizer during blending.

### 4.1.2 Morphological Changes

#### 4.1.2.1 Fluorescence studies

Previous work[48,53,128] have shown that changes occur in morphology (particle size distribution) as a function of dry blending conditions but it is unclear whether there is a simultaneous breakdown and agglomeration between grains. To investigate the behaviour of the T K Fielder laboratory mixer on

morphology of the powder blends experiments were performed in which a small portion of PVC powder, heated at 190°C for 10 minutes and incorporated into the untreated powder grains, was examined with the UV fluorescence microscope after dry blending.

Prior to blending, approximately 10% of a desired range of size fraction was sieved out and heated at 190°C for 10 minutes in an oven, and returned to the batch. After premixing thoroughly the heated and unheated resin additives were then incorporated and a dry blend prepared in the normal manner. Two sets of size fractions in the ranges of <75 μm and from 150 μm to 212 μm were treated in this manner. Four blends of different blending speeds were prepared for each set of size fraction.

For UV fluorescence microscopy observation a representative sample of approximately 50g (see sampling technique Section 4.1.1.1) was taken from each blend and sieved to obtain several size fractions ranging from <75 μm to >250 μm. Five of these fractions, including the size fraction of the original heated grains were examined and photomicrographs obtained for morphological analysis.

#### 4.1.2.2 Powder densities

In a given sample of powder it is obvious that the density will depend upon the treatment the powder has received. Bulk and apparent densities of PVC powder blends have been reported by several workers[129-132], to be affected significantly by blending parameters. In extrusion changes in densities of PVC markedly affect the outputs and batch sizes[49,131] so that for efficient control of a process consistency in batches density is required.

In the present study bulk and apparent densities were measured by the usual methods.

*Bulk Density:* Bulk density was carried out in accordance with BSS 2782, Part 5, Method 501A, 1970. A preweighed standard cup of 80 $cm^3$ was filled from a funnel containing about 100g of PVC powder blend and coaxially placed 10 cm above it. Using the edge of a cardboard sheet the powder in the cup was gently levelled off and the cup reweighed. The bulk density was calculated from the values of the powder weight and effective volume of the cup.

*Apparent Density:* Apparent density was determined by BSS 1460, 1967 method for determination of the apparent density of dry-powders. While this method was originally developed for precipitated calcium carbonate it has been successfully accepted for powders generally. Apparent density depends on the closeness of the packing of the particles of which the powders is composed. Hence it is affected by the size and shape of the particles, and depends on the true density of the material.

In this study, 100g of powder was transferred to a tall glass cylinder. The cylinder was then placed in a tap-pack volumeter and dropped for 30 minutes (to obtain a constant volume) at the rate of one drop per 2 seconds. The apparent density was obtained from the weight of the unit volume after a specified compression.

#### 4.1.2.3 Flow rate of powder blends

To measure the flow rate, 25g of powder blend was allowed to flow freely through the funnel and time in seconds was recorded. The flow rate was measured using a narrow-throat funnel but the same procedure as described for the bulk density.

#### 4.1.2.4 Particle size analysis

Blending parameters and formulation variables are reflected in the powder properties such as densities, powder flow and particle size and size distribution. The latter has not only been

used to determine the effect of various amounts of additives in blends but also useful for determining the batch-to-batch uniformity of resin[129,132]. During processing, large resin particles would require more processing to break them down and the time to achieve this would depend on bulk density of the powder. In direct powder processing, more often than not, particle size is a controlling factor. It is, therefore, desirable in any event for the resin to have particle size distribution containing medium-sized particles with some fines to fill the interstices between the larger particles.

It was thought descrete that analysis of particle size distribution of the blends and heat-treated grains is of paramount importance in understanding the distribution of additive and the effect of blending conditions on powder grains respectively. The simplest method and most widely used on a routine basis is by sieve analysis using a stack of standard sieves in the range of 45 μm to 300 μm BS mesh sizes. However, other methods have also been employed. The efficiency and choice of technique depends to a large extent on the shape and size of particles to be analysed. Normal lower limits for various methods of particle size analysis may be broadly classified as follows:

| | Method of Analysis | Lower Limit (μm) |
|---|---|---|
| 1. | Sieves | 50 |
| 2. | Elutriation | 10 |
| 3. | Relative motion between particles and fluid: | |
| | a) Sedimentation; gravitational | 2<br>1<br>(with control temp.) |
| | b) Centrifugal | 0.1 |
| 4. | Microscopical measurements: | |
| | a) Visible light (optical method) | 0.2 |
| | b) Ultraviolet light in air | 0.1 |
| | c) Electron microscope (scanning) | 0.01 |
| | d) Transmission electron microscope (TEM) | 0.005 |

A more detailed classification and choice of methods of particle size analysis can be found in references 133-137.

In the present work the particle sizes were analysed by optical method. The results obtained are dependent to some extent on the physical principles used and assumptions or conventions involved - for instance it was assumed that the shapes of the particles are spherical and that they have the same density. The unique feature of optical methods is that particles are measured individually instead of being grouped statistically by some process of classification. The optical method involves using a Zeiss TG 23 particle size analyser[138]. This equipment has been modified to include an Apple micro-computer system which records data from each channel and produces an immediate graphical display allowing a minimization of the number of particles counted.

To use this instrument, photographs at a total magnification of X100 were prepared from a representative sample of the blend concerned. The photomicrograph was positioned on a Plexiglass plate and the particle to be evaluated was positioned over the centre of a circular beam of light. By adjusting the iris diaphragm the diameter of the light beam is altered to equal that of the particle. If a particle deviates from the circular shape, the circular light spot must be so adjusted that the total area of protruding portions of the crystal becomes equal to that of the re-entrant areas. A foot switch is then depressed which actuates the correlated channel and simultaneously gives a DC voltage output which is proportional to the spot size. This allows particle sizes to be logged automatically, and with the aid of the computer programme developed within the department, subsequent calculation and immediate graphical display were produced. At least 1800 particles were analysed for each specimen.

### 4.1.3 Fusion Characteristics

By using the Brabender Plasticorder the fusion characteristics of the blends from Fielder and Henschel laboratory mixers were assessed. Many workers[54,139,140] have employed this technique to show the relative fusion or gelation characteristics of both plasticised and unplasticised PVC. A detailed description of operating techniques can be found in the published literatures[139,140], the experimental conditions however are given below.

To assess the fusion time of the 14 different formulations (see Tables 2.3 and 2.4), after dry blending, the following operating parameters were employed:

| | |
|---|---|
| Jackettemperature | 190$^{o}$C |
| Rotor speed | 50 rpm |
| Sample volume | 57 cm$^{3}$ |

The oil heated mixing chamber was allowed for an hour to attain an equilibrium temperature before starting the first measurement. In subsequent measurements on the day, 15 minutes interval, was found suitable. Accurately measured samples were rapidly charged into the chute and a load cell of 4 kg placed over the chargingpiston to aid in pressing down the sample as the twin screws rotated at selected speed of 50 rpm.
Figure 4.2 shows a typical plastogram for the evaluation of unplasticised PVC dry blend at a fixed temperature and speed.

A torque curve developed for several minutes reaching an initial torque peak C and sharply falling to a near perfect plateau D for the rest of the mixing period. The fusion time was obtained as the time between charging the sample and relative fusion temperature C.

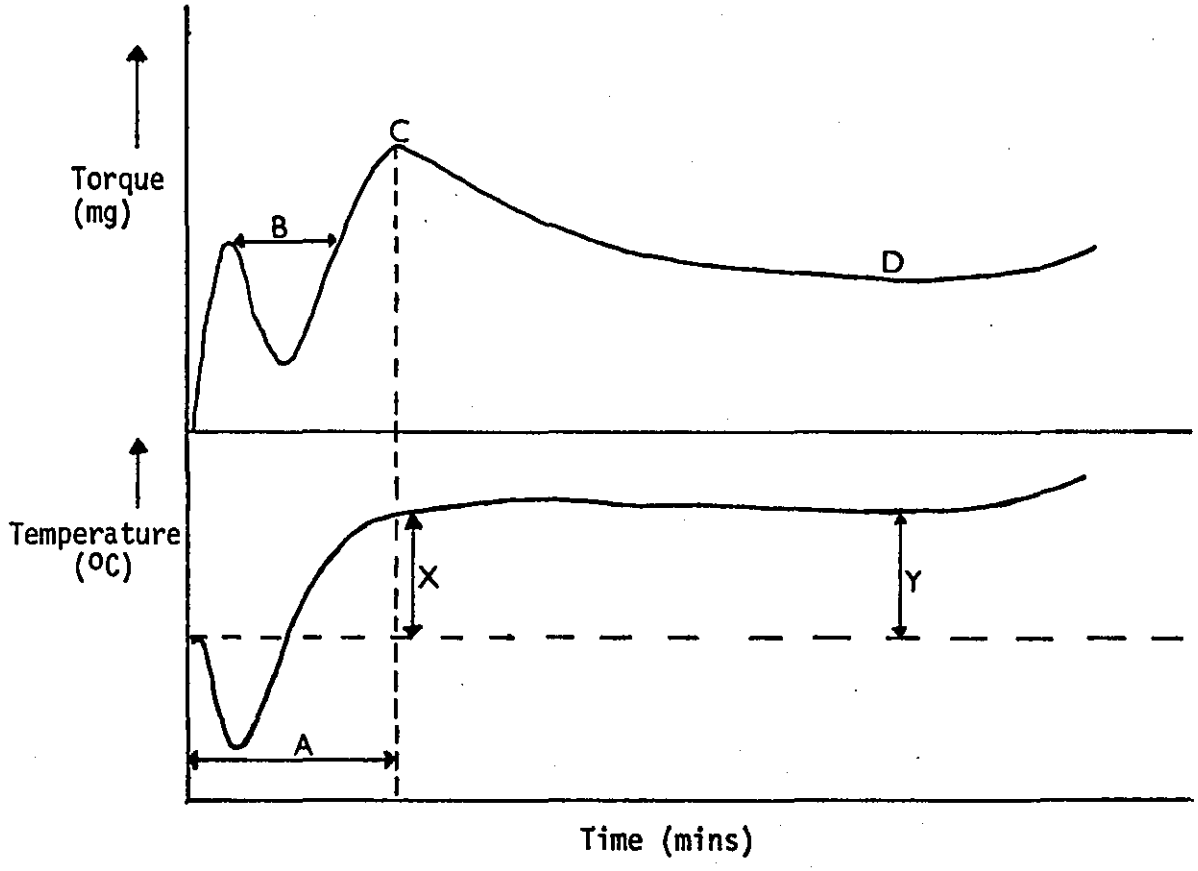


FIGURE 4.2: Typical plastogram of an unplasticised PVC blend

A = fusion time
B = fusion range
C = fusion peak
D = equilibrium torque
X = fusion temperature difference
Y = equilibrium temperature difference

### 4.1.4 Cast-film Technique[106,172]

The cast-film technique was used in an attempt to determine the possible thermal protection that could be given to a PVC grain by a single stabilizer particle, assuming that the stabilizer particles were homogeneously distributed during blending. To do this, sufficient amounts of PVC resin, to make up to 30%

concentrated solution, was dissolved in tetrahydrofuran (THF). A few of the largest sized particles of dibasic lead stearate (~ 75 μm diameter - obtained by standard sieve method) were then added to this solution. After distributing the stabilizer particles by mixing vigorously with a glass stirrer, the solution was cast on a dust-free standard glass slide to obtain very thin films - with the stabilizer particles randomly distributed on the PVC film surfaces. The films were left for three days to ensure complete evaporation of all traces of THF.

The cast-films were then heated at 190°C in an oven at various heating times. The results of the observation made with UV fluorescence microscope and photomicrographs obtained are illustrated in the discussion chapters.

## Section 4.2: PROCESSED MATERIALS - EXTRUDATES AND COMPRESSION MOULDING

### 4.2.1 Microscopical Studies

A number of sample preparation techniques for microscopical studies, such as fracture, sectioning, polishing, etching and replicating have been applied in attempts to study the internal structure of processed polyvinylchloride. In actual fact, none have proved to be completely satisfactory, although each has proved useful for a particular area of interest. For instance, sectioning has been used successfully to study the fusion of primary particles whereas grain fusion is best studied by examining fractured surfaces. To study the morphological changes, as a result of processing the dry blends by extrusion and compression moulding, the following sample preparation techniques have been used viz polishing, sectioning and fracture.

Other techniques such as replication and chemical etching, also exploited, were largely unsuccessful in the elucidation of the features within this project.

#### 4.2.1.1 Petrological technique

This technique was originally developed for geological materials but has been successfully employed, with minor variations, on a variety of materials, ranging from resins to metals. The availability of automatic polishing machines means that many materials can now be polished in substantially less time, and to a superior finish.

In this experiment, samples of about 0.3 mm thick with highly polished surfaces were obtained. Each polished specimen was obtained by grinding a representative sample on Nos 300 through to 500 abrasive paper. After finishing on the No 500 grit paper, the specimen was ground on a Selvyt SR polishing cloth with 1μ alumina powder for about one hour. This step removes the scratches left by papers, and this was checked with the stereomicroscope in the reflectance mode. Polishing was completed using ¼μ metadi diamond paste and polished for a further one hour.

When a highly polished surface was obtained the sample was trimmed to a thickness of about 2 mm, and the polished surface glued onto a standard glass slide using Canada Balsam. The reverse surface was in turn ground on Nos 300 through to 500 abrasive paper to obtain a thin section. This surface was polished in the usual manner to obtain a specimen suitable for optical examination in the transmittance mode.

#### 4.2.1.2 Brittle-fracture technique

To prepare the specimens for scanning electron microscopy (SEM) examination, samples were embrittled in liquid nitrogen (temperature -195.8°C) and fractured while brittle. The extruded strips were cut into test bars (approximately 62 x 14 x 4 mm), notched and each wrapped in aluminium foil. These were then cooled to about -195.8°C for 4 hours while immersed in the liquid nitrogen contained in a Dewar flask. After removal from the liquid

nitrogen, the aluminium wrapper was partially slipped off and the bars (gripped in the jaws of a bench-clamp) were fractured, in the vicinity of the notch, with a hammer. The aluminium foil prevented contamination and retained the fragments, most of which would have been lost when the sample shattered. The fractured samples were placed in a desiccator, to dry and attain room temperature.

For SEM examination of the fractured surfaces, desired sections were cut from the samples leaving an excess of about 4 mm in order to keep from disturbing the fracture surface. These sections to be examined were then attached to aluminium stubs with Agar silver-paint glue. This was followed by coating the sample in a sputter coater SP240. A gold-palladium alloy was used and a coating of approximately 200$^{o}$A (20 nm) in thickness was applied. The actual observation and micrographs were obtained with a Cambridge Stereoscan S4-10 scanning electron microscope which had a magnification factor of from 20X to X100K.

4.2.1.3 Microtomy

Microtomy is a specialised technique for preparing thin sections of specimen for light and electron microscopy. It is a basic technique in biological studies. Thin sections (less than 40 μm) are cut readily from the sample, which, if soft or to simplify handling, is often embedded in a block of polymer. When applied to the study of the structure of polymers, which are on the 0.02 μm to 130 μm average scale for PVC, difficulties are encountered. This is in part because of the surface deformation produced by the microtome knife, and in addition, the low degree of structural differentiation in a polymer results in low contrast. These difficulties can be overcome substantially by using a knife of high quality blade - that is, blade free from marks.

Microtome is used mainly for preparing thin sections of thickness from 1 to 40 μm. The sample is moved against the fixed

knife (which could be a glass, diamond or steel knife) and automatically raised through the required micrometer value before each cutting action. When thin sections of less than 1 μm thickness are required, an Ultratome is employed. This instrument has been designed to advance the sample very slowly, usually by thermal expansion of the metallic holder. Both equipments have been used in this experiment to prepare sections for light and electron microscopy respectively.

For light microscopical examination of the processed material, thin sections of 10 μm thickness were cut using a Leitz 1400 microtome with a 'D' profile blade. These sections were mounted between a glass slide and cover slip using a non-fluorescing immersion oil as the mountant. The specimens (80 nm thickness) for transmission electron microscopy examination were obtained using Ultratome (LKB Bromma 880) with a freshly made glass-knife. These sections were collected on copper discs (3.05 mm size) and examined with the Jeol JEN-100CX model electron microscope. Results of the observation made and micrographs obtained are illustrated in the discussion chapters.

### 4.2.2 Impact Strength Measurement

Impact strength measurements were obtained with the Advanced Ceast Fractoscope impact tester, using Izod notched method. The equipment is designed to give not only the trace of force levels as a function of time but also the normal maximum energy values that cause sample failure. It was calibrated (before the experiment) to give a direct reading of the impact energy in joules as the pendulum struck a sample.

The specimens for the impact strength measurements were prepared by machining to remove the surface layers, and then ground on No 400 abrasive paper to 'smooth' the edges. Six test pieces were prepared for each formulation and notched. The dimensions of the specimens are as given below:

| | | |
|---|---|---|
| Length | = | 62 ± 0.25 mm |
| Width | = | 12 ± 0.2 mm (unnotched) |
| Thickness | = | 3.5 ± 0.25 mm |
| Depth of notch | = | 2 mm |
| Notch angle | = | $30^{o}$ |

The tests were made in accordance with BSS 2782, test method 306A, part 3 (1970). (Specimen thickness was about 2.9 mm short of the BSS minimum thickness due to the die size used, but this does not affect the overall result). The impact strength is calculated from the values of the impact energy and effective specimen area.

### 4.2.3 Molecular Orientation Measurements

To study the orientation introduced with the sample during the extrusion process two conventional methods were employed: shrinkage measurement and birefringence measurement by optical techniques. The results obtained from preliminary birefringence test were too negligible to be of any significance to the project objectives. This is presumably an indication of the molecular orientation introduced in this particular 'profile' extrusion being small.

#### 4.2.3.1 Shrinkage measurement

For shrinkage measurement the extruded strip was cut to obtain a sample of approximately 50 mm in length (see Section 4.2.2 for dimensions of the sample), and the experiment was performed in accordance with BSS 2782, test method 106E. Both ends of the sample were carefully ground on No 400 abrasive paper to obtain 'smooth' and flat surfaces. The dimensions of the sample were accurately measured with a Vernier caliper and the sample conditioned in an oven at $130^{o}C$. After 30 minutes it was removed and conditioned in a room temperature of $21^{o}C$ for 12 hours. The final dimensions of the sample were measured and the changes in dimension

calculated. Percentage shrinkage was calculated from the equation:

$$\% \text{ shrinkage} = \frac{L_0 - L_1}{L_0} \times 100$$

where $L_0$ = original length
and $L_1$ = final length.

### 4.2.4 Surface Skin Thickness Measurement

Depending on the conditions of processing and type of process, a specimen can exhibit surface skin texture quite different from that of the 'core' region. This 'skin' formation can be due to either orientation or perfect structural arrangement or both. In injection moulded PVC, skin formation is a common phenomenon - being that the hot melt solidifies in a much lower temperature mould. The skin has been reported to be due to orientation, and found to be highly birefringent which on subsequent heating exhibits considerable shrinkage[146,147]. In extrusion, however, the surface skin will largely depend on temperature differential between the extruded melt and its cooling environment. This means, in effect, that molecular orientation will be relatively lower, as well as the birefringence.

In this study, the extruded strips were found to exhibit two different, but not clearly distinctive, structural features (a finely structured 'skin' and a coarse 'core' region) when they were examined with common light microscopy. This surface skin was found to vary with processing parameters and additive types, and appeared to arise as a result of difference in morphological features than molecular orientation. To elucidate the development of this skin with respect to processing parameters, the polarising microscopy technique was employed - a method which has been used by several workers for surface skin measurement in processed/highly oriented polymer[149,150].

The polarising microscope usually consists of an ordinary compound light microscope to which is fitted a polariser (below the condenser unit), an analyser (above the objective), a rotatable stage and strain-free optical elements - (see Figure 1.6). The polariser and analyser (mostly made with inexpensive 'polaroid' sheet) transmit light vibrating in one plane only. When the polariser and analyser are arranged so that their vibration directions are at right-angles to each other, no light can be transmitted by the microscope. This arrangement is known as crossed-polar, and was used in this study.

For a specimen having at least two principal refractive indices there will exist some directions in the specimen along which the polarised light may travel without its plane of polarisation being modified - this direction is known as the optic axes. Polymers, in general, are anisotropic - that is, can be described in terms of 2 or 3 principal refractive indices - $n_x$, $n_y$ (and $n_z$) in the optic axes x, y (and z). (Interested readers can refer to refs. 151,153 for a comprehensive account on this - as it is outside the scope of this thesis). The difference between such indices is known as the birefringence of the material.

When a birefringent specimen is viewed between crossed-polars the polarised light splits into two beams relative to the optic axes, and thus the specimen appears luminous (bright or if $\frac{1}{4}\lambda$ plate is used - different colours) By rotating the specimen stage through $45^0$ angle some areas will show maximum brightness than others. The reasons for these phenomena are well discussed in refs. 151-153, but in its simplest form this is because the beams from the specimen are vibrating in different axes from those of the crossed-polar. In other words, in anisotropic specimens the velocity of light and its state of polarisation is dependent upon the direction of the light entering the material relative to the optic axes x, y (and z). By these methods, regions of different structural features can be readily observed.

In this experiment, very thin sections (5 μm thickness) of the extrudates were obtained along the direction of extrusion, and mounted in a tricresyl phosphate immersion oil. These were then viewed under crossed polars (that is between polariser and analyser), and on rotating the sample stage to $45^0$ position a maximum brightness of the sample skin was obtained - while light in the 'core' region was extinct. From the photomicrographs obtained the 'surface skin' thickness was calculated using the equation below:

$$\text{Skin thickness} = \frac{W_T - W_C}{2 \times \text{Mag}}$$

where $W_T$ = total width of the sample

$W_C$ = width of sample 'core'

and Mag = magnification of the photomicrographs

### 4.2.5 Solvent Absorption Test

Acetone absorption test was used to evaluate the physical properties of the extrudate. Representative samples cut from the extrudates were skinned and the edges and sides smoothed to avoid any side effects as a result of crazes and scratches. The samples of constant dimensions (20 x 12 x 3.5 mm) for extrudates, or constant weight (2g) for extruder 'core' samples were accurately weighed. These were placed in sample bottles of 50 $cm^3$ volume (to allow enough room for swelling phenomenon). About 25 $cm^3$ of acetone AR-type was added into the sample bottles and covered. After two hours interval, the sample was removed from the acetone, rapidly dried with filter paper and reweighed. The percentage acetone absorption was calculated from the equation:

$$\% \text{ acetone absorption} = \frac{W_2 - W_1}{W_1} \times 100$$

where $W_1$ = weight of sample
and $W_2$ = weight of sample + acetone

### 4.2.6 Differential Scanning Calorimetric Technique

Thermal Analysis has become a widely employed technique for characterising the thermal history of polymers. Several workers[141-144,148] have used DSC for measuring phase transitions (such as glass transition temperature (Tg), degree of cure, temperature and heat of fusion) in polymers. The Du Pont DSC cell makes use of a constantan disc as the primary means of heat transfer to both sample and reference positions. Temperatures at the raised sample and reference platforms are monitored by chromel-constantan thermocouples formed by the junction of the constantan disc with a chromel wire at each platform position. The difference signal between these two thermocouple junctions is fed to the amplifier in the 990 cell base module and then monitored on the Y-axis of the recorder. Sample temperature is recorded using a chromel-alumel thermocouple below the sample and recorded on the X-axis.

Since a small sample size (~10-15 mg) is normally used and the size of the container is small (maximum dimensions about 1 x 6 mm diameter), it has been tacitly assumed that the sample temperature is uniform,

and equal to that of its aluminium container.

In this work, Du Pont model 910 differential scanning calorimeter with 990 temperature programmer and recorder were used to measure the heat of fusion of processed PVC. The operating conditions as calibrated for standard measurement were used. These parameters are as follows:

| | |
|---|---|
| Sample weight | 15.5 mg |
| Starting temperature | $25^{o}C$ |
| Limit temperature | $240^{o}C$ |
| Sensitivity | 2 mV $cm^{-1}$ |
| Programme rate | $20^{o}C$ $min^{-1}$ |

From the thermograms obtained the areas of endothermic curves were measured. These raw data were then used to calculate the heat of fusion from the equation given below:

$$\Delta H_f = \frac{A}{m} (60\ B.\varepsilon.\ \Delta_{qs})\ Jg^{-1}$$

where A = area of endothermic curve ($cm^2$)
m = mass of sample (g)
B = programme rate (in this case = 0.5 min/cm)
$\Delta_{qs}$ = sensitivity
and $\varepsilon$ = a constant whose value depends on the ~~specification of the~~ DSC cell used (in this case was found/ calculated to be 0.257).

The derivatives of B, $\Delta_{qs}$ and $\varepsilon$ are well described in the manufacturer's manual[145].

# CHAPTER 5

# POWDER BLENDING STUDIES

## 5.0 Results and Discussion

The results obtained from experiments carried out on powder blends will be discussed under the following headings: distribution of additives in dry blends; effect of blending parameters on morphological changes; effect of concentration of stabilizer on nature of distribution and morphological changes, and; effect of formulation variables on additive distribution and morphology of blend.

## 5.1 Distribution of Additives in Dry Blends

### 5.1.1 Nature of Solid Additives Distribution on PVC Grains

The powder blends obtained under normal blending conditions were examined with the transmitted light differential interference contrast (DIC) microscope. It was observed that the solid additives were deposited on the surface of the grains. Typical examples are shown in Figure 5.1 (a, b, c and d) which are respectively DIC micrographs of polymer with no additives, blend with 0.4 phr calcium stearate, 2.5 phr dibasic lead stearate (DBLS) and 2.5 phr tribasic lead sulphate (TBLS). Blends with no additives (Figure 5.1a) showed the PVC grains to have poor contrast in the liquid of near matching refractive index. To understand whether the poor contrast was peculiar with suspension type polymer it was compared to PVC-mass grains prepared under similar conditions. It was found that the surface appearance of both grain-types was similar, and therefore 'skin-effect' of suspension-PVC grains is not visible or responsible for the observed topography of the grain. By the incorporation of 0.4 phr calcium stearate, a lubricant, contrast was significantly improved (Figure 5.1b). The lubricant is clearly seen on the surface of the grains, although only in isolated areas

FIGURE 5.1: Distribution of individual additive as a function of dry blending.

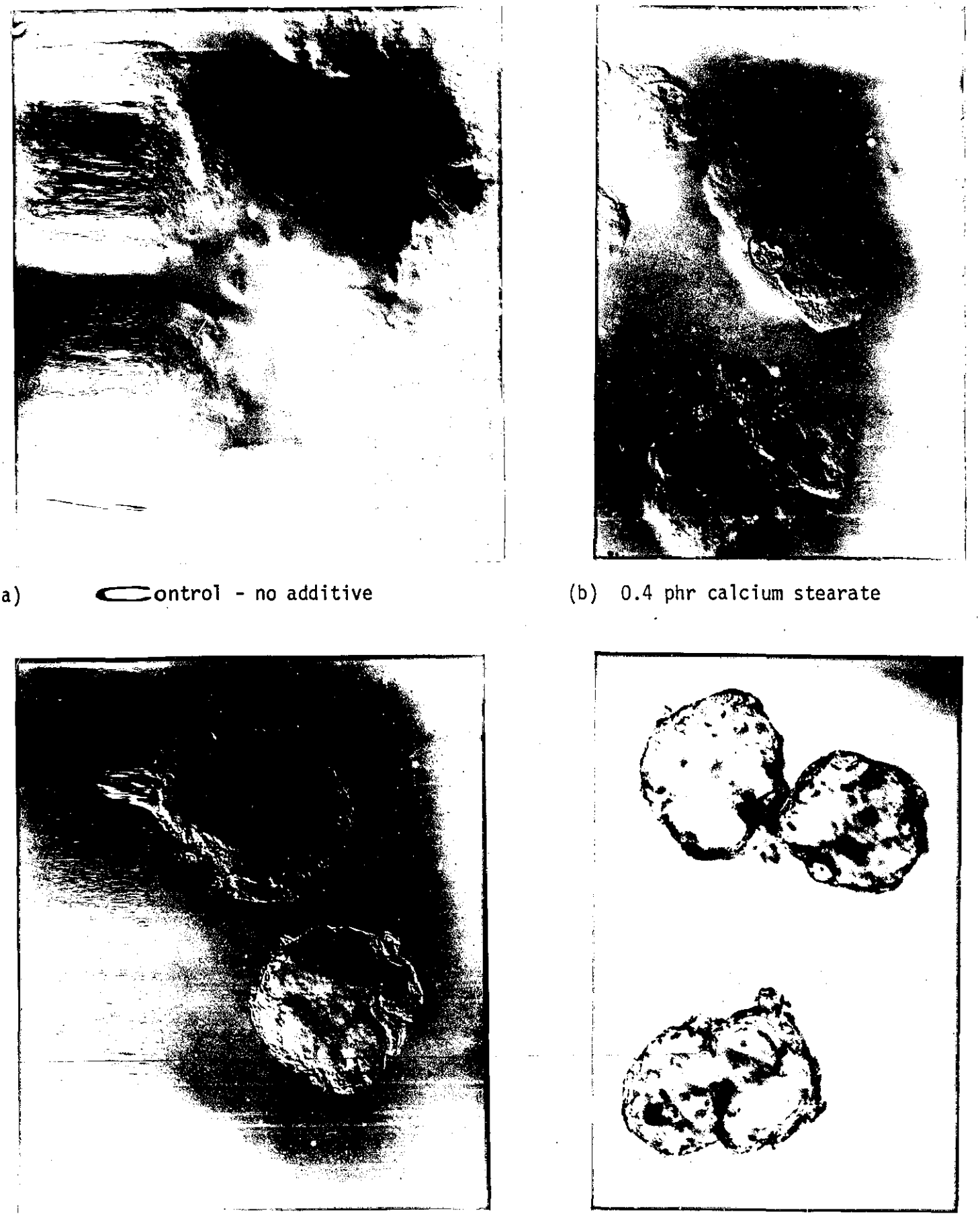


(a) Control - no additive

(b) 0.4 phr calcium stearate

(c) .5 phr DBLS

(d) 2.5 phr TBLS

(e.g. the circled region in Figure 5.1b). This is partly due to the quantity of calcium stearate in the formulation being small (i.e. 0.4 parts per hundred of resin), and partly due to the fact that the lubricant melts near the blend discharge temperature.

In Figure 5.1c, the grains contour is clearly more visible by the incorporation of 2.5 phr dibasic lead stearate stabilizer. The stabilizer is distributed on the surface of the grains, almost completely coating the entire surface of each grain. This could be attributed to the fact that the quantity of DBLS incorporated into the formulation was much larger than that of calcium stearate and, moreover, it does not melt anywhere near the blend discharge temperature. Although the grain surface appears to be completely coated, the stabiliser is not uniformly distributed due to the grains topography (see Section 5.1.2). A few areas are still devoid of stabilizer, but they are extremely negligible (Figure 5.1c) when compared to the blend containing calcium stearate (Figure 5.1b). In general terms, there is no evidence of the solid additives being absorbed into the resin grains.

These observations have also been reported by Gale[49], Hemsley et al[48] and Allsopp[50] using either different sample preparation techniques or microscopy methods on other solid additives. Hemsley et al[48] have studied the precise location, dispersion, distribution and function of tribasic lead sulphate and calcium stearate in powder blends of mass and suspension types polymer. By examining the thin sections of grains embedded in Araldite with light and electron microscopes, they observed that solid additives are usually well distributed and located on PVC grain surfaces. The same pattern of solid additives distribution have been reported by Allsopp[50] on examining microtomed sections of suspension grains embedded in epoxy with differential interference contrast microscopy method. With the common light method also he observed that the solid additive (tribasic lead sulphate)

appeared as black 'specks' on the grain surface.

In all cases, they reported that additives distribution is strongly influenced by grain topography. This fact is evident in Figure 5.1d where more TBLS particles are seen to accumulate in the re-entrant areas of the surface of PVC grains. Tribasic lead sulphate was used to illustrate this fact because its blend shows a higher refractive index contrast compared with dibasic lead stearate blend.

From this section, it is apparent that solid additive - in this case stabiliser - deposits on the surface of PVC grains during high-speed blending.

### 5.1.2 Effect of Particle Size and Shape on Additive Distribution

In order to study more systematically the distribution of additives as a function of particle size and topographical features, representative samples of blends of different blending speeds were each sieved into several size fractions. A typical example is shown in Figure 5.2 (a, b and c) - the DIC micrographs of three different size fractions, (a) $<45\ \mu m$; (b) retained in 106 μm sieve; and (c) $>250\ \mu m$, of blend produced at 3600 rpm. Observations show that for each blending speed, there is no difference in additives distribution among grains of different sizes. Additives appear to coat the grains 'uniformly' whether large, small or medium size grains. But the effect of particle topography is clearly evident. The uniformity of the distribution is largely a function of the grain topography with much of the additives located in the re-entrant regions of the grain (Figure 5.2c).

The effect of grain shape/topography on additives distribution also strongly depends on the polymer type. With mass-polymer the accumulation of 'excess' additive in the 'valleys' on the

FIGURE 5.2: Effect of grain size and shape on additives distribution

(a)

Size fractions <45 µm

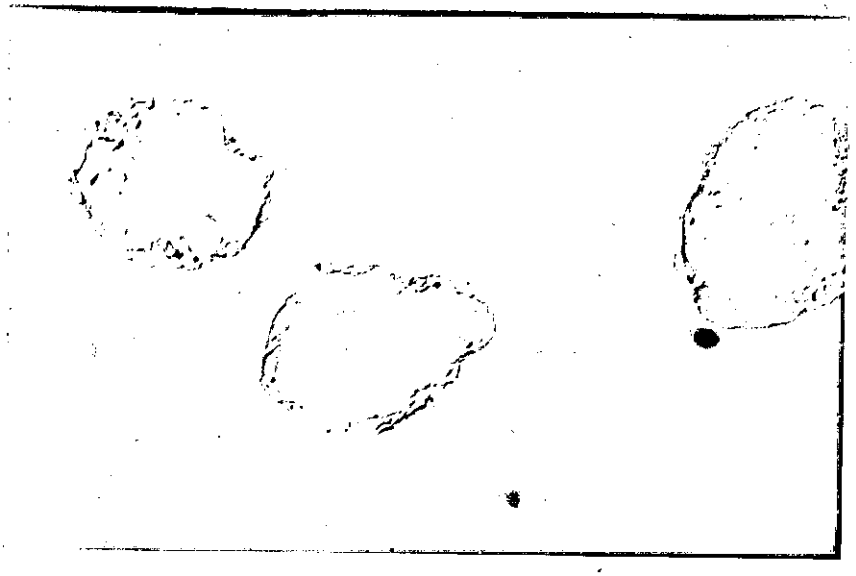

(b)

Size fractions retained in 106 sieve

(c)

Size fraction >250 µm

100µm

FIGURE 5.3: DIC micrographs of PVC powder blends

(a) Mass-PVC powder blend

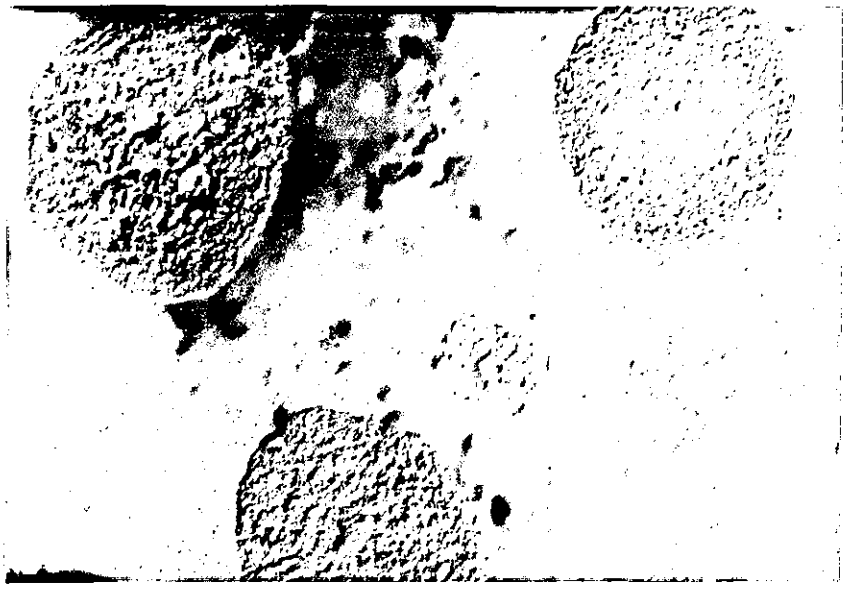

(b) Emulsion-PVC powder blend

100$\mu m$

surface peculiar to suspension-type polymers was not observed. This is due to the fact that the mass-polymer grains have a 'strawberry-like' topography. The 'strawberry-like' surface enables additives to be distributed easily and uniformly on the grain surface, and moreover, readily permits the thickest additive coating on the grain surface compared with the suspension and emulsion type polymer grains. Figures 5.3a and 5.3b show respectively the DIC micrographs of mass and emulsion grains blended under similar conditions as the suspension grains.

The emulsion grains, unlike suspension and mass grains, are spherical. Hence it will be very rare to have an 'excess' accumulation of additive particles on any region of its surface. But one major disadvantage is that, unlike its counterparts, the spatial homogeneity of the blend will be difficult to achieve (see Figure 5.3b). This is because smoothness of the grain surface may not call for proper adhesion of additive particles.

In the succeeding sections, the effect of blending conditions on the extent to which stabilizer protects the PVC grain surface from thermal treatment and morphological changes will be discussed. The results to be discussed have been obtained primarily from the qualitative and quantitative methods of fluorescent thermal analysis.

### 5.1.3 Effect of Blending Conditions on Distribution of Additives

#### 5.1.3.1 Blending speed

Blends prepared at different blending speeds were examined with differential interference contrast (DIC) technique. Also examined was the blend prepared by mixing thoroughly the ingredients by hand for about 10 minutes. Figure 5.4 (a, b and c) shows the typical examples of DIC micrographs of blends at three extreme mixing conditions: Figure 5.4a - handmixed (premix)

FIGURE 5.4: The DIC micrographs of resin blended at different blending speeds

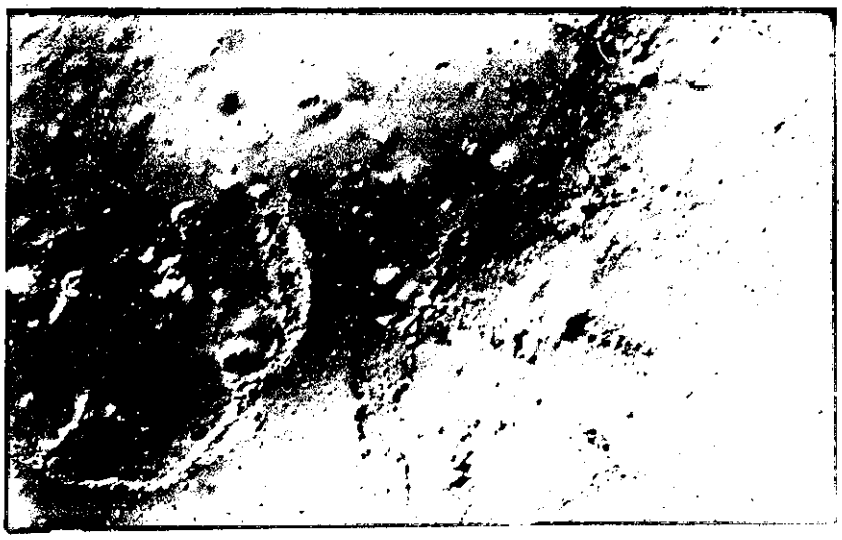

(a) Premix

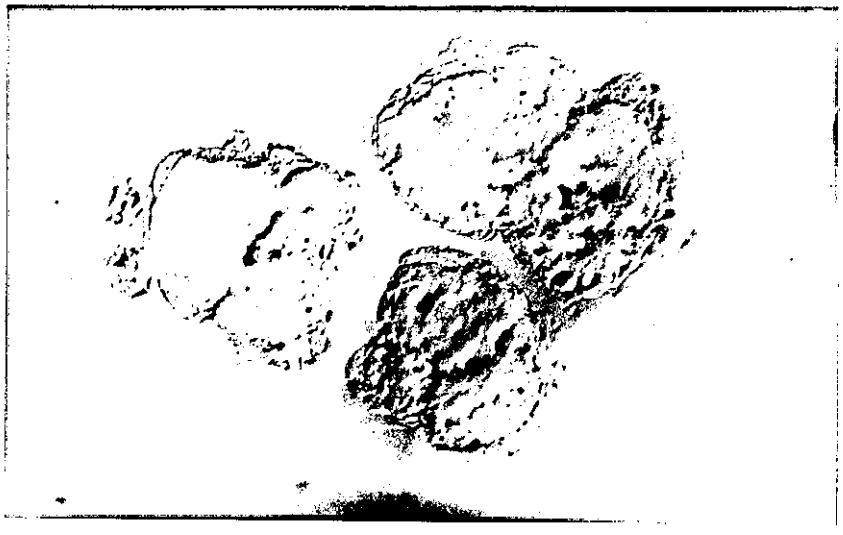

(b) 1800 rpm

(c) 3600 rpm

100um

blend, Figure 5.4b - Fielder blend at 1800 rpm and Figure 5.4c - Fielder blend at 3600 rpm. In the premix blend (Figure 5.4a), although the additives were deposited on the PVC grain surface, dispersion is extremely poor. Agglomerated additives particles are visible on the grain surface, and some loose additives particles can also be seen not absorbed on the resin grains. The reason is quite apparent, since there was no heating (either by external or internal sources) and literally no shear and frictional forces during premixing, the solid additives failed to 'breakdown' and/or 'adhere' to the resin grains.

When the blends were mixed at different blending speeds between 1800 rpm and 4200 rpm in an 8 litre T K Fielder blender, significant improvement in additives dispersion and distribution occurred compared with premix blend. Typical examples of DIC micrographs of blends from two vastly different blending speeds (1800 rpm and 3600 rpm) are respectively shown in Figures 5.4b and 5.4c. However, among the blends prepared at high blending speeds no significant difference in additives distribution is observed. The additives are well distributed and located on the PVC grains surface. Many workers[49,50,55] in this field of study have used embedding techniques (with mostly epoxy) to show that additives coat PVC grains surfaces, but they have shown little interest in the distribution of additives as a function of blending speeds, perhaps because of the limitations in the embedding technique.

This area (effect of different blending speeds) has been closely investigated using fluorescence analysis (see Chapter 4) - a method developed to study the extent of grain protection from heating by stabilizer (quantatitive method) and to precisely understand the morphological changes during blending (qualitative method).

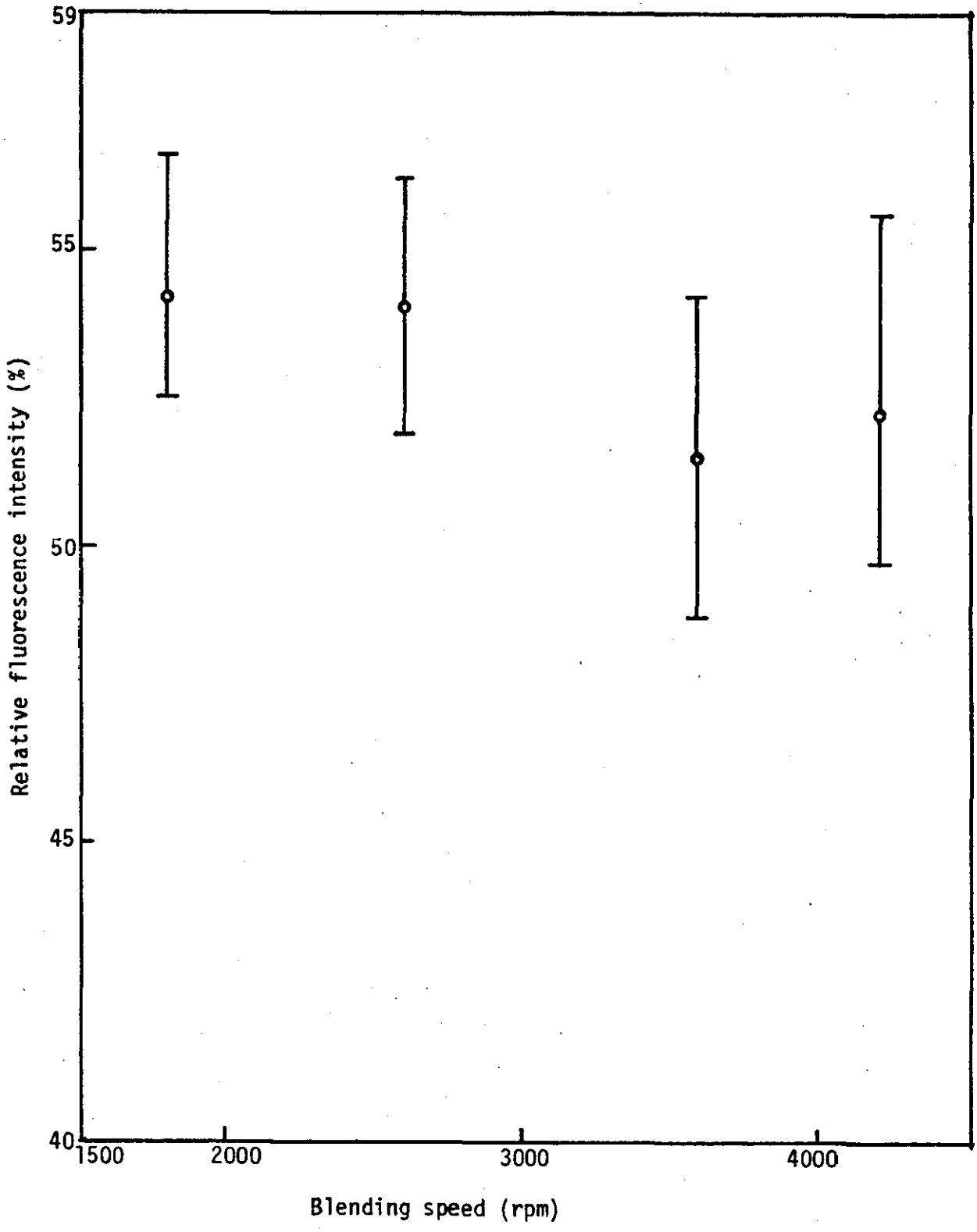


FIGURE 5.5: Relative fluorescence intensity of dry-blends at different blending speeds after heating to 190°C

By the quantitative method, increased level of fluorescence intensity means higher degree of degradation and in this situation, therefore, could be interpreted as 'poor' distribution of solid stabilizer. In Figure 5.5 it is observed that the relative fluorescence intensity slightly decreases with increase in blending speeds up to 3600 rpm before increasing slightly. This decrease in fluorescence intensity (FI) with increasing blending speed is negligible and insignificant considering that variation in FI between heat-treated grains of a specimen could be up to 5% due to particle size differences.

Therefore, it appears that blending at high-speeds, of the type that generates high shear and internal/frictional heat, produce blends with minimal variation in additives distribution. This observation again suggests that when any of the additives melt during blending, the effect of variation in blending parameters on distribution is negligible - in agreement with the results of DIC microscopy (Figure 5.4) and those reported by Allsopp[154] and Gale[49]. The results obtained from quantitative fluorescence analysis are collated in Table 5.1.

### 5.1.3.2 Effect of blending time

Blending temperature has always been constant for standard blending conditions at 120°C, and invariably controls the blending time. Therefore, if the standard formulation is being blended at standard conditions - 3600 rpm, 120°C discharge temperature and 75°C jacket temperature - in an 8 litre T K Fielder blender it will take a minimum of 18 minutes blending time to reach the discharge temperature. This has been the normal blending time, but in order to compare the effect of blending time on additive distribution, it was thought prudent to blend for times longer and shorter than normal.

TABLE 5.1

Relative fluorescence intensity of dry-blends at different blending speeds

| Blending Speed (rpm) | Relative fluorescence intensity (%) | | | | | | |
|---|---|---|---|---|---|---|---|
| | 1 | 2 | 3 | 4 | 5 | 6 | Average |
| 1800 | 56.8 | 53.5 | 52.4 | 52.9 | 52.8 | 56.6 | 54.17 |
| 2600 | 56.2 | 53.3 | 51.9 | 56.4 | 53.9 | 52.4 | 54.02 |
| 3600 | 50.6 | 52.6 | 53.3 | 48.9 | 50.0 | 54.3 | 51.62 |
| 4200 | 49.8 | 55.3 | 55.7 | 50.7 | 50.2 | 52.2 | 52.32 |

TABLE 5.2

Relative fluorescence intensity of dry-blends at different blending times for Fielder and Henschel blenders

| | Blending time (mins) | Relative fluorescence intensity (%) | | | | | | |
|---|---|---|---|---|---|---|---|---|
| | | 1 | 2 | 3 | 4 | 5 | 6 | Average |
| Fielder Blender | 5.5 | 64.4 | 67.8 | 60.2 | 66.8 | 64.2 | 63.9 | 64.55 |
| | 10 | 55.6 | 59.6 | 61.9 | 57.5 | 61.8 | 56.6 | 58.83 |
| | 15 | 52.5 | 57.9 | 58.9 | 52.5 | 51.4 | 51.5 | 54.12 |
| | 19.5 | 53.3 | 50.6 | 52.6 | 48.9 | 50.0 | 54.3 | 51.62 |
| | 25 | 49.7 | 53.9 | 52.1 | 51.4 | 48.5 | 50.8 | 51.07 |
| Henschel Blender | 5 | 70.1 | 69.7 | 70.2 | 72.8 | 70.2 | 73.5 | 71.12 |
| | 10 | 67.6 | 69.6 | 71.0 | 67.5 | 71.8 | 66.6 | 69.02 |
| | 15 | 62.5 | 57.9 | 58.9 | 62.5 | 61.4 | 61.5 | 60.78 |
| | 20 | 53.9 | 52.1 | 54.1 | 49.9 | 56.1 | 52.3 | 53.07 |
| | 25 | 54.4 | 49.2 | 49.2 | 53.2 | 56.0 | 50.8 | 52.17 |
| | 30 | 50.9 | 54.5 | 49.5 | 52.4 | 53.9 | 49.8 | 51.85 |

The blends were examined with differential interference contrast microscope. They seemed to show no difference in additives distribution Figure 5.6 (a and b) shows the micrographs of samples blended at two extreme blending times (5.5 mins and 19.5 mins respectively). This means that 'uniform' distribution of additives in a high-speed blender is achieved at the early stage of the blending cycles. Hemsley et al[48] have studied the effect of blending cycles on additives distribution using electron microscopy. They have suggested, after other physical property measurements such as powder density for instance, that poor additives distribution is observed only at very short blending cycles. Since the blend prepared in 5.5 minutes blending cycle was discharged at 88°C (which is well outside the melting range of the external lubricant - 98-101°C) it is obvious that distribution of the additives between PVC grains is poor.

In order to make a thorough examination of the effect of blending time, quantitative fluorescence analysis technique was employed. Figure 5.7 shows a drop in fluorescence intensity with increase in blending time. The higher fluorescence intensity observed with short blending time is a strong evidence of poor stabilizer distribution at this blending cycle. Although the additives coat the PVC grain surface, at short blending time the discharge temperature was not high enough to melt the lubricants which could have optimised the adhesion of the stabilizer on the grains surfaces. As the blending is prolonged however, a near plateau is reached (Figure 5.7) signifying that there is little difference in stabilizer distribution. This can be attributed to the fact that the discharge temperatures are higher than the melting point of the external lubricant (Table 5.5). This result agrees with previous results obtained with blending speeds (Section 5.1.3.1), and with the observations made by Allsopp[154], and other workers[48,49,156] that an optimum level of distribution of solid additives is achieved only if the mixing temperature exceeds the melting point of one of the additives.

FIGURE 5.6: The DIC micrographs of blends prepared at different blending times

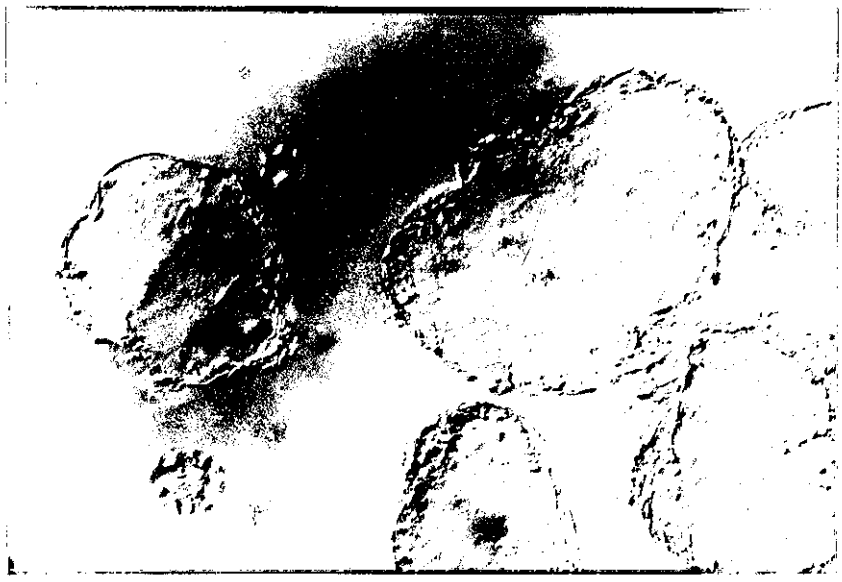

(a) 5.5 minutes

(b) 19.5 minutes

100 μm

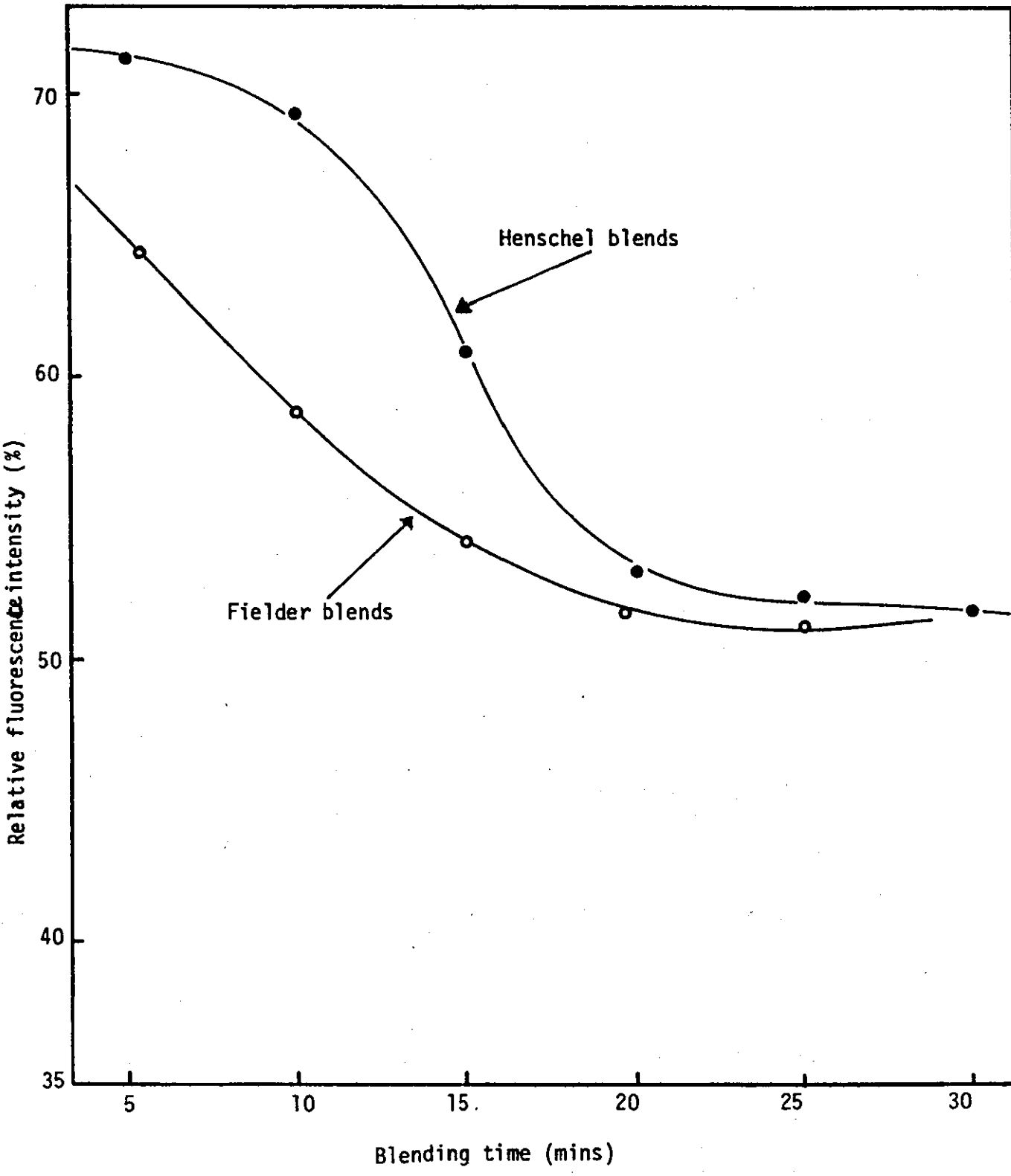


FIGURE 5.7: Relative fluorescence intensity of dry-blends after heating to 190°C

Since this fluorescence analysis convincingly appeared to be a sensitive technique for measurement stabilizer distribution, a further study was made on blends prepared with a 10 litre Henschel mixer. The use of the Henschel intensive mixer provides not only a means of proving the non-subjectivity of this fluorescence analysis method but also the elucidation of the effect of mixer blade configurations on additives distribution. The Henschel mixer has a single-layer blade arrangement, while in the T K Fielder mixer a double-layer blade arrangement was used (see Appendix 3). Previous work by Katchy[155] in IPT, Loughborough University, using different blade arrangements on the 8 litre T K Fielder mixer showed that a single-layer arrangement is less intensive. He reported that the low bulk density values found with the latter blade arrangement implies 'poor' distribution of stabilizer. In this experiment the result was found to follow the same trend as those obtained with the T K Fielder blends. That is, fluorescence intensity decreases with increase in blending time - indicating better stabilizer distribution. However, unlike the Fielder blends, the values of fluorescence intensity for Henschel blends are much higher (Figure 5.7).

From this study it has been clearly proven that blade configuration affects additive distribution, and more important, the sensitivity of this technique is - to a greater extent - certified.

The results of the FI measurements for the two blenders are given in Table 5.2.

### 5.1.3.3 Influence of charge weight on additive distribution

The quantity of material charged into a blender in a single blending operation has been known to affect blend properties. Although previous work[132,155,157] has shown that design of the mixing chamber and mixing range (maximum and minimum) of the equipment are some of the factors which affect powder blend

FIGURE 5.8: Effect of charge weight on additives distribution

(a) 1 kg

(b) 2 kg

(c) 3 kg

100μm

properties due to charge weight, little is known of their effects on additives distribution. In this experiment, blends prepared in an 8 litre T K Fielder blender at five different charge weights (1 kg, 1.5 kg, 2 kg, 2.5 kg and 3 kg) were investigated. This blender was used because the configuration of the propeller permits, with more ease, the blending of the considered minimum and maximum charge weights compared with the 10 litre Henschel blender. Each blend was examined and analysed with differential interference contrast (DIC) and UV fluorescence microscopy methods.

With the DIC microscopy the additives appeared to have distributed uniformly on the grains surfaces at all charge weights. Figures 5.8a and c show the micrographs of samples of 1 kg and 3 kg charge weights respectively. From these micrographs it appears that the differences in additives distribution amongst blends of different charge weights are obviously small - observing better distribution with increase in charge weight.

The use of quantitative fluorescence thermal analysis showed identical trends, except that optimum distribution is identified with 2 kg charge weight. Figure 5.9 shows the graph of relative fluorescence intensity of the blends and different charge weights. It is evident (from the observed lowest fluorescence intensity) that optimum distribution of additives is obtained when the optimum quantity of material is blended. The reason is because at this charge weight maximum 'work' is done on the blend in a manner which allows the lubricants to melt just after all the additives have been well distributed on the PVC grains surfaces. This reason agrees with the fact that best distribution of additives is associated with 'prolonged' blending time.

From the shape of the graph (a quarter moon shape) it can be deduced that blending higher, instead of lower, than the normal charge weight is advisable if good distribution of additives is to be achieved. The results from fluorescence analysis measurements are given in Table 5.3.

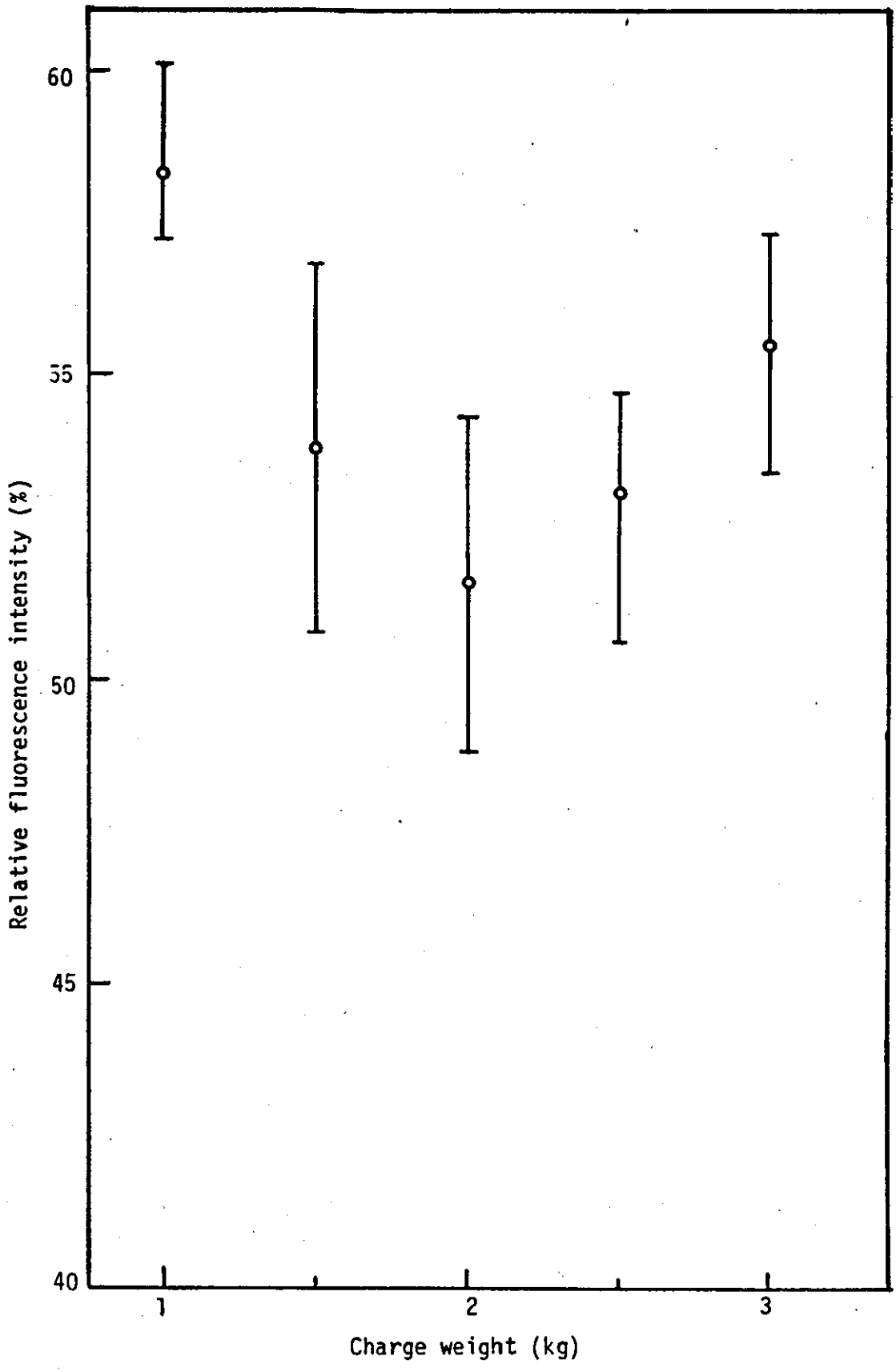


FIGURE 5.9: Relative fluorescence intensity of dry-blends at different charge weights after heating to 190°C

TABLE 5.3

Relative fluorescence intensity of dry-blends at different charge weights

| Charge Weight (kg) | Relative fluorescence intensity (%) | | | | | | |
|---|---|---|---|---|---|---|---|
| | 1 | 2 | 3 | 4 | 5 | 6 | Average |
| 1 | 58.2 | 57.3 | 58.3 | 60.1 | 58.1 | 57.6 | 58.32 |
| 1.5 | 50.7 | 52.9 | 56.9 | 55.7 | 53.7 | 52.6 | 53.75 |
| 2 | 54.3 | 52.6 | 53.3 | 48.9 | 50.6 | 50.0 | 51.62 |
| 2.5 | 54.2 | 54.7 | 52.1 | 50.6 | 53.1 | 53.4 | 53.02 |
| 3 | 56.3 | 54.8 | 53.4 | 53.8 | 57.3 | 56.2 | 55.47 |

## 5.2 Effect of Blending Parameters on Morphological Changes

The effects of blending parameters on dry blend properties such as densities, flow-rate, particle size and size distribution have been studied. The results obtained are as listed in Tables 5.4 to 5.6 and plotted in Figures 5.10 to 5.14. The blending parameters investigated were, as before, blending speed, blending time and charge weight so that at the end an attempt will be made to correlate additives distribution with morphological changes.

In Figure 5.10 powder density is seen to increase with higher blending speed. Bulk density increases steadily at first up to 3000 rpm. Above 3000 rpm it increases sharply to reach a near steady increase again. The tap-density also increases in the same manner as the bulk density but has higher values. This increase in powder density is due to the higher shear environments associated with higher blending speeds[49,131,132]. For example, the pronounced difference in densities between blends prepared at 1800 rpm and 3600 rpm could be attributed to the formation of more smaller particles in the latter[128]. Morohashi[132] reported an increase in bulk

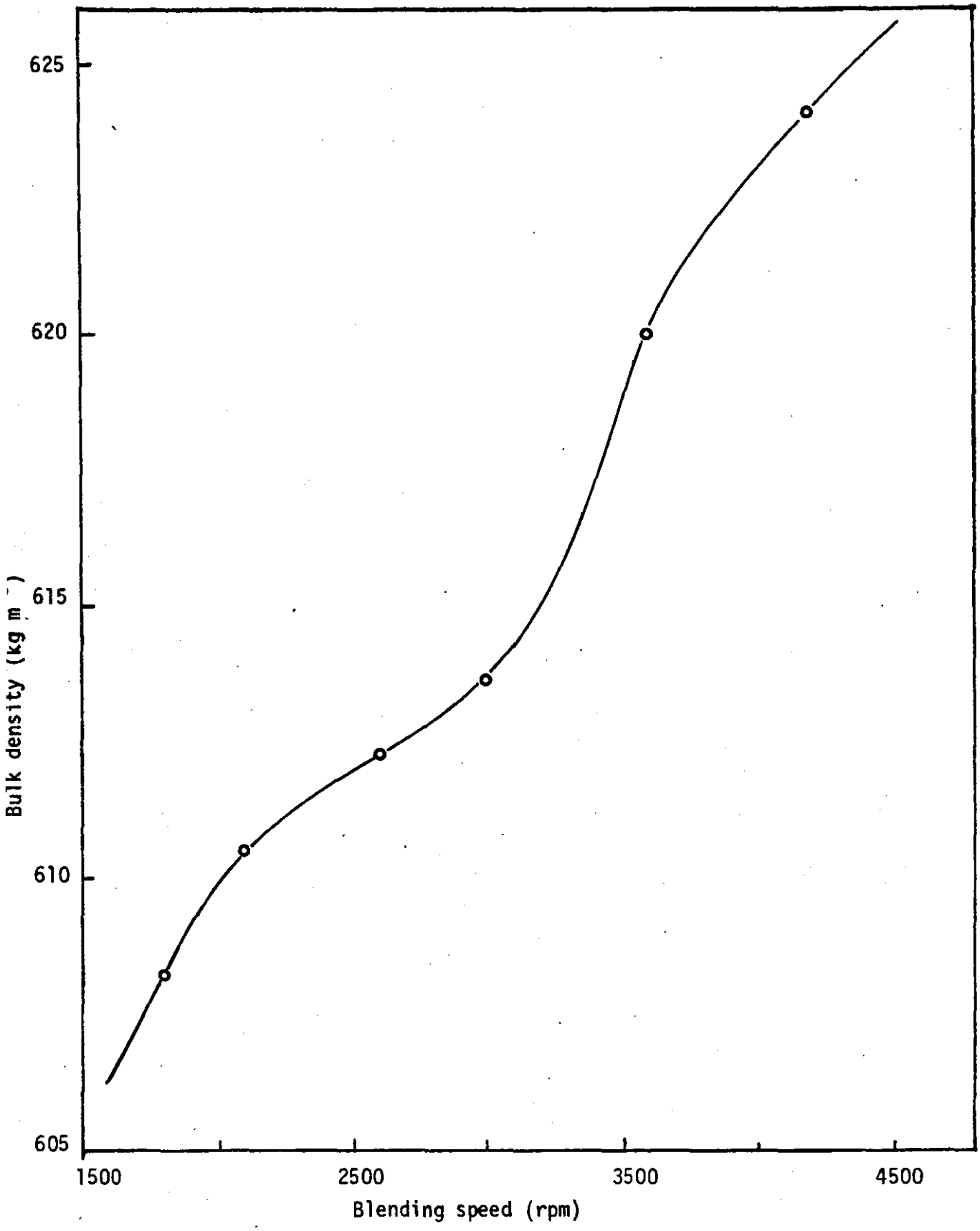


FIGURE 5.10 Variation of bulk density with blending speed

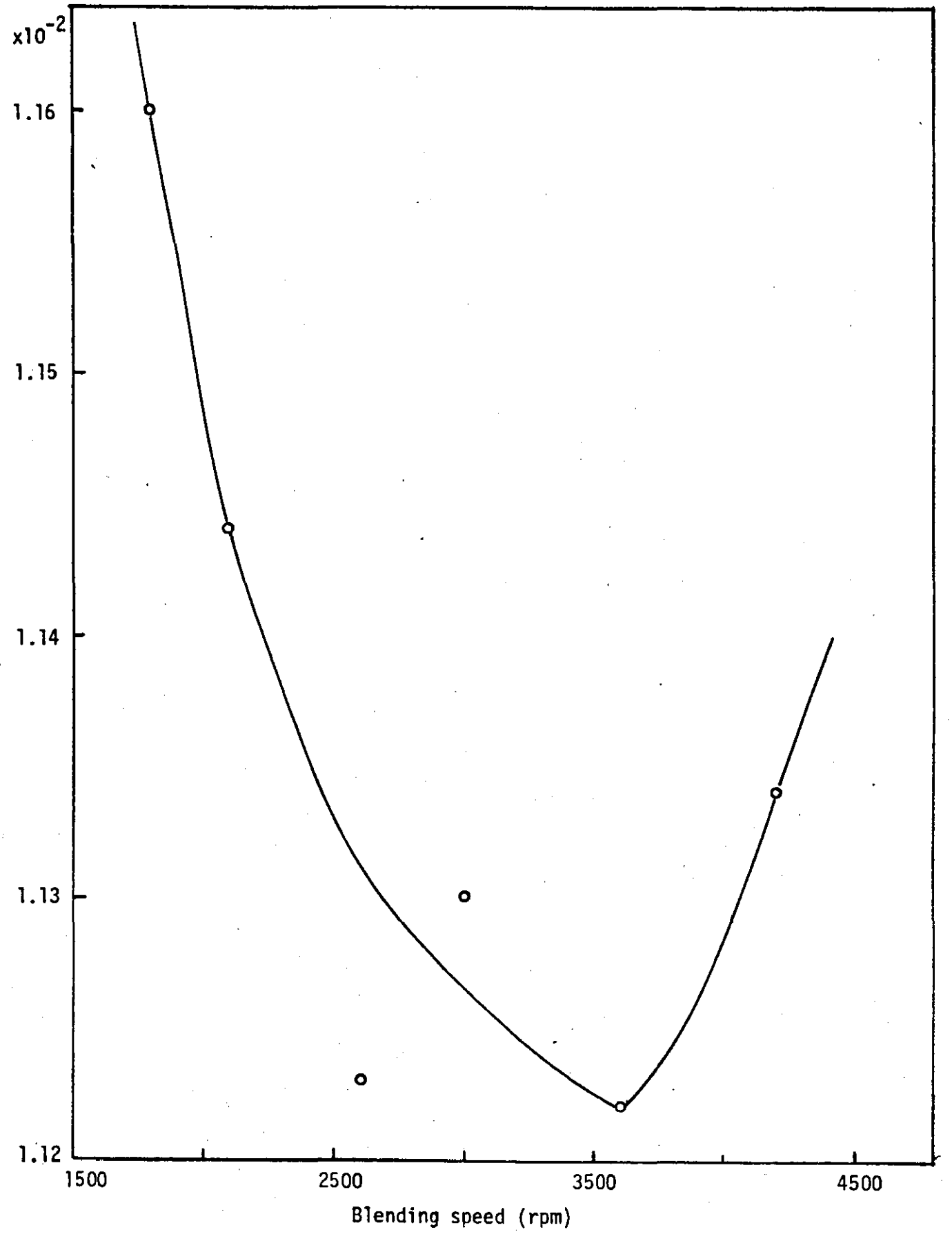


FIGURE5.11:Effect of blending speed on powder flow rate

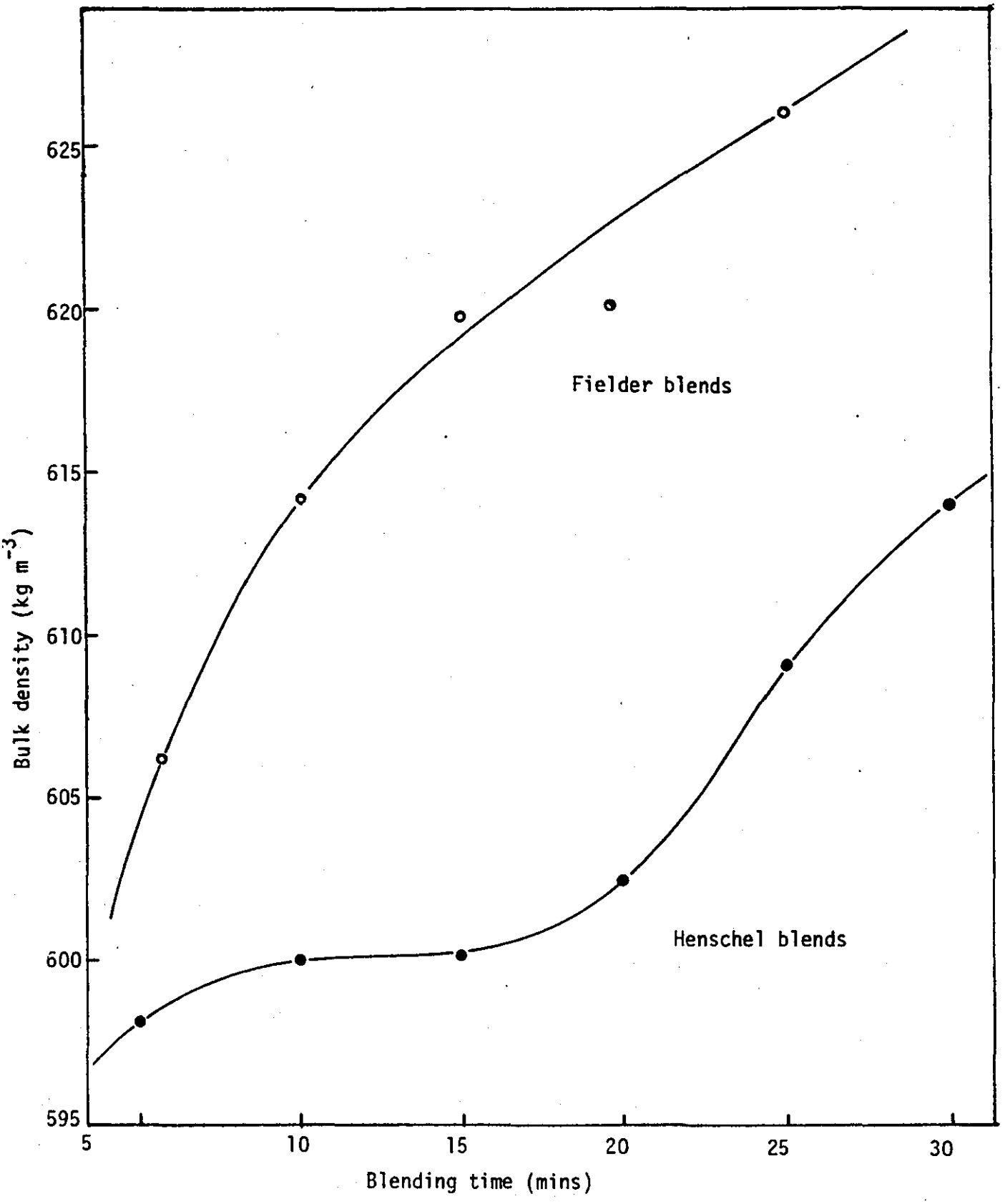


FIGURE 5.12:Variation of bulk density with blending speed for two blender types

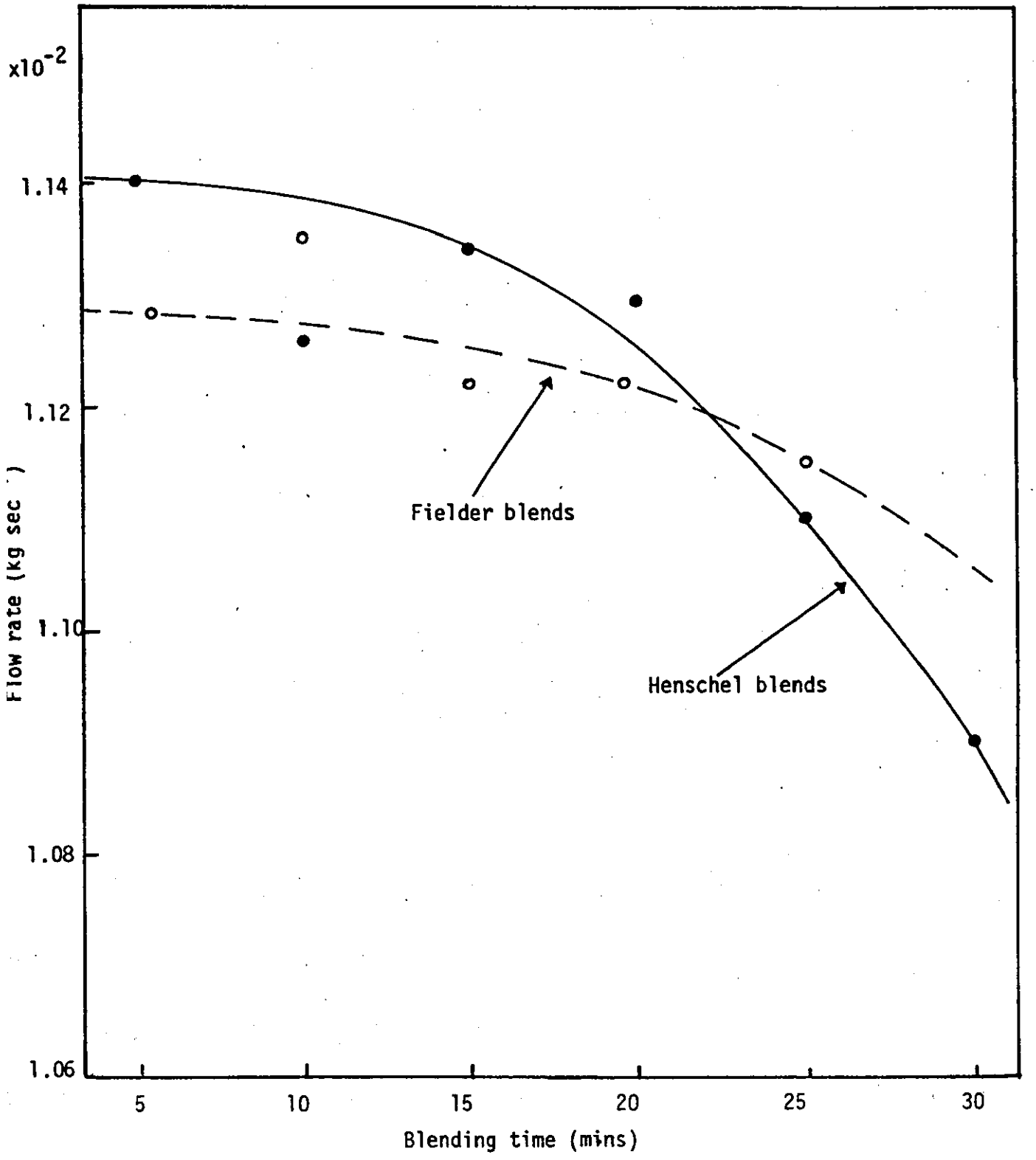


FIGURE 5.13 Effect of blending speed on powder flow rate for two blender types

density to be due to formation of smaller particles at high blending speed. He showed blends prepared in a Henschel mixer at low speed to have lower powder density compared with those prepared at high speed. Although at 1800 rpm to reach the normal discharge temperature has required a longer blending period, the effect of this 'prolonged' blending in this context is negligible. The reason is that, at different blending speeds, the effect of blending time on density changes is insignificant because the blends are produced at the same discharge temperature (120$^{o}$C). Conversely, at different blending speeds, if the blends are discharged at the same blending time but different blending temperatures the effect of discharge temperature on density changes precedes that of blending speeds. The effect of temperatures on powder densities has been reported by several workers to precede other parameters[131,132]. Therefore to avoid temperature effect the blends were discharged at the same temperature.

The effect of blending speeds on changes in grains morphology during blending was further investigated with semi-quantitative and qualitative methods of UV fluorescence analysis. These were used to determine the particle size and size distribution of heated grains of specific size range. To do this, 10% of grains with particle sizes from 150 to 212 μm and particle sizes below 75 μm were sieved out and heat-treated (full details of this experiment are given in Chapter 4, Section 4.1.2). The blends containing heated grains were obtained for blending speeds from 1800 to 4200 rpm.

Figure 5.14 compares the size distribution of the heated grains at two different blending speeds (1800 and 3600 rpm). A shift in particle size of heated grains from the original size fraction is observed. This indicates that 'breakdown' of grains occurs during blending, and is most pronounced for samples blended at 3600 rpm. This can be attributed to the higher particle interactions associated with the high shear rate - environment at high blending speed[158]. Figure 5.15 shows/compares the size distribution

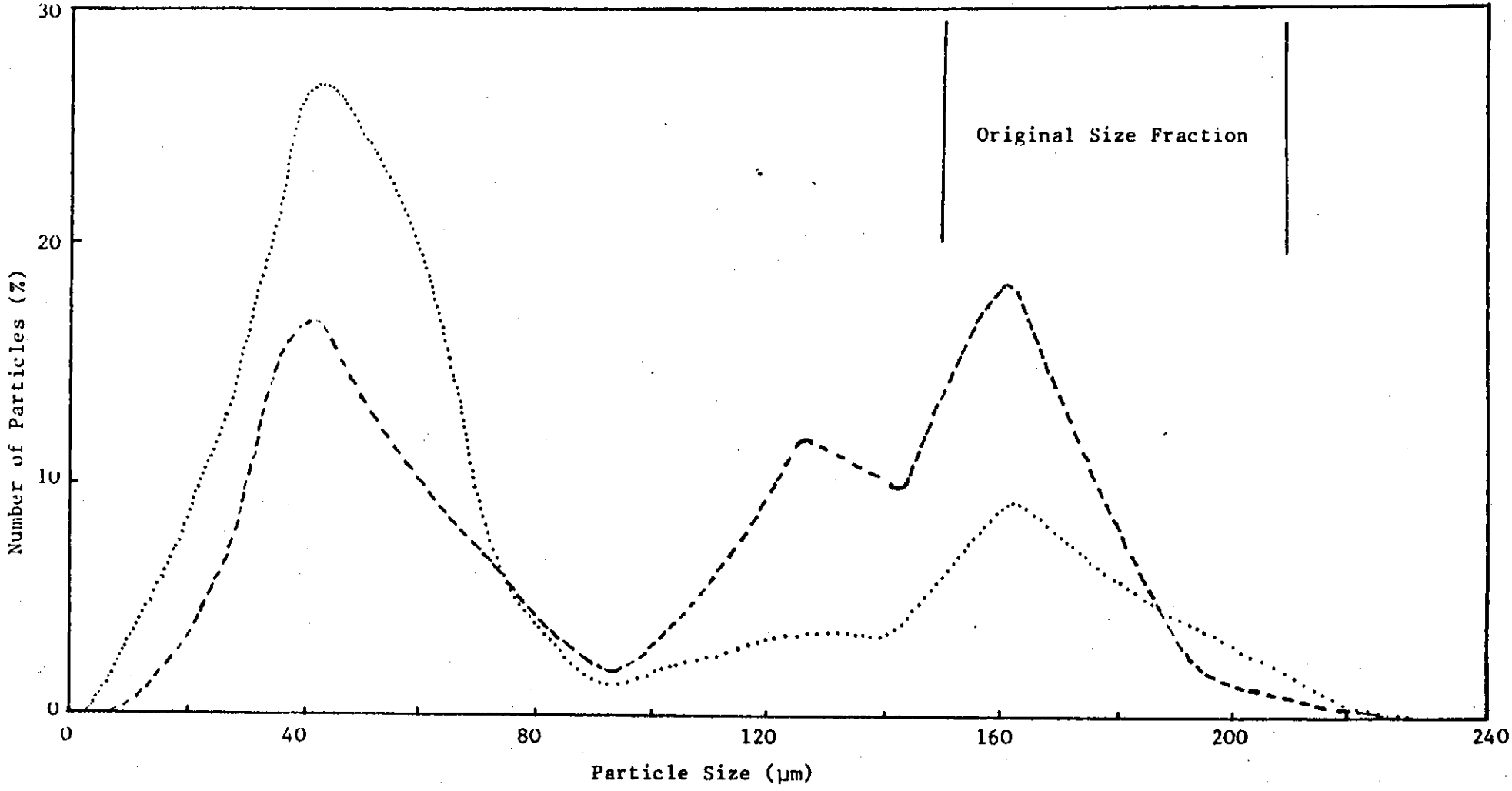


FIGURE 5.14: Effect of blending speed on the size changes of heated grains of size from 150-212μm. (T K Fielder blender) ( --- ) 1800 rpm, (···) 3600 rpm.

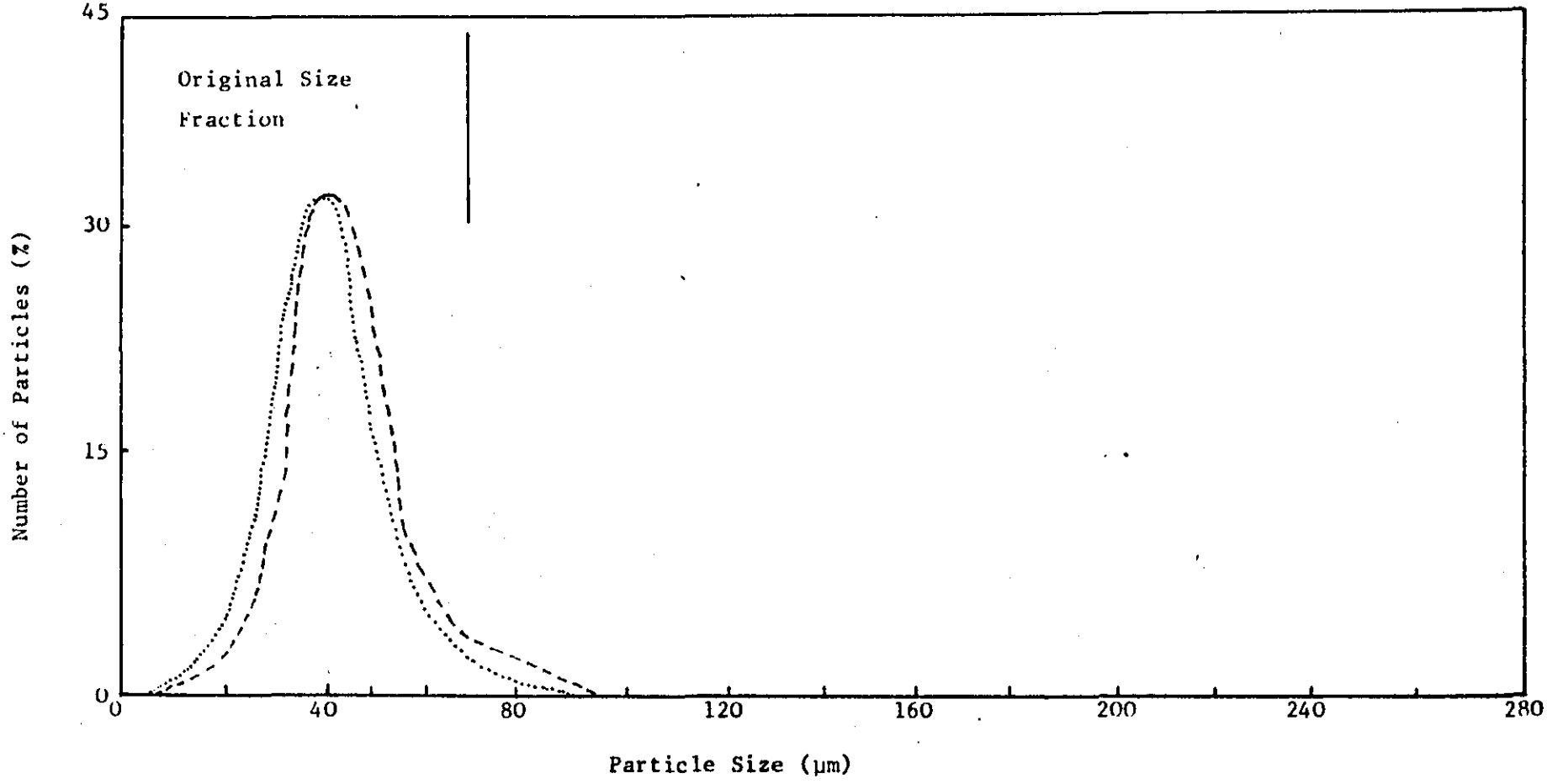


FIGURE 5.15: Effect of blending speed on the size changes of heated grains of <75μm size. (T K Fielder blender) (----) 1800 rpm, (····) 3600 rpm.

of heated grains of <75 μm again at two blending speeds. No significant shift in distribution is observed to either lower or higher size range. Therefore very little agglomeration occurs during blending. This is supported by the observations made with qualitative fluorescence analysis method on several size fractions from the blends. It was observed that very little adhesion occurs between grains (Figure 5.16) compared with particle 'breakdown'. Perhaps another important point clarified by the use of this technique is particle adhesion. After examining samples of many blends (randomly sampled) it can be concluded that it is rare- if ever it does exist - to see 2 equal size grains/fragments adhering to each other. However, small fragments mostly are seen to adhere to large grains - especially with blends prepared at high blending speeds. This explains the fact that higher powder density is observed with increase in blending speed.

Powder densities also increase with increasing charge weight (Figure 5.17). In this figure a sharp rise in bulk density is observed on increasing the charge weight from 1.5 to 2 kg - presumably indicating a region of optimum charge weight. On further increase in charge weight to 2.5 kg a maximum bulk density value is reached, but the dependency is much more reduced. This strongly suggests that the 'vortex' flow of powder is greatly restricted. In other words, another increase in charge weight will result in a sharp drop in bulk density (Figure 5.17) - due to less interaction between the particles. The sharp increase in densities from minimum to optimum charge weights is due to the intense mixing action associated with optimum charge weight - which causes not only reduction in particle size but also the additives to be quickly dispersed in the mix.

In general terms, powder density and flow rate measurements have been employed quite extensively by workers[131,159,160] to elucidate the effects of blending parameters on powder blend. Hemsley et al[48] reported that significant changes of bulk density are observed in a normal blending process even at relatively low

E 5.16: Fluorescence micrographs of samples from four different size fractions (original size fraction 150-212 μm) 3600 rpm

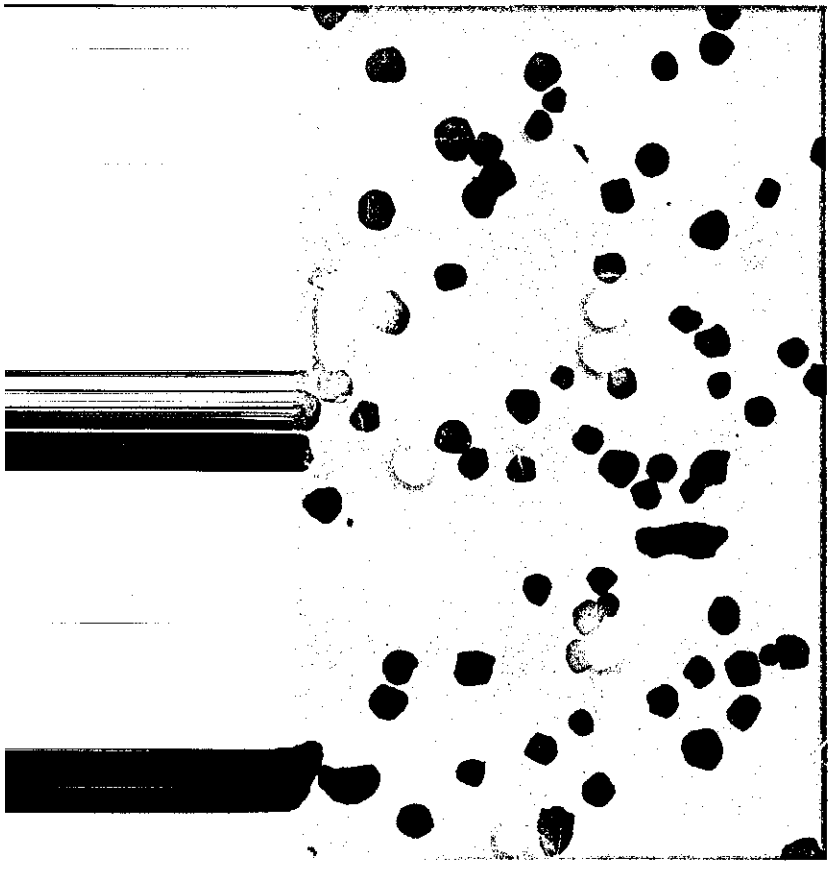

53 μm

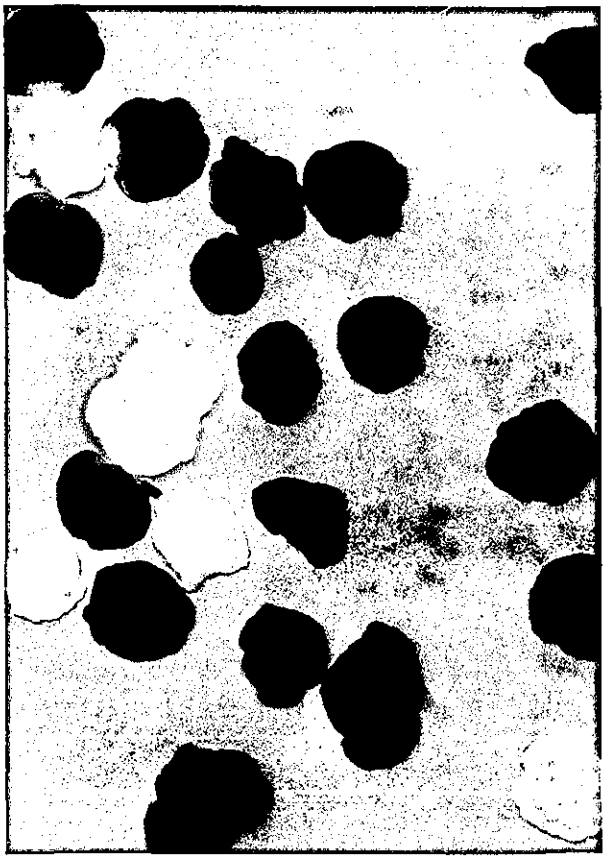

(b) 90-106 μm

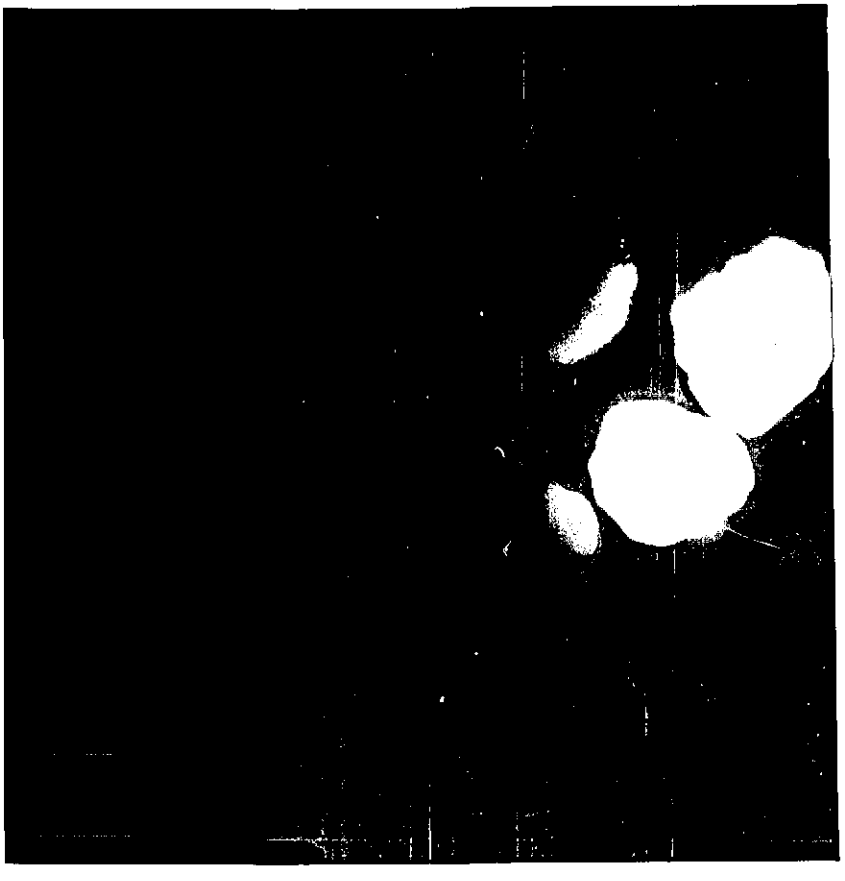

180-212 μm

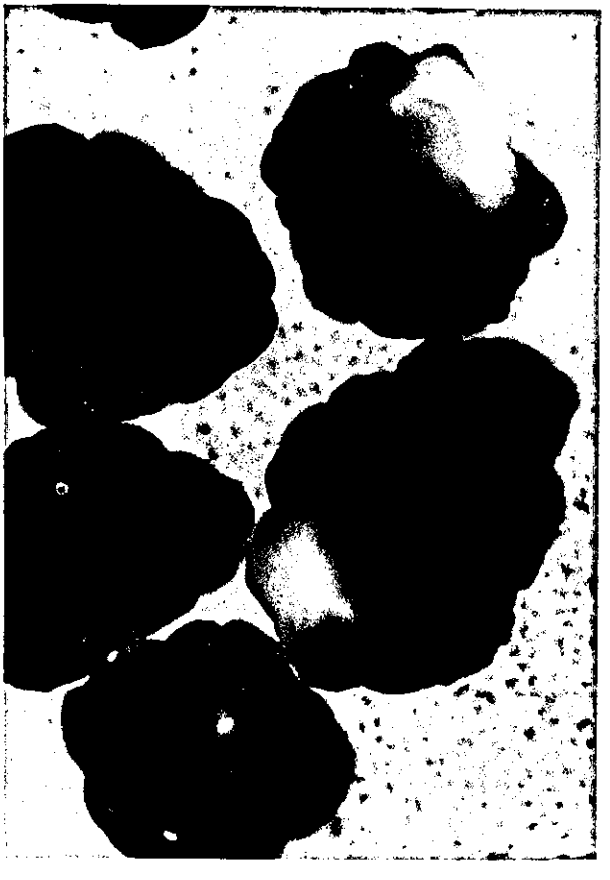

(d) >250 μm

150μm

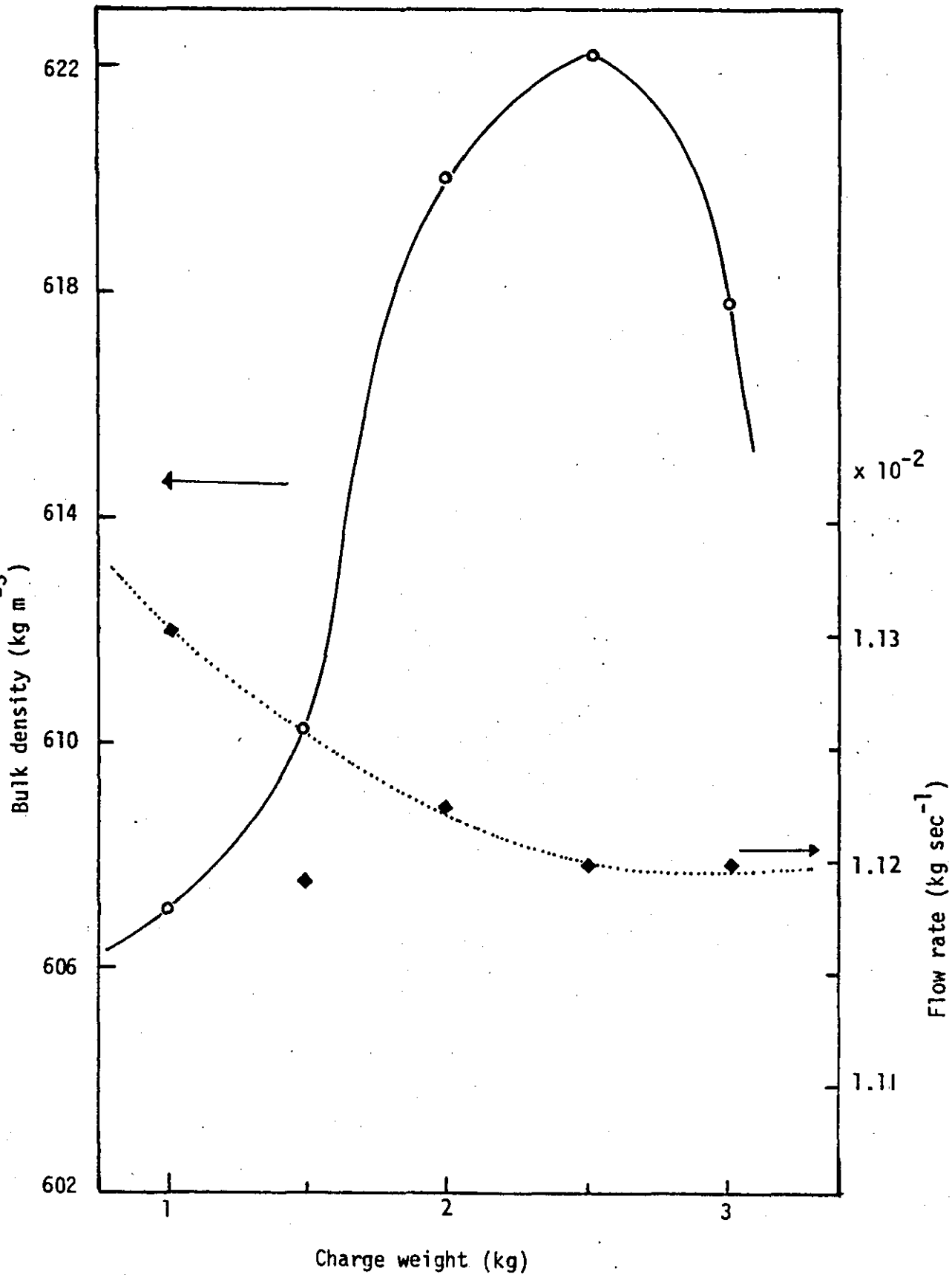


FIGURE 5.17 Variation of powder-blend properties with charge weight

shear effects. Guimon[131] has also indicated that powder densities increase very rapidly within the first 3 minutes of blending cycle and would soon be at a maximum but for temperature. High density blends are reported to be due to particle size reduction[159]. Since higher density and reduction in flow-rate are associated with 'prolonged' blending cycle, high charge weight, and high blending speed, reduction in particle size occurs at these conditions. This is confirmed by the broad agreement between the results obtained from fluorescence microscopy techniques and conventional methods.

TABLE 5.4

Effect of blending speed on dry-blend properties

| Blending speed (rpm) | Discharge time (mins) | Bulk density ($Kgm^{-3}$) | Tap Density ($Kg\ m^{-}$ ) | Flow-rate x $10^{-2}$ ($Kg\ sec^{-1}$) |
|---|---|---|---|---|
| 1800 | 35.0 | 608.22 | 649.90 | 1.16 |
| 2100 | 30.5 | 610.50 | 654.23 | 1.144 |
| 2600 | 28.0 | 612.28 | 654.91 | 1.123 |
| 3000 | 24.0 | 613.72 | 655.96 | 1.13 |
| 3600 | 19.5 | 620.00 | 662.84 | 1.122 |
| 4200 | 14.5 | 624.15 | 665.20 | 1.134 |

TABLE 5.5

Effect of blending time on dry-blend physical properties

| | Blending time (mins) | Discharge Temp. ($^{o}C$) | Bulk density ($Kgm^{-3}$) | Tap Density ($Kgm^{-3}$) | Flow-rate $x10^{-2}$ ($Kg\ sec^{-1}$) |
|---|---|---|---|---|---|
| | - | - | 590.01 | 650.82 | 1.111 |
| | 5.5 | 85.3 | 606.80 | 655.10 | 1.128 |
| Fielder | 10 | 97.8 | 614.22 | 657.94 | 1.135 |
| Blender | 15 | 107.9 | 619.70 | 660.40 | 1.122 |
| | 19.5 | 120.0 | 620.00 | 662.86 | 1.122 |
| | 25 | 125.0 | 625.98 | 669.25 | 1.115 |
| | 5 | 81.0 | 598.42 | 652.10 | 1.14 |
| | 10 | 90.0 | 599.08 | 653.71 | 1.126 |
| Henschel | 15 | 100.5 | 600.13 | 654.55 | 1.134 |
| Blender | 20 | 106.5 | 602.70 | 656.32 | 1.129 |
| | 25 | 109.0 | 609.01 | 657.10 | 1.11 |
| | 30 | 112.5 | 614.10 | 661.14 | 1.09 |

TABLE 5.6

Effect of charge weight on dry-blend physical properties

| Charge Weight (Kg) | Discharge time (mins) | Bulk density ($Kgm^{-3}$) | Tap density ($Kgm^{-3}$) | Flow-rate $x\ 10^{-2}$ ($Kg\ sec^{-1}$) |
|---|---|---|---|---|
| 1.0 | 28.0 | 607.07 | 649.90 | 1.130 |
| 1.5 | 22.5 | 610.17 | 654.50 | 1.119 |
| 2.0 | 19.5 | 620.00 | 662.86 | 1.122 |
| 2.5 | 16.0 | 622.30 | 661.94 | 1.120 |
| 3.0 | 11.5 | 617.94 | 661.98 | 1.120 |

## 5.3 Effect of Concentration of Stabilizer on Nature of Distribution and Morphology

The effect of stabilizer loading on its distribution between powder grains was studied with fluorescence and differential interference contrast microscopes. Stabilizer loadings from 1 phr to 4 phr were examined with DIC and their micrographs are as shown in Figure 5.18. More stabilizer is observed on the surface of the PVC grains in Figure 5.18b than the surface of grains in Figure 5.18a. An image contrast is developed as the stabilizer concentration is increased. Since the polymer grains and immersion liquid have similar refractive index the development of image contrast is due to index difference from the stabilizer[161]. An optimum image contrast is observed at near 3 phr stabilizer concentration. At this ratio a saturation level appears to have been reached and further addition of stabilizer made no significant different to its image contrast. It means that more stabilizer particles are deposited/absorbed on the PVC grains of blends containing higher concentration, and that a saturation level is reached at about 3 phr. These observations made with DIC were further/closely investigated with quantitative fluorescence analysis method on heated grains. Because of thermal instability of PVC the extent to which the PVC grains is protected from thermal degradation/discolouration would largely depend on the quantity of stabilizer on its surface. Conversely relative fluorescence intensity depends on the level of degradation (see Chapter 4).

Figure 5.19 shows a decrease in relative fluorescence intensity as a function of stabilizer concentration. After the initial sharp drop, the fluorescence intensity appears to have reached a plateau at 2.5 phr stabilizer loading. This is in broad agreement with the observation made with DIC - that a level of saturation is attained after 2.5 phr loading. This is expected because the amount of lead stabilizer normally used in industry has been 3 phr[97,162]. This result not only confirmed the DIC observation but also emphasised the sensitivity and non-subjectivity of the

FIGURE 5.18: Effect of DBLS loading on distribution

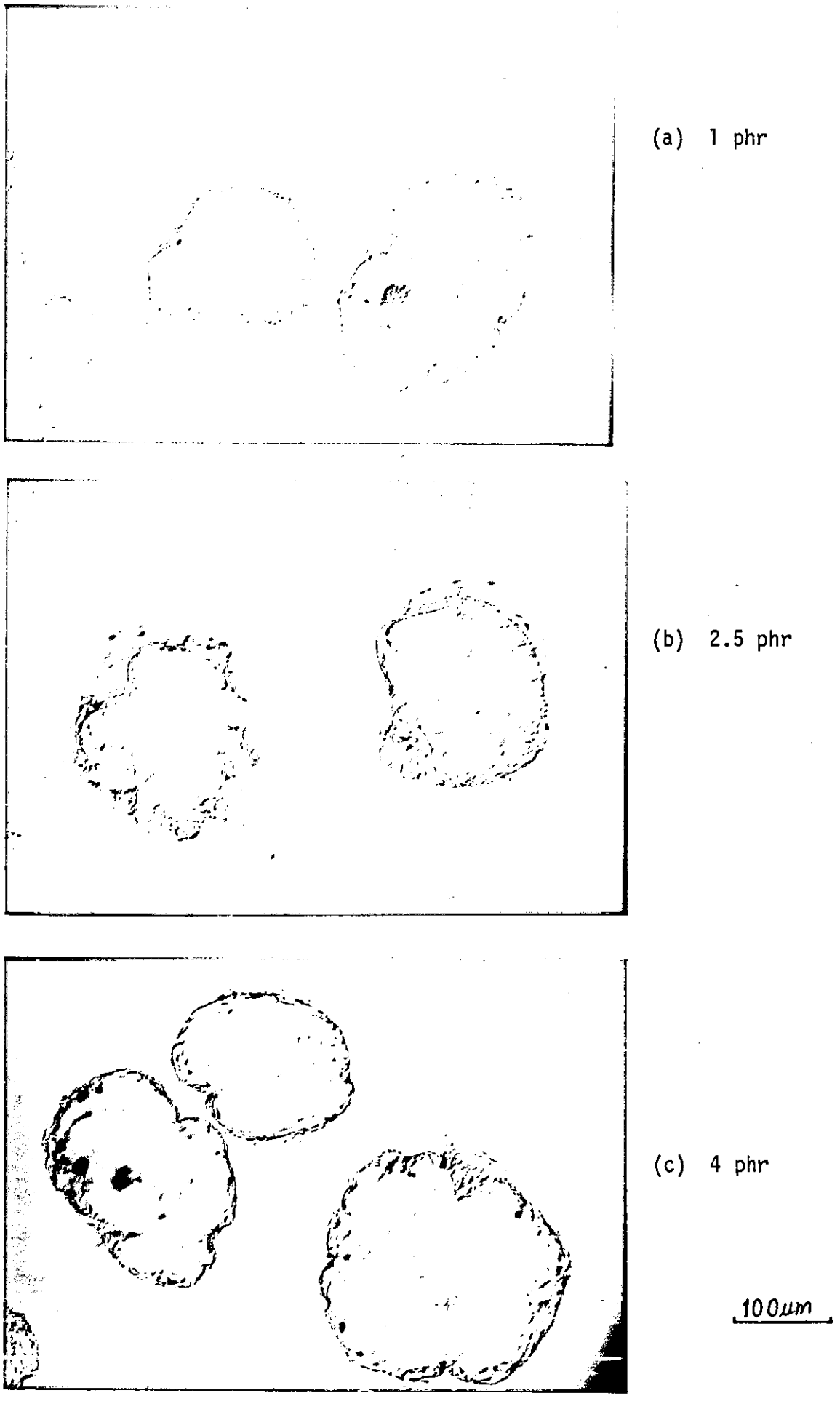

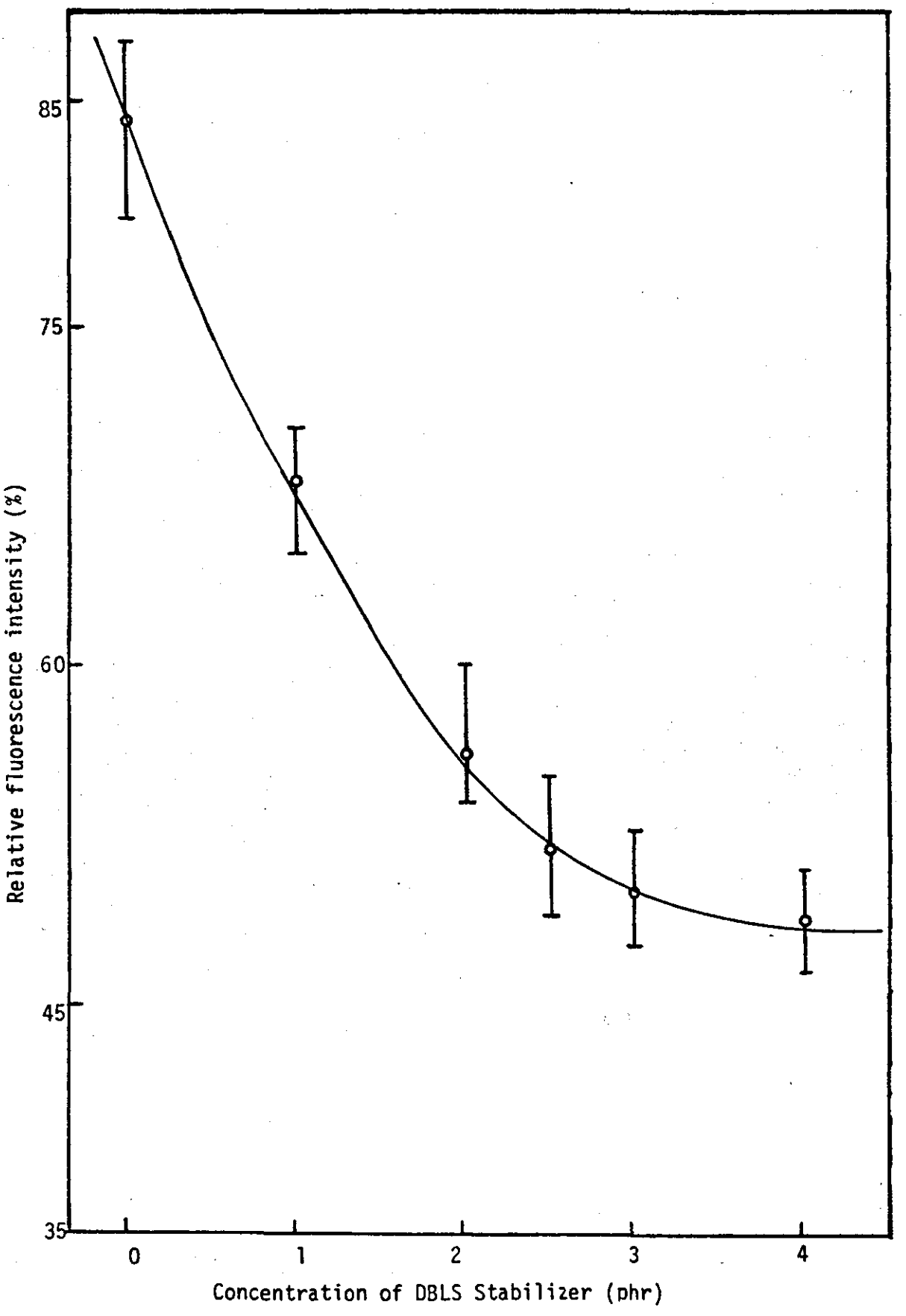


FIGURE 5.19: Relative fluorescence intensity of dry-blends containing different loadings of DBLS stabilizer after heating to 190°C

UV fluorescence analysis. The result from the fluorescence measurement is given in Table 5.7.

The effects of stabilizer concentration on physical properties such as densities, flow rate and particle size distribution (determined to substantiate the microscopical observations) are given in Figures 5.20 and 5.21 respectively, and are listed in Tables 5.8 and 5.9. Results from flow rate measurement show the values to decrease with increase in stabilizer concentration (Figure 5.20). The decrease in powder flow rate is due to rise in surface friction between the grains as thicker layers of stabilizer are formed on their surfaces. This effect has been reported by other workers[129,131]. Corry et al[129] have shown that flow-rate of suspension PVC decreases with increased amounts of secondary organic additive. High stabilizer ratio, therefore, suggests an increase in the density of the blend - and in fact the bulk density was found to increase sharply with increasing stabilizer concentration up to 3 phr. It must be stated that the dependency reduces as the stabilizer loading increases. A small drop in bulk density at 4 phr is observed. This drop in density could be explained in terms of a lower discharge temperature (Table 5.8) - caused by excessive lubricating effect of the stabilizer observed only at higher concentration.

The particle size distribution of blends with different stabilizer loading are compared in Figure 5.21. Distance between the bimodal distribution peaks appears to have narrowed down with increased amounts of stabilizer. This effect could suggest a possible surface modification of the PVC grains - caused by increased stabilizer loading. This change in particle size distribution also reflects on the powder density due to alteration in packing characteristics of the blend[128]. By sieving the blends to BS 410: 1969, 'test sieve', a trend was obtained between particle breakdown and stabilizer concentration (Table 5.9). More particles were found to pass through the 180 μm mesh size as the DBLS concentration was increased. This seemed to agree with the

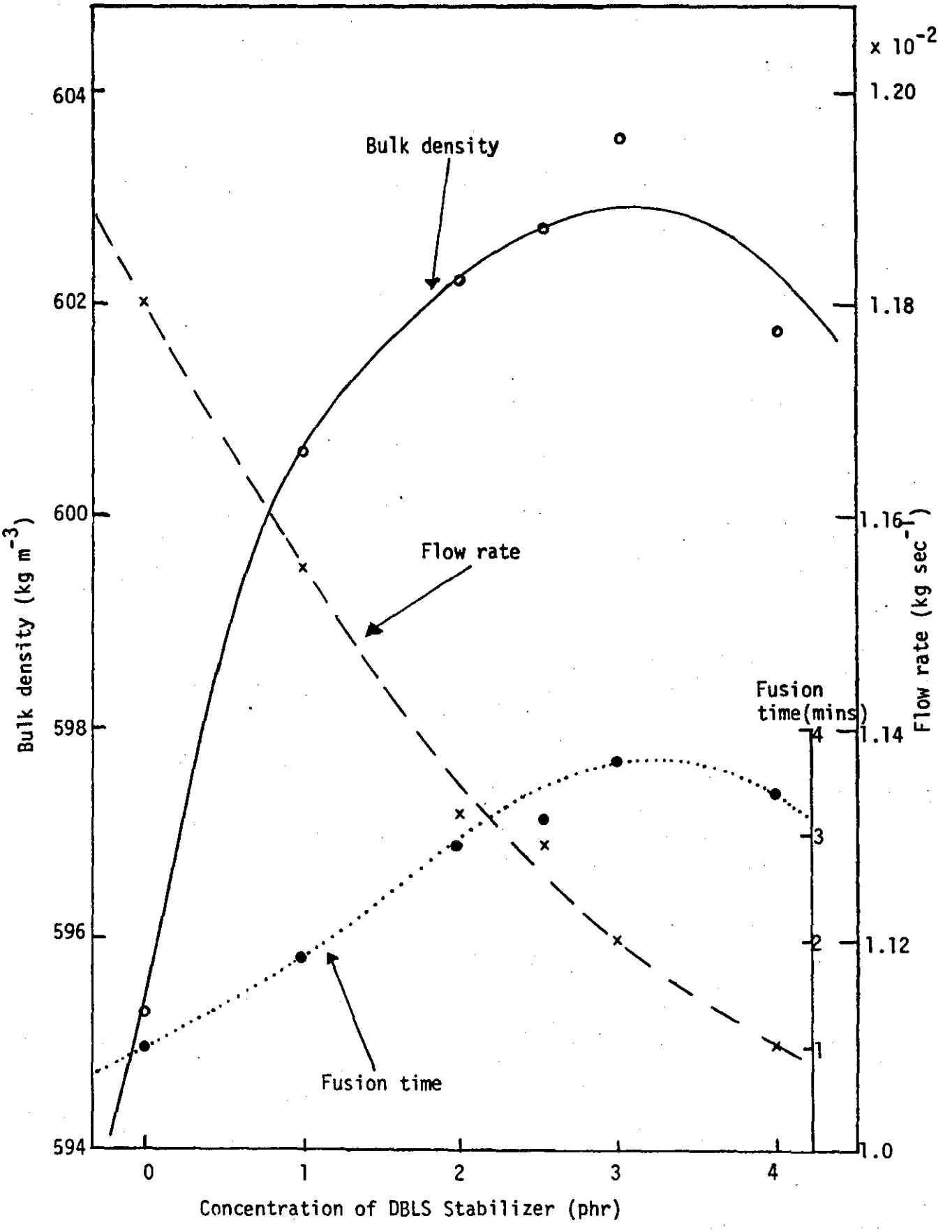


FIGURE 5.20 Relationships of powder-blend properties to the concentration of dibasic lead stearate (Henschel blender)

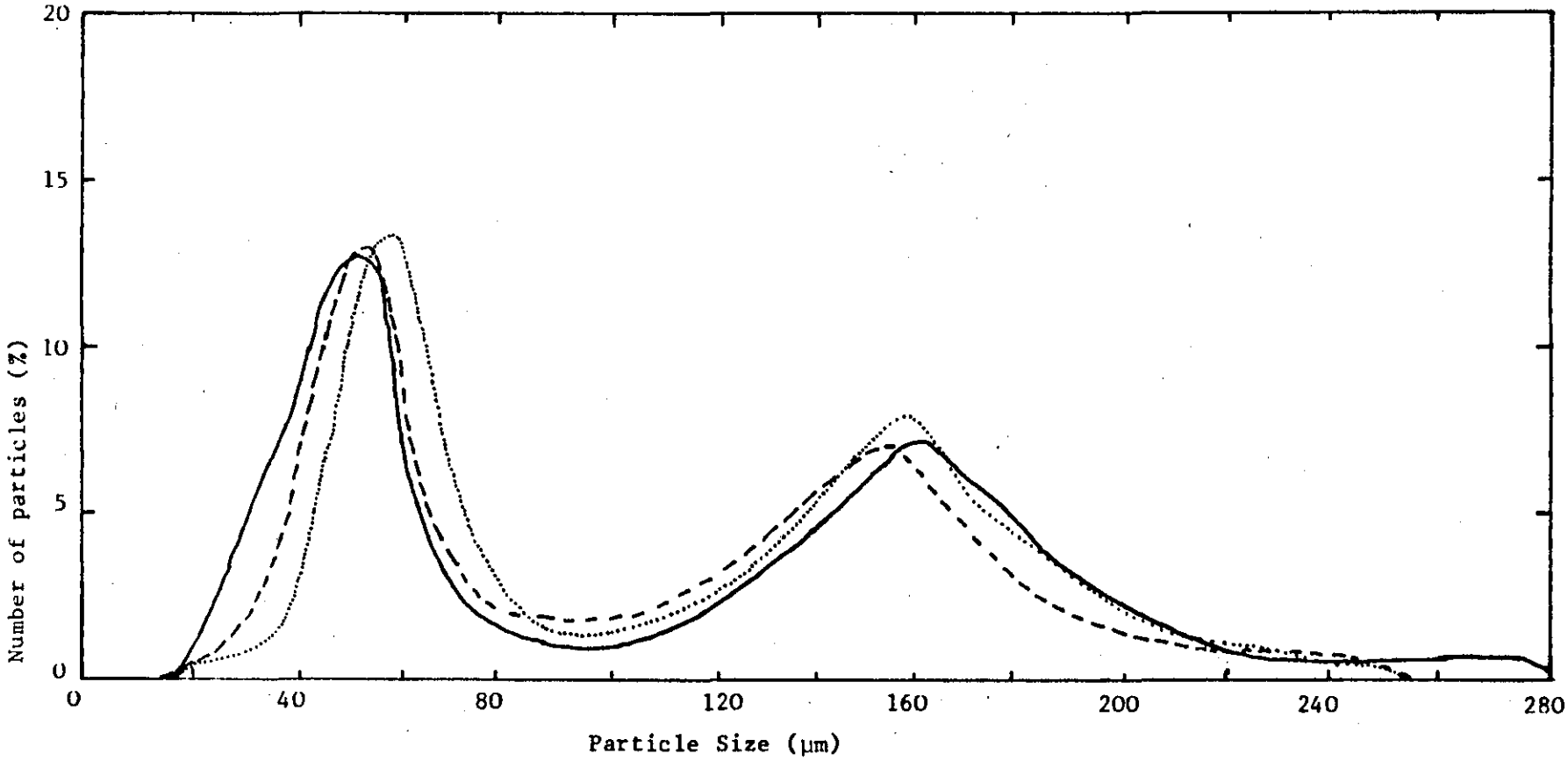


FIGURE 5.21: Effect of stabilizer concentration on the particle size distribution of blends. (Henschel Blender)
( ____ ) 0 phr, (- - - - -) 2.5 phr, ( • • • ) 4 phr.

particle size distribution in Figure 5.21 - where an imaginary drawn vertical line at 180 μm particle size would cut through, first at 2.5 phr and lastly 0 phr distribution curves. In other words, more particle 'breakdown' is obtained with increasing stabilizer concentration. This tendency decreases after 2.5 phr - due to, perhaps, the effect of low surface friction between particles, and between particles and surface of mixing chamber. Assessment of particles retained in 250 μm mesh size evidently showed the 'breakdown' of particles to occur largely at higher particle size fraction (Table 5.9). However, at higher stabilizer concentration (above 2 phr) only small change in particle size was observed at high particle size fraction.

As expected, the Brabender fusion time was found to increase with increase in the concentration of DBLS. However, at 4 phr of DBLS a decrease in fusion time was observed (Figure 5.20). The reason for this is not exactly known, but it is certain that a saturation level is reached at about 3 phr - in broad agreement with the observations of DIC and fluorescence microscopy methods. The results of these measurements are illustrated in Tables 5.7 to 5.9.

TABLE 5.7

Relative fluorescence intensity of dry blends containing different concentration of dibasic lead stearate (DBLS) - Henschel blender

| Concentration of DBLS (phr) | Relative fluorescence intensity (%) | | | | | | |
|---|---|---|---|---|---|---|---|
| | 1 | 2 | 3 | 4 | 5 | 6 | Average |
| 0 | 84.4 | 87.8 | 80.2 | 86.8 | 84.2 | 83.9 | 84.55 |
| 1 | 69.7 | 64.9 | 68.1 | 70.4 | 65.5 | 70.8 | 68.23 |
| 2 | 55.3 | 60.2 | 56.8 | 57.4 | 55.4 | 57.2 | 57.05 |
| 2.5 | 54.4 | 49.2 | 49.2 | 53.4 | 56.0 | 50.8 | 52.17 |
| 3 | 52.6 | 53.3 | 49.6 | 50.1 | 47.7 | 48.6 | 50.32 |
| 4 | 51.2 | 49.7 | 47.4 | 50.1 | 46.5 | 49.6 | 49.08 |

TABLE 5.8

Relationships of powder blend properties to the concentration of dibasic lead stearate (DBLS) - Henschel blender

Discharge time = 18mins.

| Concentration of DLBS (phr) | Discharge Temp. (°C) | Bulk Density ($kgm^{-3}$) | Tap Density ($kgm^{-3}$) | Flow rate $\times 10^{-2}$ ($kgsec^{-1}$) | Brabender fusion time (mins) |
|---|---|---|---|---|---|
| 0 | 102.5 | 595.26 | 642.30 | 1.180 | 1.00 |
| 1 | 104.5 | 600.60 | 649.46 | 1.155 | 1.85 |
| 2 | 106.5 | 602.23 | 653.66 | 1.132 | 2.90 |
| 2.5 | 106.5 | 602.70 | 656.32 | 1.129 | 3.15 |
| 3 | 107.0 | 603.64 | 658.20 | 1.120 | 3.70 |
| 4 | 95.5 | 601.73 | 652.30 | 1.100 | 3.45 |

TABLE 5.9

Relationship of particle size to concentration of dibasic lead stearate

| Concentration of DBLS (phr) | Wt. of particles through 180μ mesh size (%) | Wt of particles retained in >250μ mesh size (%) |
|---|---|---|
| 0 | 73.52 | 0.51 |
| 1 | 75.18 | 0.33 |
| 2 | 76.30 | 0.40 |
| 2.5 | 77.15 | 0.50 |
| 3 | 77.17 | 0.51 |
| 4 | 77.80 | 0.63 |

## 5.4 Effect of Formulation Variables on Additive Distribution and Morphological Changes

Variations on the basic formulation were made to obtain simple yet readily processable formulations (see Section 3.2). Apart from varying the lubricant concentrations, small amounts of 'secondary' additives also have been incorporated into the basic formulation. The effects of these minor variations, in the basic formulation, on additives distribution and powder morphology will be discussed under the following headings: effect of varying the ratios of lubricants and effect of addition of 'secondary' additives.

### 5.4.1 Effect of Varying the Ratios of Lubricants

The effect of varying the ratios of external and internal lubricants in the basic formulation was studied with transmitted light differential interference contrast (DIC) technique. By this method it was found that neither lower nor higher ratio of both lubricants have significantly changed the spatial homogeneity of the blends. This is because the variations made in the ratios of these lubricants were too small to impart any visible change in image contrast between the blends. Figure 5.22 shows the DIC micrograph of typical example of additives distribution observed with both higher and lower than normal concentrations of the lubricants. It is evident when compared with Figure 5.1 that no significant change in distribution has occurred.

Table 5.10 shows the results from physical properties measurements. At low ratio of internal lubricant (calcium stearate) reduction in external lubricant concentration produced blend with lowest bulk density. At high calcium stearate concentration reduction in external lubricant concentration slightly lowered the bulk density. However, when both the external and internal lubricant concentrations were simultaneously increased, the bulk density was found to increase. This suggests perhaps that the shape of

FIGURE 5.22: Effect of lubricants concentrations on additive distribution
(a) .15 phr GS wax; (b) .8 phr calcium stearate;
(c) .15 phr GS wax; .8 phr calcium stearate

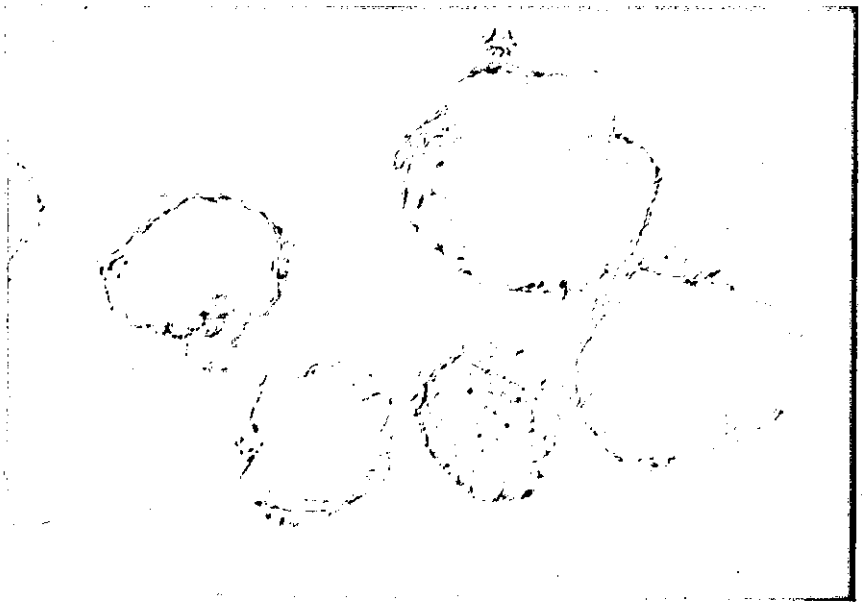

(a)

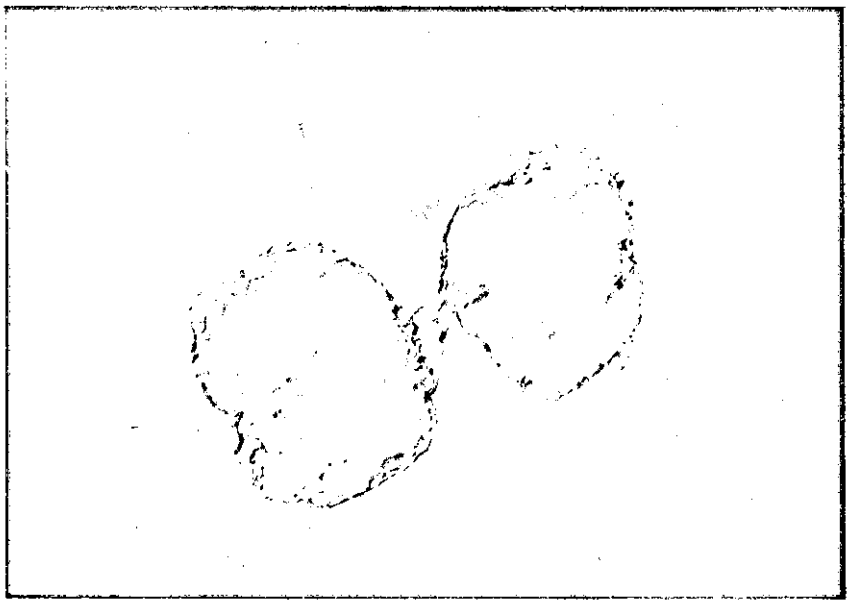

(b)

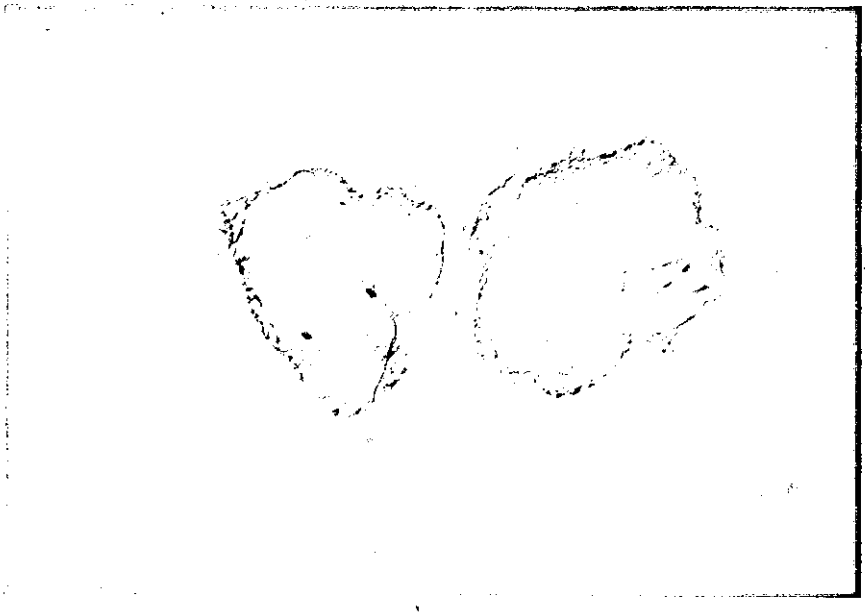

(c)

100μm

TABLE 5.10

Variation of different formulations with physical properties of powder-blends

| Formulation Number | Additive type and ratios (phr) | | Bulk Density ($kgm^{-3}$) | Tap Density ($kgm^{-3}$) | Flow rate $x10^{-2}$ ($kgsec^{-1}$) | Brabender fusion time (mins) |
|---|---|---|---|---|---|---|
| | Cal.St. | G.S. wax | | | | |
| 1* | 0.4 | 0.3 | 620.00 | 662.86 | 1.122 | 2.98 |
| 2 | 0.4 | 0.15 | 620.51 | 665.04 | 1.123 | 2.45 |
| 3 | 0.8 | 0.3 | 626.51 | 669.41 | 1.125 | 3.40 |
| 4 | 0.8 | 0.15 | 624.74 | 668.11 | 1.126 | 3.26 |
| 5** | 0.2 | OPW | 621.62 | 664.13 | 1.182 | 3.30 |
| 6** | 0.4 | GMS | 626.18 | 668.55 | 1.144 | 3.10 |
| 7** | 1.5 | K120N | 632.09 | 673.20 | 1.129 | 2.70 |
| 8** | 1.5 | NLS | 639.33 | 685.46 | 1.137 | 5.30 |
| 9 | 2.5 | TBLS | 631.93 | 679.10 | 1.099 | 2.65 |

* = standard formulation

** = standard formulation containing the 'secondary' additive indicated

OPW = Oxidised polyethylene wax

GMS = Glycerol monostearate

K120N = Paraloid K120N

NLS = Normal lead stearate

Cal.St. = Calcium stearate

G.S. wax= G.S. Wax 2411P

the particles has been greatly modified - due to large amounts of lubricants. Flow rates of the blends did not follow the same trend as the bulk density. However, it is observed that increase in calcium stearate produced blends with higher flow rate for blends containing lower or higher ratios of external lubricant (Table 5.10) compared with the standard blend. To further substantiate the effect of lubricants concentration on powder properties fusion time of these blends were determined with Brabender Plasticorder - a method which has been used by several workers[139,164] to determine the fusion time of PVC. Table 5.10 shows the longest fusion time to be associated with the blend with highest concentration of lubricants. This is expected since the lubricants will significantly reduce interparticle friction hence delaying the gelation period[44,165,166,168]. The effect of this on processing will be discussed in the next two chapters. It is worth noting the pronounced effects variation in ratios of lubricants have on the fusion characteristics of the blends. For instance, 50% reduction of GS Wax (external lubricant) ratio reduced the fusion time by merely a quarter. The results are collated in Table 5.10.

### 5.4.2 Effect of Addition of 'Secondary' Additives

The results obtained by determining the physical properties of blends containing various 'secondary' additives are given in Table 5.10. Additions of external lubricants (oxidized polyethylene wax and glycerol monostearate) do not significantly affect the stabilizer distribution. This is partly because small amounts of the lubricants were incorporated which, in the basic formulation, will have little effect compared with other components. Moreover, the melting points of oxidized polyethylene wax and glycerol monostearate as determined by differential scanning calorimeter (DSC) method are 80°C and 110°C respectively - which is below the blend discharged temperature of 120°C. Since both external lubricants melted during blending, the difference in stabilizer distribution between their blends is

negligible (Figure 5.23). The same observation is made with blends containing 1.5 phr normal lead stearate - which melts at 120°C. These additives, on melting, are absorbed into the PVC grains and thus are tacitly assumed to improve distribution of stabilizer[48-50]. However, the small difference observed in stabilizer distribution between Figure 5.23c and 5.23a is largely due to the high concentration of normal lead stearate. Figure 5.23b shows the transmitted light DIC micrograph of blends containing 1.5 phr impact modifier - which has a very high melting point. The particles of impact modifier and DBLS appear to be spatially distributed on the PVC grains surface. The micrograph shows these additive particles as 'specks' on the PVC grains surfaces.

The effect of these 'secondary' additives on morphological changes is quite pronounced. Bulk density of the blend increases with the addition of 'secondary' additives. The increase in density observed with blends containing external lubricants and normal lead stearate, is apparently due to the large differences between the melting points of the 'secondary' additives and blend discharge temperature. For instance after the additives have melted blending continued for about five more minutes before attaining the required discharge temperature of 120°C. During this period, smoothing and sphericality of the PVC grains occur thus producing blends with high bulk density (Table 5.10). This effect is reflected also on the flow property of the blends (Table 5.10). The less spherical grains with lower ratio of lubricant have highest flow rate, because surface friction between particles is reduced. Similar results were obtained with blends containing 1.5 phr impact modifier. The bulk density and flow rate increased compared with that of the basic formulation. This is expected because the impact modifier, like DBLS, does not melt during blending but distributes on the PVC grains surfaces.

In Table 5.10 the Brabender fusion result shows that the normal lead stearate incorporated into blend 8 resulted in a

FIGURE 5.23: Effect of addition of 'secondary' additives on stabilizer-distribution.
(a) .4 phr GMS; (b) 1.5 phr Paraloid K120N, (c) 1.5 phr normal lead stearate

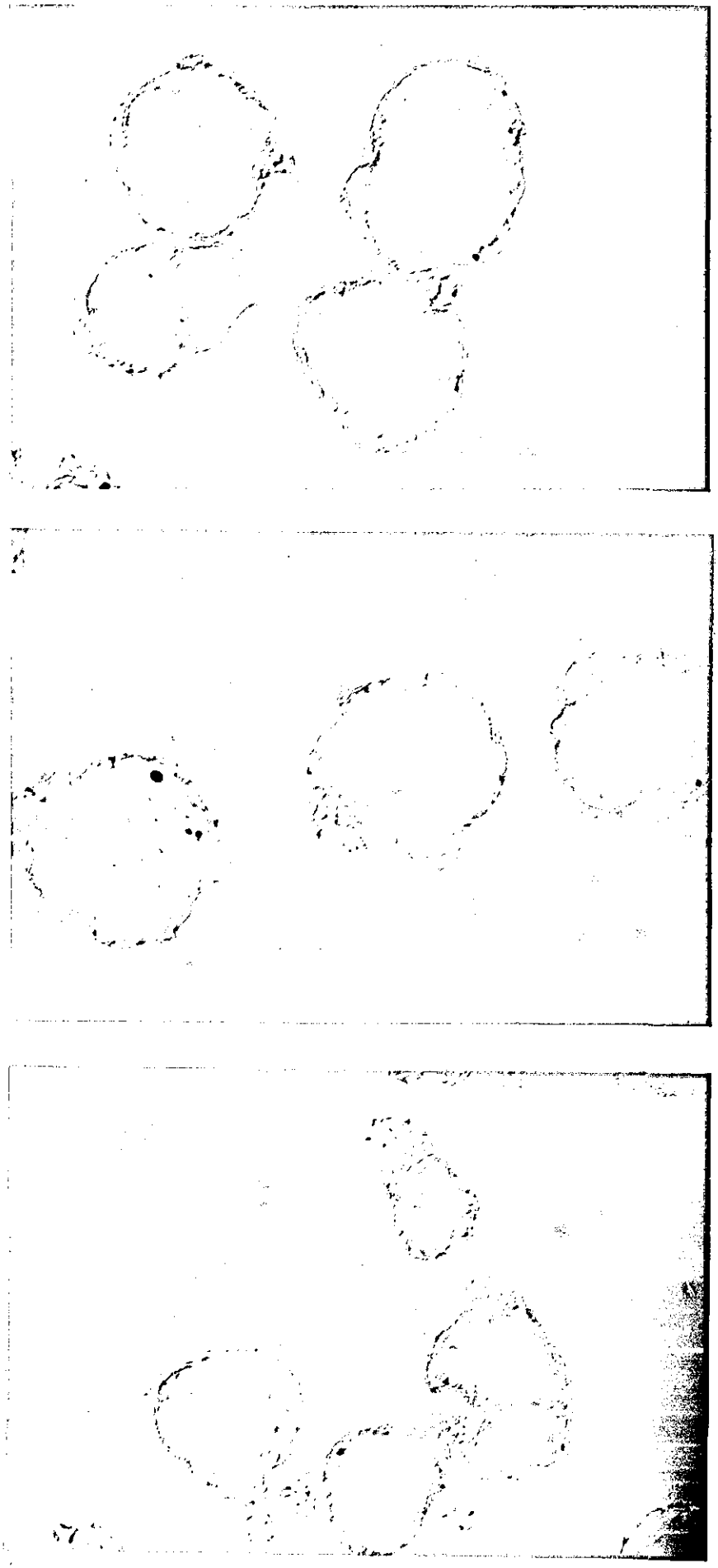

prolonged fusion time. The normal lead stearate has an internal lubricating effect, as well as stabilising action, which prolonged the fusion time of the blend. This prolonged fusion time, although could lead to an improvement in stabilizer distribution, will result in products of relatively poor mechanical properties (as will be shown in the next chapter). In general, incorporation of lubricant (external or internal) prolonged the fusion time, but the opposite trend was observed with impact modifier (Table 5.10).

## 5.5 Conclusion

The UV fluorescence microscopy has been used to show that a systematic relationship exists between stabiliser distribution, morphological changes and blending conditions. From the results and observations made with both fluorescence and differential interference contrast microscopy methods, the following conclusions can be drawn:

1. Solid additives are found to coat PVC grains surfaces in a manner which is typical of their surface topography. The pattern of distribution differs between suspension, mass and emulsion grains. For suspension polymer grains more additive accumulate in the re-entrant surface, poor additive distribution is observed with emulsion polymer grains due to their 'glossy' surfaces; and the mass polymer grains showed the best distribution of additives because of their strawberry-like surfaces. For a specific polymer type the size of grains does not affect distribution of additive.

2. Good additives distribution is obtained at early stages of blending, but the optimum level is achieved only if one component in the formulation melts at least 5 minutes before the complete blending cycle. This 5 minute period allows some loose additive particles to be absorbed onto the 'wet' polymer grains.

3. It is evident, from the discussion section, that different blenders produce dry blends of varying morphological properties and degree of stabilizer distribution. The effectiveness of a blender, among other things, is dependent on the blade arrangements. Double layer blade arrangement gave dry blends with better stabilizer distribution and physical property than a single layer blade mixer. However, their dry blends properties show similar trends in the way they vary with blending parameters.

4. Blending cycle affects the distribution of stabilizer. Fluorescence analysis of blends prepared at different blending times and heated to 190°C shows that prolonged blending time (before one component in the formulation melts) results in optimum distribution of additives. However, after the melting of the lubricant prolonged blending (e.g. for more than 5 minutes) did not have any significant difference on blend property.

5. Particle breakdown and agglomeration occur simultaneously during dry blending, but the former is much more pronounced no matter what the blending condition. In fact it is very rare to see two equal size grains adhering to each other as a result of dry blending, but fragments breaking from and attaching to large grains are a dominant feature at higher blending speeds.

6. Increase in the concentrations of both stabiliser and lubricant were found to increase dry blend properties such as density, flow rate and fusion time. These properties, also, were very sensitive to variations in formulation. For instance, the addition of an impact modifier and a normal lead stearate into the standard formulation resulted in higher powder density. Also impact modifier reduced the fusion time whilst an increase in fusion time was observed with blends containing normal lead stearate stabilizer.

# CHAPTER 6

# EXTRUDATE STUDIES

## 6.1 Literature Review

The extrusion of rigid PVC pipe from powder blend compounds of intensive mixers has become widely accepted by pipe fabricators and the industry in general. The extrusion of powder blend compounds offers several potential advantages over the use of diced/pelletized compounds: greater economy, greater production rates, less total heat history and improved physical properties. The use of a twin-screw machine and the continual improvement in its quality have largely contributed to the increase in powder blend extrusion. Several publications[49,52,154] have shown that pipes and other rigid profiles produced with a twin-screw extruder have better mechanical properties and improved gelation level. Rolls and Weill[52] reported that pipes extruded directly from a powder compound are equal in strength and chemical resistance to pipes made from mill-mixed and diced compounds.

Recent writers have mainly concentrated on elucidating the relationship between structure, property and morphology[56,148,169,154]. It has been found that structural modification takes place on processing the powder blend, and, in most cases, leads to the presence of residual grains in the end product. Allsopp[154] also used microscopical evidence to show that a superficially homogeneous melt usually contains residual grains. He suggested that the quality of rigid PVC products is largely undermined by residual grains and undispersed additives. Gale[165] showed that gelation level is affected by lubricant type and concentration. On the effect of undispersed additives a cavity transfer mixing head (CTM) developed in RAPRA[170,171] was shown to improve the dispersion/distribution of additives.

In this part of the programme, fluorescence and differential interference contrast (DIC) microscopy methods(as the two main microscopy methods) have been used in an attempt to obtain information on the structural modification of UPVC. To substantiate the observations of these two methods, other conventional microscopy methods (normal light, SEM and TEM) and physical property methods were also used.

The physical property methods used were impact test, solvent absorption and shrinkage test. A close study was also made on morphological changes along the extruder screws as a function of extrusion parameter. The use of UV fluorescence microscopy, it is hoped, would clearly reveal the structural changes and dispersion of stabilizer in the processed samples.

## 6.2 Results and Discussion

The results obtained with the microscopy techniques used in studying the morphological changes and the distribution of stabilizer in UPVC extrudates and extruder screw samples are reported in this section. For convenience the results will be discussed under the following headings. Effect of varying the concentration of lubricants; influence of the presence of 'secondary' additives; effect of different extrusion speeds and effect of different extrusion temperatures.

The results obtained also by physical experimental techniques employed will be used simultaneously to support or substantiate the microscopical observations.

### 6.2.1 Effect of Varying the Concentration of Lubricants

The two lubricants incorporated into the standard formulation are calcium stearate and GS Wax, and these are respectively internal and external lubricants. In order to study their effects on morphology and stabilizer distribution their ratios were varied

FIGURE 6.1: Micrographs of two vastly different formulations

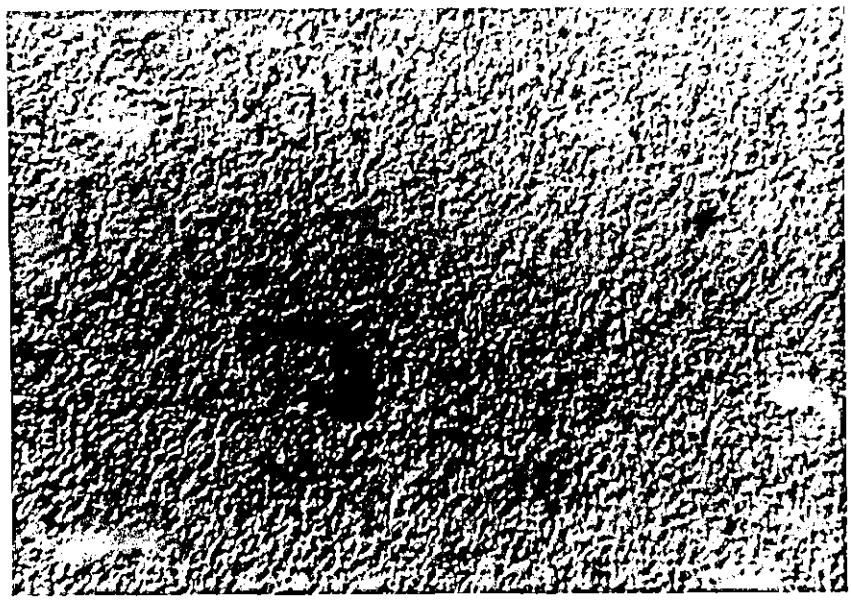

(a) Formulation 1
Contains 0.4 phr Cal. St.
0.3 phr Wax

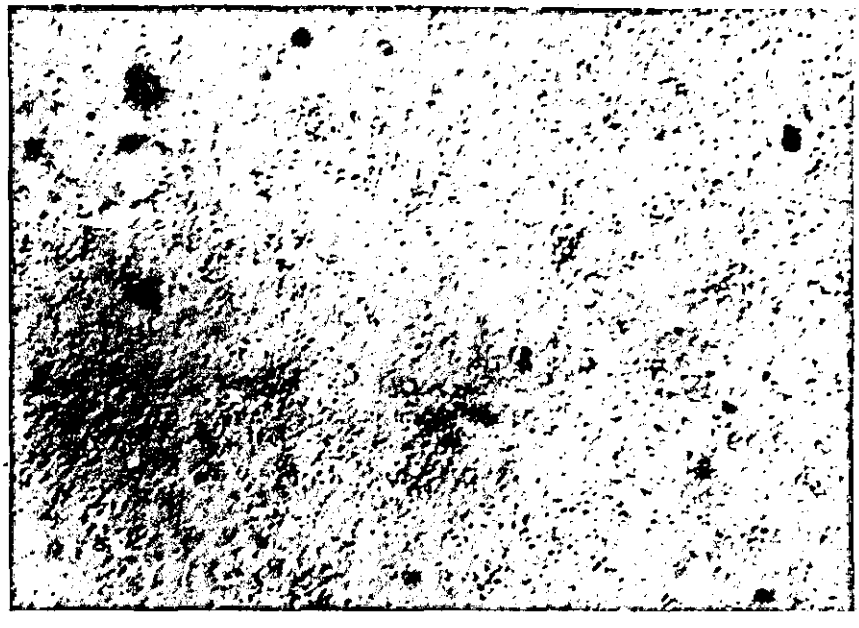

(b) Formulation 4
Contains 0.8 phr Cal. St.
0.15 phr Wax

30 μm

as indicated in formulations 1 to 4 (see Chapter 2, Section 2.2). In Figure 6.1 (a and b) is shown the differential interference contrast (DIC) micrographs of typical examples of samples prepared from formulations 1 and 4 respectively. Better homogeneity of matrix is evident in the blend containing higher level of internal lubricant (Figure 6.1b). The DIC micrographs of formulations 2 and 3 are not shown here because the homogeneity levels of their matrixes are similar to that of formulation 1. It is perhaps necessary to state that only a few sub-grains were observed by using UV fluorescence microscopy (Figure 6.2), even in the extremely less homogeneous matrix of formulation 1. This can be explained as a result of random distribution of stabilizer particles which in effect 'masks' the fluorescent property of the residual grains. In other words, large amounts of unfused residual grains (sub-grains) could be contained in the extrudates, although they were not all visible under the UV fluorescence microscope. To examine the presence of sub-grains a petrological technique of sample preparation was used to obtain thin sections of highly polished surfaces (see Chapter 4, Section 4.2.1.1). This technique minimises the stresses introduced into the specimen during preparation and, moreover, the specimen is free of knife marks which often lead to image misinterpretations. The thin sections were then examined with normal light microscopy method in the transmitted mode. Figure 6.3 (a, b, c and d) shows that there are significant amounts of sub-grains in the extrudates - indicating poor fusion of particles. The degree of homogeneity or grain fusion appears to depend on the composition of the formulations. The highest amount of sub-grains is observed in the standard formulation. By either decreasing the quantity of external lubricant or increasing that of the internal lubricant the number of sub-grains was greatly reduced. Simultaneous reduction and increment of the external and internal lubricants respectively produced samples with very little residual grains Figure 6.3(c and d)). This strongly suggests that the degree of homogeneity of UPVC matrix is affected by the concentration of

FIGURE 6.2: Fluorescence micrographs of different formulations

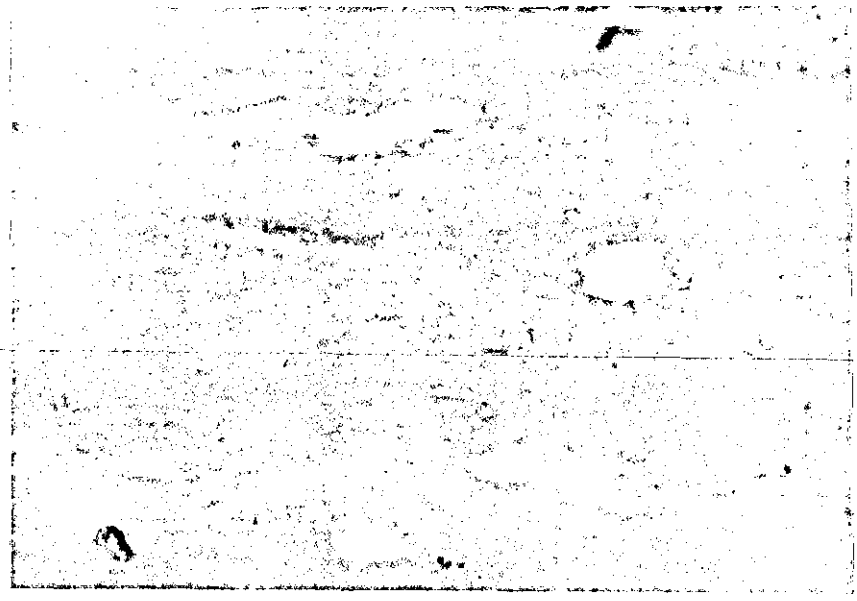

(a) Formulation 1 (standard formulation)
Contains 0.4 phr Calcium stearate
0.3 phr Wax

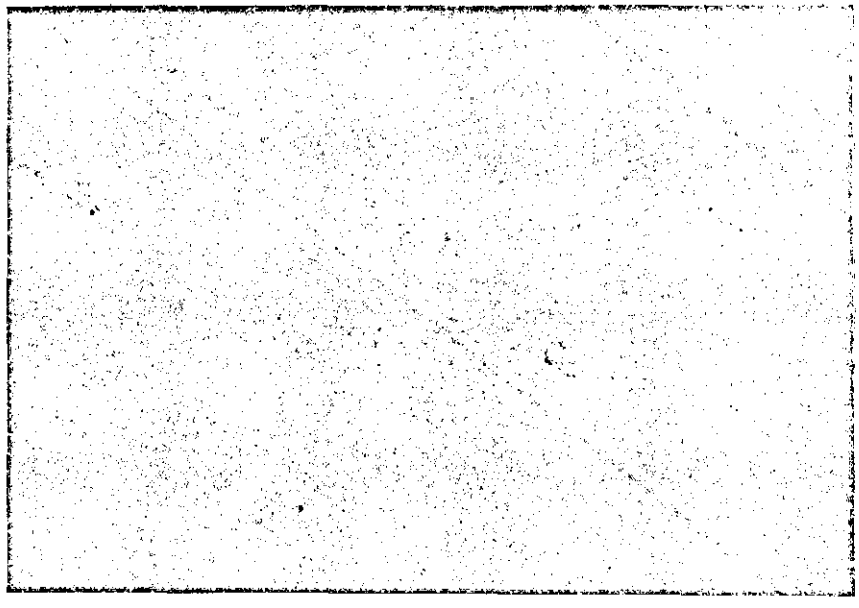

(b) Formulation 4
Contains 0.8 phr Calcium stearate
0.15 phr Wax
(No evidence of sub-grains in the matrix)

50μm

6.3: Normal light photomicrographs of samples prepared by petrological technique showing influence of lubricants' concentrations on morphology and distribution of stabilizer

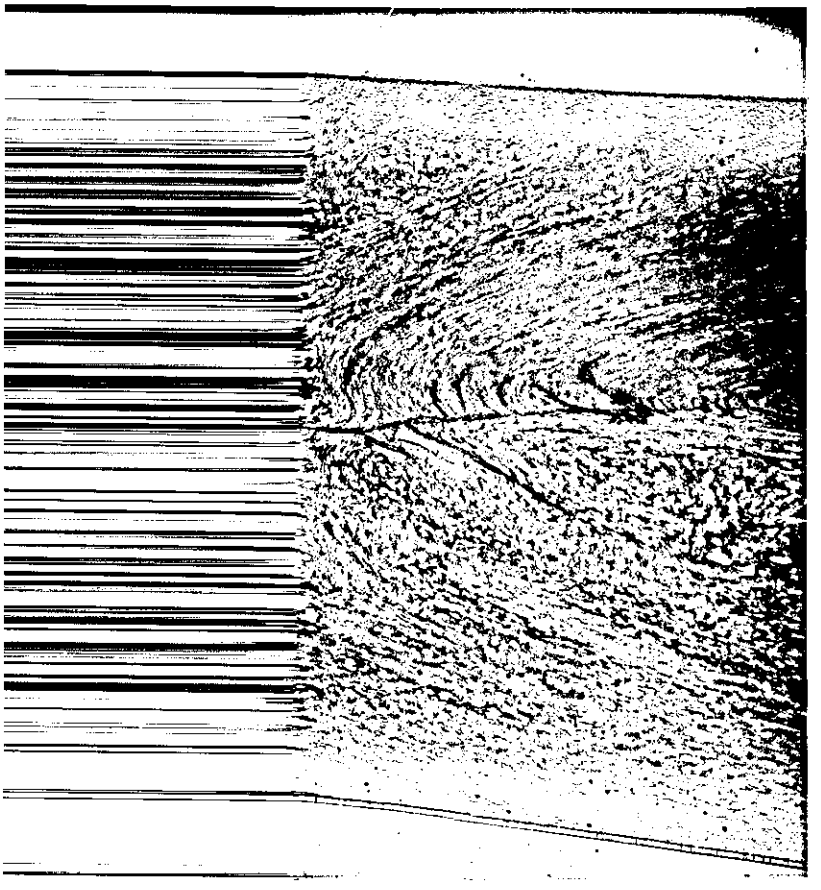

ormulation 1; Cal St 0.4;
Wax 0.3 phr
standard formulation)

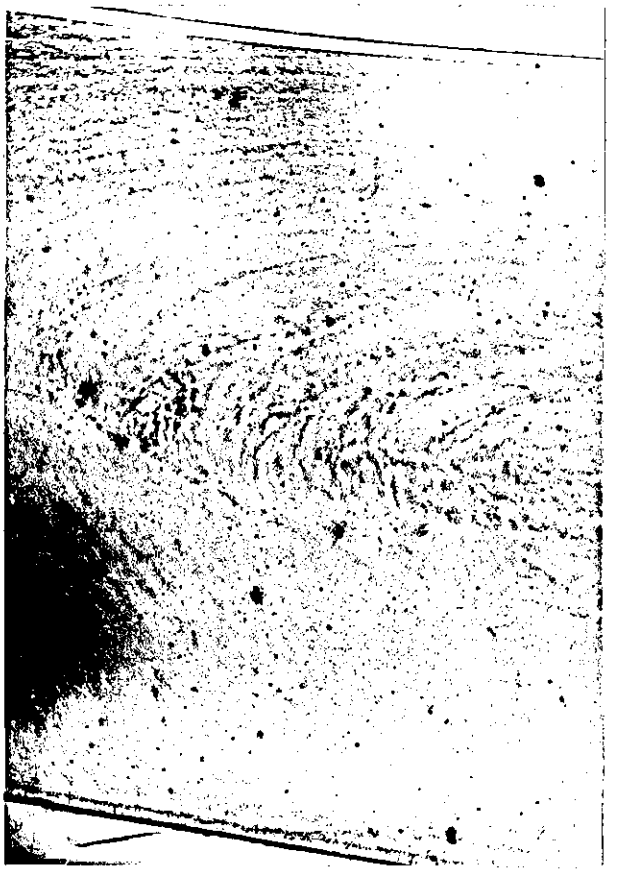

(b) Formulation 2: Cal St 0.4;
Wax 0.15 phr

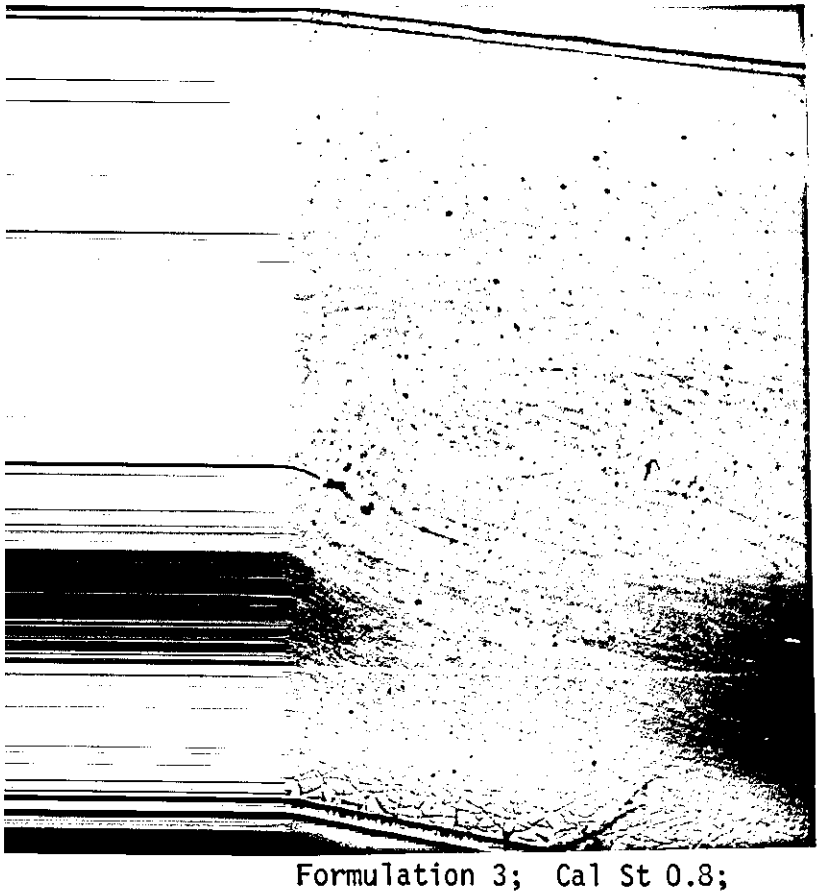

Formulation 3; Cal St 0.8;
Wax 0.3 phr

(d) Formulation 4; Cal St 0.8;
Wax 0.15 phr

500um

lubricant, in broad agreement with the observations of Gale[165] and Berens et al[65]. This experiment also confirmed that the loss of fluorescence intensity or fluorescing structure is largely due to random dispersion of the stabilizer particles.

Since high degree of mixing is closely associated with better distribution of additives, the comparison of micrographs a, b, c and d in Figure 6.3 show that the distribution of the lead stabilizer is best in formulation 4 and worst in formulation 1. Apart from poor stabilizer distribution the degree of fusion of primary particles is also found to be lower in formulation 1 than in formulation 4. In Table 7.6 the result from differential scanning calorimeter test shows that high heat of fusion is identified with formulations containing higher concentration of internal lubricant. The result agrees with the absence of sub-grains in formulation 4 (which contains high concentration of internal lubricant), since higher fusion implies higher chain entanglement density. To closely investigate the distribution of stabilizer particles the transmission electron microscope was used - a method that can show the detailed distribution of the lead stabilizer and the presence of, perhaps, micro-voids. However, with this method very little difference in stabilizer distribution between the formulations was observed, but it revealed the presence of micro-voids. Typical examples are shown in Figure 6.4 (a and b) which are respectively TEM micrographs of formulations 1 and 4. The micro-voids (average size of approximately 0.5 μm) are clearly seen to be associated with the stabilizer. They seem to occur where there are stabilizer agglomeration in the UPVC matrix and predominantly in the centre of the extrudates. By comparison, more micro-voids were found in formulation 1 than in formulation 4. This is probably because of the greater difference in ratio between external and internal lubricants in formulation 4 - which permits an increase in melt elasticity of the material and subsequent increase in degree of fusion and distribution of stabilizer. Since the stabilizer particles are

FIGURE 6.4: TEM photomicorgraphs showing stabilizer particles and micro-voids. Mag. x 20K

(a) Formulation 1

(b) Formulation 4

well distributed the micro-voids associated with stabilizer agglomeration and/or which are formed by hydrogen chloride evolution are greatly reduced. To a large extent, this observation agrees with the earlier suggestion that the absence of residual grains is associated with better stabilizer distribution.

Differences in the morphology of the extrudates were further evaluated by some physical testing methods: impact strength measurements, solvent absorption test and orientation measurements. The effect of lubricants concentration on the physical property of the extrudates is evident by comparing the data in Tables 6.1, 6.2 and 6.3. Impact strength is observed to increase with either lower levels of wax or higher levels of calcium stearate. Highest impact strength is identified with formulation 4. This confirms that the absence of sub-grains in finished products leads to improved mechanical properties. This is in agreement with the observations made with microscopy methods and observations of Gale[125] and Allsopp[50] - that the fall in impact strength is caused, among other factors, by the presence of unfused material. Solvent absorption test shows formulations with higher calcium stearate to have lower % absorption values. This is contradictory to several workers observations[173-175] that higher gelled samples absorb more solvent than poor gelled ones. This anomaly is presumably due to the effect of higher lubricant concentration rather than degree of fusion - because at high gelation level solvent test has been proven to be inadequate for grading degree of gelation[175,176,125].

The orientation measurements carried out to determine the degree of strain introduced into the materials during extrusion processing also produced results in agreement with microscopical observations. The data obtained are shown in Tables 6.3 and 6.2 respectively for surface skin thickness and percentage shrinkage of the extrudates. Surface 'skins' are evident on all specimens but are more pronounced in those containing low concentration of

TABLE 6.1

Variation of different lubricants concentrations with impact strength as a function of stabilizer distribution in extruded samples

| Formulation Number | Additive type and ratio (phr) | | Impact strength (kJ $m^{-2}$) | | | | | |
|---|---|---|---|---|---|---|---|---|
| | Cal.St. | G.S.Wax | 1 | 2 | 3 | 4 | 5 | Average |
| 1* | 0.4 | 0.3 | 16.52 | 16.26 | 16.27 | 17.63 | 16.82 | 16.70 |
| 2 | 0.4 | 0.15 | 22.32 | 19.81 | 19.69 | 18.86 | 21.05 | 20.35 |
| 3 | 0.8 | 0.3 | 28.16 | 26.80 | 29.40 | 25.86 | 28.01 | 27.65 |
| 4 | 0.8 | 0.15 | 30.20 | 28.76 | 32.33 | 27.89 | 28.19 | 29.47 |

TABLE 6.2

Variation of different lubricants concentrations with % shrinkage as a function of stabilizer distribution in extruded samples

| Formulation Number | Additive type and ratio (phr) | | % Shrinkage (%) | | | |
|---|---|---|---|---|---|---|
| | Cal.St. | G.S. Wax | 1 | 2 | 3 | Average |
| 1* | 0.4 | 0.3 | 2.58 | 2.55 | 2.62 | 2.58 |
| 2 | 0.4 | 0.15 | 9.21 | 9.35 | 9.30 | 9.29 |
| 3 | 0.8 | 0.3 | 7.92 | 8.26 | 8.30 | 8.16 |
| 4 | 0.8 | 0.15 | 7.68 | 7.20 | 7.37 | 7.42 |

* = standard formulation

Cal. St. = calcium stearate

G.S. Wax = G.S. Wax 2411P

TABLE 6.3:

Variation of different formulations with physical properties as a function of stabilizer distribution in extruded samples

| Formulation Number | Additive type and ratio (phr) | | Skin thickness (mm) | Solvent-Absorption (%) | Extruder-Output Rate (kg $hr^{-1}$) |
|---|---|---|---|---|---|
| | Cal. St. | G.S. Wax | | | |
| 1* | 0.4 | 0.3 | 0.270 | 18.16 | 7.44 |
| 2 | 0.4 | 0.15 | 0.365 | 19.04 | 7.32 |
| 3 | 0.8 | 0.3 | 0.346 | 17.77 | 7.74 |
| 4 | 0.8 | 0.15 | 0.479 | 17.91 | 7.68 |
| 5** | 0.2 | OPW | 0.221 | 17.59 | 7.53 |
| 6** | 0.4 | GMS | 0.115 | 19.93 | 7.65 |
| 7** | 1.5 | K120N | 0.167 | 25.59 | 7.74 |
| 8** | 1.5 | NLS | 0.206 | 20.15 | 8.31 |

* = Standard formulation

** = Standard formulation containing the 'secondary' additive indicated

OPW = Oxidised polyethylene wax

GMS = Glycerol monostearate

K120N = Paraloid K120N

NLS = Normal lead stearate

Cal St = Calcium stearate

GS Wax = GS Wax 2411P

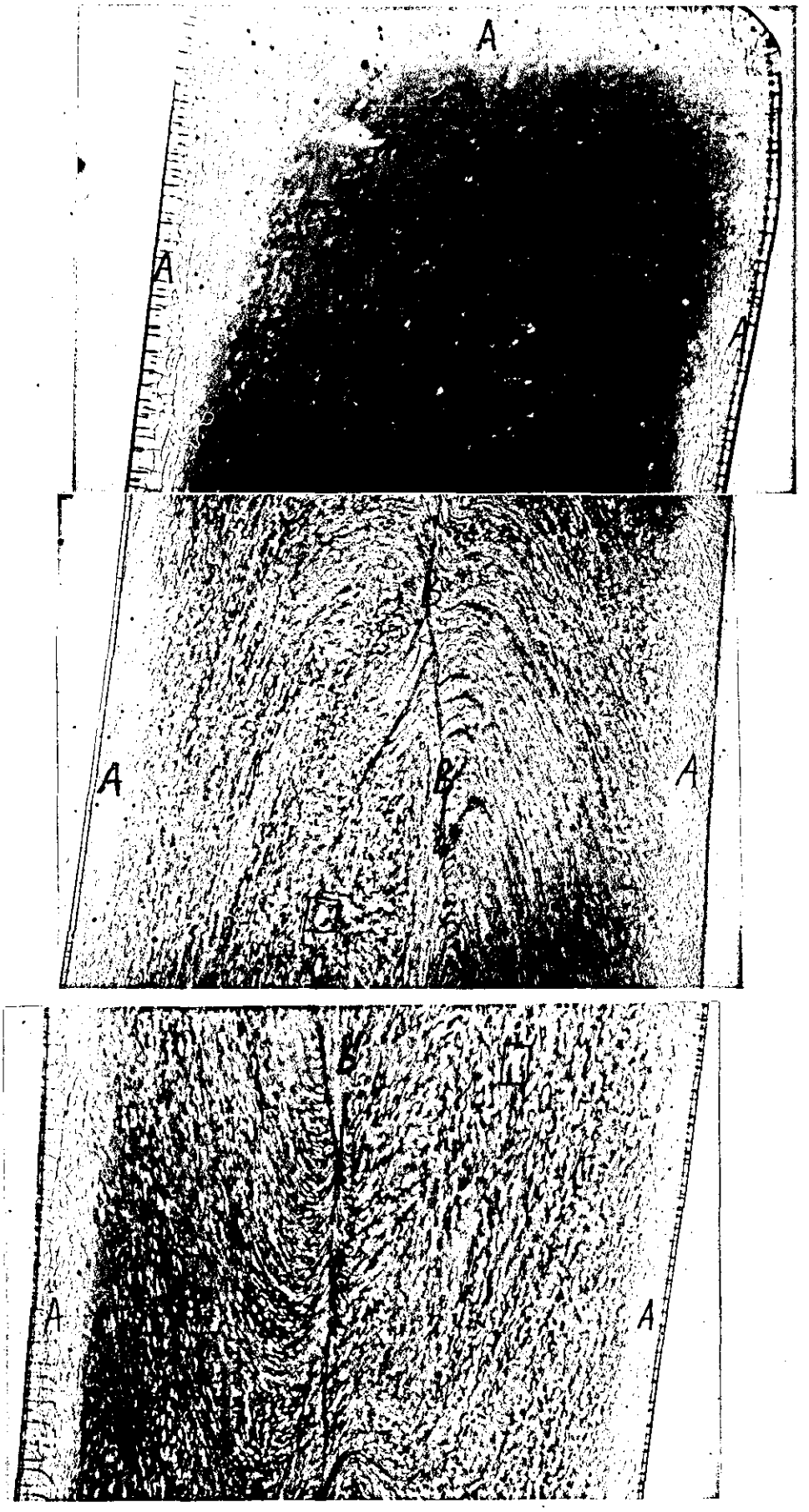


FIGURE 6.5: Normal-light photomicrograph of sample prepared by petrological technique. Sample of formulation 1 showing examples of some of the features observed in the extrudates with light microscopy.
'A' = surface skin
'B' = weld lines of polymer melts from the two screws
□ = sub-grains (residual grains) in the extrudate

external lubricant. These 'skins' are textureless and less opaque, when viewed under the normal light microscope, than the centre of the extrudate (see Figure 6.5). The topography of the matrix suggests that the presence of skin is not only as a result of the temperature difference between the extrudates and their cooling environment, but also due to the polymer flow and shear characteristics near the die surface. A similar trend was obtained from shrinkage measurement, but the effect of formulation variations on shrinkage is much more higher, as shown in Table 6.2. This result agrees very well with microscopical observations being that high shrinkage is identified with samples containing less residual grains (i.e. samples with high degree of fusion of primary particles).

### 6.2.2 Influence of the Addition of 'Secondary' Additives

Changes in morphological features and distribution of stabilizer (dibasic lead stearate) by incorporation of 'secondary' additives into the standard formulation are shown in Figures 6.6 to 6.9. The data from physical property evaluations are summarised in Tables 6.4 and 6.5. Fluorescence light and differential interference contrast (DIC) microscopical examination of formulations 1, 5, 6, 7 and 8 (respectively containing no 'secondary' additives, 0.2 phr oxidized PE wax, 0.4 phr glycerol monostearate, 1.5 phr paraloid KIZON and 1.5 phr normal lead stearate) show significant changes in morphology of formulations 7 and 8 . Only little improvement in morphology in formulations 5 and 6 was observed. In other words the addition of low concentration of slightly incompatible internal lubricants, into the standard formulation, slightly reduced the quantity of unfused sub-grains. The effect of these lubricants is clearly evident with polished specimens (Figure 6.8 (a, b, c, d and e)). However, the differential scanning calorimeter results show very little variations in their degree of fusion from the standard formulation (Table 7.6). Since both lubricants (oxidized polyethylene wax and

FIGURE 6.6: DIC micrographs of samples of different formulations

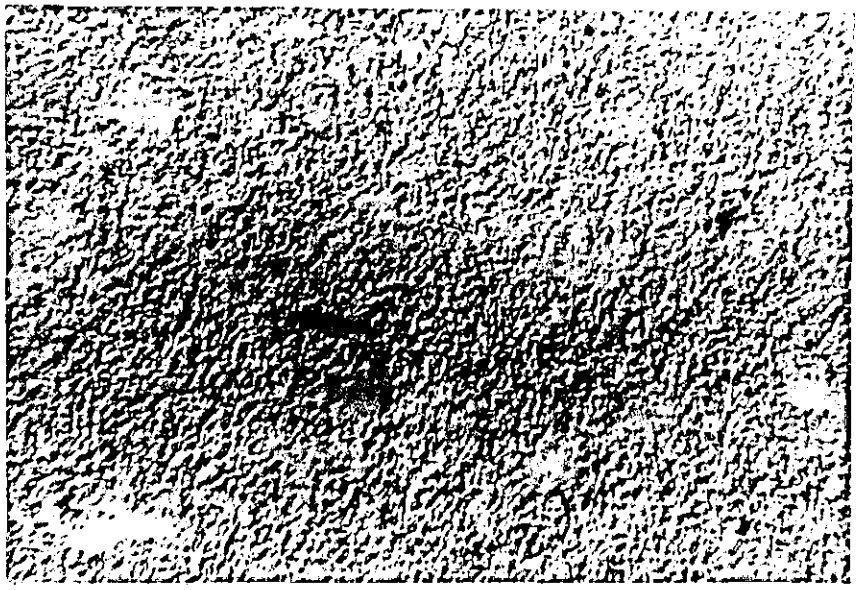

(a) Formulation 1
Contains no 'secondary' additive

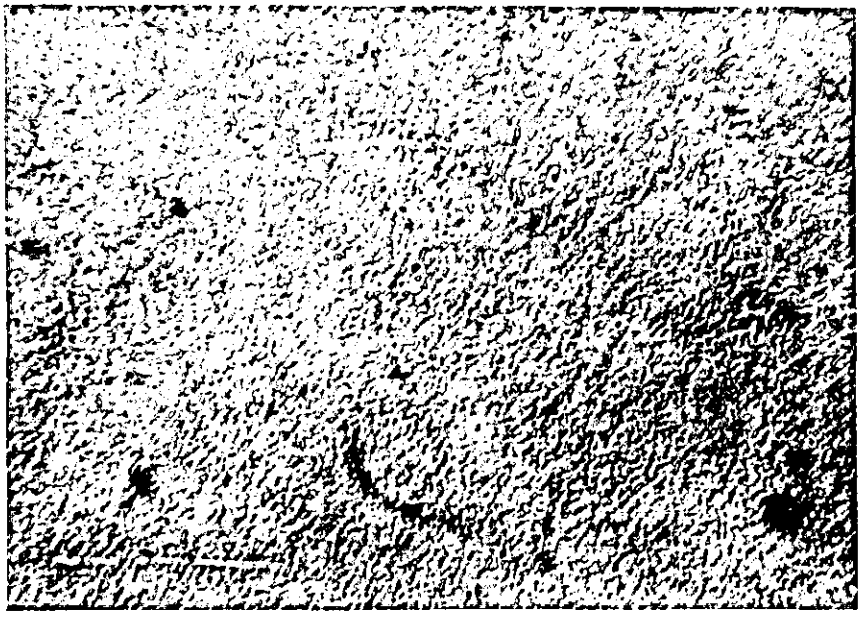

(b) Formulation 7
Contains 1.5 phr K120N (impact modifier)

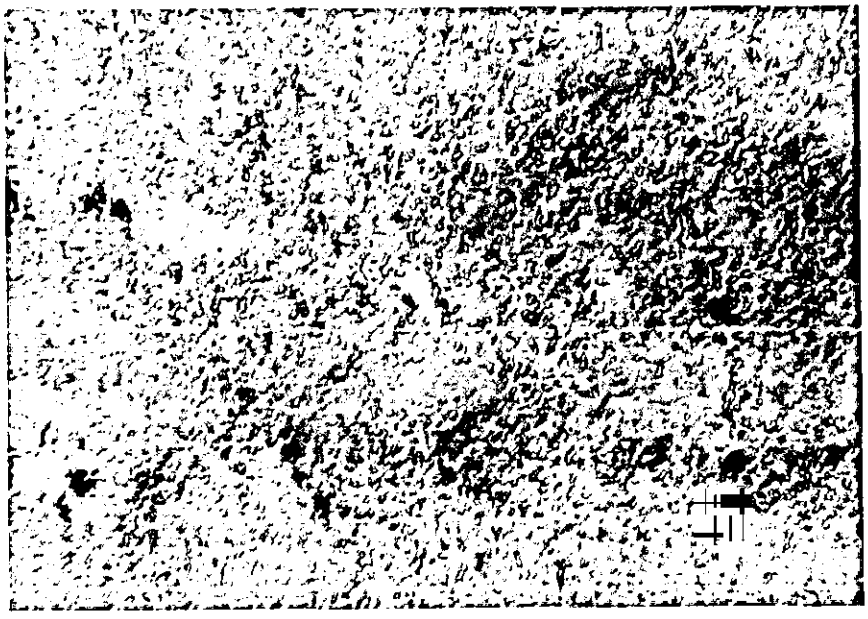

(c) Formulation 8
Contains 1.5 phr normal lead stearate

30μm

FIGURE 6.7: Fluorescence micrographs of samples of different formulations

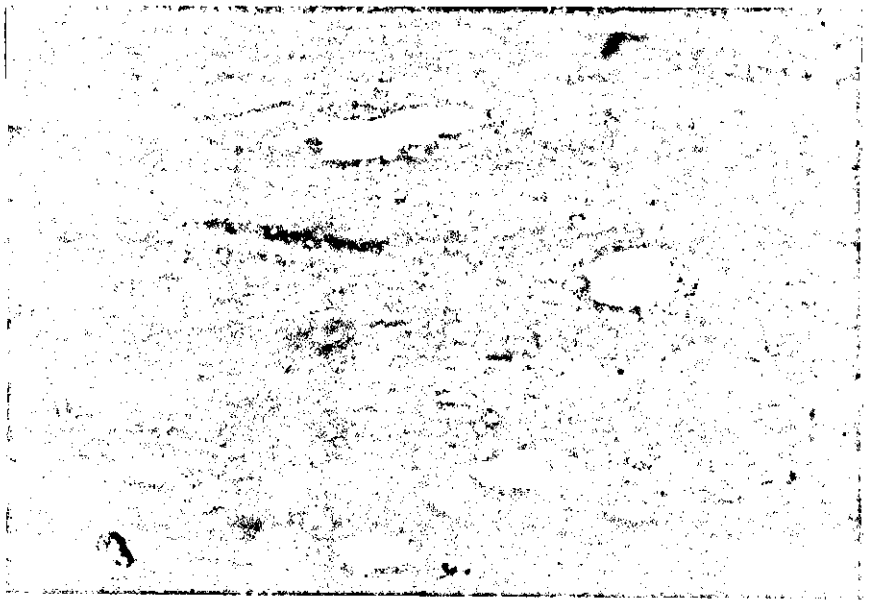

(a) Formulation 1 Does not contain 'secondary' additives

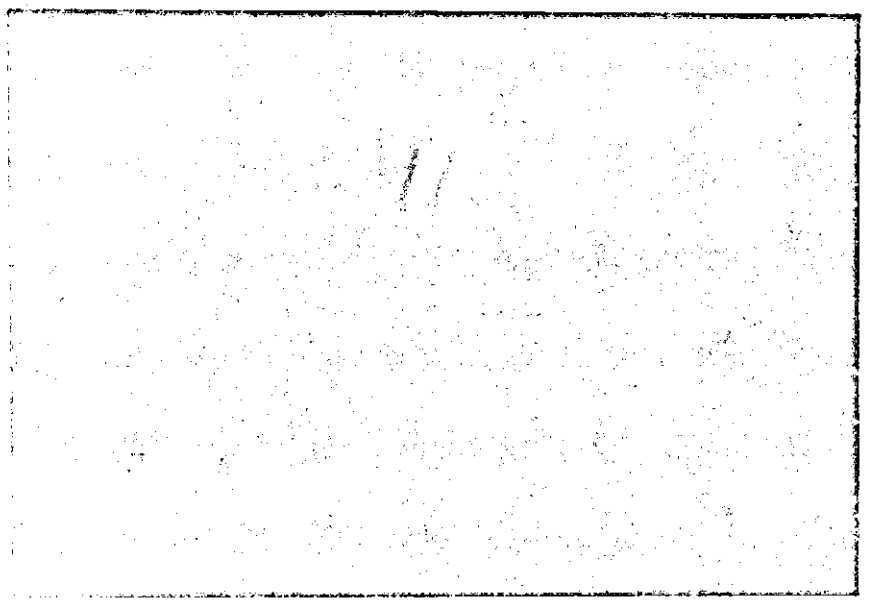

(b) Formulation 7 Contains 1.5 phr impact modifier (K120N). Reductic in the quantity c sub-grains and intensity of fluorescence

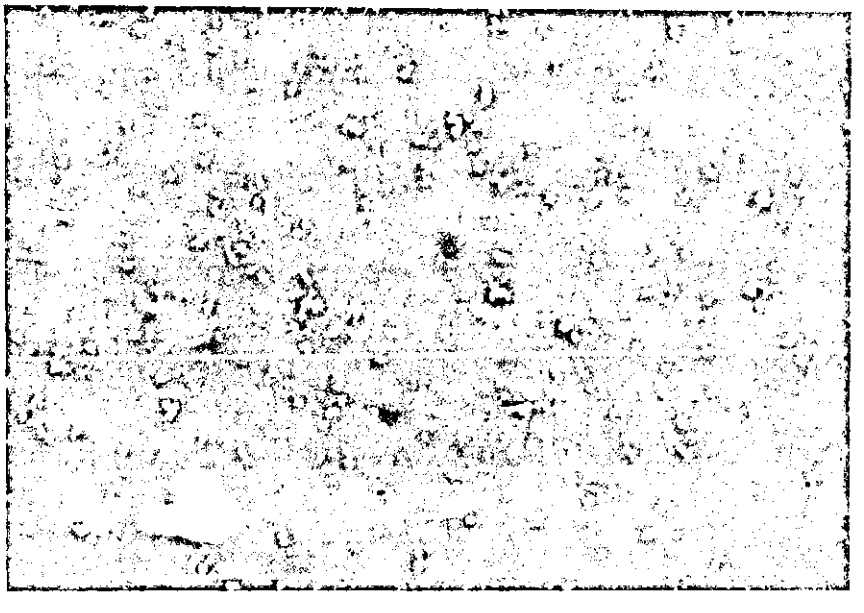

(c) Formulation 8 Contains 1.5 phr normal lead stearate stabili zer. (Poor sta- bilizer dispersio is clearly evident)

50μm

glycerol monostearate) have some external lubricating property they greatly reduce the friction between particles and surface of extruder barrel (vital for loss of particle identity), thereby promoting extrusion rate with little effect on morphology of the extrudates. This is clearly evident in Table 6.3 which shows the values of extruder output rate for formulations 5 and 6 to be higher than that of formulation 1.

Different situations occur with formulations 7 and 8 which contain respectively 1.5 phr paraloid K120N and 1.5 phr normal lead stearate. The effect of both 'secondary' additives on degree of stabilizer distribution and fusion of the sub-grains is evident from Figure 6.6 - DIC and Figure 6.7 - fluorescence micrographs and Figure 6.8 (a to e) - micrographs of polished surfaces. Paraloid K120N is an acrylic processing aid (see Chapter 2) which relaxes the molecular chains, therefore it produces extrudates whose matrix have a rubber-like texture. From Brabender fusion results (Chapter 5, Table 5.10) it was shown that the addition of Paraloid K120N reduced the fusion time of the standard formulation - suggesting that there will be fewer residual grains in its end product. In contrast, normal lead stearate is a lubricant-stabilizer hence it retards frictional heat thereby prolonging gelation period (this has also been demonstrated in the Brabender Plasticorder test in Chapter 5). Thus, the overall effect is better distribution of stabilizer particle at the expense of high degree of fusion. In Figure 6.7 (a, b, and c) the fluorescence light micrograph clearly shows that the stabilizer particles are uniformly distributed in the melt, but not seen absorbed into any of the residual grains, or even broken down into smaller sizes compared with formulations 1 and 7.

These differences in morphology of the extrudates were further examined by scanning electron microscopy (SEM) and transmission electron microscopy (TEM). Scanning electron micro-

FIGURE 6.8: Normal light photomicrographs of samples prepared by petrological technique showing influence of 'secondary' additives on morphology and distribution of stabilizer

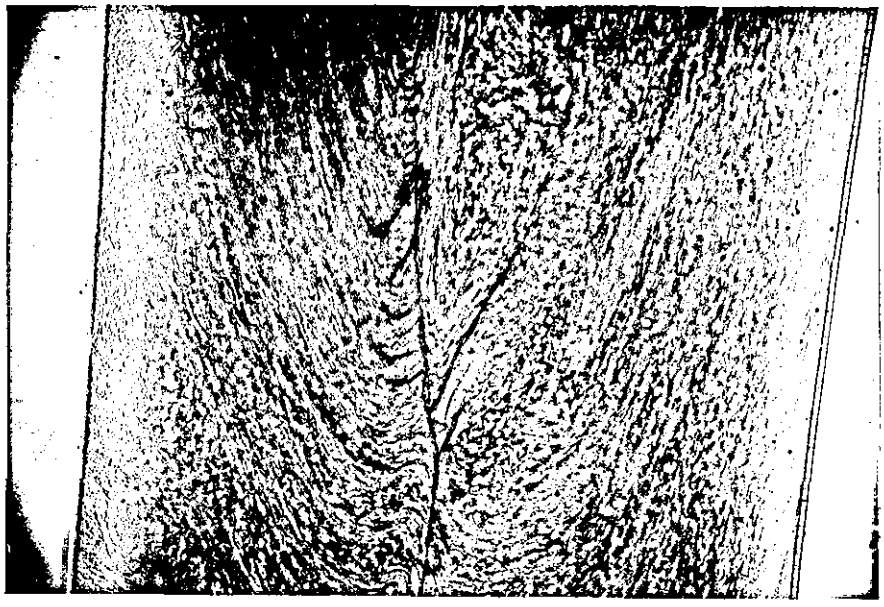

(a) Formulation 1 'secondary' additive (phr) 0; standard formulation

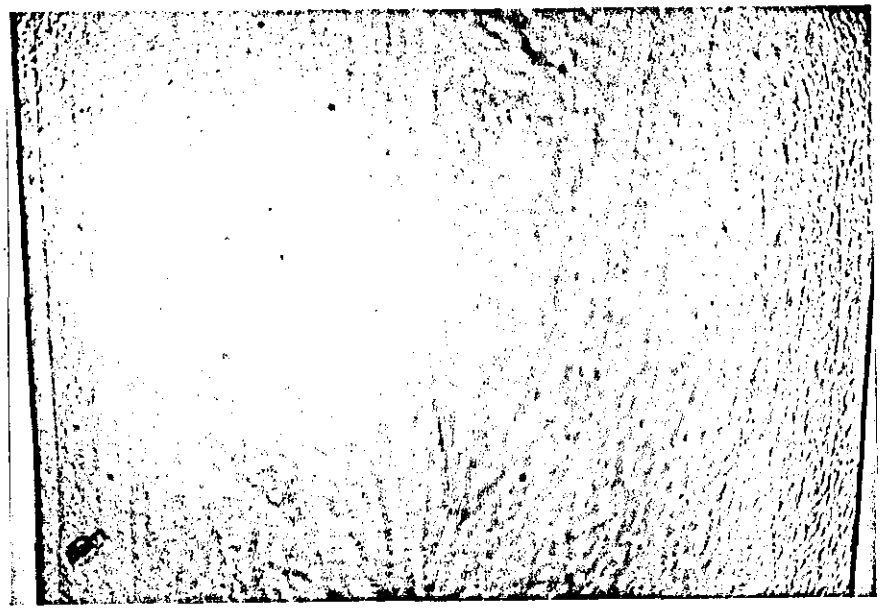

(b) Formulation 5; 0.2 phr Oxidized PHE wax

500μm

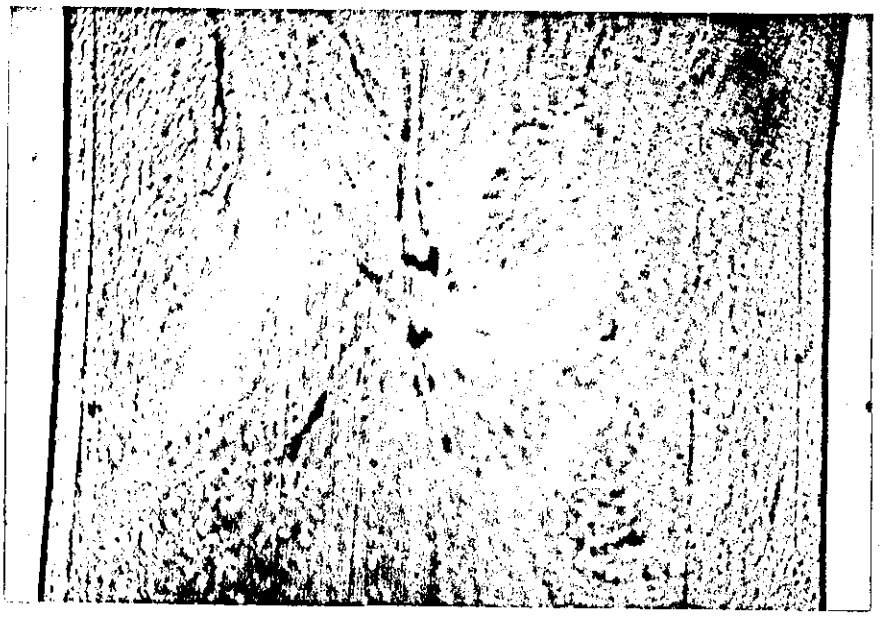

(c) Formulation 6; 0.4 phr Glycerol monostearate

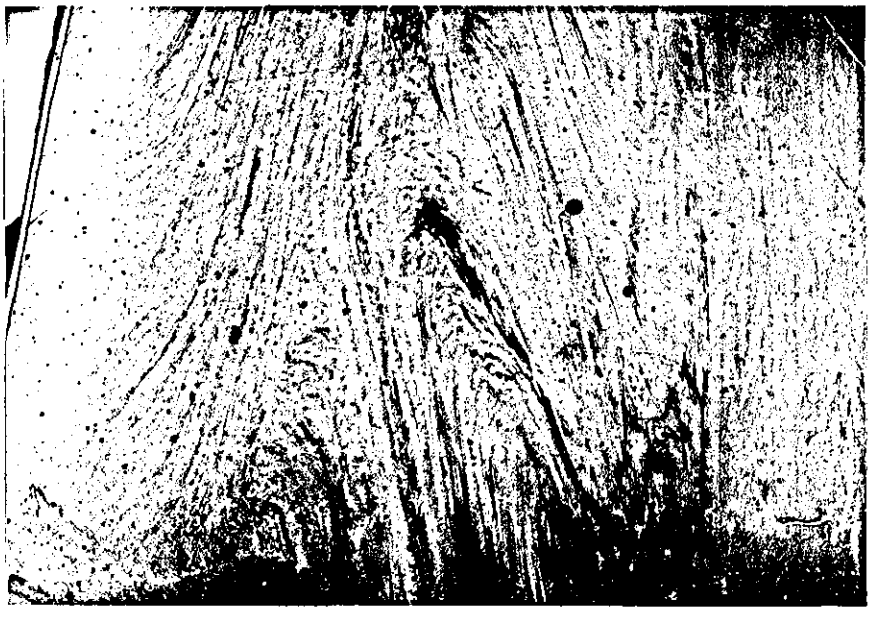

(d) Formulation 7; 1.5 phr Paraloid K120N

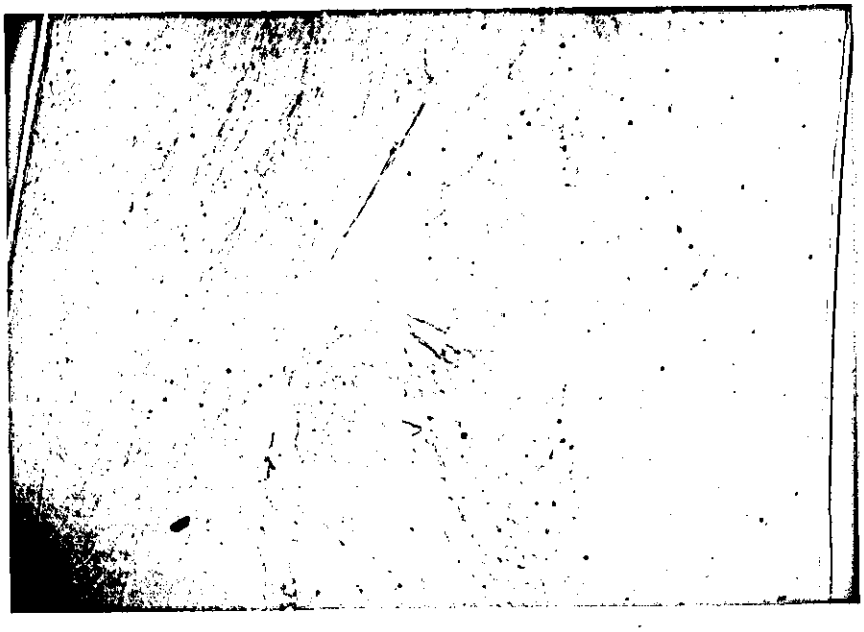

(e) Formulation 8; 1.5 phr Normal lead stearate

500μm

scopy of liquid nitrogen fractured surfaces of representative specimens of formulations 1, 7 and 8 are shown in Figure 6.9 (a, b and c). No noticeable difference in their topography is observed with this method, but primary particles and micro-voids are evident in all the samples. Examination of the surfaces of impact specimens reveals, as expected, that all the extrudates failed in a ductile manner. As transmission electron microscope (TEM) has better resolution, it was used to examine the distribution of the stabilizer and presence of micro-voids not clearly observable with SEM technique. The ultramicrotomed specimens examined show significant differences in distribution of stabilizer as well as in the presence of micro-voids between the formulations. It was observed that the incorporation of oxidized PE wax in formulation 5, and glycerol monostearate in formulation 6 appears to result in a poor stabilizer distribution in the extrudates. This is presumably due to the decrease in degree of mixing associated with higher levels of external lubricants. Since incorporation of these lubricants (external and internal) also decreases the melt elasticity it is expected to be detrimental to the physical property. However, an increase is observed in the impact strength, % shrinkage and solvent absorption while surface skin thickness decreases when compared with formulation 1. This anomalous physical property may be explained by the fact that both lubricants are regarded as possessing both internal and external lubricating properties, which means they exhibit different behaviour at different processing temperatures and formulations. Moreover, the extrudates, as shown with microscopy methods, contain slightly lower quantities of residual grains.

The TEM examination of formulation 7 shows a sporadic distribution of additive particles in the UPVC matrix. As will be clearly demonstrated in Chapter 7, the conglomerated particles are the stabilizer particles while the strips-like particles are the acrylic processing aid. In comparison with formulation 1 the micro-voids in formulation 7 were relatively fewer in number -

FIGURE 6.9: SEM photomicrographs of fracture surfaces of different formulations

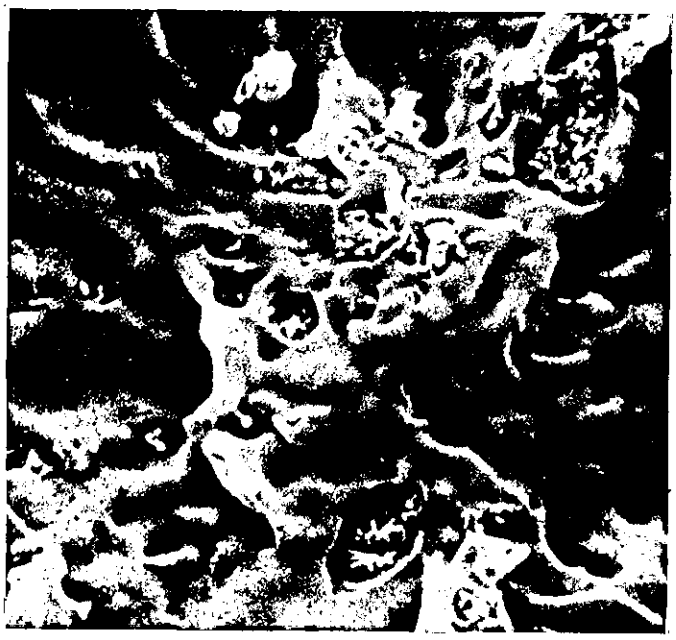

(a) Formulation 1; Contains no 'secondary' additive. Mag. x10K

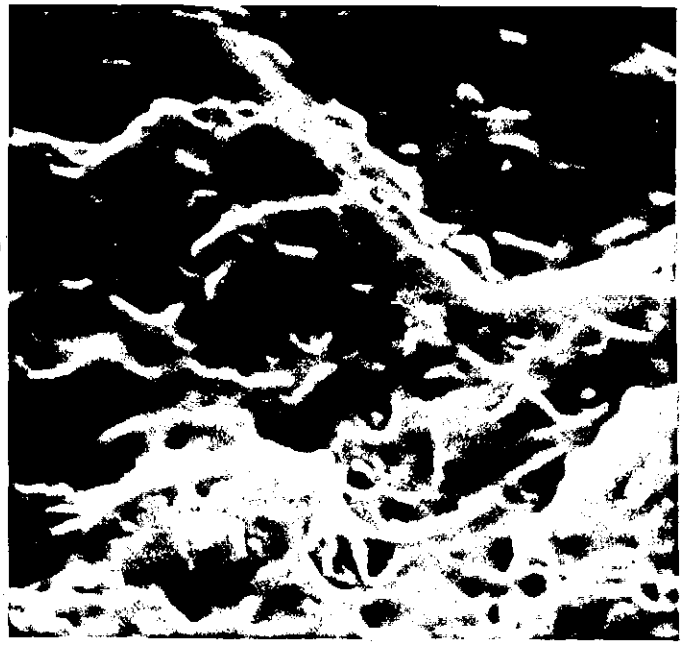

(b) Formulation 7; Contains 1.5 phr of Paraloid K120N Mag. x10K

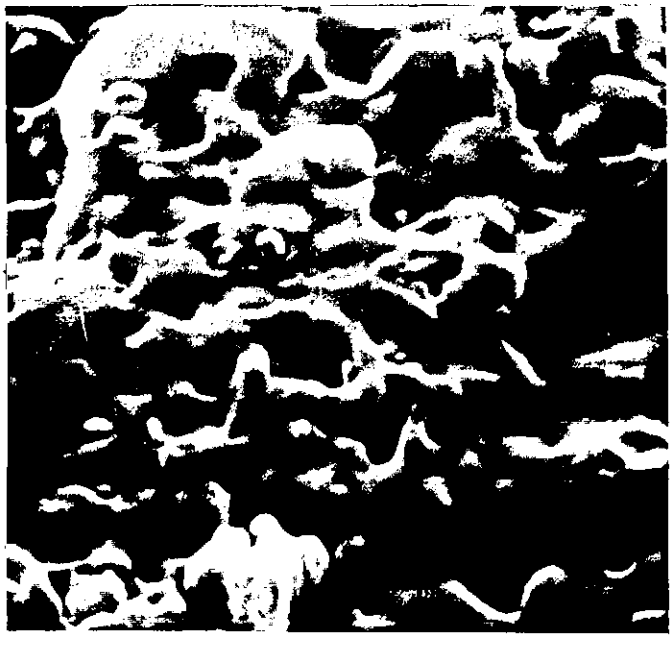

(c) Formulation 8; Contains 1.5 phr of normal lead stearate Mag. x10K

in agreement with the observation made with samples prepared by petrological technique. The fewer number of voids could be attributed to an improved level of gelation, obtained by incorporation of a processing aid[165]. This is also clearly illustrated in Table 6.4 where formulation 7 (containing acrylic processing aid K120N) shows a considerable increase in impact strength and % shrinkage over the rest of the formulations. Collins et al[177] have also shown that incorporation of acrylic processing aids with PVC compounds improves the rate of fusion and gelation level of the grains/primary particles. Decrease in surface skin thickness is also observed, presumably due to lower melt elasticity at the die. The rubber-like texture of its matrix and thin surface skin are the major factors that contributed to the pronounced absorption of solvent. This is in broad agreement with results of Menges et al[173], and confirms the higher solvent absorption principle of highly gelled samples.

Examination of ultramicrotomed sections of formulation 8 by TEM method reveals the scarcity of stabilizer particles in the extrudate, and the matrix to have low surface tension.* This is expected because of the replacement of half of the ratio of dibasic lead stearate with normal lead stearate. The morphology of this extrudate showed very little difference from that of the standard formulation. This can be explained by the fact that normal lead stearate has dual properties as an internal lubricant and a stabilizer. At normal extrusion temperature it behaves more like an internal lubricant thereby decreasing the degree of fusion of sub-grains. This is clearly demonstrated in Table 7.6 - where degree of fusion obtained by differential scanning calorimeter method confirmed that formulation 8 has the lowest heat of fusion compared with other formulations. The lower degree of fusion and surface tension also reflect on the physical property of the formulation. There is a pronounced decrease in impact strength and surface skin thickness while % solvent absorption and shrinkage are higher than in the standard formulation.

* Pronounced surface tearing during microtomy led to loss of stabilizer particles in the specimen.

TABLE 6.4:

Effect of 'secondary' additives on impact strength as a function of stabilizer distribution in extruded samples

| Formulation Number | Additive type and ratio (phr) | Impact Strength (kJ $m^{-2}$) | | | | | |
|---|---|---|---|---|---|---|---|
| | | 1 | 2 | 3 | 4 | 5 | Average |
| 1 | - | 16.52 | 16.26 | 16.27 | 17.63 | 16.82 | 16.70 |
| 5 | 0.2 OPW | 20.69 | 25.33 | 21.40 | 19.87 | 23.28 | 22.11 |
| 6 | 0.4 GMS | 24.55 | 27.81 | 26.09 | 24.83 | 26.35 | 25.93 |
| 7 | 1.5 K12ON | 36.01 | 32.84 | 31.92 | 34.46 | 29.88 | 33.02 |
| 8 | 1.5 NLS | 11.28 | 10.39 | 11.34 | 10.81 | 11.02 | 10.97 |

TABLE 6.5:

Effect of 'secondary' additives on shrinkage as a function of stabilizer distribution in extruded samples

| Formulation Number | Additive type and ratio (phr) | Shrinkage (%) | | | |
|---|---|---|---|---|---|
| | | 1 | 2 | 3 | Average |
| 1 | - | 2.58 | 2.55 | 2.62 | 2.58 |
| 5 | 0.2 OPW | 3.69 | 2.87 | 2.80 | 2.79 |
| 6 | 0.4 GMS | 8.30 | 8.27 | 8.91 | 8.28 |
| 7 | 1.5 K12ON | 10.33 | 10.50 | 10.13 | 10.32 |
| 8 | 1.5 NLS | 7.98 | 8.22 | 7.86 | 8.02 |

Evidence of its lubricating property is also shown in Table 6.3 where it is shown to exhibit the highest extrusion throughput. This means that the resident time in the extruder barrel was too little to permit complete breakdown and/or fusion of the sub-grains.

### 6.2.3 Effect of Different Screw Speeds on Extrudate Morphology

Changes in morphology and distribution of stabilizer as a function of screw speed was studied by extruding the standard formulation at screw speeds ranging from 20 to 50 rpm. The die temperature was set at 194$^{o}$C and the other zone temperatures adjusted correspondingly as listed in Table 2.7 (Chapter 2). Typical micrographs from differential interference contrast (DIC) and fluorescence light microscopical methods are shown in Figures 6.10 and 6.11 respectively. The figures show that there is little if any difference in the texture of samples extruded at two extreme speeds (compare 20 rpm with 50 rpm samples). This is because the pumping action of the screws provides the melt with little resident time in the barrel. In the fluorescence micrographs (Figure 6.11) it can be seen that at 30 rpm highest degree of particles fusion is achieved. Presumably, this is due to the existence of an equilibrium state between the mechanical input and output rate of the extruder at the screw speed. This will thus result in products of better mechanical property.

In Figure 6.12 the normal light micrographs of samples extruded at 20, 30 and 50 rpm also show that a significant increase in degree of mixing with increasing screw speed is obtained up to 30 rpm. Beyond 30 rpm larger size sub-grains are clearly visible, but the quantity of the sub-grains is small compared with samples extruded at 20 rpm.

To further study the extent of mechanical effect the SEM

FIGURE 6.10: DIC micrographs of samples extruded at different speeds

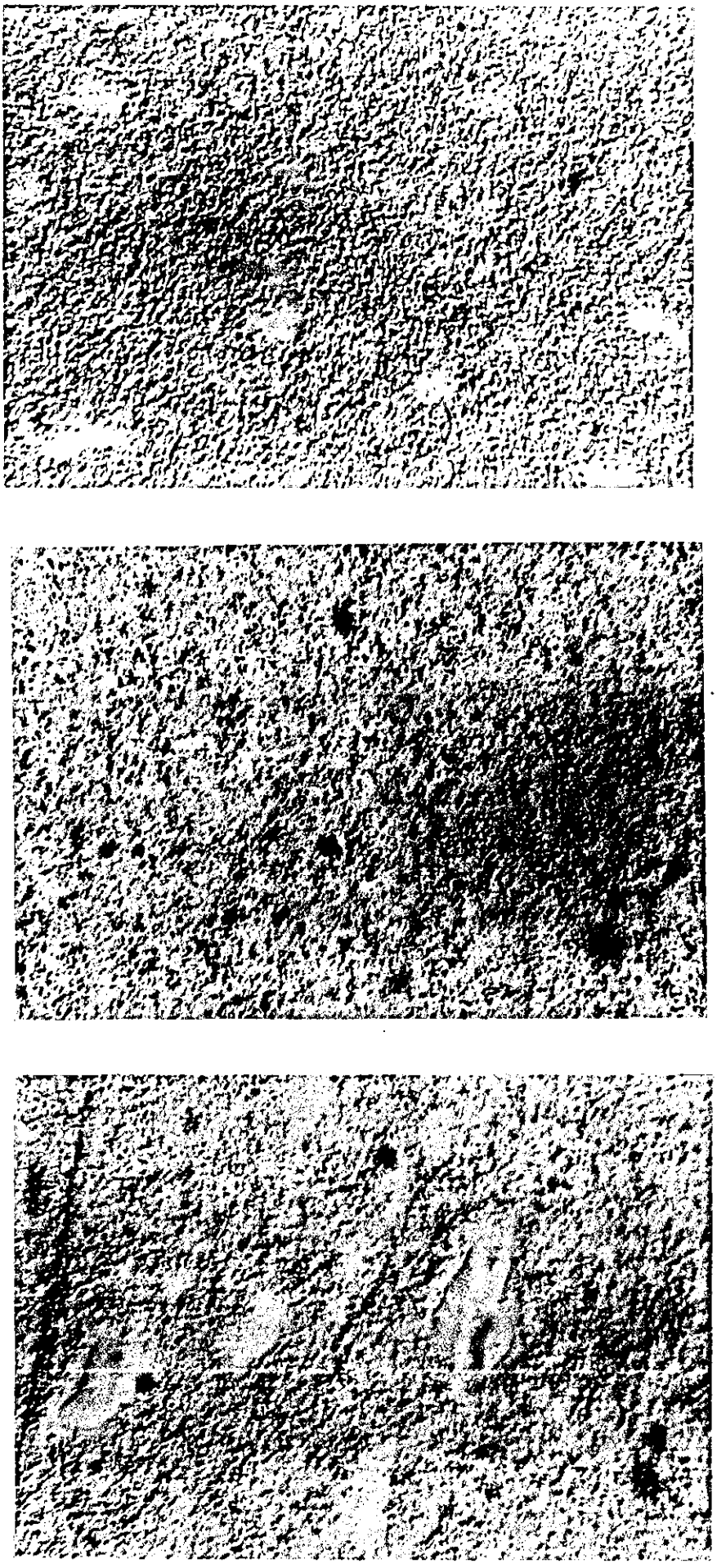

(a) Extruded at 20 rpm

(b) Extruded at 30 rpm

(c) Extruded at 50 rpm

30 μm

FIGURE 6.11: Fluorescence micrographs of samples extruded at different speeds

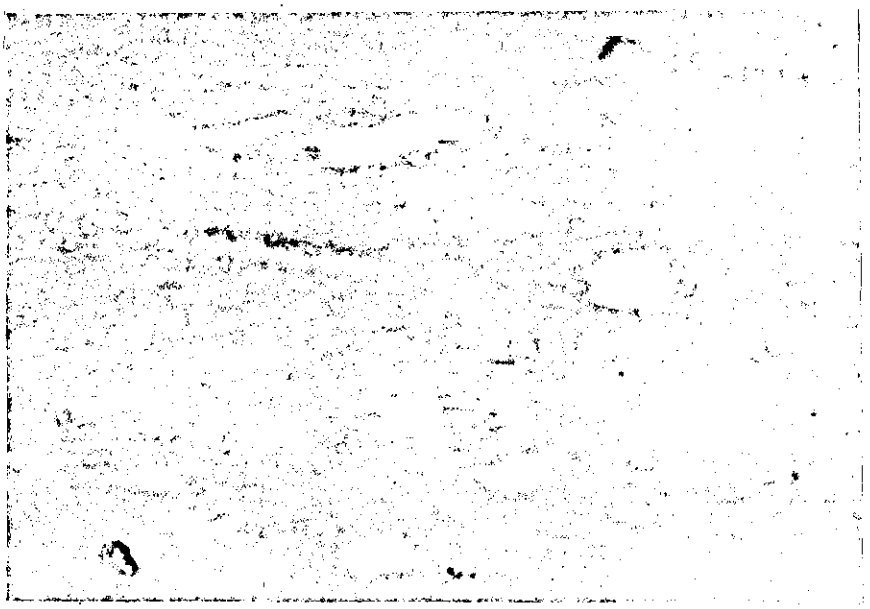

(a) 20 rpm

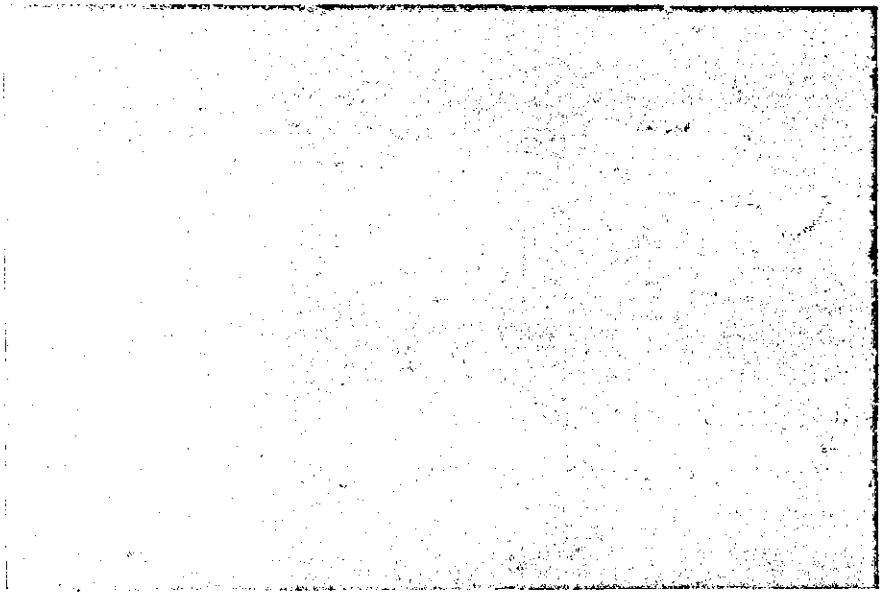

(b) 30 rpm

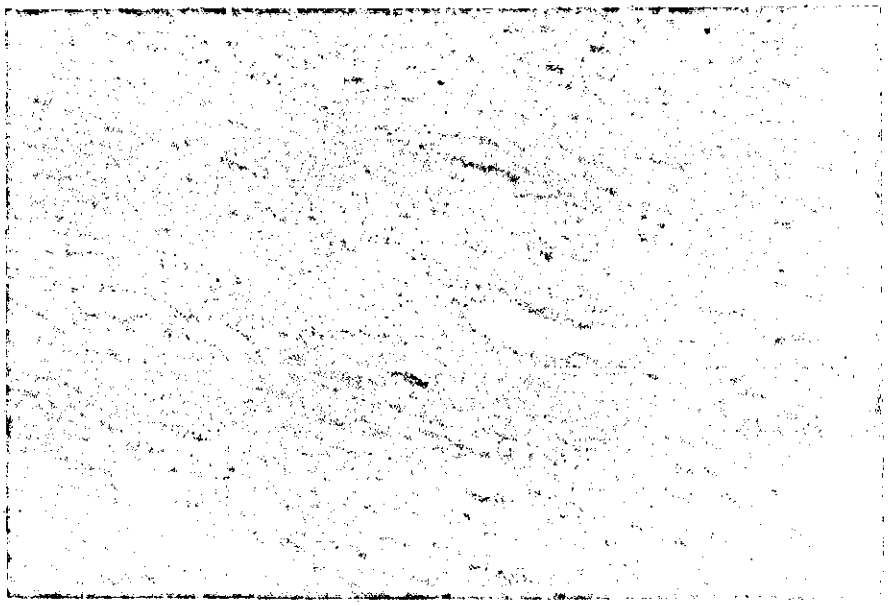

(c) 50 rpm

50μm

FIGURE 6.12: Normal light photomicrographs of samples prepared by petrological technique showing the effect of screw speed on morphology and distribution of stabilizer in formulation 1

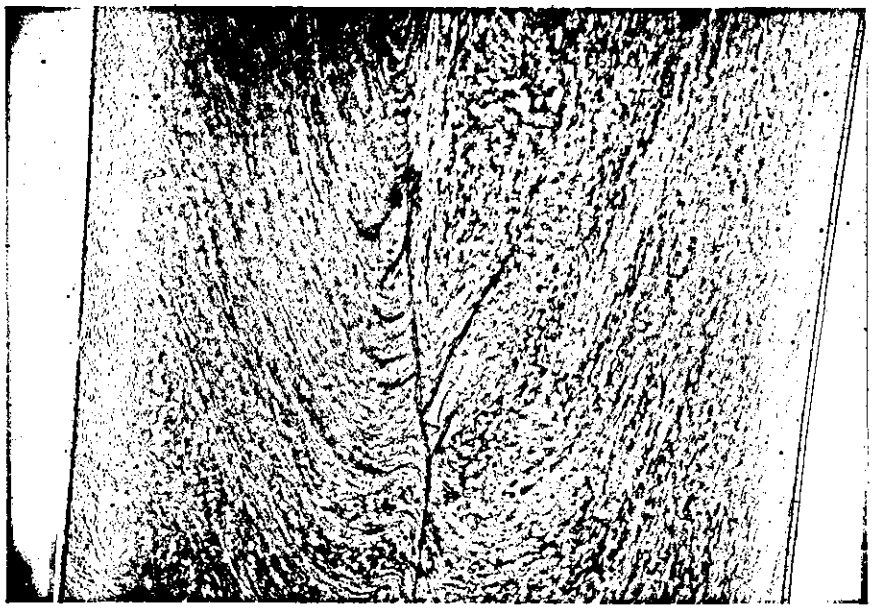

(a) Extruded at 20 rpm

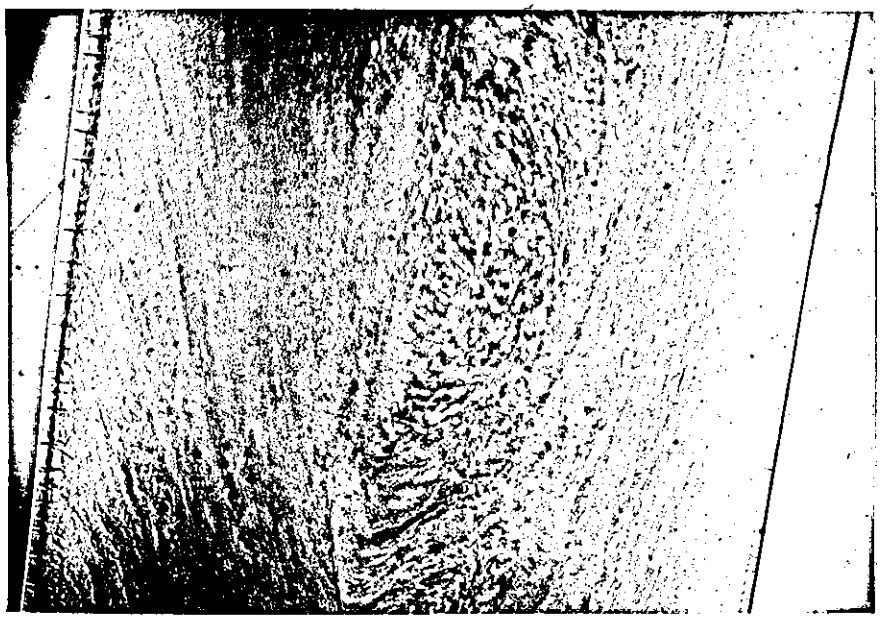

(b) Extruded at 30 rpm

(c) Extruded at 50 rpm

500 μm

was used to examine the presence of primary particles. Figure 6.13 shows that more primary particles are observed with higher screw speeds. This observation exposes two points of interest. First, high shear (mechanical) history results in mass exposure of primary particles at relatively short residence time. This means that in order to produce such a large number of primaries fairly large amounts of sub-grains must have been 'destroyed'.

. Secondly, mechanical history (screw speed) appears to have very little effect on the fusion or modification of the primary particles. This is why more primary particles were found with higher screw speed sample. This implies that the quality of product will be undermined by increase in screw speed, because of poor fusion of primary particles. (This point will be discussed later).

The short residence time of the melt in the extruder barrel will suggest less thermal history on the extrudates, and this is in substantial agreement with values of relative fluorescence intensity shown in Table 6.9. The relative fluorescence intensity is shown to increase at first - up to 30 rpm - before dropping sharply (Figure 6.14). This means that at low extrusion speed (long residence time) higher amounts of degradation are introduced into the product (but not high enough to affect the physical properties). To closely investigate the effect of shear history, the extrudates were evaluated with the differential scanning calorimeter - a method which has been successfully used to evaluate the thermal history and fusion level in processed UPVC[148,161,174,175]. Figure 6.15 shows that higher degree of fusion - which is associated with structural modification - increases with increasing screw speed. This result not only confirms the microscopical observations but also agrees with the conclusion of Gilbert et al[161] that fusion of primary particles is highly dependent on both the shear and thermal history of the PVC.

FIGURE 6.13: Fracture surfaces of samples extruded at different screw speeds

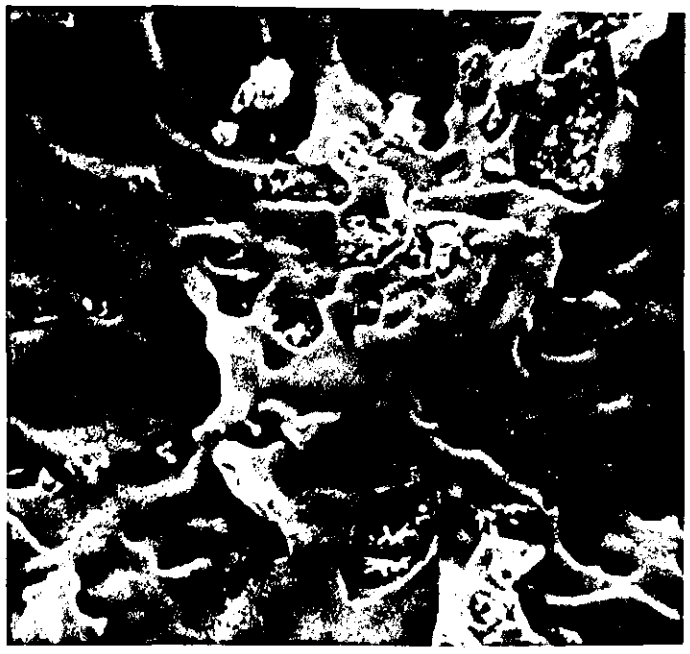

(a) Extruded at 20 rpm
Max. x10K

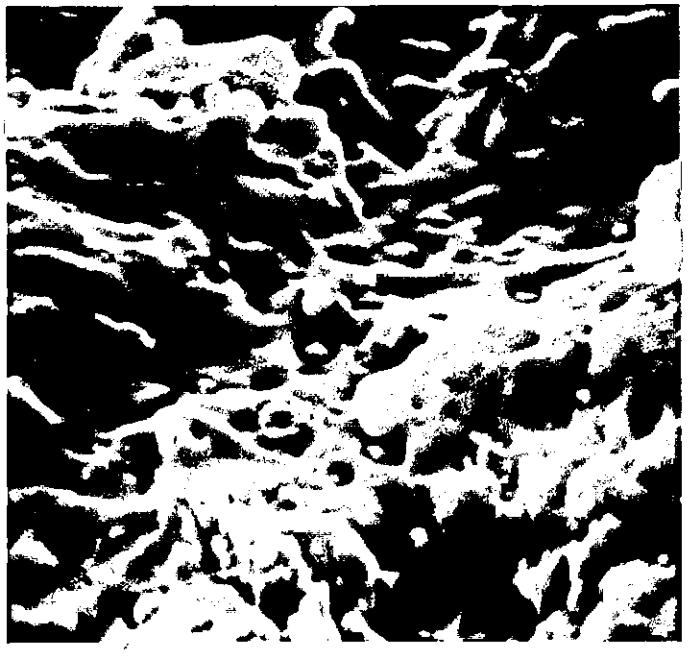

(b) Extruded at 30 rpr
Mag. x10K

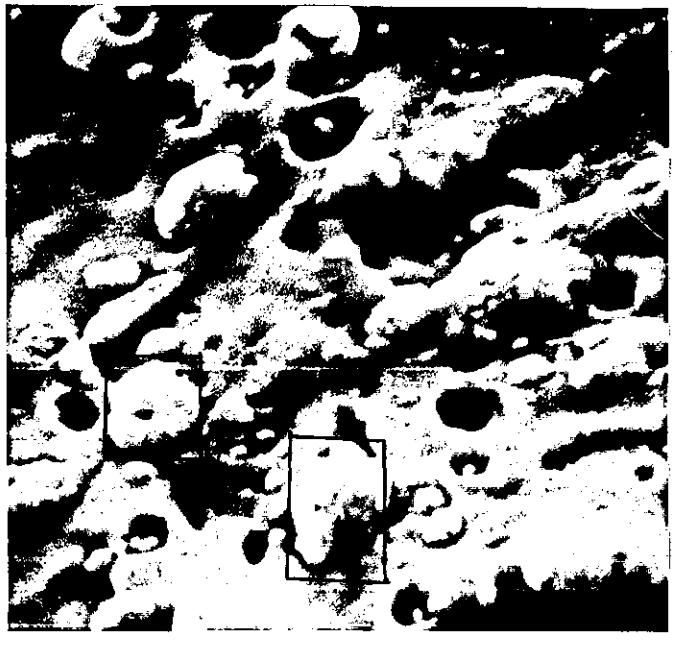

(c) Extruded at 50 rp
Mag. x10K

□ = Primary particles

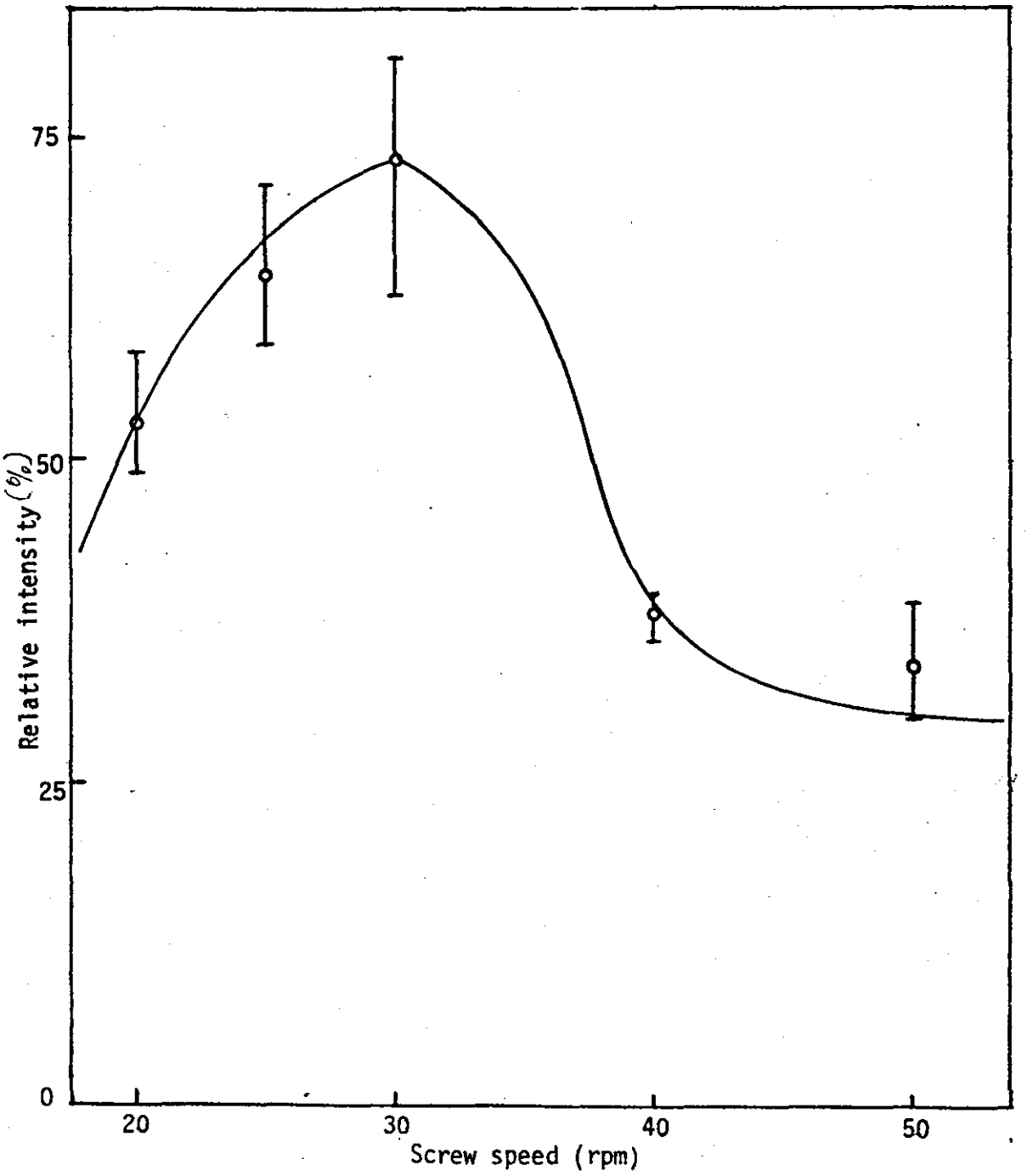


FIGURE 6.14: Fluorescence intensity of extrudates at different screw speeds

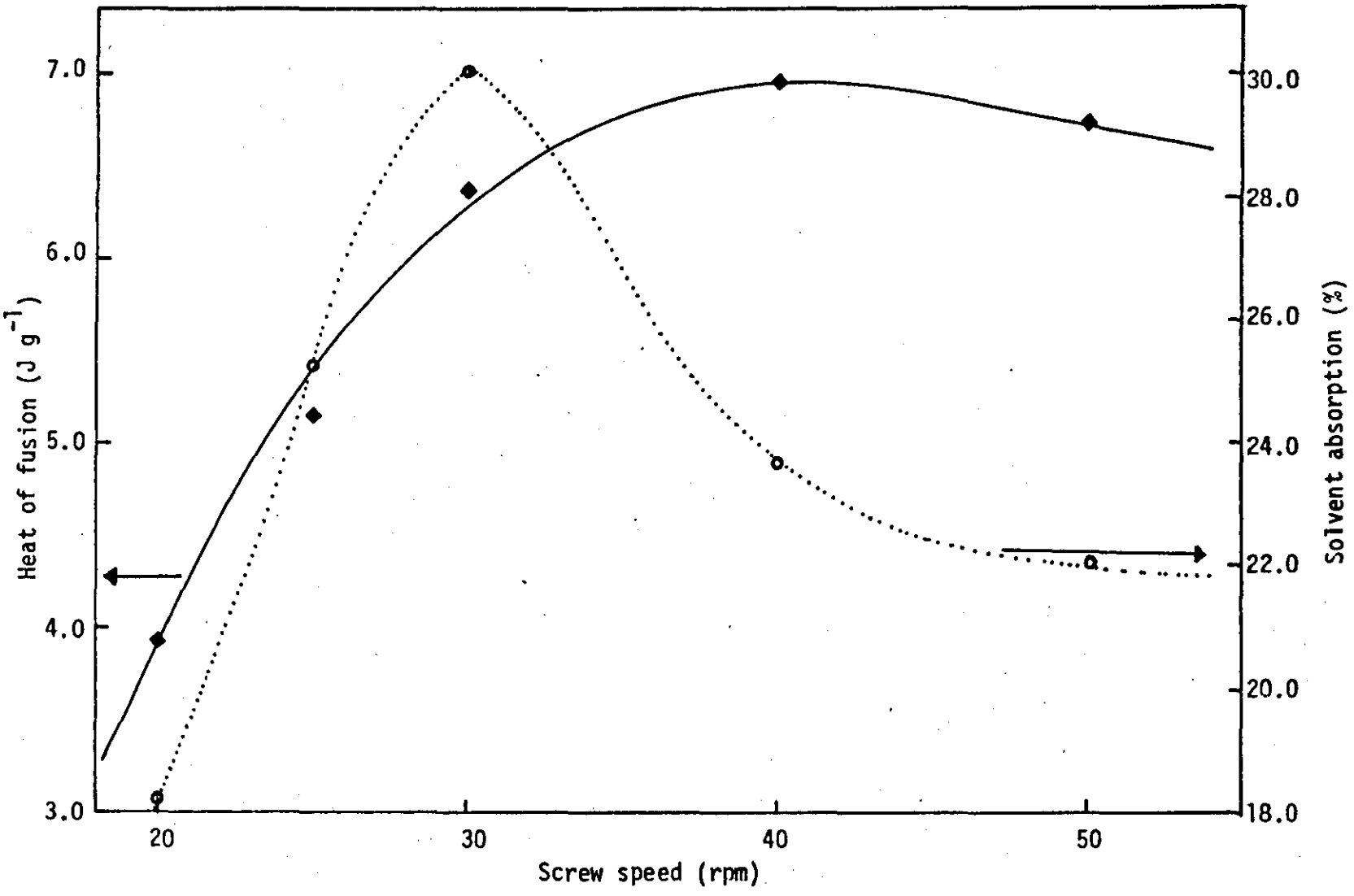


FIGURE 6.15: Variation of fusion characteristics with extruder screw speed

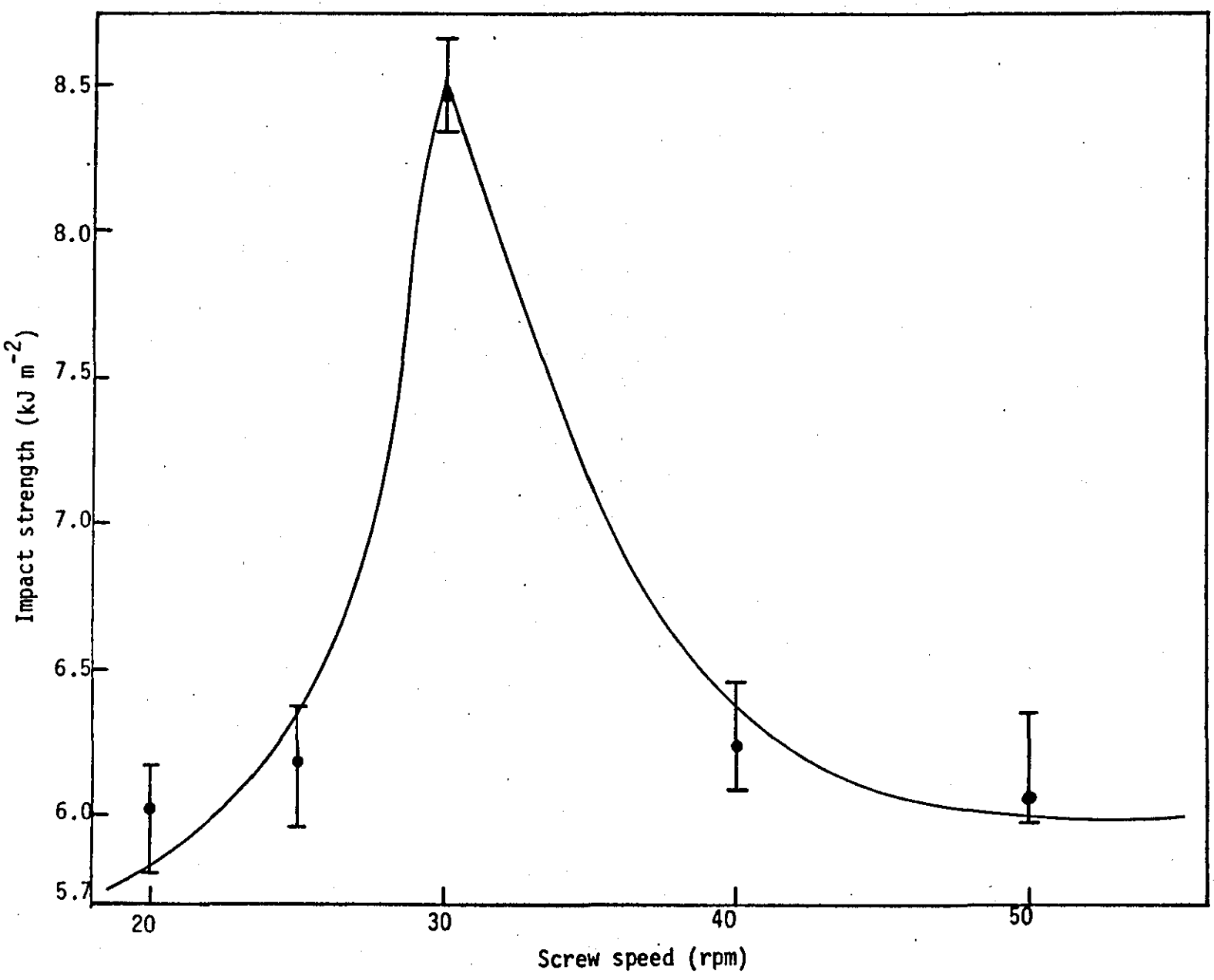


FIGURE 6.16: Variation of impact strength with extruder screw speed

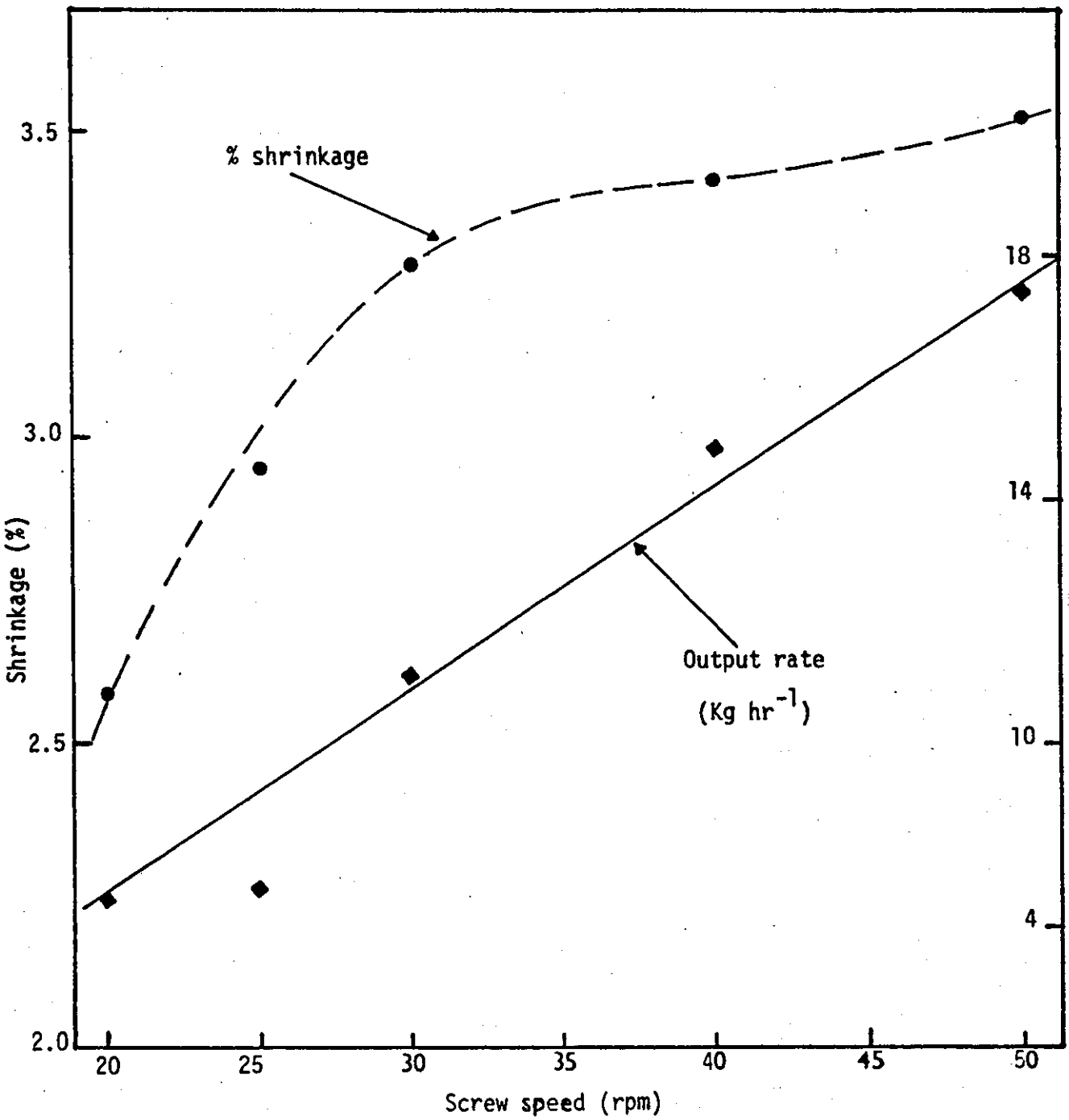


FIGURE 6.17: Effect of extruder screw speed on sample shrinkage and output rate

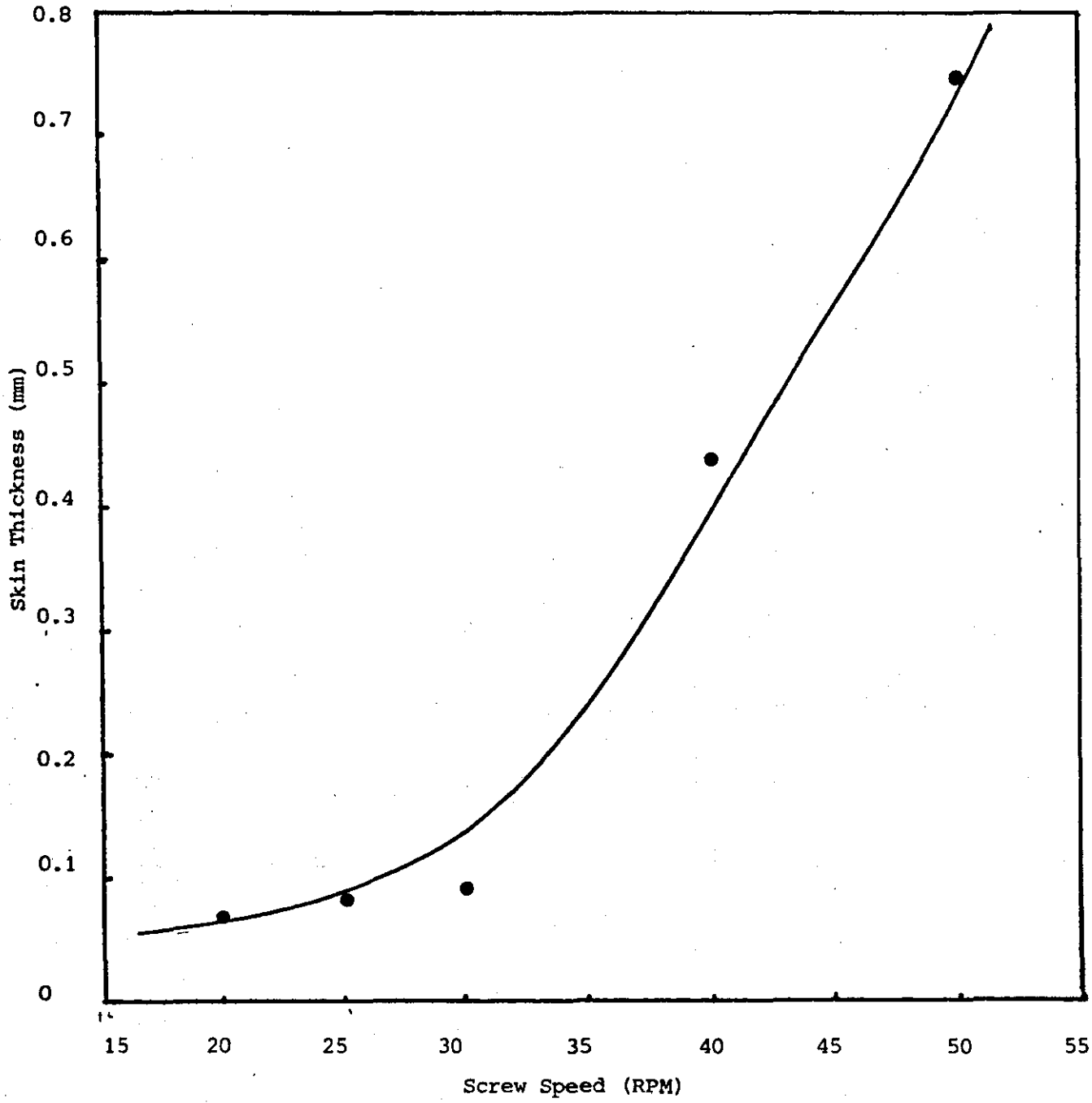


Figure 6.18: The Effect of Screw Speed on Skin Thickness of the Extrudate.

TABLE 6.6:

Effect of extrusion speed on impact strength as a function of stabilizer distribution in standard formulation

| Extrusion Speed (rpm) | Impact strength (kJ $m^{-2}$) | | | | | | |
|---|---|---|---|---|---|---|---|
| | 1 | 2 | 3 | 4 | 5 | 6 | Average |
| 20 | 5.89 | 5.92 | 5.78 | 6.16 | 5.79 | 6.00 | 6.01 |
| 25 | 6.36 | 6.15 | 6.17 | 6.06 | 6.38 | 5.96 | 6.18 |
| 30 | 8.55 | 8.32 | 8.61 | 8.45 | 8.38 | 8.46 | 8.46 |
| 40 | 6.44 | 6.22 | 6.19 | 5.98 | 6.35 | 6.18 | 6.23 |
| 50 | 6.29 | 5.92 | 6.05 | 6.19 | 5.91 | 5.92 | 6.05 |

TABLE 6.7:

Effect of extrusion speed on shrinkage as a function of stabilizer distribution in standard formulation

| Extrusion Speed (rpm) | Shrinkage (%) | | | |
|---|---|---|---|---|
| | 1 | 2 | 3 | Average |
| 20 | 2.58 | 2.55 | 2.62 | 2.58 |
| 25 | 2.92 | 2.96 | 2.96 | 2.95 |
| 30 | 3.28 | 3.30 | 3.27 | 3.28 |
| 40 | 3.45 | 3.40 | 3.40 | 3.42 |
| 50 | 3.51 | 3.50 | 3.54 | 3.52 |

TABLE 6.8:

Effect of extrusion speed on physical properties as a function of stabilizer distribution in standard formulation

| Extrusion Speed (rpm) | Skin Thickness (mm) | Solvent Absorption (%) | Extruder Output Rate ($kghr^{-1}$) | Heat of Fusion ($J\ g^{-1}$) |
|---|---|---|---|---|
| 20 | 0.270 | 18.16 | 7.44 | 3.94 |
| 25 | 0.281 | 25.26 | 7.56 | 5.13 |
| 30 | 0.292 | 30.08 | 11.10 | 6.36 |
| 40 | 0.448 | 23.66 | 14.86 | 6.99 |
| 50 | 0.750 | 22.01 | 17.40 | 6.74 |

TABLE 6.9:

Relative fluorescence intensity of extrudate at different screw speeds

| Extrusion Speed (rpm) | Relative fluorescence intensity (%) | | | | | | |
|---|---|---|---|---|---|---|---|
| | 1 | 2 | 3 | 4 | 5 | 6 | Average |
| 20 | 49.0 | 55.0 | 57.9 | 49.9 | 50.6 | 53.7 | 52.81 |
| 25 | 59.2 | 65.4 | 59.0 | 67.8 | 71.3 | 64.5 | 64.41 |
| 30 | 65.7 | 78.2 | 77.7 | 78.9 | 77.8 | 66.2 | 73.30 |
| 40 | 39.3 | 36.3 | 38.4 | 39.1 | 36.9 | 39.1 | 38.19 |
| 50 | 32.9 | 39.0 | 33.5 | 30.2 | 36.7 | 37.2 | 34.86 |

TABLE 6.10:

Relative fluorescence intensity of extrudate at different processing temperatures

| Extrusion Temp (°c) | Relative fluorescence intensity (%) | | | | | | |
|---|---|---|---|---|---|---|---|
| | 1 | 2 | 3 | 4 | 5 | 6 | Average |
| 170 | 34.4 | 35.7 | 36.3 | 35.9 | 32.6 | 36.4 | 34.93 |
| 188 | 48.3 | 49.6 | 51.3 | 52.6 | 53.2 | 49.0 | 50.59 |
| 194 | 49.0 | 55.0 | 57.9 | 49.9 | 50.6 | 53.7 | 52.81 |
| 202 | 87.9 | 104.6 | 100.5 | 80.7 | 99.6 | 101.3 | 95.71 |
| 218 | 109.2 | 107.6 | 110.4 | 110.5 | 109.0 | 102.6 | 108.22 |
| 224 | 66.2 | 73.8 | 79.2 | 70.10 | 80.0 | 72.8 | 73.80 |

The graphs of the data obtained from physical property measurements are shown in Figures 6.15 to 6.18. The graphs also show some of the physical properties to exhibit highest values at 30 rpm, in agreement with microscopical observations. The highest impact strength and solvent absorption values are observed at 30 rpm, although the opposite trend was expected from solvent absorption test - because the residual grains and primary particles do form a 'barrier' to solvent penetration into the matrix[173,175]. At higher screw speeds (40 and 50 rpm), the stabilizer is observed to be poorly distributed, but there is no discernible difference between extrudates from both speed settings. Apart from the observed decrease in impact strength and solvent absorption, a noticeable increase in shrinkage and surface skin thickness is evident (Figures 6.17 and 6.18).

The effect of surging was common at these screw speeds (40 and 50 rpm) and, by a closer assessment, the extrudate width seemed to have varied in a sinusoidal manner with a cycle time similar to one screw revolution. Since the surging occurred only at higher screw settings, it may be an indication that insufficient powder was feeding from the hopper. This will, in general, seriously affect the properties of the samples and poor distribution of stabilizer is apparent. Many workers[127,181,182] have analysed and explained surging in extruders. Fenner[182] has demonstrated that there are at least three different types of surging independently occurring in an extruder. He found one of these to be the variations associated with the rotation of the screw particularly due to the solids conveying process. It is not surprising therefore that at higher extrusion speeds (40 and 50 rpm) a poor distribution of components - that is, larger size residual grains etc - was observed.

### 6.2.4 Effect of Different Extrusion Temperatures on Morphological Changes

The standard formulation was extruded at a constant screw speed of 20 rpm but varied extrusion temperature to produce the range of

7 temperature profiles given in Table 2.7. The effect of the temperature range on the distribution of stabilizer, degradation of the polymer, fusion and morphology of the extrudates were examined. Because of the apparent effect of degradation and pronounced changes in morphology with higher temperatures, it was possible to exploit the following microscopy methods: UV fluorescence light and differential interference contrast (DIC), including other conventional microscopy methods.

The examination of samples obtained along the extruder screws at different temperatures was also carried out with these methods. For convenience, the effect of different extrusion temperatures on the morphology and stabilizer distribution in extrudates will be discussed under two headings: on final extrudates and extruder screw samples.

### 6.2.4.1 Effect of extrusion temperature on morphology of extrudates

With fluorescence light and differential interference contrast (DIC) microscopy techniques pronounced differences in morphology of the extrudates are observed. Figures 6.19 to 6.25 show the micrographs of the samples processed at different temperatures. It can be seen that the quantity of residual grains in the samples decreases as the processing temperature is raised. The fluorescence micrograph (Figure 6.21) clearly shows these residual grains (sub-grains) to fluoresce brighter than their surroundings, and the stabilizer particles to be distributed only in the melted region. A contrasting feature is observed in samples processed at 224$^{o}$C - where all the sub-grains appear to have been melted. The degree of fusion or homogeneity of the polymer melt is seen to improve with increase in extrusion temperature. With differential interference contrast microscopy this is seen as a progressive loss in image contrast (Figure 6.19). This is due to loss of sub-grains and high level of primary particle fusion.

FIGURE 6.19: DIC photomicrographs of samples extruded at different temperatures

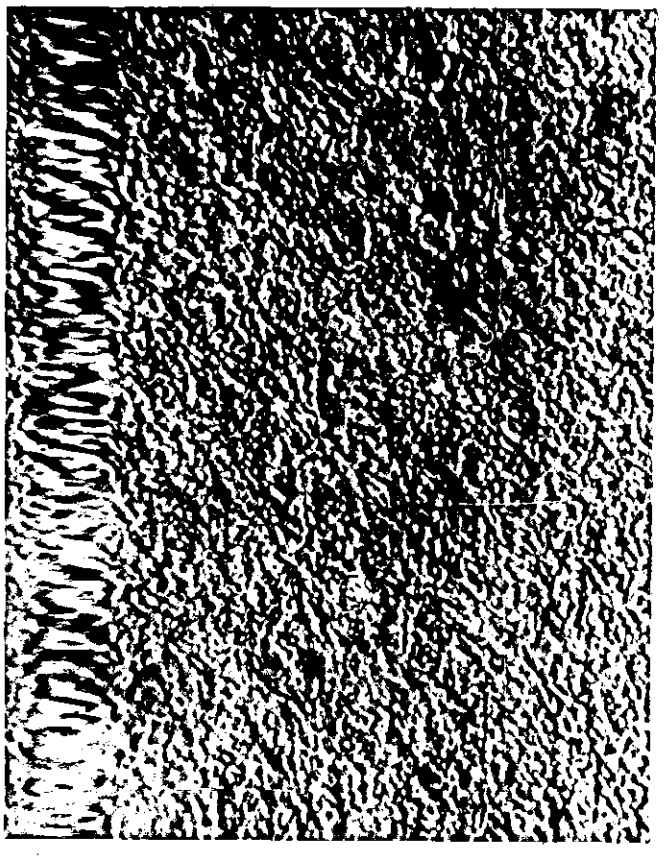

(a) Extruded at 170°C

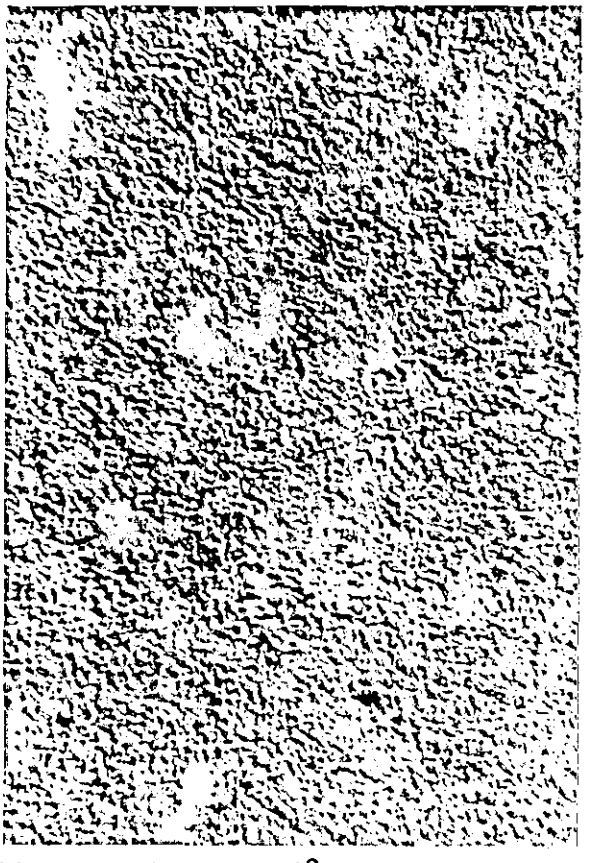

(b) Extruded at 194°C

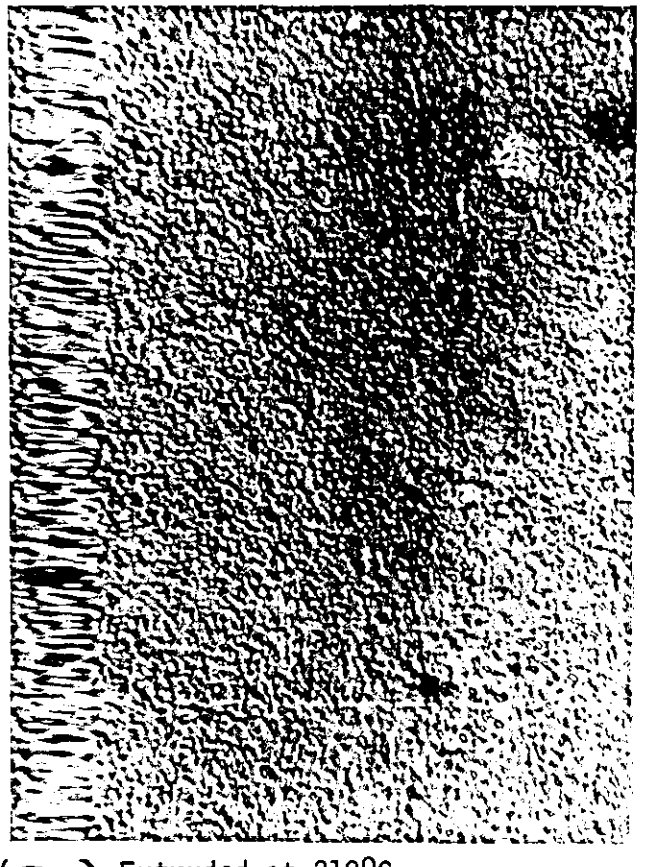

(c) Extruded at 218°C

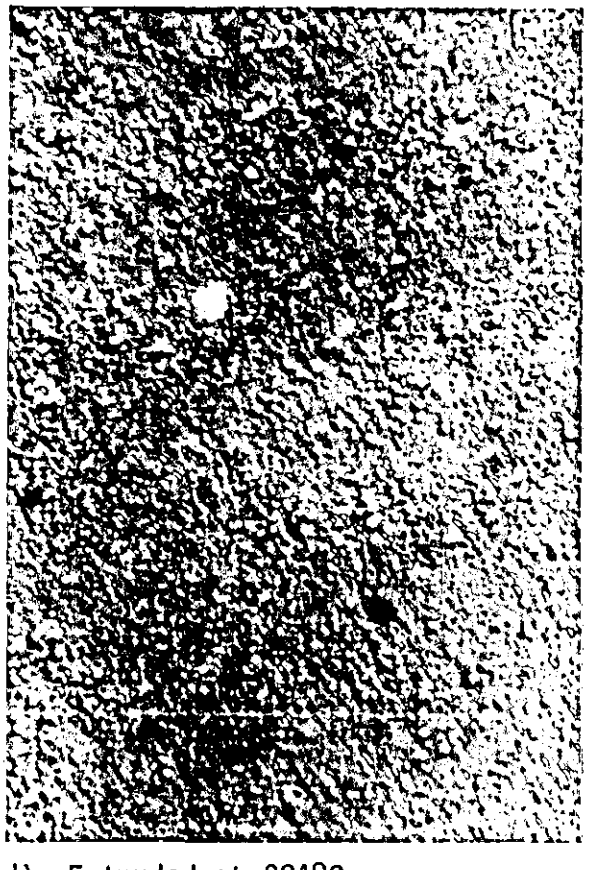

(d) Extruded at 224°C

30 μm

FIGURE 6.20: Normal light photomicrographs of samples extruded at different temperatures
Field of view is the same with the DIC photomicrographs in page

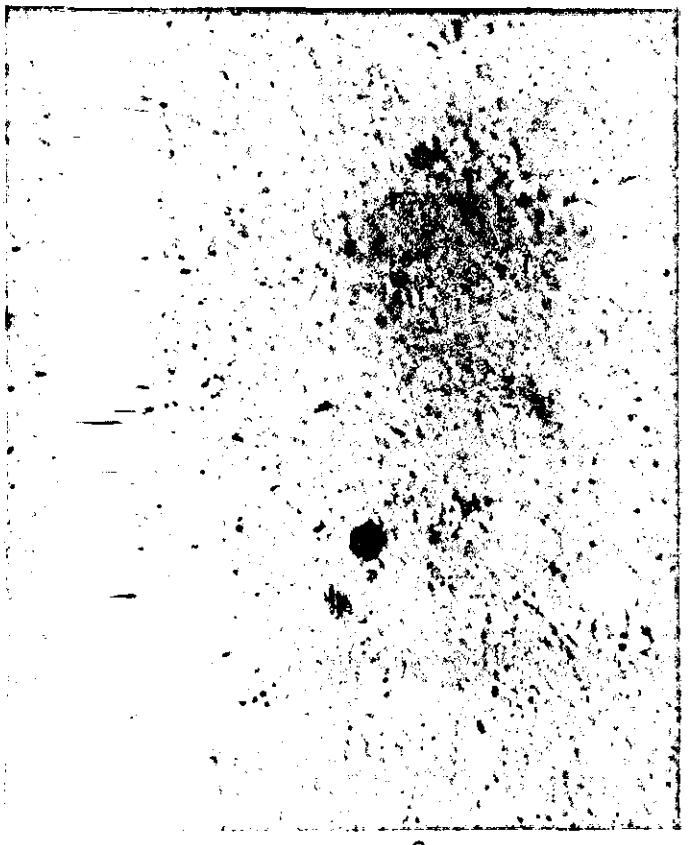

(a) Extruded at 170°C

(b) Extruded at 194°C

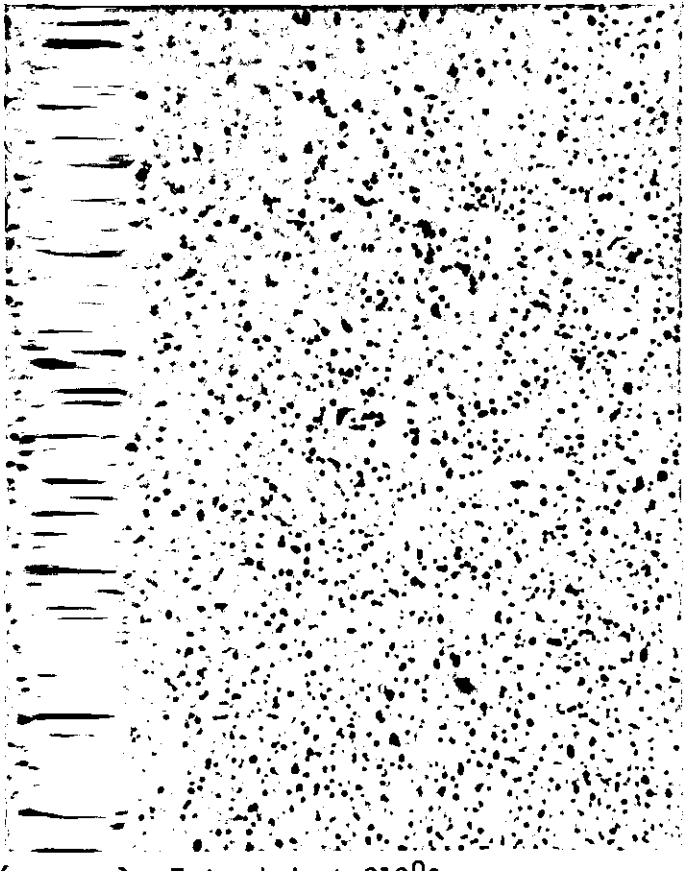

(c) Extruded at 218°C

(d) Extruded at 224°C

30μm

FIGURE 6.21: Fluorescence photomicrographs of sample extruded at two extreme temperatures
□= stabilizer particles

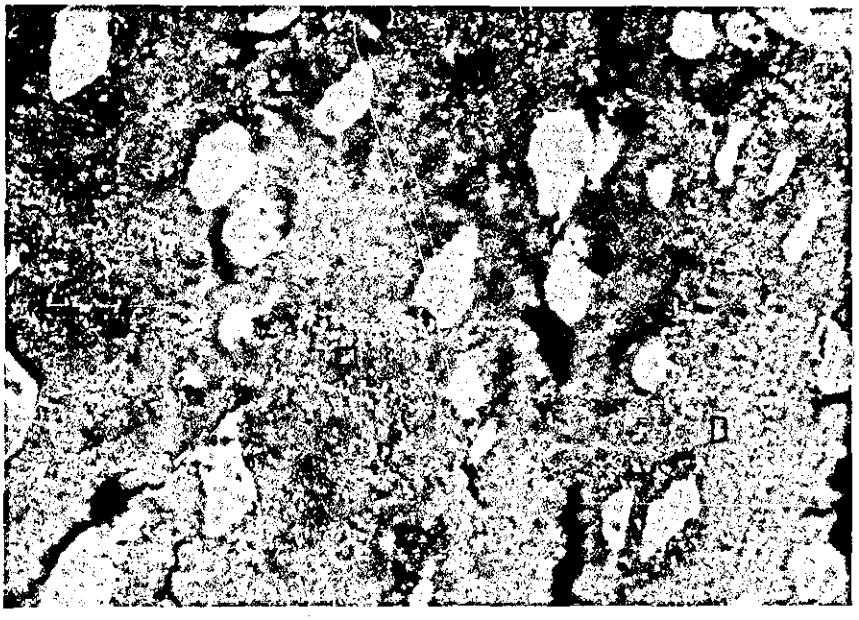

(a) Extruded at 170°C

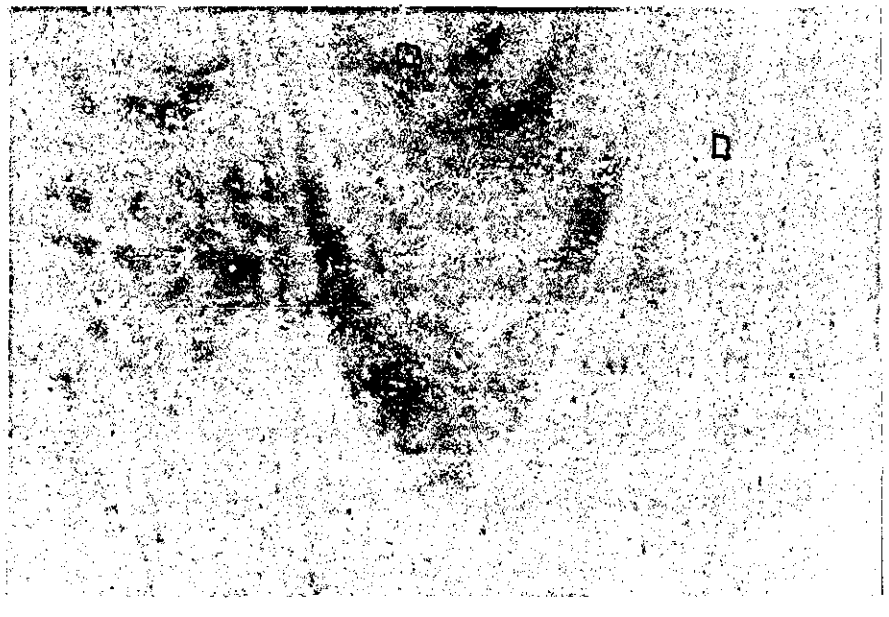

(b) Extruded at 224°C

50 um

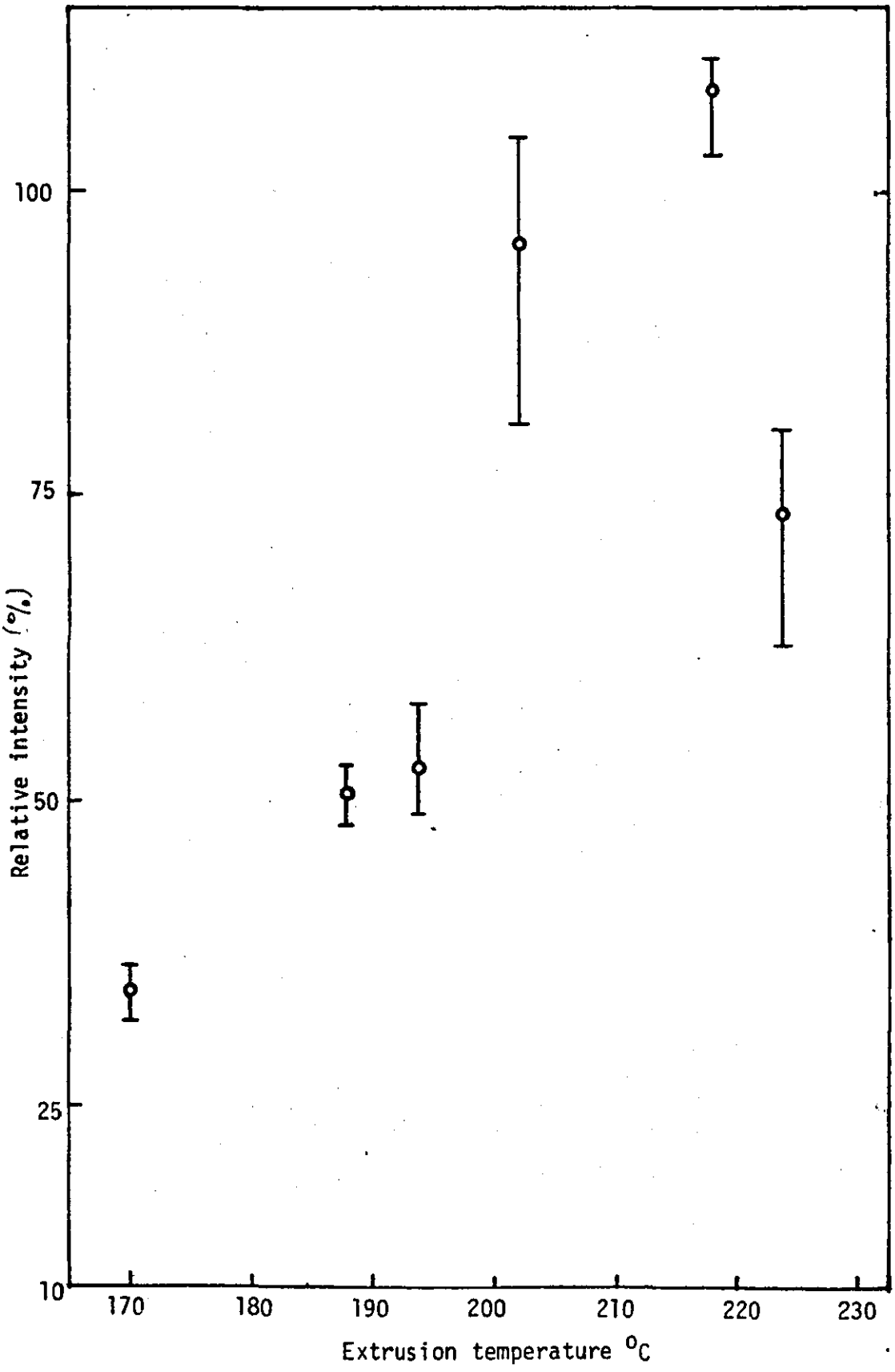


FIGURE 6.22 Fluorescence intensity of extrudates at different extrusion temperatures

Thus, the highest degree of fusion of sub-grains and primaries appears to be achieved in the sample processed at 218°C.

While keeping the same field of view the sections were re-examined with cross-polar and normal light microscopy techniques, in an attempt to explicitly interpret this change in morphological features. In Figure 6.20 it can be seen that the additional texture observed in low temperature samples with the DIC technique is not visible under a normal light microscope. It can be seen also that there is very little if any sub-grains found in samples processed above 218°C. It is clearly demonstrated that above this temperature a significant change in size and distribution of stabilizer particles occur. This means that the stabilizer particles also undergo structural modification, but mainly when there is a 'phase change' in the UPVC matrix. At normal processing temperature (194°C), where a substantial number of sub-grains is contained in the sample, random distribution of stabilizer particles is clearly evident (Figure 6.20(b)). This confirmed the suggestion that random stabiliser distribution, as well as its structure, accounts for the little or no fluorescent property of sub-grains in most end-products. However, a measure of relative fluorescence intensity as a function of extrusion temperature shows an increase in fluorescence up to 218°C (Figure 6.22). This is suggested to be due to the effect of degradation rather than stabilizer distribution. This is strongly supported by the fact that at an extrusion temperature of 224°C (where highest degradation is anticipated) a reduction in relative fluorescence intensity was observed. This agrees with a possible shift in emission band, which has been vividly explained in Chapter 3 and by Gerrard et al[122] to be associated with very high levels of degradation.

The same mechanism of gelation or topographical features were observed when specimens prepared by petrological technique were examined with normal light microscopy (see Figure 6.23). The samples

FIGURE 6.23: Normal light photomicographs of samples prepared by petrological technique showing the effect of extrusion temperature on morphology and distribution of stabilizer

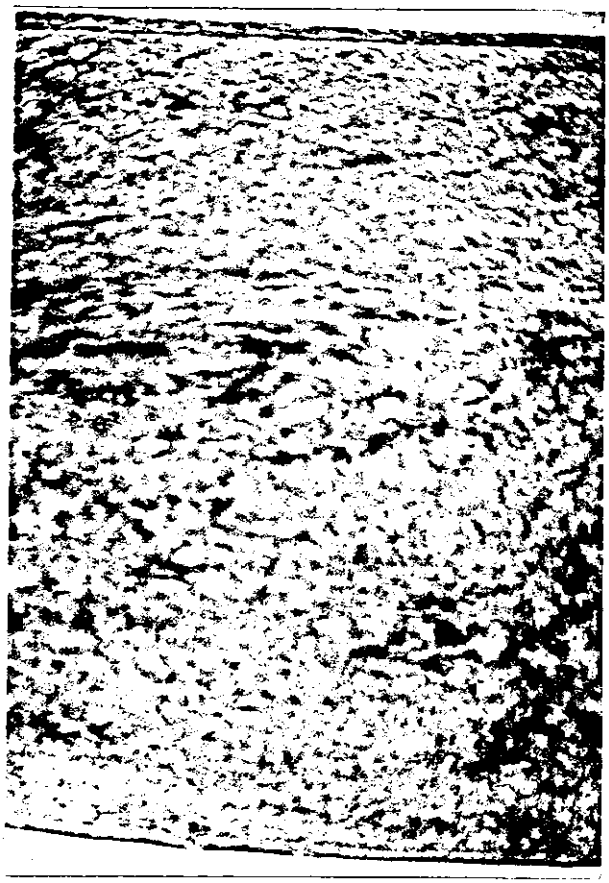

(a) Extruded at 170°C

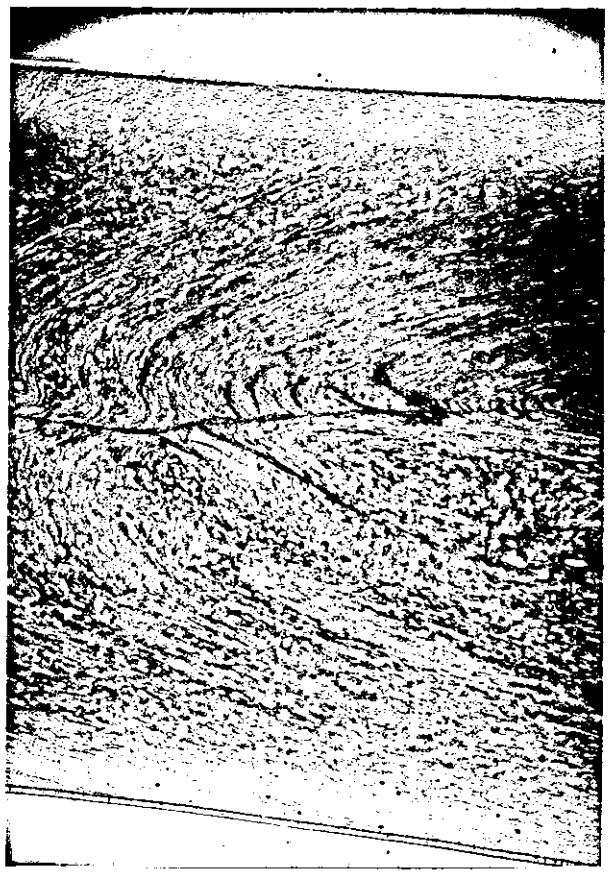

(b) Extruded at 194°C

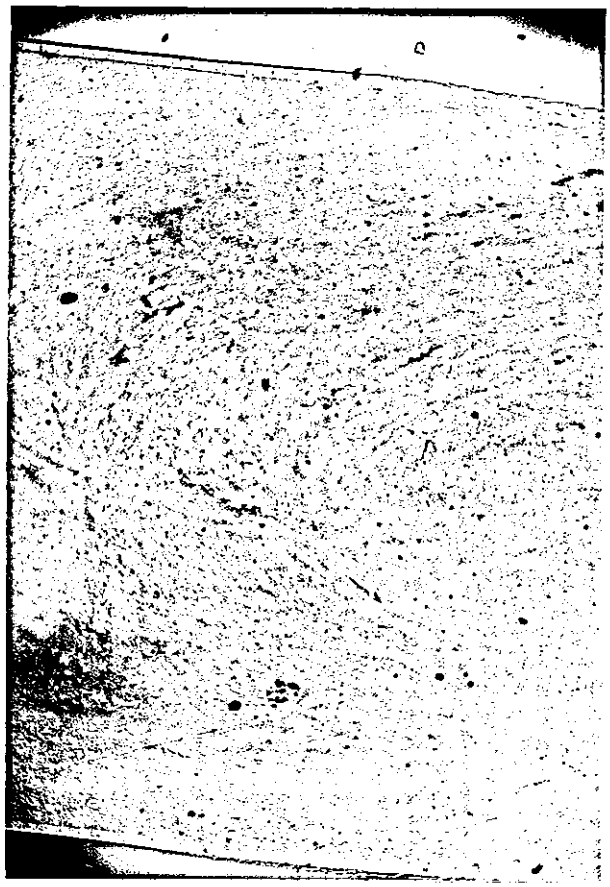

(c) Extruded at 218°C

(d) Extruded at 224°C

500μm

extruded at die temperatures lower than 210°C show the existence of large quantities of sub-grains, especially at 170°C - in substantial agreement with other microscopical methods. Perhaps it is important to point out that the petrological technique by normal light microscopy reveals sample topography similar to those observed with UV fluorescence method - which indicates a good correlation between them. At higher temperature (224°C) a molten 'streak-like' structure is observed, and there appear to be no sub-grains present in this sample. This anomalous effect of temperature on structural modifications was further examined by SEM and TEM in an attempt to obtain proper explanations. The results are depicted in Figures 6.24 and 6.25 which show respectively the micrographs obtained by SEM and TEM methods. The scanning electron microscopy (SEM) micrographs of liquid-nitrogen fractured surfaces show the presence of primary particles in 170°C to 218°C extrudates, but not in the sample extruded at 224°C. In addition, the sample extruded at 170°C appears to have fractured in a brittle manner and along weakly fused grain boundaries. This agrees with the fact that the number of primary particles revealed in the fracture surface is very low compared with higher temperature samples. Also visible, are the voids 'surrounding' the primary particles - which are still present in the 224°C sample even though the primary particles have melted. The presence of large size voids in the 224°C extrudate can be explained by the fact that evolution of hydrogen chloride at higher temperature is evident. At this temperature all residual grains (sub-grains and primary particles) have been melted - leading to the formation of very high density molecular chain entanglement network. (This suggestion has been closely studied with the DSC method and will be discussed in the latter part of this section). The above observation is in substantial agreement with the observations made with light microscopy methods. The significant difference in the distribution and nature of the stabilizer, observed with normal light microscopy method, as a

FIGURE 6.24: Fracture surfaces of samples extruded at different temperatures Mag. x10K

(a) Extruded at 170°C

(b) Extruded at 194°C

(c) Extruded at 218°C

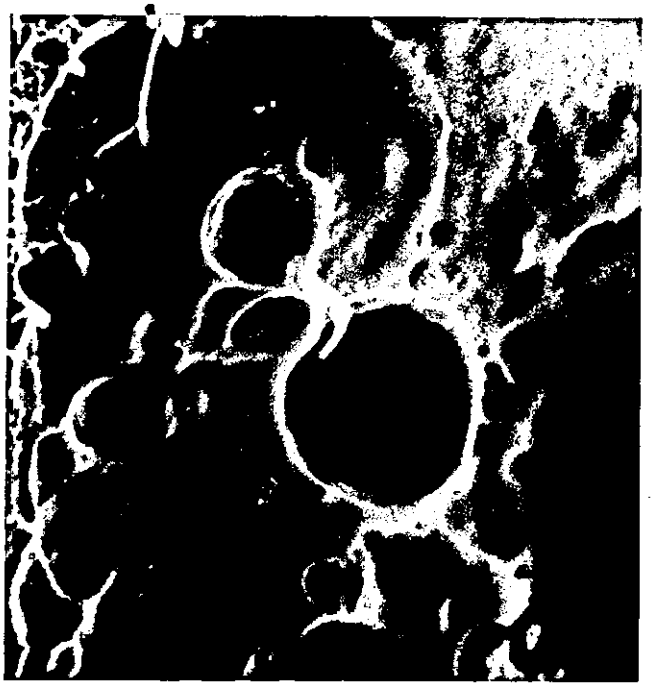

(d) Extruded at 224°C

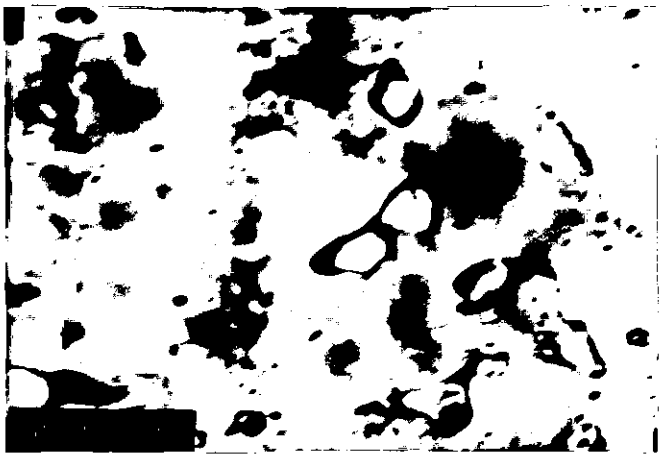

(a) Extruded at 170°C

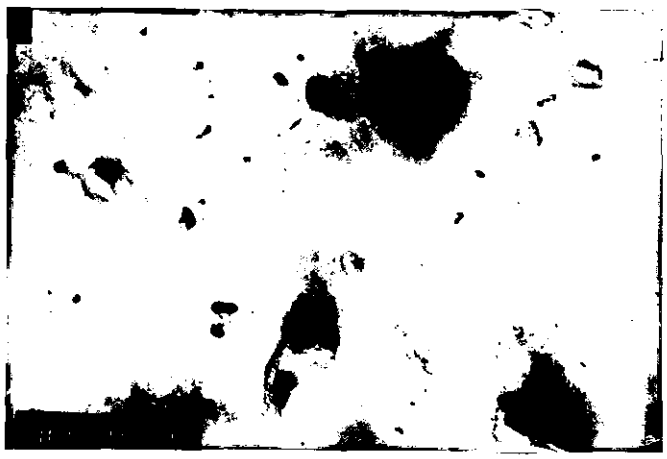

(b) Extruded at 194°C

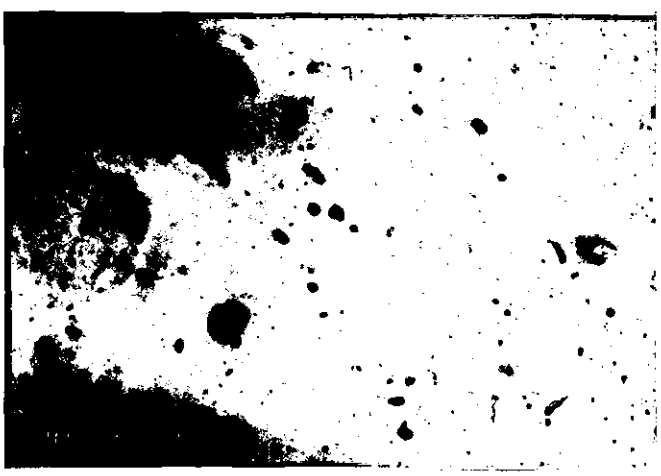

(c) Extruded at 218°C

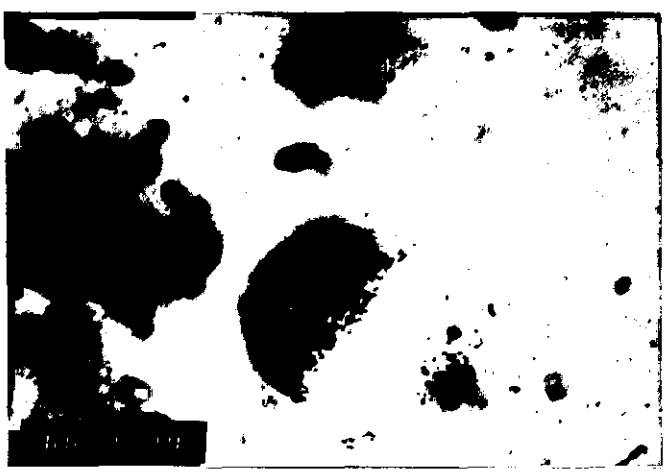

(d) Extruded at 224°C

FIGURE 6.25: TEM photomicrographs of samples extruded at different temperatures
Mag. x16K


(e) Extruded at 194°C. Showing micro-void in agglomerated stabilizer particles.
Mag. x33K

function of temperature was closely examined with a transmission electron microscopy (TEM) method. This method has also been used in the preceding sections to evaluate the presence of micro-voids. It can be seen that the stabilizer particles in samples extruded at 224$^{o}$C have melted compared with those in the lower temperature extrudates (Figure 6.25), appearing as 'ink-stains' in the polymer matrix. It is also evident, by this method, that at higher temperature voids are no longer entirely associated with agglomerated stabilizer particles (Figure 6.25(d)), but also with evolution of hydrogen chloride.

The physical properties of the extrudates plotted as a function of extrusion temperature are given in Figures 6.26 to 6.29 . It is noticed that the impact strength increases with increasing temperature up to 218$^{o}$C before dropping sharply. This confirmed the formation of very high molecular chain entanglement network beyond 218$^{o}$C. In other words highest [illegible] entanglement networks do not imply best impact property. A similar result was obtained with equilibrium solvent absorption test. Percentage sorption is seen to increase with increasing temperatures up to 218$^{o}$C, and again dropping sharply beyond this temperature (Figure 6.27). The thermograms obtained with differential scanning calorimeter, as before, show the presence of two endothermic peaks (see Appendix 4). The endothermic peaks 'A' and 'B' have been shown in several publications to represent respectively the formation of secondary crystallites and the melting of primary crystallites of various sizes and degrees of perfection[148,161]. As extrusion temperature increases, the endothermic peak 'A' was found to increase, thus the area of the peak was measured and used to calculate the heat of fusion of primary particles[161]. In Figure 6.27 it can be seen that the heat of fusion increases with increasing extrusion temperature. This dependency is reduced at higher extrusion temperature. This result, in effect, strongly suggests that at very high processing temperature (e.g. 224$^{o}$C) there is a

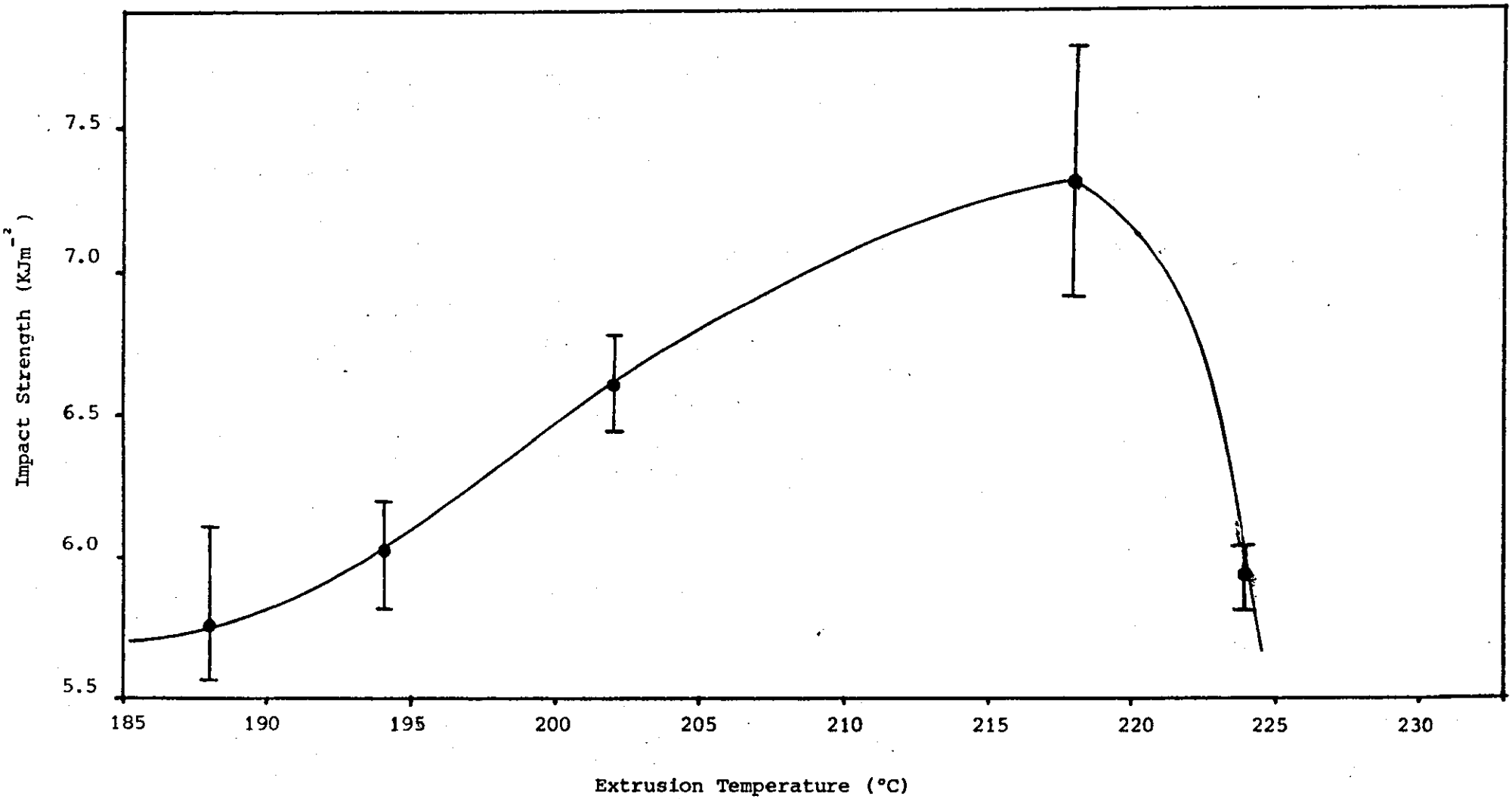


Figure 6.26 Variation of Extrusion Temperature with Impact Strength.

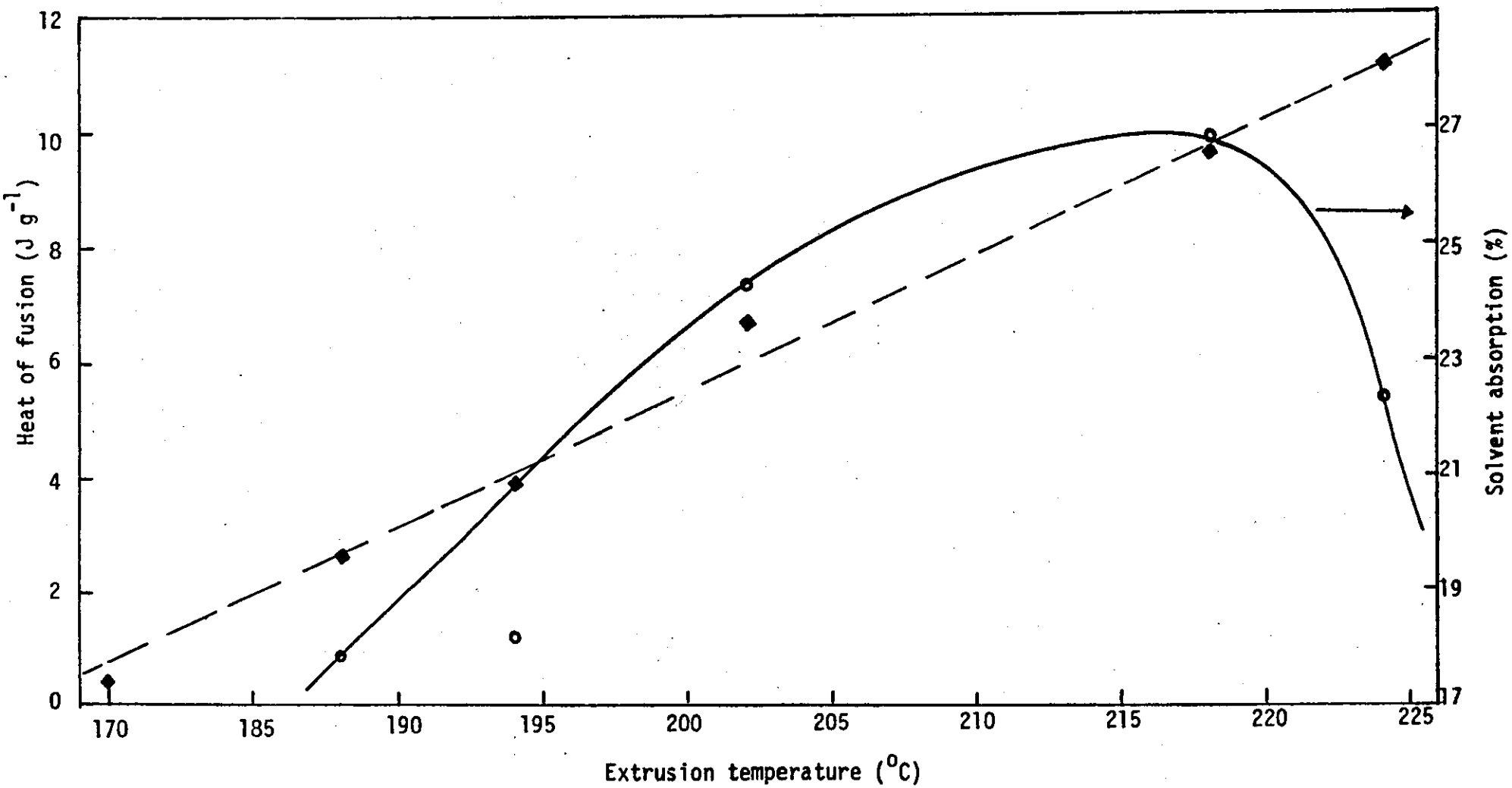


FIGURE 6.27: Variation of fusion characteristics with extrusion temperature

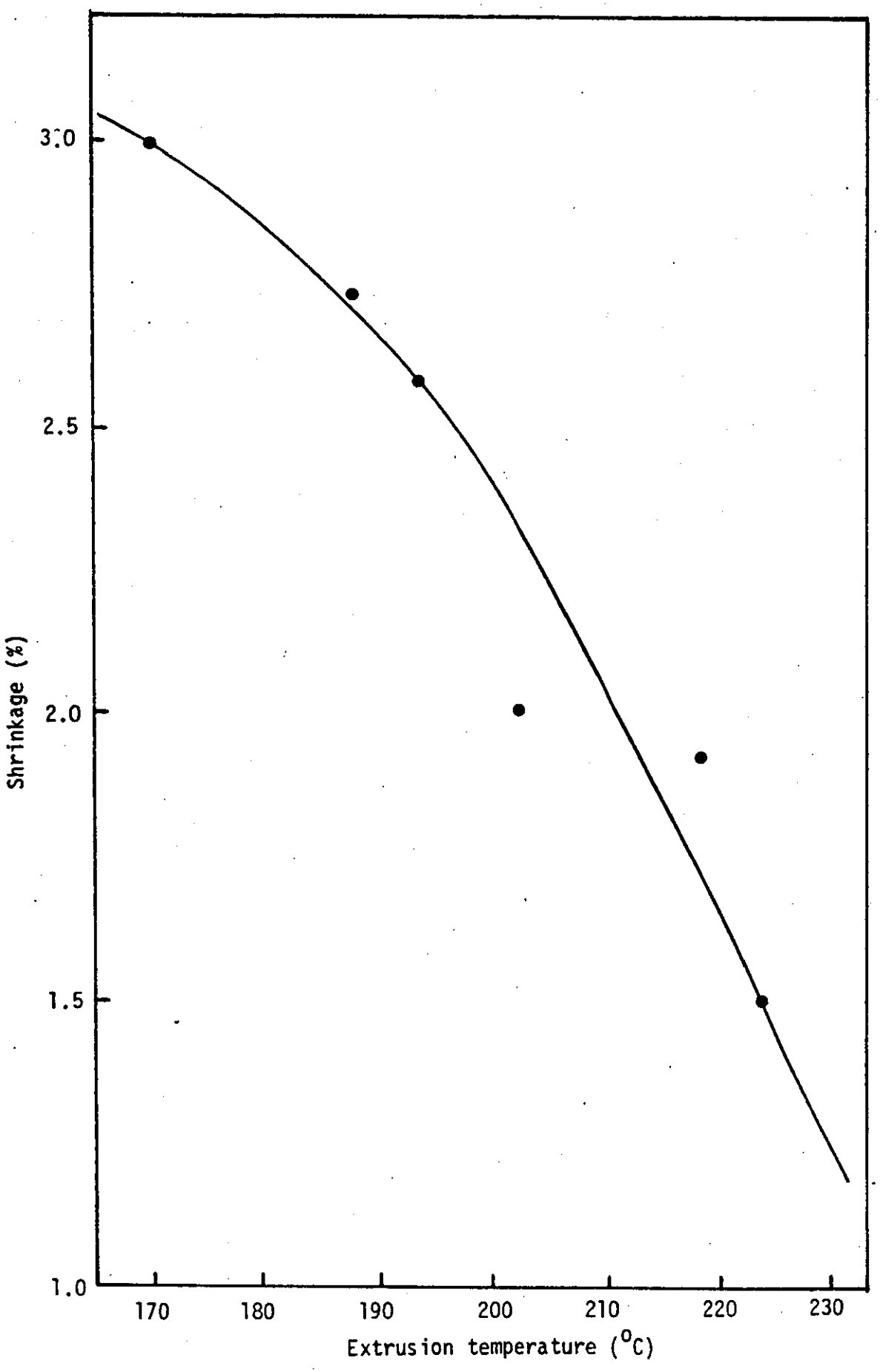


Figure 6.28 Effect of extrusion temperature on sample shrinkage

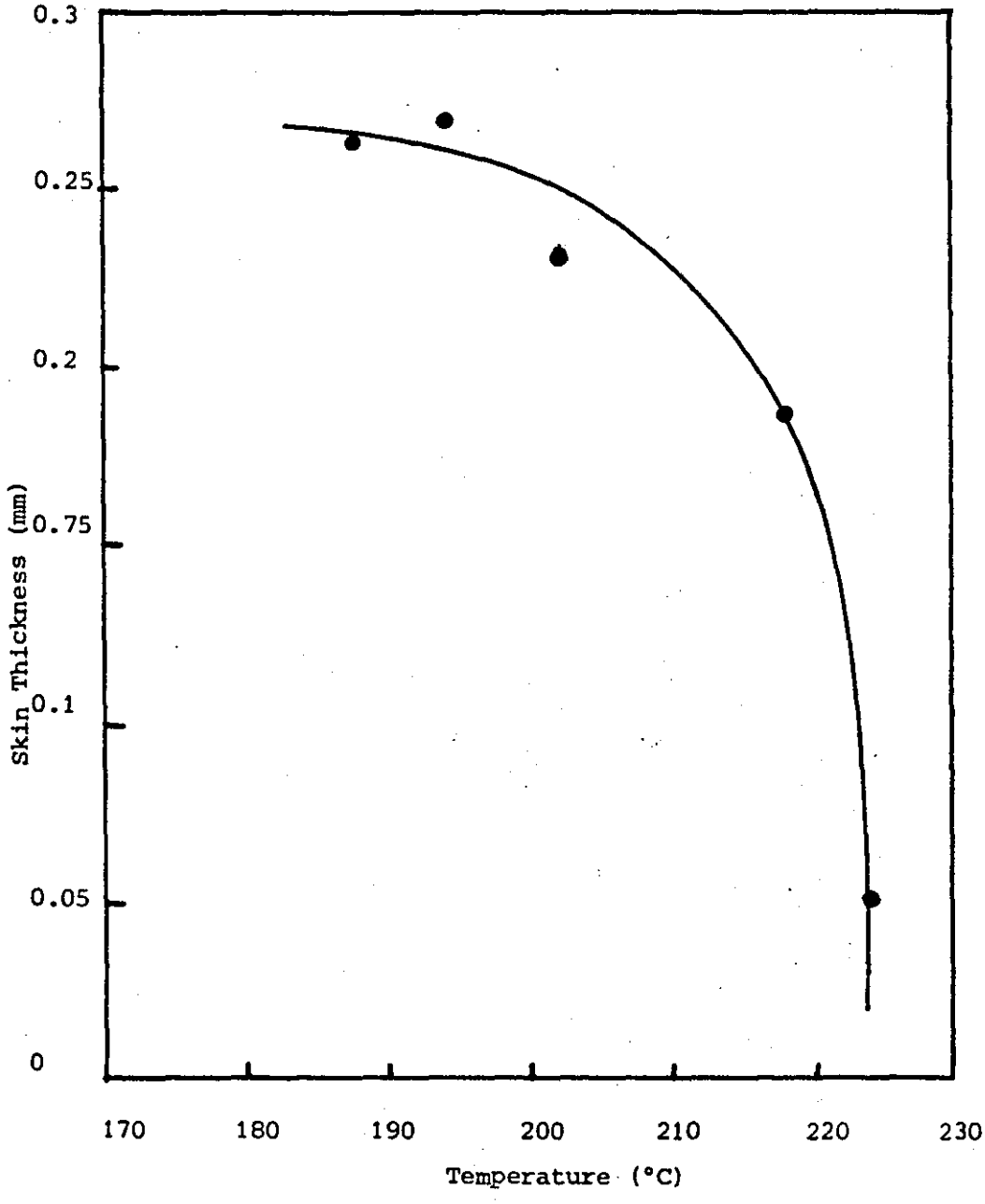


FIGURE 6.29: The Effect of Extrusion Temperature on Skin Thickness of the Extrudate.

TABLE 6.11:

Variation of extrusion temperature with impact strength as a function of stabiliser distribution in standard formulation

| Extrusion Temp. (°C) | Impact Strength (kJ $m^{-2}$) | | | | | | |
|---|---|---|---|---|---|---|---|
| | 1 | 2 | 3 | 4 | 5 | 6 | Average |
| 188 | 5.59 | 5.78 | 6.09 | 5.56 | 5.58 | 5.67 | 5.76 |
| 194 | 5.89 | 5.92 | 5.78 | 6.16 | 5.79 | 6.00 | 6.01 |
| 202 | 6.76 | 6.44 | 6.69 | 6.46 | 6.56 | 6.69 | 6.60 |
| 218 | 7.43 | 7.75 | 6.95 | 7.73 | 6.90 | 7.08 | 7.31 |
| 224 | 5.79 | 5.95 | 5.99 | 6.02 | 5.98 | 5.86 | 5.93 |

TABLE 6.12:

Effect of extrusion temperature on shrinkage as a function of stabilizer distribution in standard formulation

| Extrusion Temperature (°C) | Shrinkage (%) | | | |
|---|---|---|---|---|
| | 1 | 2 | 3 | Average |
| 170 | 2.99 | 3.00 | 2.98 | 2.99 |
| 188 | 2.74 | 2.69 | 2.76 | 2.73 |
| 194 | 2.55 | 2.62 | 2.58 | 2.58 |
| 202 | 1.95 | 2.05 | 2.05 | 2.02 |
| 218 | 1.93 | 1.97 | 1.95 | 1.95 |
| 224 | 1.53 | 1.48 | 1.50 | 1.50 |

TABLE 6.13:

Variation of extrusion temperature with physical properties as a function of stabilizer distribution in standard formulation

| Extrusion Temperature (°C) | Skin Thickness (mm) | Solvent Absorption (%) | Extruder Output Rate (kg $hr^{-1}$) | Heat of Fusion (J $g^{-1}$) |
|---|---|---|---|---|
| 170 | - | - | - | 0.31 |
| 188 | 0.264 | 17.85 | 7.42 | 2.54 |
| 194 | 0.270 | 18.16 | 7.44 | 3.94 |
| 202 | 0.229 | 24.34 | 7.62 | 6.70 |
| 218 | 0.187 | 26.93 | 7.71 | 9.67 |
| 224 | 0.052 | 22.35 | 7.84 | 11.04 |

possibility of all the primary particles being destroyed. In fact, the SEM micrographs show that at 224°C there were few, if any, primary particles left in the extrudate. It should be expected, therefore, that in a sample where nearly all the primary particles have been destroyed chain crosslinking will prevail, which will be detrimental to its physical properties. This is why poor physical and mechanical properties were observed with samples extruded at 224°C.

The shrinkage and surface skin thickness of the extruded strips plotted as a function of extrusion temperature are given in Figures 6.28 and 6.29 respectively. It is observed that the orientation (as measured by shrinkage and surface skin thickness) decreases with increasing extrusion temperature. This is due to effects of melt relaxation - in agreement with Berens and Folt[65] who have shown that minimum orientation is associated with higher processing temperatures. In other words, depending on the cooling rate, low quantity of residual grains in samples is associated with minimum orientation.

In general, best physical property and perfectly fused homogeneous extrudate as shown by microscopy methods and physical property measurements, are observed at 218°C extrusion temperature, where there is a balance between primary particles and molecular chain entanglement network.

### 6.2.4.2 Effect of extrusion temperature on morphology of screw samples

In order to make an effective study of changes in morphology and distribution of stabilizer along the extruder screw, samples were obtained at three different temperatures: 170°C, 194°C and 210°C. Because of degradation, it was not possible to obtain samples above the processing temperature of 210°C. Specimens from the screw channels for each temperature were then examined

with the following methods: fluorescent light, differential interference contrast, normal-light, TEM and SEM microscopy methods. Figures 6.30 to 6.32 compares the typical examples of micrographs of screw samples obtained at three screw zones for the three extrusion temperatures. It is observed that the degree of particle fusion in the screw samples not only increases towards the die but also differs with different temperatures. Each of the twin screws has 40-screw channels and numbering them from metering zone to feed zone, it is noticed that powder compaction and colour changes started respectively at 37 and 35 screw turns, 35 and 32 screw turns and 35 and 30 screw turns for screw samples obtained at 210$^{o}$C, 194$^{o}$C and 170$^{o}$C respectively. This means that the screw channel at which powder compaction begins is largely determined by the extrusion temperature. It can also be seen that the number of screw channels between powder compaction and first colour change decreases with increase in extrusion temperature.

At the early stage of the compaction, melting and grain fusion along their boundaries occurred. The distribution of stabilizer is within the fused boundaries of the UPVC grains as portrayed by the UV fluorescence and DIC micrographs in Figures 6.30 and 6.33. As the powder moves along the screw zones via feed, compression, vent and metering zones the molten grains are sheared and broken down, thus exposing the primary particles which form the unit of flow. During this period short chain entanglement network along the molten boundaries occurs, through interdiffusion of chain segments from adjacent grains. Since the solid stabilizer particles coat only the surfaces of UPVC grains, the obliteration of the grain boundaries results in a random distribution of the stabilizer particles in these boundaries. By fluorescence light microscopy these areas with stabilizer do not fluoresce, while areas (the exposed sub-grains) devoid of stabilizer fluorecesce intensely (see Figure 6.31). Towards the tail end of the metering zone (depending on temperature and shear rate the fluorescing sub-grains are nearly completely disappeared signifying not only a

FIGURE 6.30: Fluorescence micrographs of 'core' samples of a twin-screw extruder at 170°C

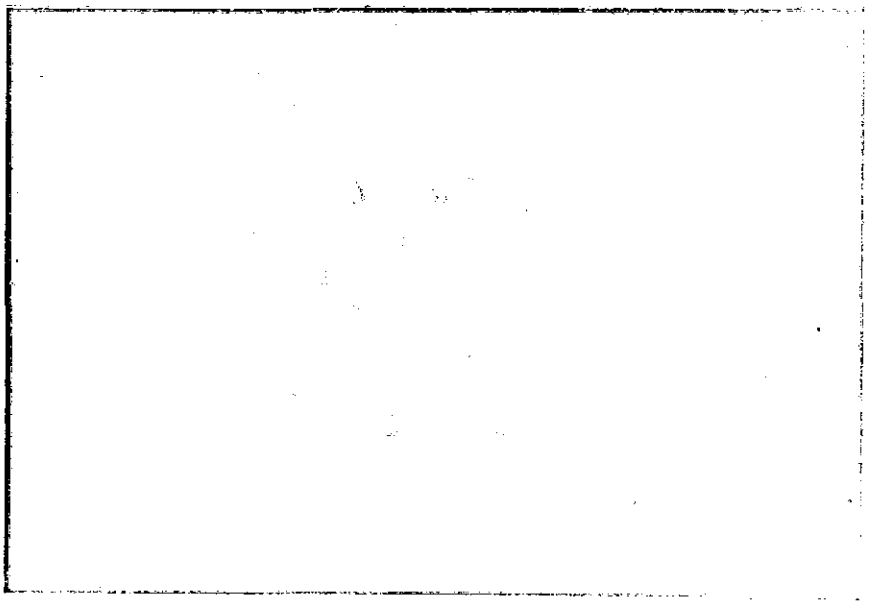

(a) 1st screw turn

(b) 12th screw turn

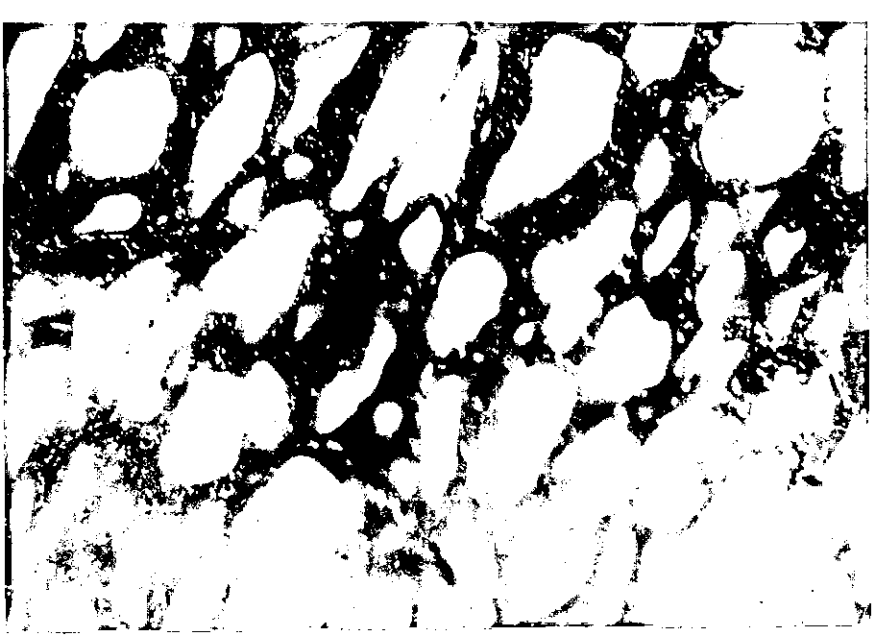


(c) 29th screw turn

FIGURE 6.31: Fluorescence micrographs of 'core' samples of a twin-screw extruder at 194°C

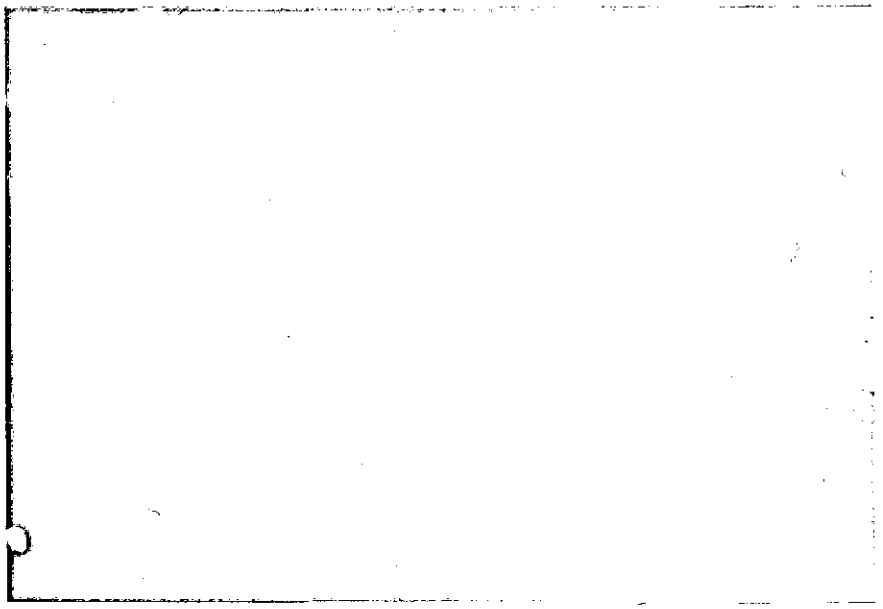

(a) 1st screw turn

(b) 12th screw turn

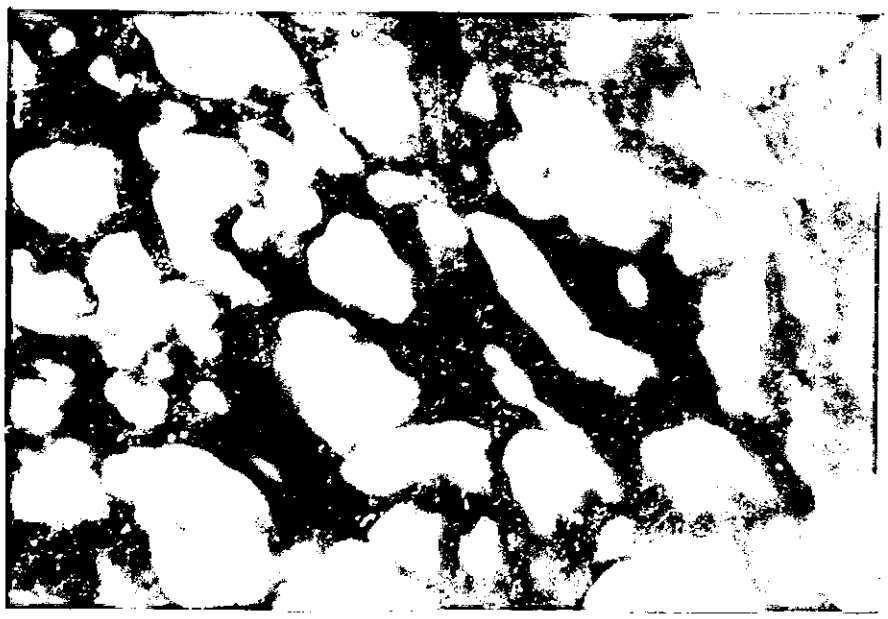


(c) 29th screw turn

FIGURE 6.32: Fluorescence micrographs of 'core' sample of a twin-screw extruder at 210°C

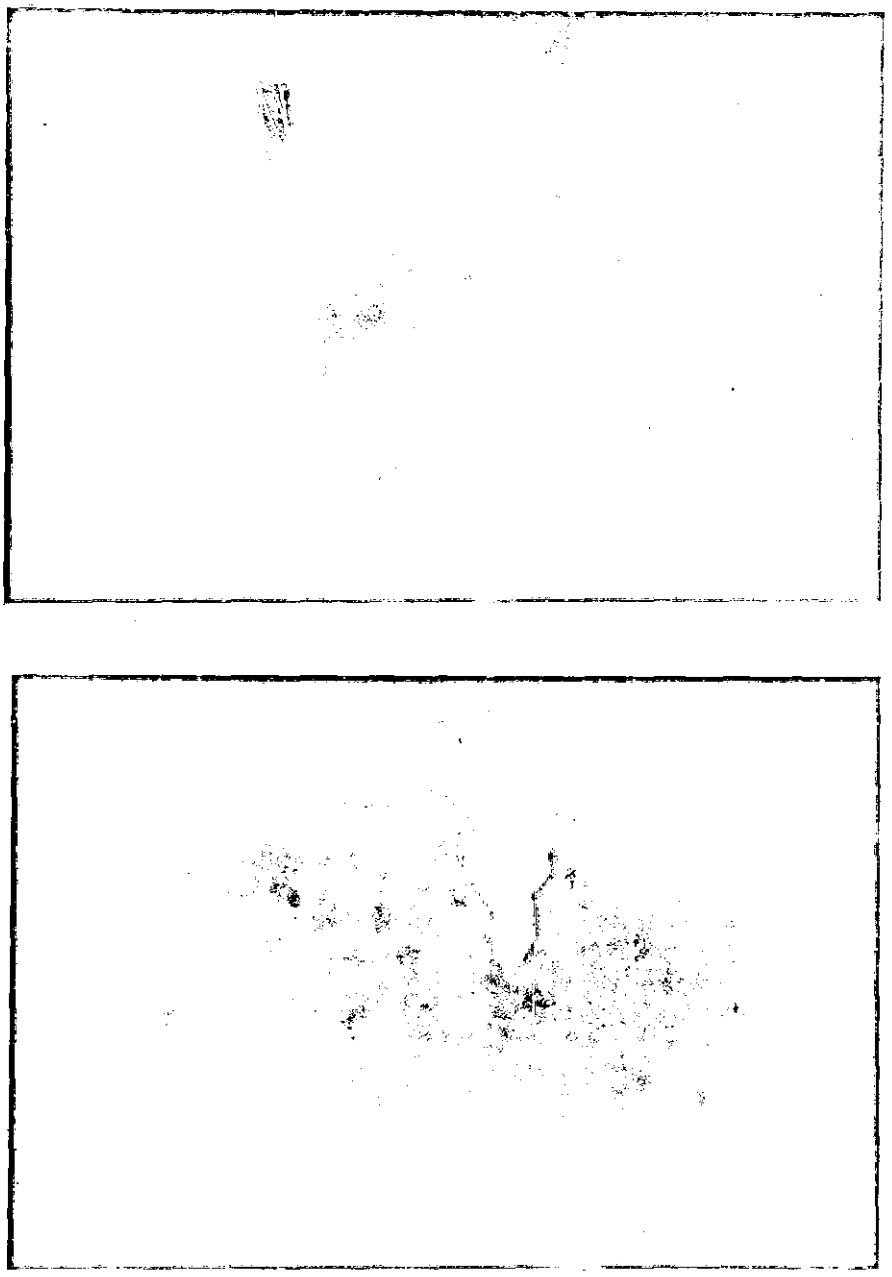

uniform distribution by stabilizer particles but also the higher distruc tion or melting in the number of sub-grains. Allsopp[50] has also reported this loss in fluorescence intensity towards the end of the metering zone of a twin-screw extruder, but suggested that it is a result of better stabilizer distribution. In fact, the loss in fluorescence can be explained as a result of two factors. First, the random distribution of stabilizer particles due to material fluxing. This is in agreement with microscopical observations and the suggestion of Allsopp. This was further investigated by determining the relative fluorescence intensity of the screw samples. In Figure 6.34 it can be seen that the fluorescence intensity decreases as the melt is fluxed and moved towards the extruder die for all the three temperature samples. These results, as well as showing the effect of degradation, are strongly related to colour changes along the screw zones. By this method therefore changes in colour can be more accurately related to the degree of degradation compared with the conventional visual method. The second factor can be explained in terms of the disappearance of sub-grains (uniformity of melt) leading to a 'perfectly fused' homogeneous melt at the end of the melting zone. By using differential scanning calorimeter (DSC) method, it was found that the degree of fusion of primary particles (or more appropriately - the formation of chain entanglement network) increases as the UPVC melt is moved towards the die (Figure 6.35). This confirms not only the loss in fluorescence but also the suggestion that low density entanglement network is formed at the early stages of grain compaction which progressively becomes denser as the melt is moved towards the die. Berens et al[65], using two different polymer types, also suggested that at low temperature moulding the coherent mass is weakly held together by interdiffusion of short chain segments between particle boundaries - in broad agreement with the DSC results.

The SEM and TEM micrographs also show the existence of powder grains and distribution of stabilizer along the screw feed

FIGURE 6.33: DIC photomicrographs of 'core' samples of a twin-screw extruder produced at different extrusion temperatures

A: 1st screw turn

(i) 170°C

(ii) 194°C

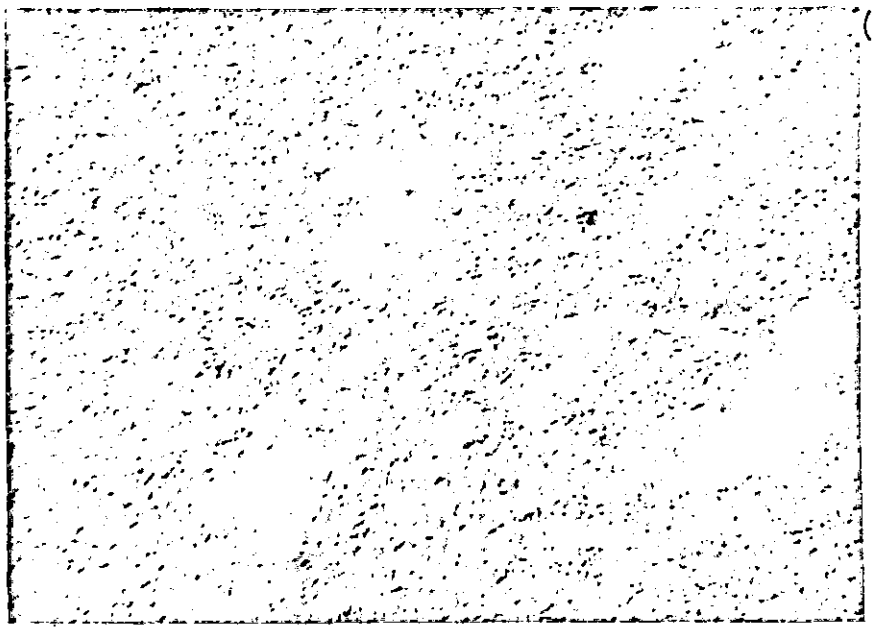

(iii) 210°C

30μm

B: 12th screw turn

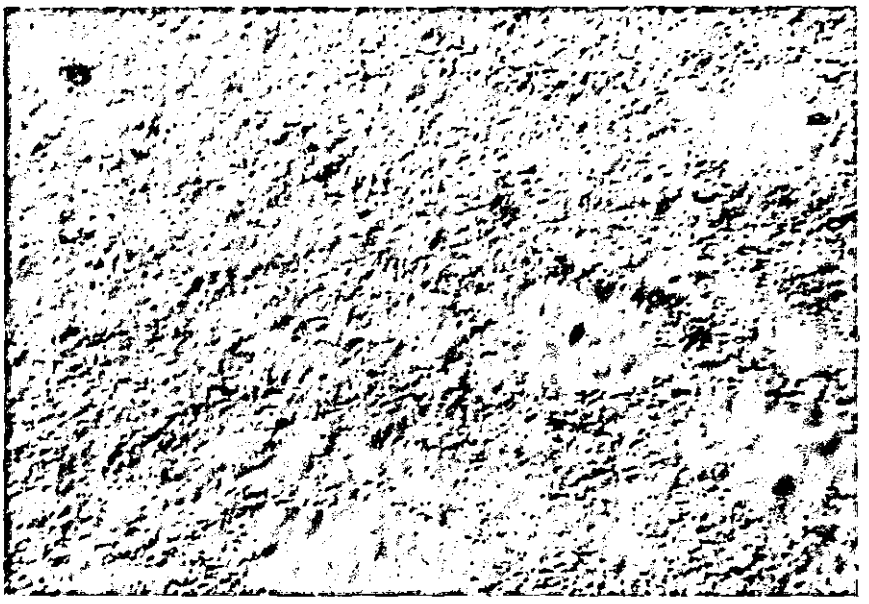

(i) 170°C

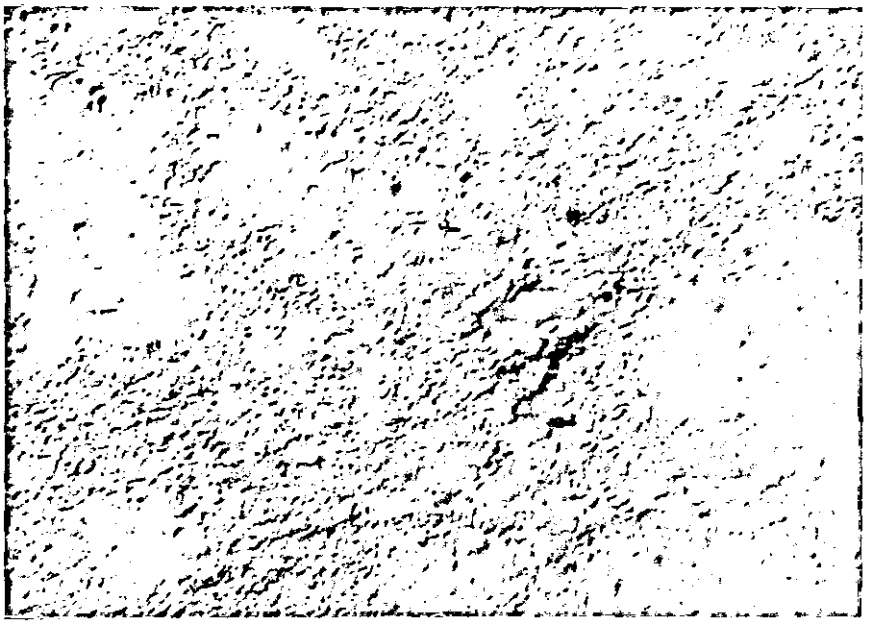

(ii) 194°C

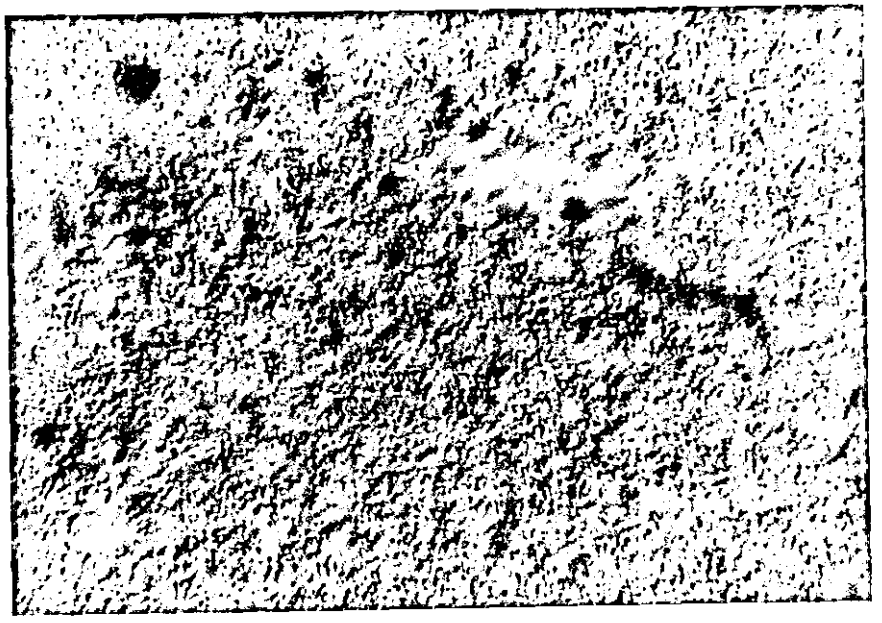

(iii) 210°C

30 μm

C: 29th screw turn

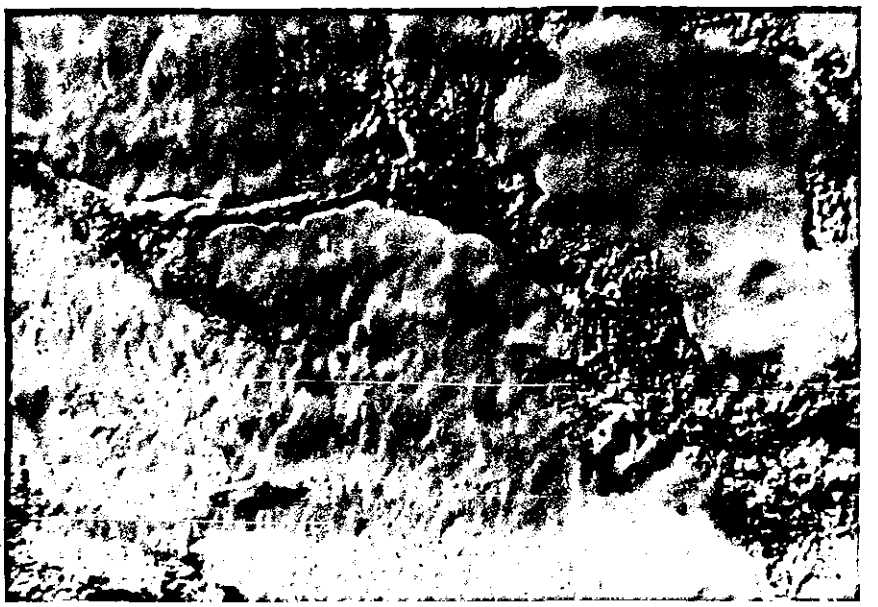

(i) 170°C

(ii) 194°C

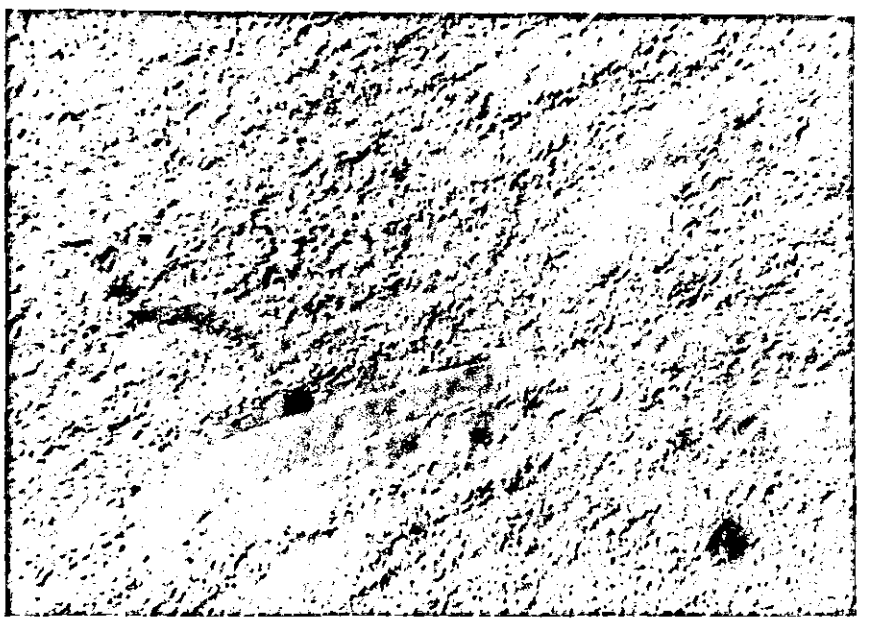

(iii) 210°C

30 um

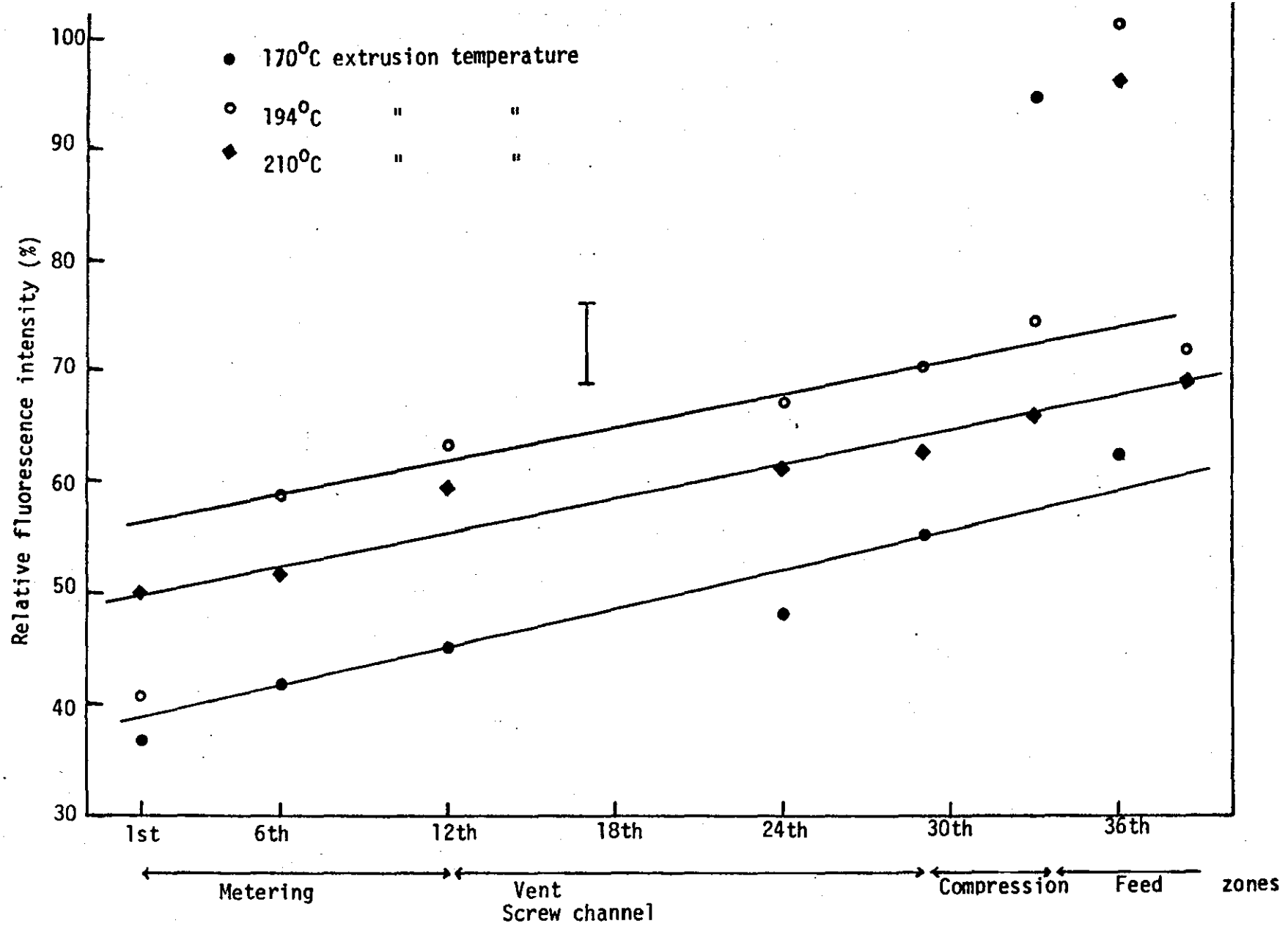


FIGURE 6.34 Relative fluorescence intensity of extruder screw-samples at different temperatures. (The error bar included illustrates the average deviation from the points plotted)

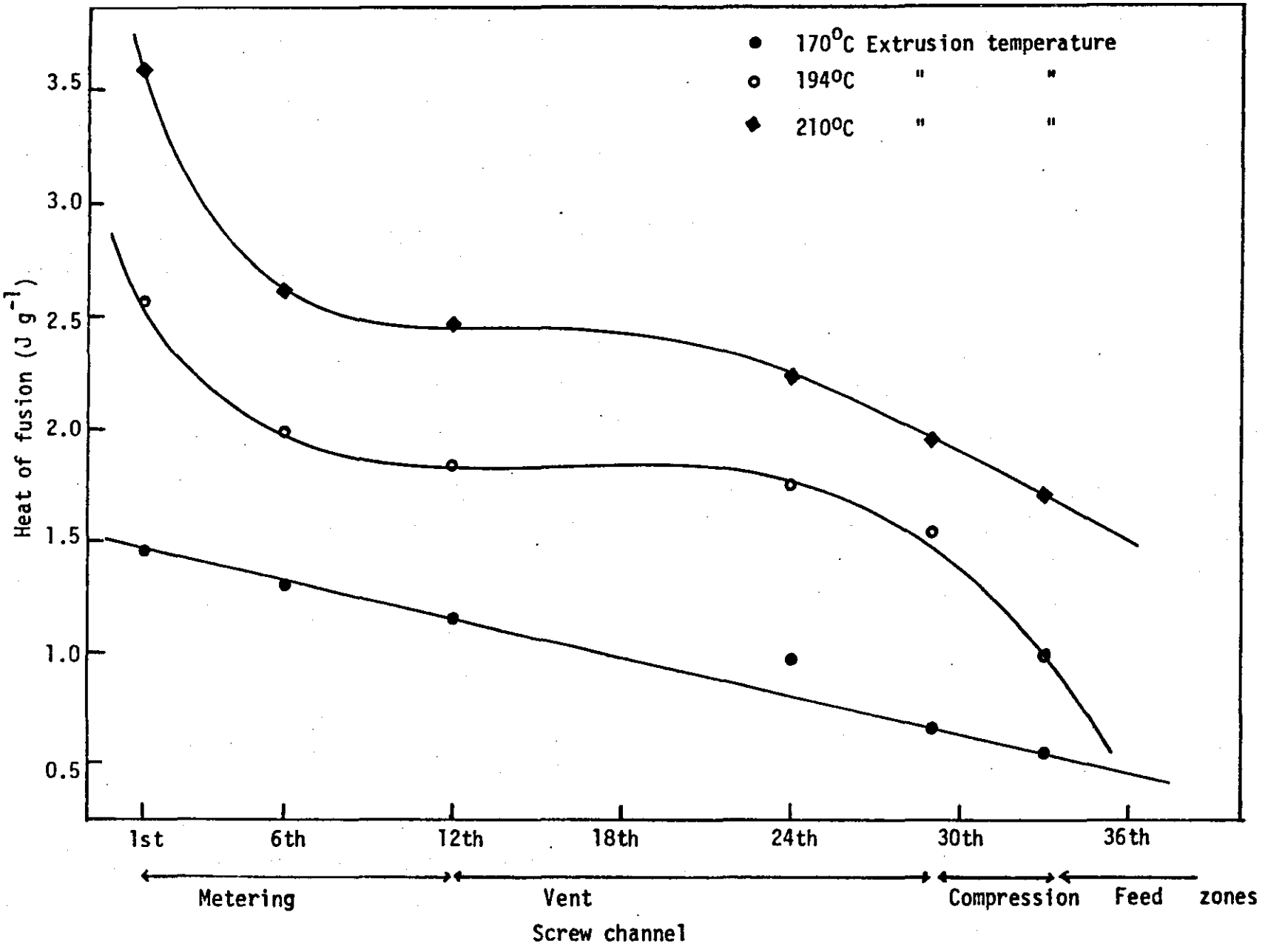


FIGURE 6.35 Heat of fusion of extruder screw samples of different temperatures

and compression zones to be very similar to that of compression moulding (Figure 6.36). However, at the end of the metering zone (1st screw channel), better stabilizer distribution, degree of mixing and fusion of primary particles are observed, and also the presence of voids are becoming more pronounced. Comparing these observations for screw samples produced at different temperatures (170, 194 and 210$^{o}$C), it is noticed that at any screw turn degree of fusion of primary particles, distribution of stabilizer and, where applicable, presence of micro-voids increase with increasing processing temperature. This can be explained by the fact that, for example, at the 29th screw channel particle fusion increases in the order 210$^{o}$C > 194$^{o}$C > 170$^{o}$C as shown earlier on by UV fluorescence and DIC micrographs in Figures 6.30 and 6.33.

Owing to the spiral shape of the screw samples the only physical property experiment successfully carried out is solvent absorption test. The result is plotted against the number of screw channels for each temperature in Figure 6.37, and are also summarised in Table 6.16. The reasons for the observed anomalous solvent absorption along the screw for different temperatures are due to compaction effect and thermo-mechanical variations at different zones - as summarised in the same Table 6.16. Comparing the graphs in Figure 6.37 it can be noticed that solvent absorption is higher at 194$^{o}$C than at 170$^{o}$C processing temperatures. The trend observed with higher temperature (210$^{o}$C) screw sample is mainly due to the effect of higher melt temperature than the presence of microvoids. In other words the results depended more on the structural modifications than micro-voids effect. The higher sorption value observed at high processing temperature (210$^{o}$C) compared with samples prepared at 170$^{o}$C is due to the formation of higher chain entanglement network in the former.

During examination of the screw samples a cross-section of fluorescence micrographsfrom screw surface to the barrel surface regions were obtained. Figure 6.38 shows typical examples of such

FIGURE 6.36: Fracture surface of 'core' samples produced at two extreme temperatures

A: Produced at 170°C

(i) 1st screw turn
Mag. x5K

(ii) 37th screw turn
Mag. x200K

B: Produced at 210°C

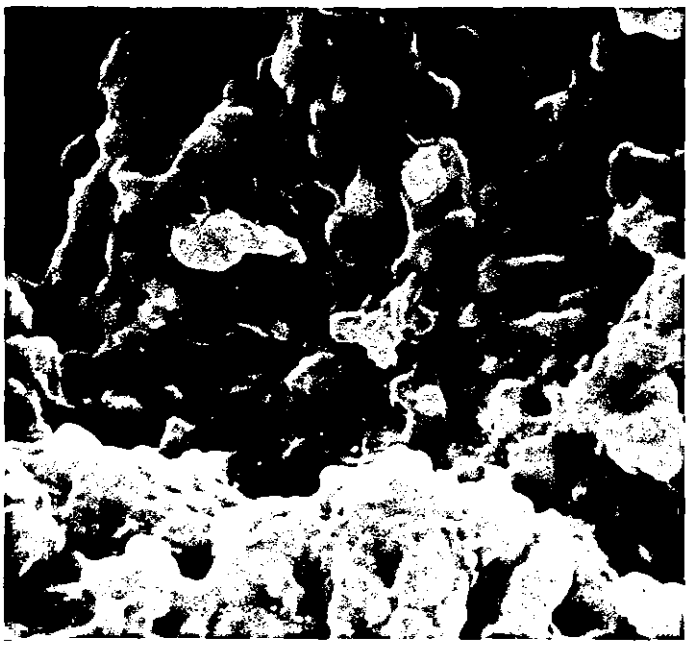

(i) 1st screw turn
Mag. x5K

(ii) 37th screw turn
Mag. x200K

(iii) 37th screw turn
Mag. x1K

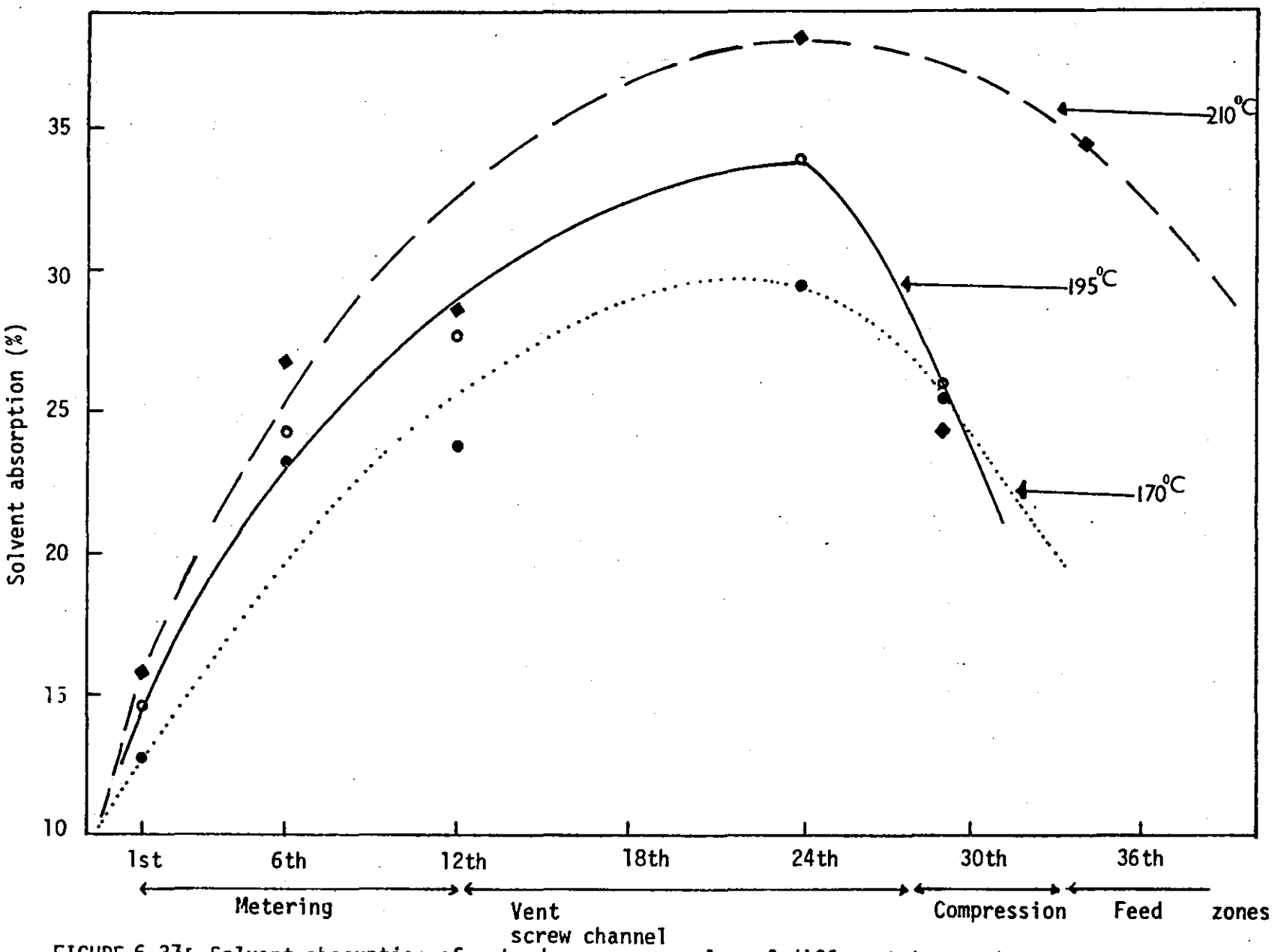


FIGURE 6.37 Solvent absorption of extruder screw samples of different temperatures

FIGURE 6.38: Fluorescence photomicrographs showing cross-sectional view of 'core' sample from screw surface to barrel surface.
Temperature of extrusion: 170°C
Sample position in screws: 19th screw turn

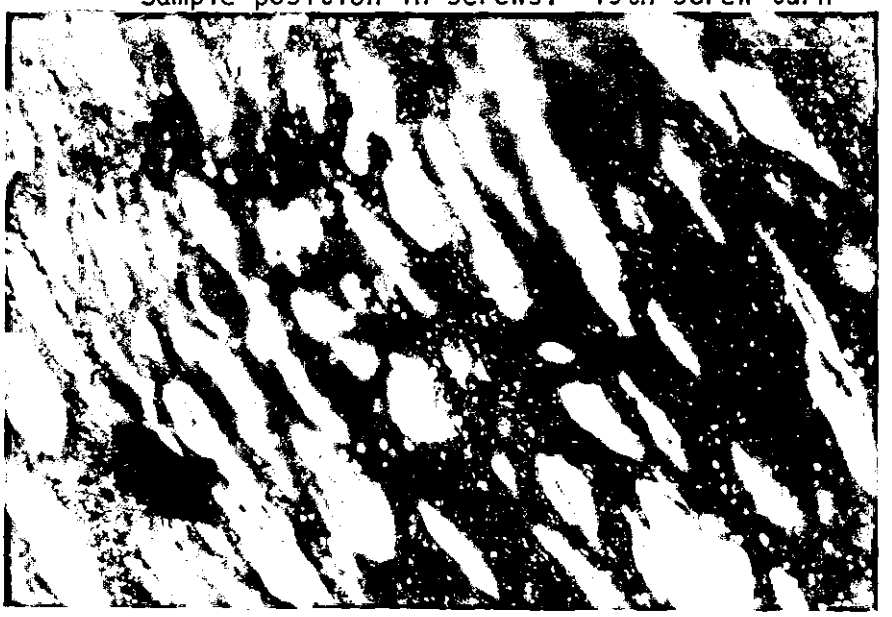

(a) Screw surface

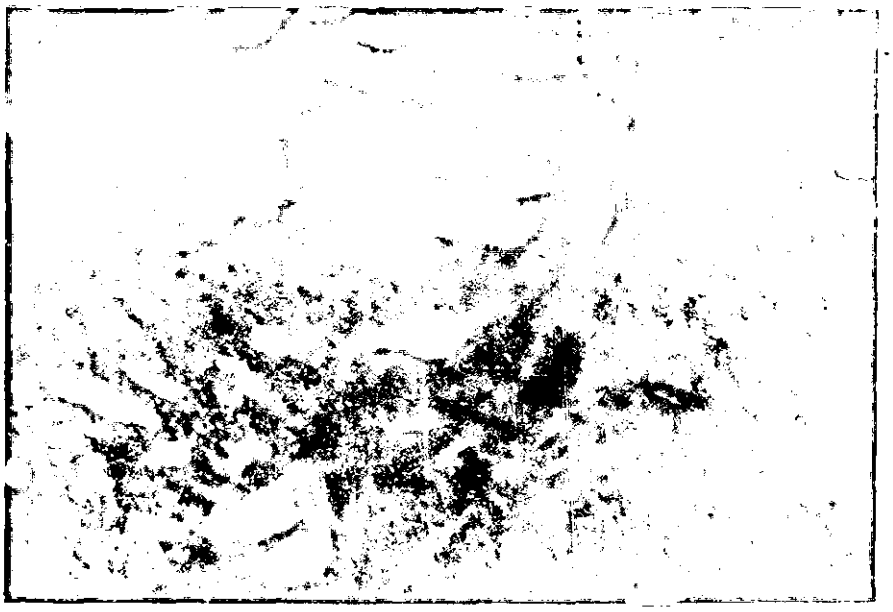

(b) Middle

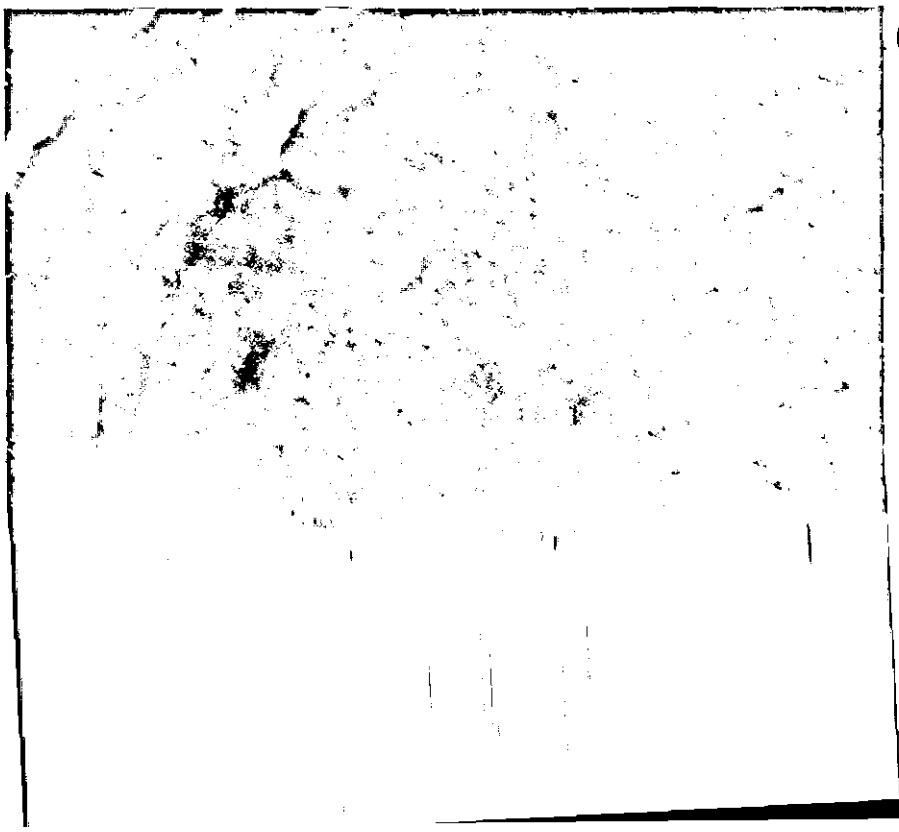

(c) Barrel surface

cross-sectional views made on specimens obtained from the 19th screw channel of normal processing temperature sample. More sub-grains are observed in the region nearer to the screw than in that nearer to the barrel (compare Figure 6.38 (a and c))- indicating that bulk structural modification takes place when the polymer melt is sheared against the barrel surface - than when sheared against the screw surface. It is also noticed that the sub-grains are elongated as they are moved from the screw surface towards the barrel surface. This process continues along the screw channels to deliver a superficially homogeneous melt to the extruder die.

TABLE 6.14:
Relative fluorescence intensity of extruder screw samples of different temperatures

| Screw Channel | Relative fluorescence intensity (%) | | |
|---|---|---|---|
| | 170°C | 194°C | 210°C |
| 1st | 36.73 | 41.62 | 50.37 |
| 6th | 41.78 | 59.13 | 53.38 |
| 12th | 45.02 | 63.13 | 58.60 |
| 24th | 48.75 | 67.48 | 59.85 |
| 29th | 55.02 | 70.85 | 62.75 |
| 33rd | 94.60 | 74.83 | 66.07 |
| 36th | 62.37 | 109.63 | 96.20 |
| 38th | - | 72.05 | 69.93 |

TABLE 6.15:

Heat of fusion of extruder screw samples of different temperatures

| Screw Channel | Heat of Fusion ($Jg^{-1}$) | | |
|---|---|---|---|
| | 170°C | 194°C | 210°C |
| 1st | 1.44 | 2.59 | 3.58 |
| 6th | 1.30 | 1.99 | 2.61 |
| 12th | 1.14 | 1.85 | 2.49 |
| 24th | 0.98 | 1.78 | 2.23 |
| 29th | 0.65 | 1.54 | 1.96 |
| 33rd | 0.54 | 0.96 | 1.72 |
| 36th | - | - | - |
| 38th | - | - | - |

TABLE 6.16:

Variation of screw turns with solvent absorption at different extrusion temperatures as a function of stabilizer distribution in standard formulation

| Screw-turns | Solvent absorption (%) | | | Reasons for some observed effect |
|---|---|---|---|---|
| | 170°C | 194°C | 210°C | |
| 1st | 12.73 | 14.71 | 15.93 | |
| 6th | 23.30 | 24.30 | 26.85 | |
| 12th | 23.78 | 27.65 | 28.47 | |
| 24th | 29.45 | 33.90 | 38.51 | |
| 29th | 25.44 | 25.95 | 24.40 | Compaction and degradation especially at 210°C - in the early stages of extrusion |
| 34th | - | - | 34.61 | Samples of 170°C & 194°C disintegrated in the solvent |

### 6.2.5 Conclusion

The following conclusionscan be drawn from the results and discussions given in the chapter:

1. At normal processing condition the degree of particle fusion and distribution of stabilizer depends on the composition of the formulation. Therefore increase in the amount of calcium stearate promotes the breakdown of sub-grains resulting in a higher degree of fusion and better distribution of stabilizer, while the same effects are at their minimum when the proportion of GS wax (an external lubricant) is reduced.

2. Incorporation of slightly incompatible internal lubricants (0.2 phr oxidised PE wax and 0.4 phr glycerol monostearate) in the standard formulation show very little improvement in the degree of particles fusion. However, when an impact modifier and a lubricant-stabilizer (respectively 1.5 phr paraloid K120N and 1.5 phr normal lead stearate) were separately incorporated there were significant changes in both particle fusion and stabilizer distribution. Products containing the impact modifier exhibited best mechanical performance, while those containing normal lead stearate showed lowest impact strength due to reduction in melt elasticity.

3. Changes in extrudates morphology and distribution of stabilizer are found to be affected by extrusion variables; extrusion screw speed and temperature. Best product performance is observed at 30 rpm, and beyond this screw speed the effect of 'surging' is evident. At this screw speed the sample contains fewer sub-grains and small-size primary particles, but large-size primary particles are dominant at higher screw speeds. The best distribution of

stabilizer and the highest homogeneity of matrix are also observed at 218°C extrusion temperature, where the extrudate seems to contain no sub-grains. At 170°C the extrudate fluoresces intensely from stabilizer devoid large-size sub-grains, while at 224°C the sub-grains melt and exhibit intense fluorescing striations along the flow regions. The absorption of solvent increases with increase in extrusion temperature up to 218°C. This is due to increase in molecular chain entanglement, but above 218°C cross-linking results leading to low solvent sorption.

4. There are two conditions which introduce voids in the UPVC matrix; when agglomeration of additive particles occurs and by evolution of hydrogen chloride-bubbles. The former occurs mostly at low extrusion temperature, whilst the micro-voids formation by HCl evolution occurs at high extrusion temperature and they become larger in diameter with increase in temperature.

5. The study of screw samples of a twin-screw extruder has shown that regardless of the processing conditions degree of fusion of particles and distribution of stabilizer improve with the movement of the polymer melt towards the extruder die. Final changes in the morphological features of the polymer melt are not achieved along the zones of the extruder screws. Taking any screw channel, the 'best' homogeneity of matrix is observed in regions nearer to the barrel surface than those closest to the extruder screw-surface.

6. 'Surface skin' is observed on all extrudates, but no evidence of this phenomenon is found in screw samples. Therefore, the presence of 'surface skin' is largely due to orderly alignment of residual grains in the melt, resulting from polymer flow and shear characteristics near the die surface.

# CHAPTER 7

# COMPRESSION MOULDING

## 7.0 Results and Discussion

The dry blends were compression moulded into sheets of similar thickness to the extrudates. Mouldings were prepared using a range of temperatures (150-230$^{o}$C) from standard formulation. Since the rates of shear in compression moulding are relatively low - in the order of 1-10 $sec^{-1}$ - compared to extrusion ($10^{2}$ - 3000 $sec^{-1}$), it presents an ideal situation to study the effect of temperature on morphological properties. Compression mouldings were also prepared from powder blends containing various additives and different concentrations of stabilizer. The object was to establish whether there exists any relationship between distribution of additives and morphological changes at a low shear, and at early stages of extruder core samples.

This chapter will be discussed under the following headings: Effect of temperature on morphology, and distribution of additive, Effect of concentration of stabilizer on particle fusion and Influence of formulation variations on changes in morphology.

## 7.1 Effect of Temperature on Morphology and Distribution of Additive

### 7.1.1 Distribution of Additive

The effect of moulding temperatures on distribution of stabilizer was studied using differential interference contrast, UV fluorescence and transmission electron microscopy. By the use of DIC, the stabilizer can be observed on the boundaries of the sintered powder (Figure 7.1) held in the form of a network. This is mostly observed with high processing temperature - from 170$^{o}$C. Below this temperature, it was not unexpected to find

FIGURE 7.1: DIC micrographs of samples moulded at different temperatures

(a) Moulded at 170°C

(b) Moulded at 190°C

(c) Moulded at 210°C

(d) Moulded at 230°C

100um

that compaction and densification of the grains was extremely poor. The original grains remained structurally unchanged. Although thin sections were obtained (with extreme difficulty) for the samples, there was no significant difference in structure between these sections and powder blends. This indicates that temperature, as well as shear, is vital if any change is to be observed in good agreement with the results obtained by X-ray study[1] and differential scanning calorimeter[148,175]. The effect of temperature is clearly visible in Figure 7.1 (DIC micrographs of samples moulded at 190°C and 210°C) which shows a significant change in morphology to be associated with increase in temperature. The grain boundaries are less visible, which should suggest that most of the stabilizer particles have diffused into the melt pool. It is also noted that, unlike liquid stabilizer blends used by several workers[148,179,180], even at higher moulding temperatures, a homogeneous matrix was not obtained. This is presumably due to the stabilizer particles still in abundance around the periphery of the grains. In order to verify this assumption the UV fluorescance and transmission electron microscope were employed.

The fluorescence micrograph of samples moulded at 190°C is shown in Figure 7.2. It is evident that the PVC grains periphery fluoresce brighter than the centres. Two different fluorescent areas can be identified viz. light-blue colour (at periphery of grains) and dark-blue (at centre of grains). The light-blue colour observed at the periphery of the grains is apparently due to the presence of stabilizer which prevents catastrophic degradation in these regions. It is not surprising that since distribution of the stabilizer is mostly on the communal boundaries of the PVC grains, the mouldings produced at higher temperatures (from 210°C) will have a substantially reduced fluorescent property as a result of higher degradation. This is confirmed by the absence of the light-blue fluorescent colour in samples of higher moulding temperatures. By the use of this

FIGURE 7.2: Fluorescence micrographs of sample moulded at different temperatures

(a) Sample moulded at 190°C

(b) Sample moulded at 210°C

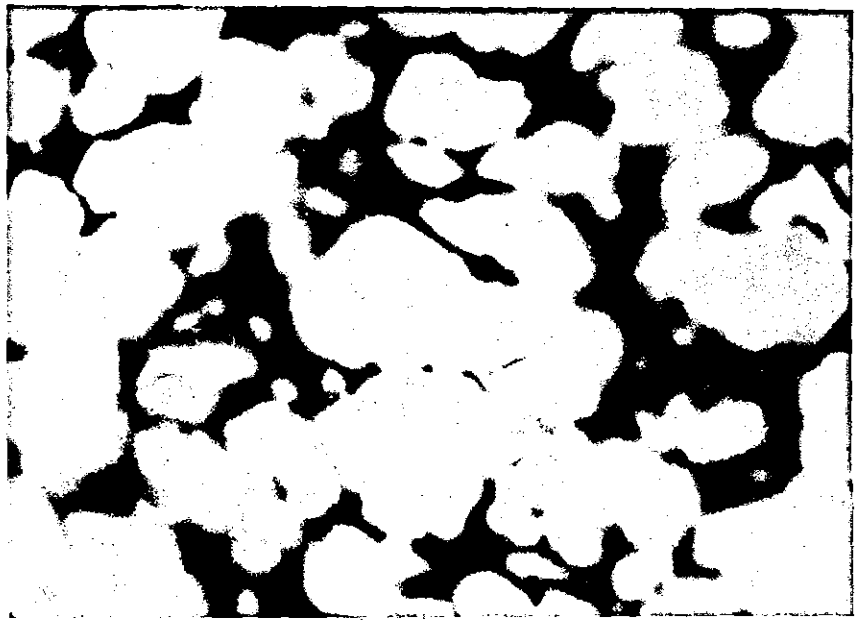

(c) Sample moulded at 230°C

50μm

technique, it was also observed that at 200°C (before loss of fluorescence due to degradation) the obliteration of the grains boundaries increases and some of the stabilizer particles previously located in those boundaries can be seen distributed in the resultant 'melt' pool or matrix.

The photomicrographs obtained by transmission electron microscopy (Figure 7.3) also provided a clear evidence that stabilizer particles, at 190°C and below, are within the boundaries of the PVC grains. It is clearly apparent that the dibasic lead stearate stabilizer which coated the grains during high speed blending remains as a coating even at this temperature and therefore forms a network pattern throughout the bed of sintered powder. This prevents catastrophic degradation, but is inadequate to prevent the generation of a brown colour because of degradation which occurs at the particles centres.

A similar observation was made in the feed section of extruder core samples (see Figure 6.31), but unlike the compression moulding, fluxing of the grains resulted in earlier appearance of sub-grains, thus a considerable improvement in stabilizer distribution and consequently in the colour of the materials. In a compression moulding process, even at higher moulding temperatures where the grains boundaries are partially obliterated (as shown earlier on), to permit a better distribution of the stabilizer the absence of fluxing still results in intense discolouration of materials.

Several workers[154,155,157] have shown that solid additives form a 'network' throughout the bed of sintered powder due to its 'failure' to penetrate into the supermolecular structure of PVC. This is unique with compression moulding of dry blends containing solid stabilizer. Similar observations also have been reported by Hemsley et al[48], and they have shown that solid additives remain at the periphery of the grains in compression moulding. However, none of the workers observed the colour change in fluorescence microscopy as a result of degradation.

FIGURE 7.3: TEM micrographs showing stabilizer distribution

(a) Sample moulded at 190°C. Stabilizer particles are still within grain boundaries. Mag. x6.6K

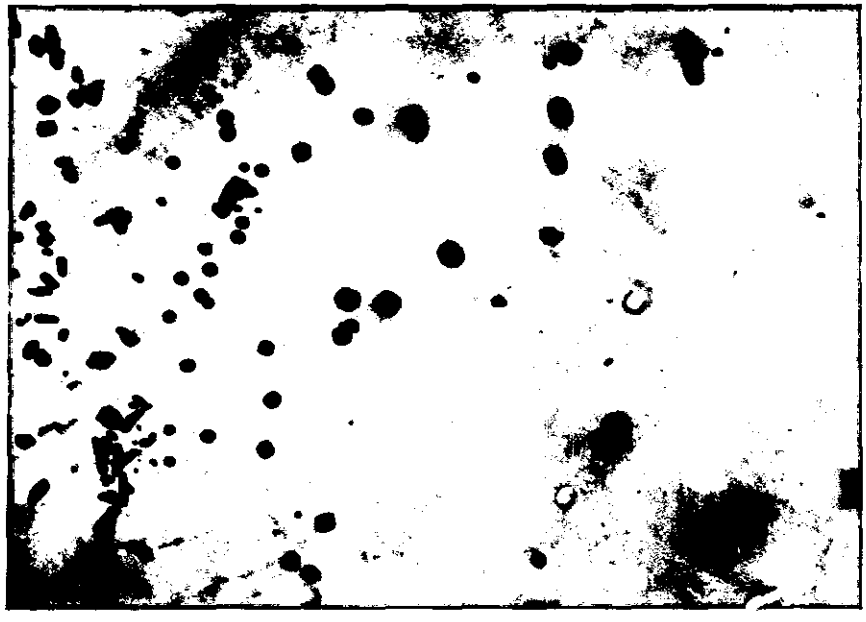

(b) Sample moulded at 210°C. Stabilizer particles migrated into grains due to boundary obliteratio Mag. x16K

(c) Sample moulded at 230°C. Mag. x16K

### 7.1.2 Effect of Temperature on Morphological Changes

Changes in the morphological features of PVC particles moulded by using a minimum of shear have been studied with differential interference contrast (DIC) microscopy. By examining thin sections of mouldings prepared at different temperatures (ranging from 150-230$^{o}$C) it was observed that increase in moulding temperature leads to structural modification. However, the rates of structural modification (morphological changes) were found to decrease with increase in moulding temperature. This can be attributed to the absence of fluxing and high shear which otherwise could have readily destroyed the original grain structure. Typical examples are shown in Figure 7.1 - which are DIC micrographs of samples moulded at 170$^{o}$C, 190$^{o}$C, 210$^{o}$C and 230$^{o}$C. At low moulding temperature (less than 170$^{o}$C) intra-particle fusion was observed, leading to the loss of particle porosity. Fusion between ajdacent grains was extremely weak - even sectioning the samples was difficult. Apart from high densification there was no evidence of grain modification.

Inter-particle fusion of appreciable strength begins to form from 170$^{o}$C. The PVC grains start to lose their original shape as the moulding temperature is raised, and subsequently the melted grains fused into a form of a network pattern (see Figure 7.1). This is attributed to the presence of solid stabilizer - which has already been discussed in Section 7.1.1. At higher moulding temperatures (from 210$^{o}$C) although the network pattern is still retained, some of the primary particles are revealed. However, there was no evidence of substantial loss of grain identity at this or higher moulding temperatures. This was closely studied by moulding samples at series of temperatures above 230$^{o}$C to include some badly degraded materials. On examining the thin sections of these materials, it was found that the grain memories were still visible in even the badly degraded samples. In other words, primary particles fusion is largely intra

(occurring within a grain) rather than inter (occurring between grains). This strongly suggests that although considerable amounts of primary particles fusion may result by processing at higher temperatures, the resultant grain entanglement network will largely be localised within the grain. This means that the product will be highly brittle - as shall be determined by an impact test in Section 7.1.3. The mode of fusion of the primary particles, thus, depends not only on the processing conditions and presence of additives but also on the type of process. In other words, the fusion of primaries can be readily achieved, among other things, by the correct combination of process and formulation.

The fusion or change in the morphological features of PVC grains during processing has been studied by many workers[154,161]. Gilbert et al[161] have reviewed a number of techniques for assessing PVC fusion and, using optical methods, they have shown that fusion of primaries is highly associated with shear and thermal history of the PVC. They also postulated a fusion mechanism of melting and recrystallising process which, like Allsopp[154], leads to an entanglement network formation at the later stages of a process. The observations made here are, to an extent, outside their findings and fusion models. They did not observe that fusion of primary particles occurs predominantly within the grains in low shear process. Presumably, it is because their fusion models were based on an extrusion process and other higher shear rates processes.

### 7.1.3 Effect of Temperature on Fusion Properties of Compression Mouldings

The assessment of fusion properties was further made with conventional methods, such as impact test, differential scanning calorimeter and solvent absorption. The findings will be related to microscopical observations made in the preceding sections. The results obtained from these experiments are shown in Tables 7.1 and 7.2 and are plotted in Figures 7.4 and 7.7. Impact strength

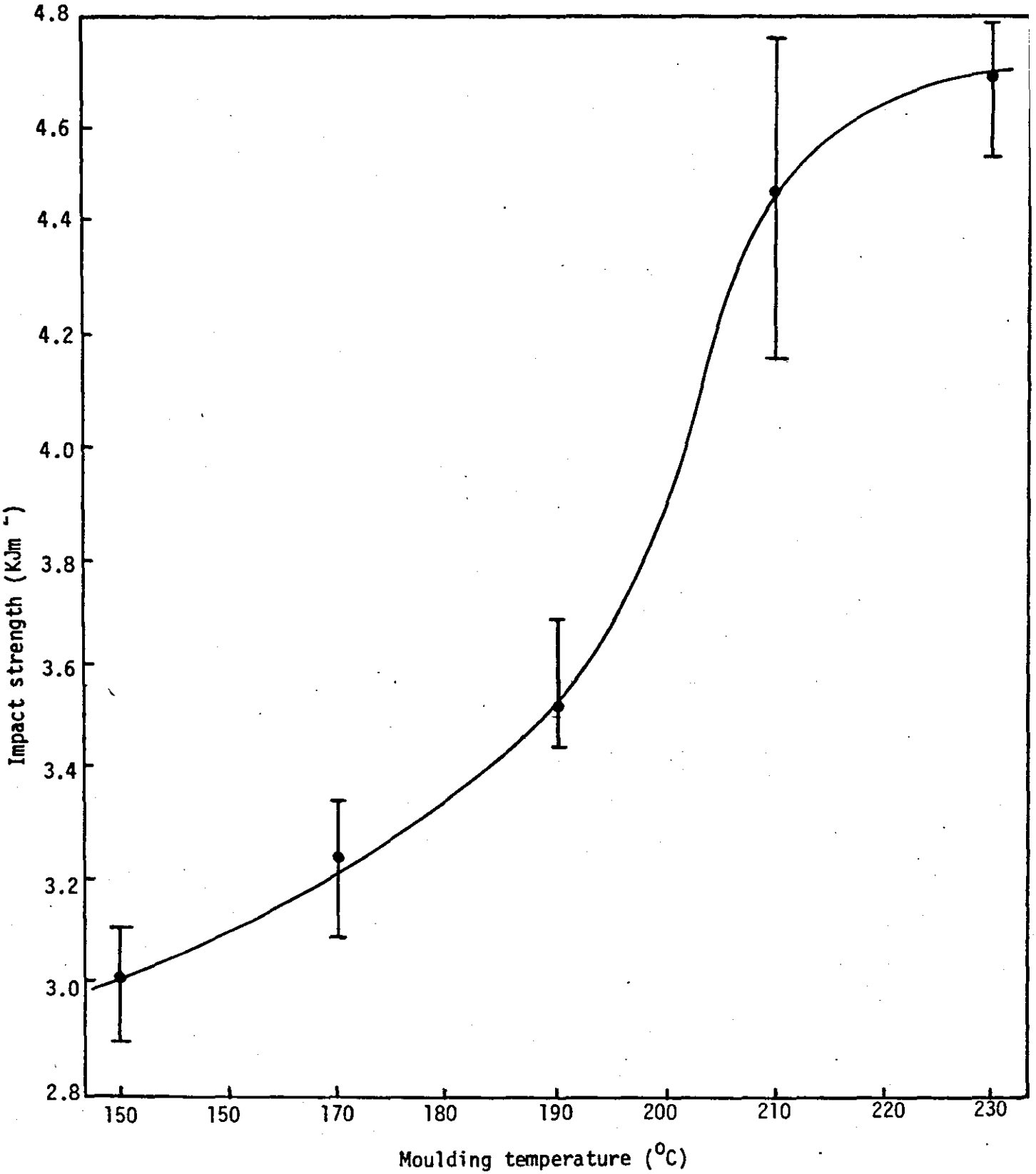


FIGURE 7.4: Variation of impact strength with moulding temperature

FIGURE 7.5: SEM micrographs of fracture surfaces of compression mouldings Mag. x5K

(a) 150°C

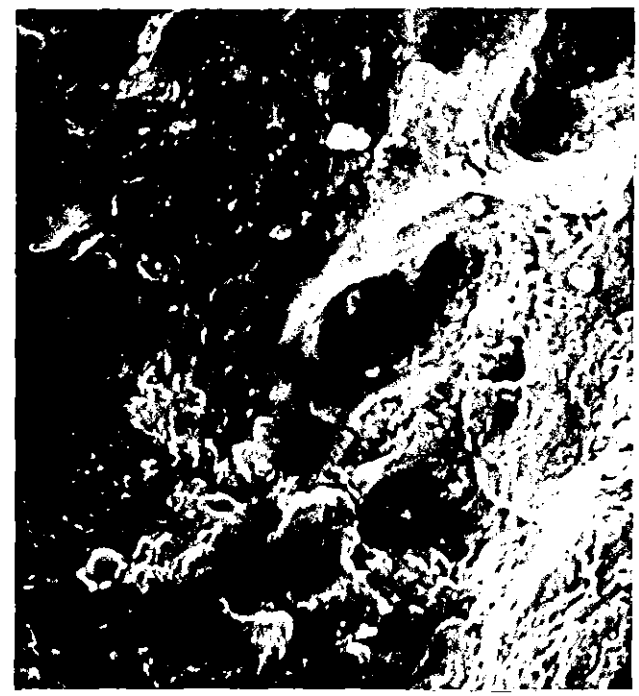

(b) 190°C

(c) 210°C

(d) 230°C

was observed to increase almost linearly with increase in moulding temperature up to 210°C, indicating presumably the occurrence of high grain compaction prior to their boundaries fusion[49,50]. Above this moulding temperature the dependency is much reduced, which should suggest that after certain temperature a lowering in impact strength, relative to the earlier increase, is apparent[161] - due to molecular chain cross-linking.

The fracture surfaces of the impact specimens were examined using scanning electron microscopy. Figure 7.5 (a, b, c and d) show the fracture surfaces of samples moulded at 150°C, 190°C, 210°C and 230°C respectively. From the micrographs it is evident that samples moulded at temperatures below 190°C failed in a brittle manner, occurring at the periphery of the 'fused' grains (that is, wholly inter-particle fracture). At 190°C some inter-particulate failure is observed, and at 210°C the failure is clearly ductile with fracture occurring mostly through the grains (that is, intra-particle fracture). Hemsley et al observed a similar mode of fracture when tensile strength measurement was made on samples compression moulded at different temperatures[48]. The graphic traces of fracture mechanisms of the samples are shown in Figure 7.6, where the single peak and double peaks are respectively indications of samples failing in a brittle and dutcile manner - in agreement with formation of short chain segments at low temperatures.

The results obtained with a differential scanning calorimeter are shown in Figure 7.7. This method measures the formation of secondary crystallites and presence of primary crystallinity as a function of thermal history[148,178]. From the raw data obtained, the heat of fusion ($\Delta H_f$) has been calculated (see Section 4.2) and presented in Table 7.2. It is shown that heat of fusion is not recorded for samples of low moulding temperatures. In other words, for samples of lower moulding temperature there is little or no difference in morphological features between them and

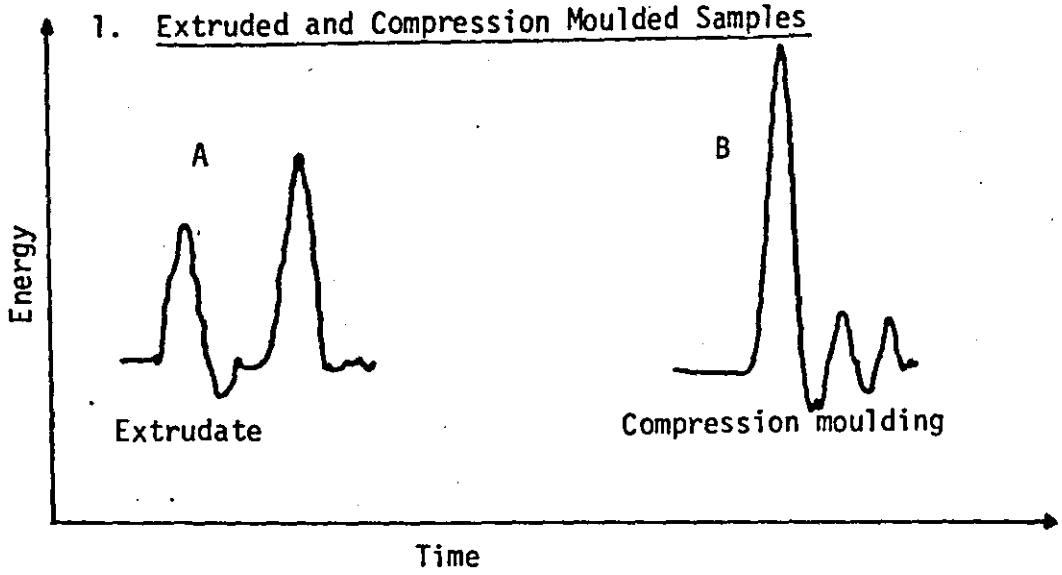


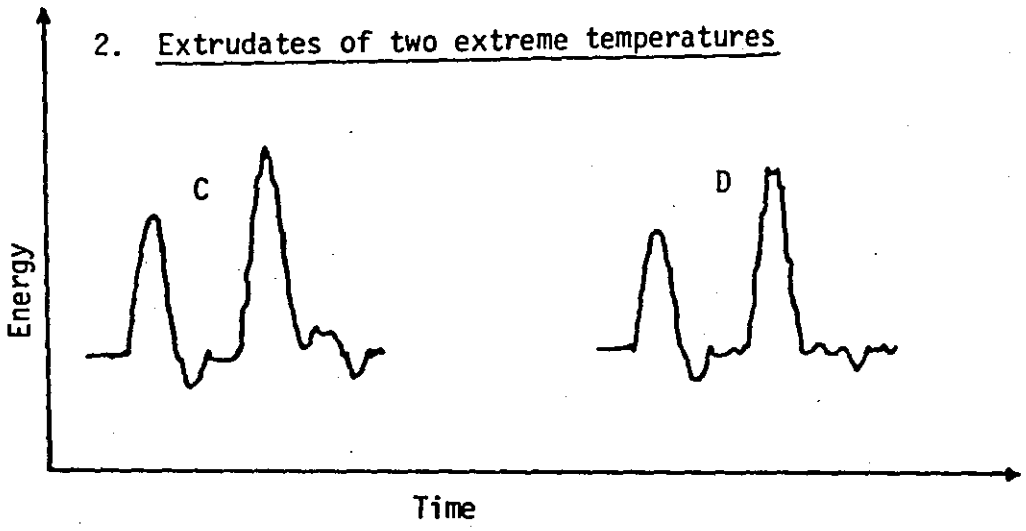


FIGURE 7.6(a) Comparison of graphic traces for the fracture mechanisms of impact test samples

| | A | B | C | D |
|---|---|---|---|---|
| Processing Temp ($^{o}C$) | 194 | 190 | 188 | 224 |
| Breaking Force (N) | 340 | 218 | 340 | 320 |
| Mode of Failure | Ductile | Brittle | Ductile | Ductile |

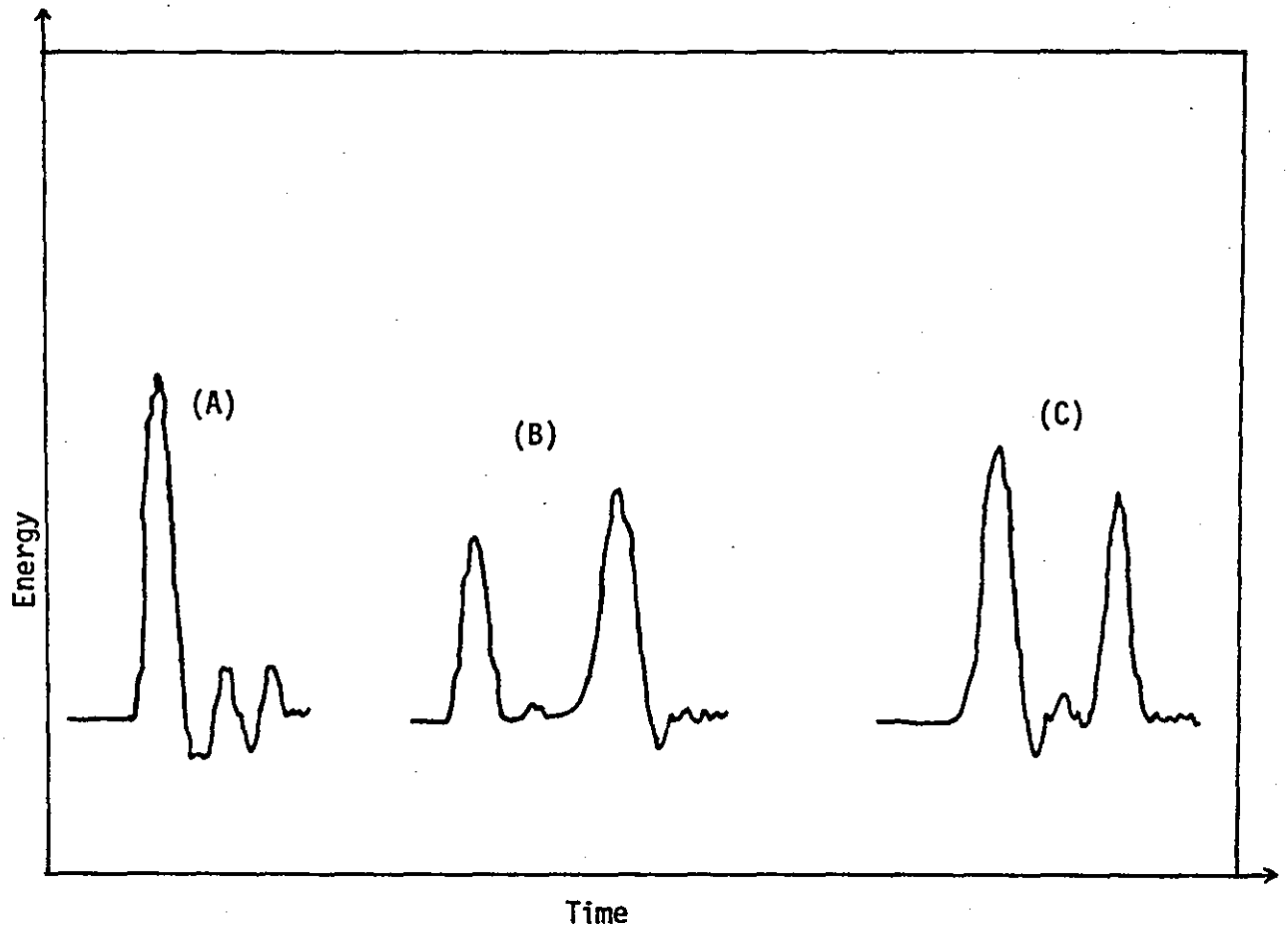


FIGURE 26(b) Comparison of graphic traces of fracture mechanisms of compression moulded samples

| | A | B | C |
|---|---|---|---|
| Moulding temperature ($^{o}$C): | 170 | 210 | 220 |
| Breaking force (N) | 240 | 160 | 180 |

powder blends - at least not in samples of such high section thickness as used here. This result is in good agreement with microscopical observations made in the preceding section. For higher temperature mouldings heat of fusion increases steeply with temperature up to 210°C, and above this temperature the dependency is again much reduced (Figure 7.7). Terselius et al[178] and Gilbert et al[148] have used this method to investigate the gelation of rigid PVC. They have shown that the appearance and subsequent increase of the broad endothermic peak, as a function of moulding temperature, may be due to the formation of secondary crystallites. Since this secondary crystallite is associated with structural modification, it is apparent that only grain compaction had occurred below 170°C. This also indicates that grains compaction could occur, most times, without simultaneous fusion of primary particles and entanglement network.. This nearly always produces a friable sample. The thermograms from these measurements are shown in Appendix 4. The overall result is considerably low compared with DSC results of the extruded samples (Figure 6.27). This large difference in value could be due to fluxing and shearing, as well as heating, associated with extruded samples. Solvent absorption results (Table 7.2) show a similar trend to impact strength and differential scanning calorimeter results. Percentage solvent absorption was found to decrease with increasing moulding temperature. It is important to emphasise again that the test period was short - 15 minutes - to avoid misleading results due to flaking of the samples. An entirely different result can sometimes be obtained if the samples are left in acetone for several hours[173-175]. This is only suitable for highly gelled or fused samples such as extrudates, where flaking rarely occurs. In this study when the test period was doubled to 30 minutes, samples moulded at lower temperatures (150°C and 170°C) were almost completely disintegrated, and flaking was common with high temperature mouldings.

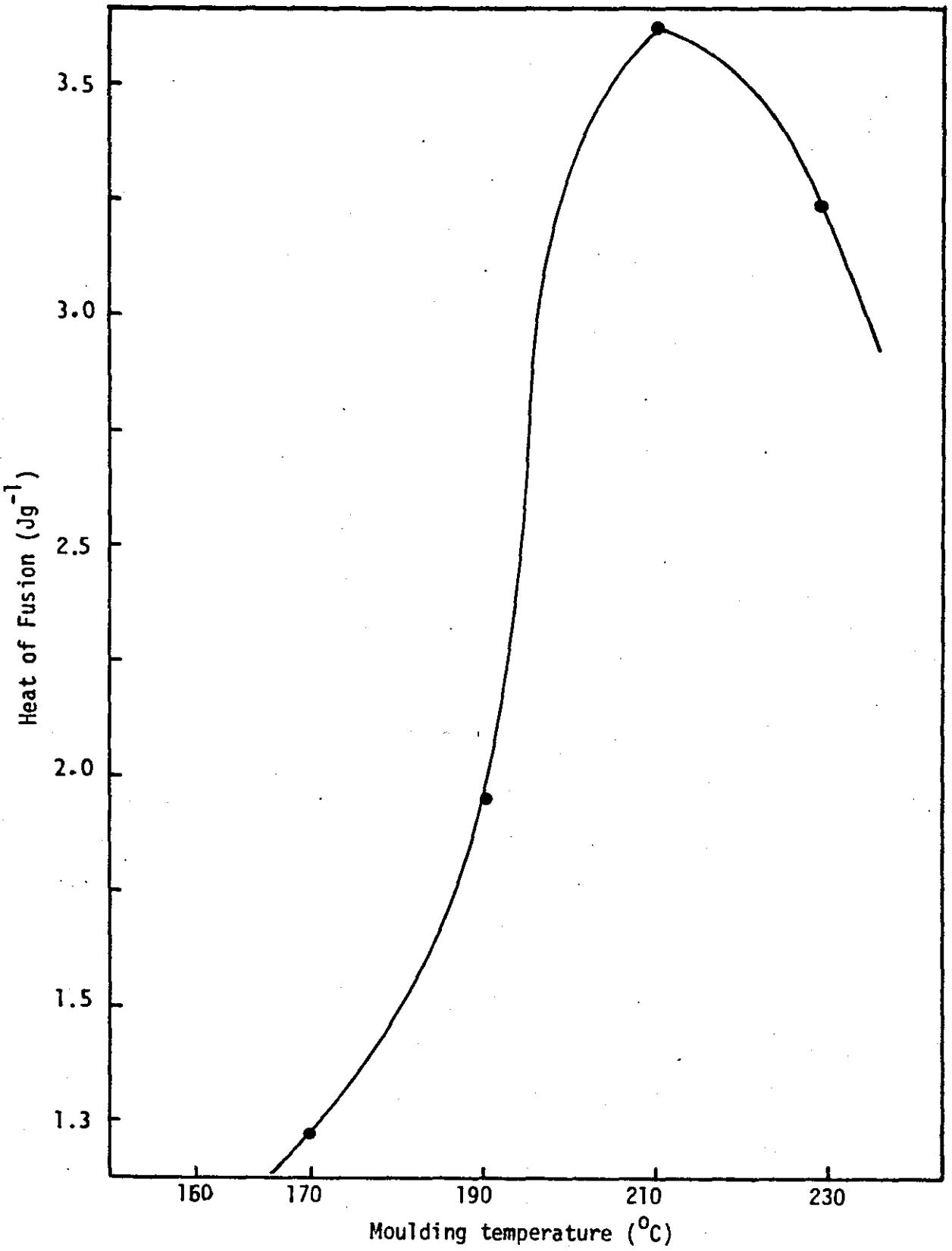


FIGURE 7.7 : Effect of temperature on heat of fusion in compression mouldings

TABLE 7.1:

Variation of impact strength with temperature in compression moulding

| Temperature (°C) | Impact Strength (kJ $m^{-3}$) | | | | | | |
|---|---|---|---|---|---|---|---|
| | 1 | 2 | 3 | 4 | 5 | 6 | Average |
| 150 | 3.10 | 2.98 | 2.90 | 3.07 | 2.95 | 2.98 | 3.00 |
| 170 | 3.28 | 3.26 | 3.08 | 3.33 | 3.27 | 3.22 | 3.24 |
| 190 | 3.54 | 3.46 | 3.55 | 3.68 | 3.48 | 3.49 | 3.53 |
| 210 | 4.23 | 4.59 | 4.33 | 4.57 | 4.78 | 4.17 | 4.45 |
| 230 | 4.73 | 4.50 | 4.57 | 4.80 | 4.69 | 4.53 | 4.64 |

TABLE 7.2:

Effect of temperature on fusion properties of compression mouldings

| Temperature (°C) | Heat of Fusion $\Delta H_f$ ($Jg^{-1}$) | Solvent Absorption (%) |
|---|---|---|
| 150 | - | - |
| 170 | 1.25 | - |
| 190 | 1.95 | 4.96 |
| 210 | 3.61 | 4.63 |
| 230 | 3.30 | 4.23 |

These results obtained with 'conventional' methods are not wholly in agreement with microscopical observations made in the preceding sub-sections - especially for samples moulded at lower temperatures. For instance, the DSC, unlike microscopy techniques, did not record any fusion at lower moulding temperatures. Similarly, no result was obtained by solvent absorption tests for lower temperature samples. It could, therefore, be assumed that at lower moulding temperature the percentage ratio of compaction to inter-particle fusion is in the range of 95:5. This means that only very small percentage of grain fusion, perhaps not measurable with these 'conventional' methods, is occurring at lower moulding temperatures.

## 7.2 Influence of Dibasic Lead Stearate Concentration on Morphological Changes

Variations in the amount of stabilizer in the standard formulation were made in order to clearly understand the relationship between stabilizer distribution and morphological changes under a minimum of shear. In the preceding section (Section 7.1) it has been demonstrated that stabilizer distributes around the periphery of the PVC grains in compression mouldings. This was shown to be responsible for a form of 'network' pattern observed in the sintered powder, which at higher moulding temperatures was still visible.

In this section, mouldings containing different concentrations of dibasic lead stearate stabilizer have been examined using both light and electron microscopy techniques. Figure 7.8 (a, b, and c) shows the micrographs obtained with differential interference contrast, Figure 7.9 (a, b and c) shows UV fluorescence micrographs and Figure 7.10 shows the transmission electron micrographs. The topography of the moulding can be seen to change as the concentration of lead stabiliser is increased. In moulding with low concentration of DBLS (< 1.5 phr) the boundaries of the grains are almost completely obliterated. As expected this feature is

FIGURE 7.8: DIC micrographs of samples containing different concentrations of DBLS stabilizer

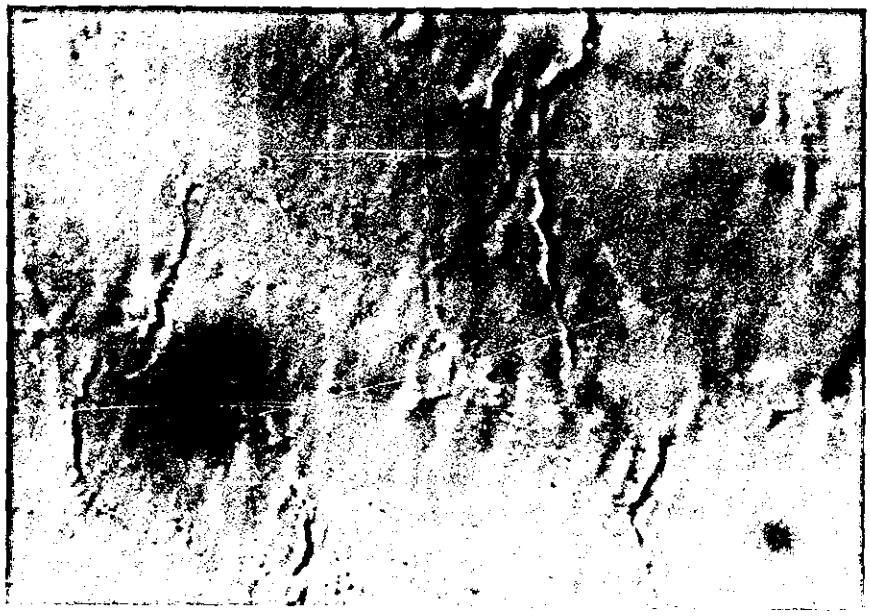

(a) Contained no stabilizer

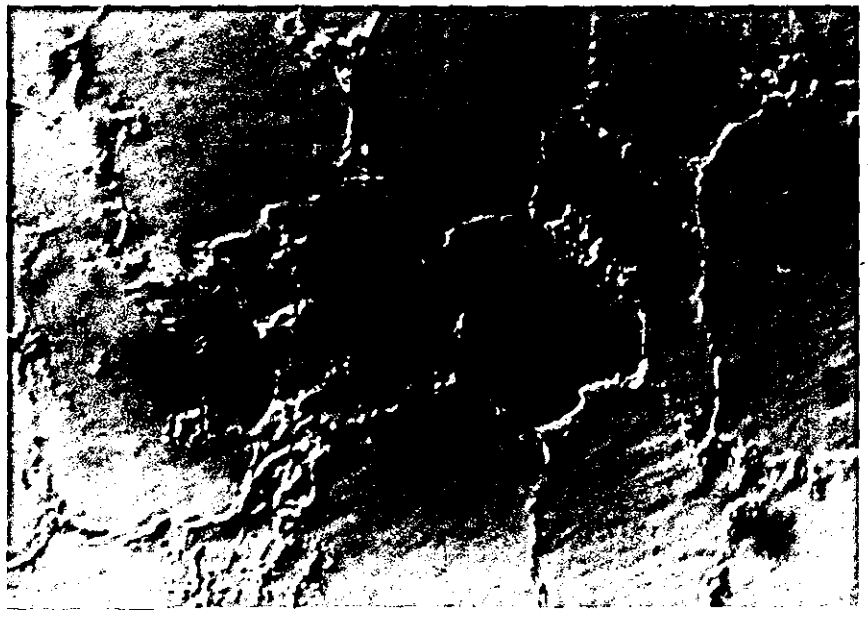

(b) Contained 2.5 phr dibasic lead stearate stabilizer

(c) Contained 4 phr dibasic lead stearate stabilizer

100um

FIGURE 7.9: The UV fluorescence micrographs of samples containing different concentration of DBLS stabilizer

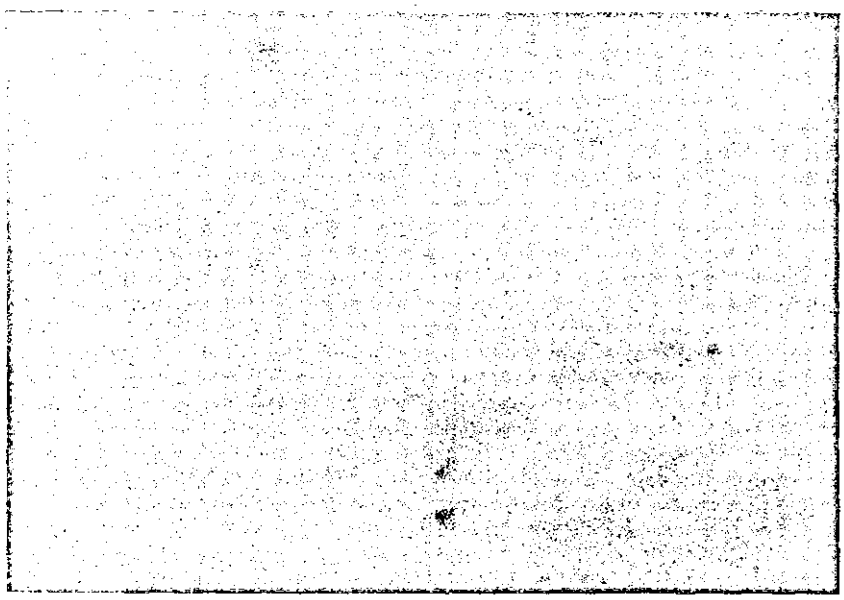

(a) Contained no stabilizer. Grains boundaries not visible

(b) Contained 2.5 phr of stabilizer Grains fluorescence differ from that of boundaries due to stabilizer

(c) Contained 4 phr of stabilizer. Grains boundaries are very visible due to excess stabilizer

50 μm

most pronounced in the mouldings with no stabilizer (Figure 7.8a) indicating that solid stabilizer is responsible for the presence of the 'network' pattern seen in the mouldings. Figure 7.9 (a, b and c) shows respectively the fluorescence micrographs of samples containing 0 phr, 2.5 phr and 4 phr of stabilizer. As the stabilizer concentration is increased the grain boundaries become more visible - fluorescing much brighter than the grains centres. This Figure 7.9 also clearly indicates that solid stabilizers do not penetrate into PVC grains during blending. Katchy[155] demonstrated the distribution of solid and liquid stabilizers in compression mouldings, but failed to observe this difference in topography between the samples containing these stabilizers. However, he pointed out that the liquid tin stabilizer was wholly absorbed into the PVC grains, while the solid stabilizer remained on the periphery of the grains. In other words, since the liquid stabilizer was absorbed into the grains during blending it is obvious that a high degree of fusion would be observed in the moulded samples[148,173,179]. In comparison with blends containing solid stabilizer, there was hardly any grain boundary found in those mouldings.

As the concentration of stabilizer increases (up to 4 phr) its quantity on the grains boundaries increases and the samples become highly brittle. Evidence of stabilizer particles agglomeration is clearly shown in Figure 7.10 (micrographs from TEM studies). A void near the agglomerated stabilizer particles apparently arising from poor grain compaction is also clearly seen. In general, there is no evidence of gross structural modification observed in mouldings containing either lower or higher DBLS concentration. The obvious relationship which exists between stabilizer concentration and morphological changes, as a function of stabilizer concentration, is that at higher concentration the material thermal history is highly reduced - that means reduction in degree of fusion of primary particles.

FIGURE 7.10: TEM micrographs of compression moulding samples containing different DBLS concentrations

(a) Contained 1 phr of DBLS.
Mag. x33K

(b) Contained 2.5 phr of DBLS.
Mag. x6.6K

(c) Contained 4 phr of DBLS.
Mag. x6.6K

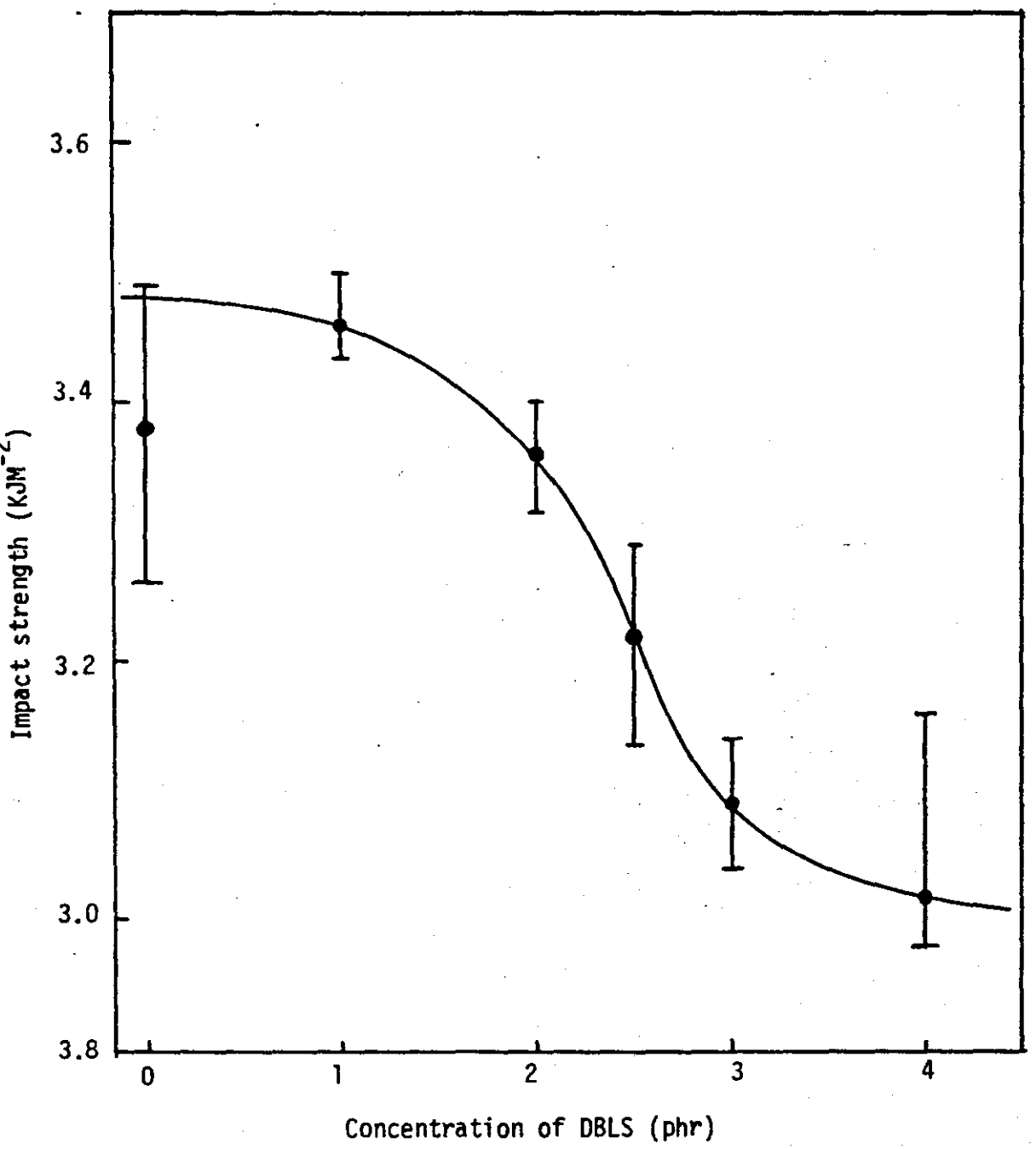


FIGURE 7.11 Effect of dibasic lead stearate concentration on impact strength of compression samples

This suggests that the impact strength of the moulding will be affected by higher ratio of stabilizer; and in fact the impact strength was seen to decrease with increasing stabilizer concentration (Figure 7.11). The low value of impact strength observed with non-stabilized samples compared with samples containing 1 phr stabilizer is presumably due to the effect of degradation. At 4 phr (higher stabilizer loading) the dependency increases. This is attributed to lower compactibility between the PVC grains. Examination of fracture surfaces of impact test bars revealed that the failure is clearly brittle and entirely inter-particle. The brittle failure in non-stabilized samples is largely due to high chain ( cross linking ) as a result of degradation.

Solvent absorption and differential scanning calorimeter results (Tables 7.3 and 7.4) also showed that lower degree of fusion is associated with higher ratio of stabilizer. Figure 7.12 shows the results obtained from DSC to decrease, and solvent absorption to increase with increasing stabilizer concentration. This indicates that the fusion level and grain compactibility are reduced as the amount of stabilizer is increased, in general agreement with the results of differential interference contrast microscopy.

In a further attempt to elucidate the relationship between stabilizer distribution and morphological changes, it was thought necessary to interchange dibasic lead stearate (DBLS) with tribasic lead sulphate in the standard formulation. The latter has not only higher lead content but also wider range of particle size distribution (see Section 2.1 ). From Figure 7.13 it can be seen that the grain boundaries are more visible in mouldings containing tribasic lead sulphate (TBLS) than in those containing DBLS (Figure 7.13). As a result poorer stabilizer distribution is observed due to lower degree of grain fusion. This suggests a fall in the impact strength of the standard formulation. The results obtained from impact strength and solvent absorption tests are

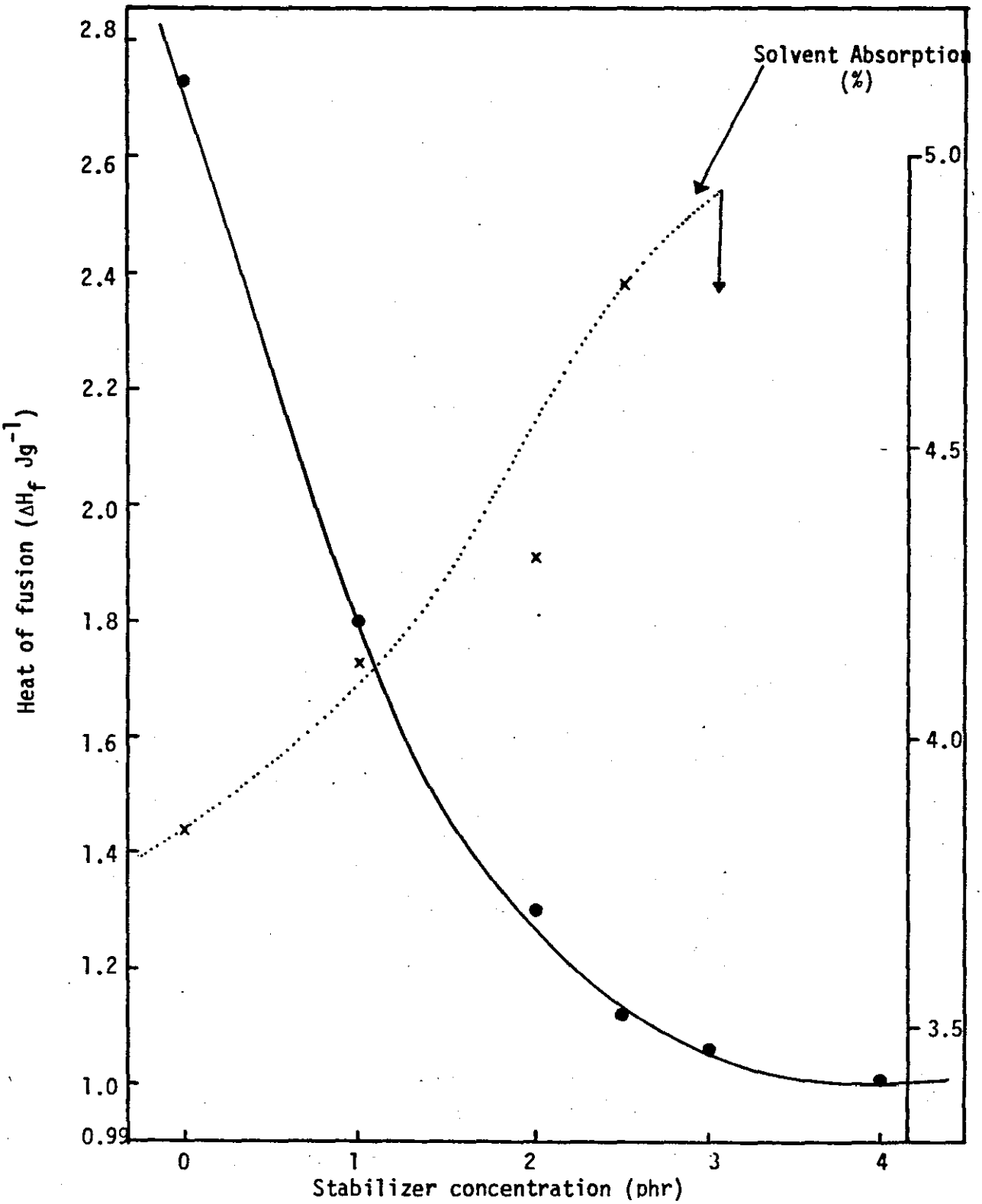


FIGURE 7.12: Effect of stabilizer concentration on fusion properties of compression mouldings

FIGURE 7.13: The micrographs of samples containing different stabilizers

(a) Sample containing dibasic lead stearat stabilizer. (DIC micrograph)

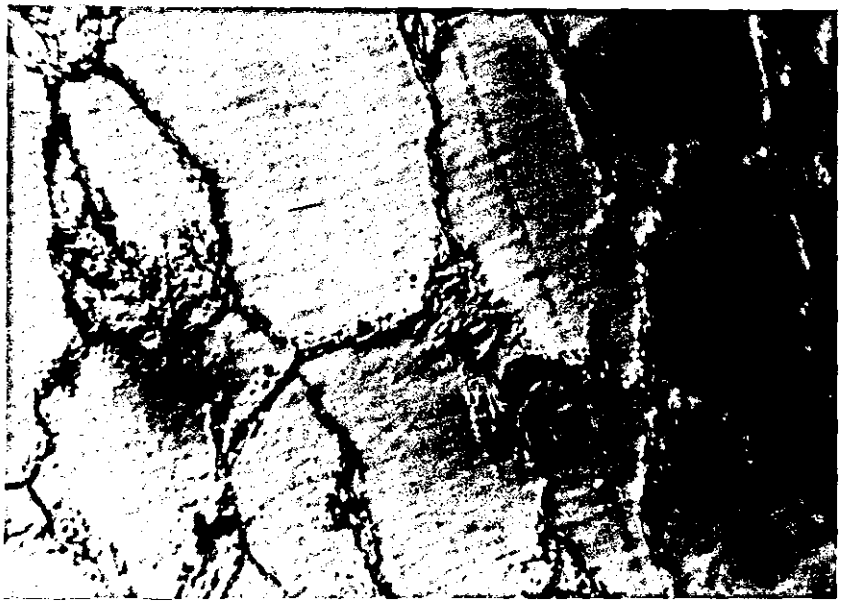

(b) Sample containing tribasic lead sulphate stabilizer. (DIC micrograph)

100μm

(c) Sample containing tribasic lead sulphate stabilizer. (Fluorescence micrograph. Compare it with Figure 7.2a)

50μm

TABLE 7.3:

Effect of stabilizer concentration on impact strength of compression moulding

| Concentration of DLBS (phr) | Impact Strength (kJ $m^{-2}$) | | | | | | |
|---|---|---|---|---|---|---|---|
| | 1 | 2 | 3 | 4 | 5 | 6 | Average |
| 0 | 3.33 | 3.49 | 3.32 | 3.26 | 3.42 | 3.45 | 3.38 |
| 1.0 | 3.45 | 3.50 | 3.44 | 3.48 | 3.45 | 3.46 | 3.46 |
| 2.0 | 3.40 | 3.34 | 3.35 | 3.36 | 3.32 | 3.38 | 3.36 |
| 2.5 | 3.13 | 3.19 | 3.26 | 3.19 | 3.24 | 3.29 | 3.22 |
| 3.0 | 3.14 | 3.10 | 3.06 | 3.10 | 3.09 | 3.04 | 3.09 |
| 4.0 | 2.89 | 3.11 | 2.89 | 3.14 | 2.92 | 3.16 | 3.02 |

TABLE 7.4:

Effect of stabilizer concentration on fusion properties of compression mouldings

| Concentration of DBLS (phr) | Heat of fusion $\Delta H_f$ ($Jg^{-1}$) | Solvent Absorption (%) |
|---|---|---|
| 0 | 3.68 | 3.84 |
| 1.0 | 2.22 | 4.13 |
| 2.0 | 1.46 | 4.31 |
| 2.5 | 1.34 | 4.78 |
| 3.0 | 1.26 | - |
| 4.0 | 1.21 | - |

shown in Table 7.3. However, although no structural modifications was observed, less discolouration (which gave low fluorescence intensity) was observed with this moulding. This is presumably due to the higher lead content and better heat properties associated with tribasic lead sulphate stabilizer[31].

## 7.3 Effect of Different Formulations on Morphology of Moulding

In order to make an in-depth study of the influence of various additives on stabilizer distribution in dry blends, the blends were again moulded under a low shear. By this method it is possible to perhaps understand readily the influence of certain additives in the distribution of stabilizer in mouldings.

From the formulations (Section 2.2), it will be most convenient to discuss this section under two headings: effect of varying the ratios of lubricants and effect of incorporation of 'secondary' additives into the standard formulation.

### 7.3.1 Effect of Varying the Ratios of Lubricants

In this sub-section, the influence of lubricant concentration and lubricant type in relation to fusion and distribution of stabilizer are discussed. The external and internal lubricants used were respectively G.S. wax and calcium stearate. The concentrations of the G.S. wax and calcium stearate used in the standard formulation were varied as shown in Table 2.4. Figure 7.14 (a, b and c) shows the micrographs of formulation 4 obtained with (a) DIC, (b) fluorescence, and (c) TEM respectively. It can be seen that simultaneous reduction and increment in G.S. wax and calcium stearate respectively resulted in better distribution of the stabilizer - that means the 'obliteration' of grain boundaries. It is evident from the DIC micrographs that the grain boundaries are less seen, and that most of the stabilizer particles have penetrated into the grains. A typical distribution pattern observed with TEM in most regions (in about 70%) of the matrix is shown in

FIGURE 7.14: The micrographs of formulation containing high concentration of calcium stearate

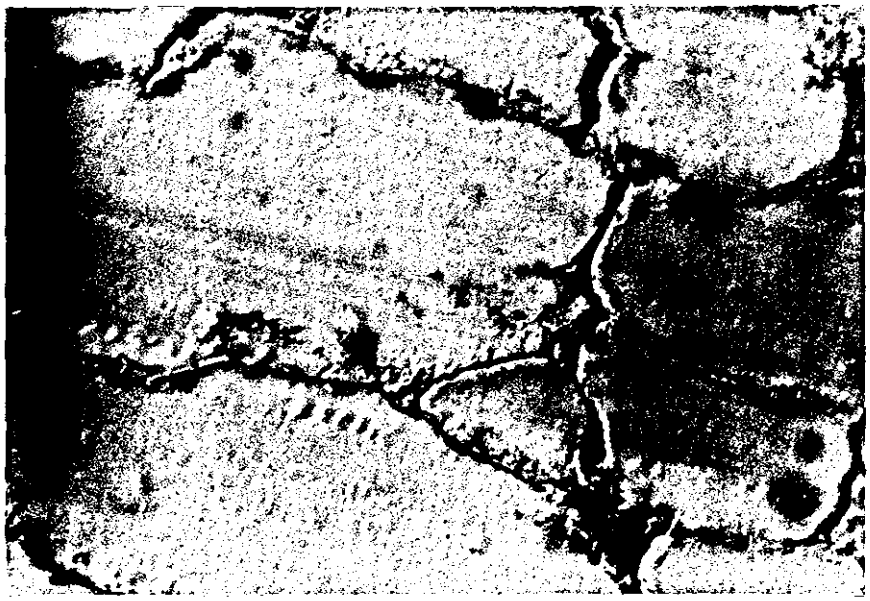

(a) DIC micrograph. Compare with standar formulation Fig 7.1b (Less stabilizer particles in the grain boundaries).

50um

(b) Fluorescence micro-graph. Compare with Fig 7.2a (Loss of grains boundaries is evident

50um

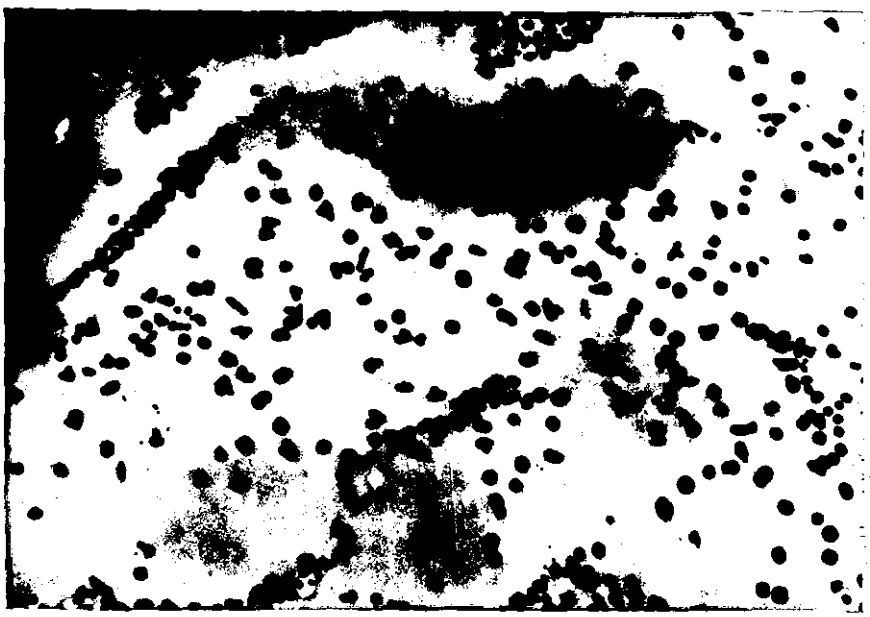

(c) TEM micrograph. Compare with Fig 7.3a (Better stabilizer dispersion into the PVC grains)

Mag. x66K

TABLE 7.5:

Variation of impact strength with formulations in compression moulding

| Formulation No. | Additive type and ratio (phr) | | Impact Strength (kJ $m^{-2}$) | | | | | | |
|---|---|---|---|---|---|---|---|---|---|
| | | | 1 | 2 | 3 | 4 | 5 | 6 | Average |
| | Cal.St. | Wax | | | | | | | |
| 1* | 0.4 | 0.3 | 3.54 | 3.46 | 3.55 | 3.68 | 3.48 | 3.49 | 3.53 |
| 2 | 0.4 | 0.15 | 3.48 | 3.57 | 3.43 | 3.41 | 3.57 | 3.46 | 3.48 |
| 3 | 0.8 | 0.3 | 3.60 | 3.38 | 3.46 | 3.65 | 3.59 | 3.63 | 3.55 |
| 4 | 0.8 | 0.15 | 3.63 | 3.58 | 3.56 | 3.64 | 3.66 | 3.59 | 3.61 |
| 5 | 0.2 | OPW | 3.61 | 3.53 | 3.59 | 3.49 | 3.53 | 3.56 | 3.55 |
| 6 | 0.4 | GMS | 3.57 | 3.61 | 3.64 | 3.58 | 3.55 | 3.54 | 3.58 |
| 7 | 1.5 | K120N | 3.25 | 3.15 | 3.17 | 3.39 | 3.28 | 3.26 | 3.25 |
| 8 | 1.5 | NLS | 3.27 | 3.40 | 3.28 | 3.38 | 3.43 | 3.26 | 3.34 |
| 9 | 2.5 | TBLS | 3.51 | 3.47 | 3.42 | 3.44 | 3.45 | 3.47 | 3.46 |

TABLE 7.6:

Effect of different formulations on fusion properties in compression moulding

| Formulation Number | Heat of Fusion $\Delta H_f$ ($Jg^{-1}$) | Solvent Absorption (%) | Heat of Fusion for Extrudates ($Jg^{-1}$) |
|---|---|---|---|
| 1* | 1.75 | 4.96 | 3.94 |
| 2 | 1.71 | 1.3 (flake) | 4.02 |
| 3 | 1.92 | 4.39 | 8.05 |
| 4 | 1.61 | 3.66 | 7.60 |
| 5 | 1.69 | 4.45 | 4.48 |
| 6 | 2.05 | 1.74 (flake) | 3.12 |
| 7 | 1.52 | - | 2.21 |
| 8 | 1.72 | 4.43 | 2.93 |
| 9 | 1.95 | - | - |

* = standard formulation
OPW = oxidized polyethylene wax
GMS = glycerol monstearate
K120N = paraloid K120N
NLS = normal lead stearate
TBLS = tribasic lead sulphate (formulation contains no DBLS)
Cal.St. = Calcium stearate

Figure 7.14c. In addition and as expected, better distribution of stabilizer observed in this formulation leads to increase in impact strength and reduction in percentage solvent absorption (Tables 7.5 and 7.6). The former is due to fewer numbers of agglomerated stabilizer particles in the matrix which otherwise could have lowered the impact strength.

When the G.S. wax concentration only was reduced, no significant change was observed in both morphology and distribution of stabilizer. On increasing the concentration of calcium stearate only, again no change in both morphology and stabilizer distribution was observed. However, there was an increase in impact strength in the latter case, while in the former the impact strength was reduced. Since stabilizer distribution is not affected, the change in impact strength could be due to higher melt elasticity associated with high concentration of internal lubricant[65]. Solvent absorption tests gave results of no apparent tendency - due to flaking observed with both samples (Table 7.6).

It means therefore that grains compaction and fusion, and distribution of solid stabilizer depends substantially on the ratio of external lubricant to internal lubricant. Higher external lubricant concentration will affect structural modification. This indicates that the external lubricants of low melting point (such as G.S. wax - see Appendix 2) form an ultra-thin film layer on the grains of dry blend, in agreement with the results of DIC microscopy of samples containing only lubricants and those reported by Naturman[167], Gale[49] and Allsopp[50]. This ultra-thin film increases in thickness with increase in concentration of the lubricant and, thus, affects inter-particle fusion adversely.

### 7.3.2 Effect of Incorporation of 'Secondary' Additives

The influence of 'secondary' additives on morphological changes and distribution of stabilizer was studied by incorporating oxidized polyethylene wax, glycerol monostearate, paraloid K120N impact modifier and normal lead stearate into the standard formulation

FIGURE 7.15: TEM micrographs of formulations containing 'secondary' additives. Mag. ×6·6K

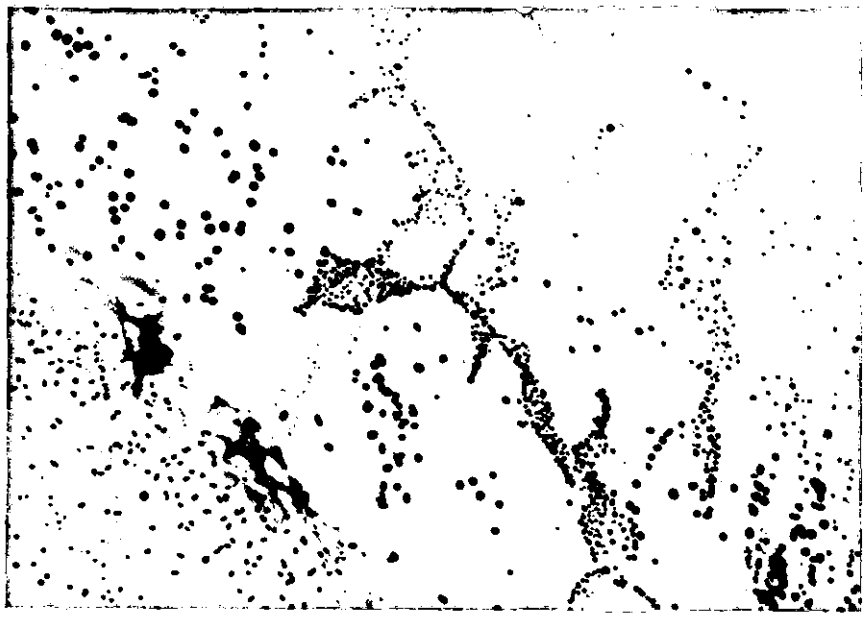

(a) Contains 0.4 phr glycerol monostearate Loss of some grains boundaries permits better stabilizer distribution

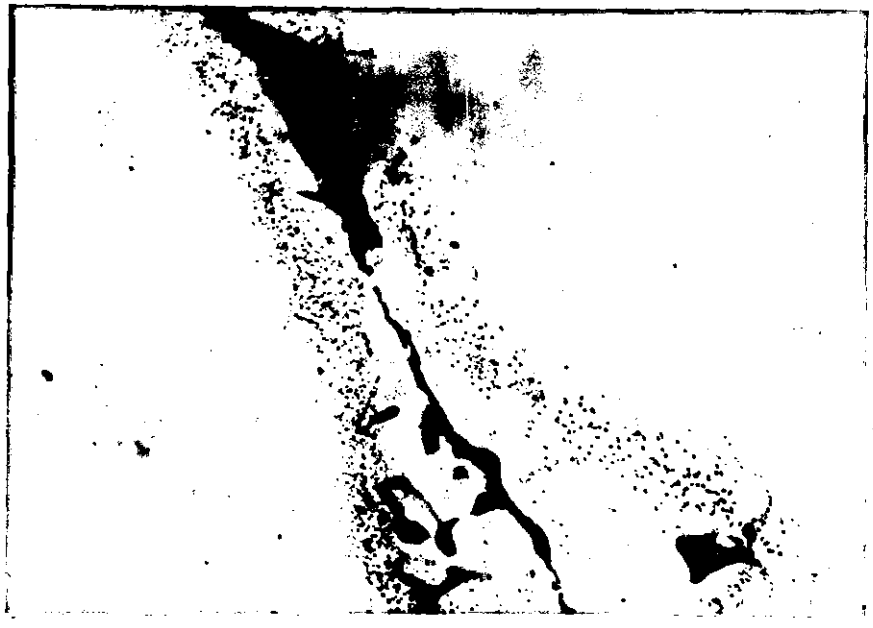

(b) Contains impact modifier. Stabilizer and impact modifier particles remained mainly within grain boundaries

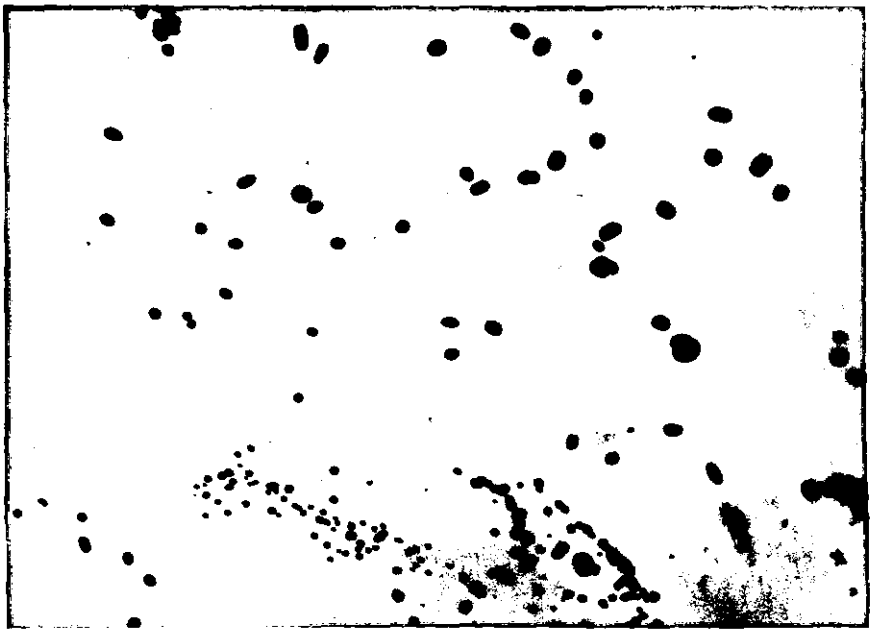

(c) Contains normal lead stearate. Loss of grain boundaries allows best stabilizer distribution

(Section 2.2 ). The results of impact strength and solvent absorption are given in Tables 7.5 and 7.6 respectively. Figure 7.15 (a, b and c) shows that better distribution of stabilizer particles is obtained with moulding containing these 'secondary' additives. It can be seen from the TEM micrographs that the stabilizer particles have penetrated into the matrix of the mouldings. This is because of the internal lubricating effect of oxidized PE wax, glycerol monostearate and normal lead stearate[163]. Since their melting points are relatively lower than the moulding temperatures, they easily 'diffused' into the grains carrying some stabilizer particles with them. Rolls and Weill have observed a similar penetration of solid stabilizer into the grains in lightly pressed dryblends[52]. This is also confirmed by the fact that, unlike external lubricants, the internal lubricants do not form thin films on melting.

The best distribution of stabilizer, in the context of this study, is observed with mouldings containing normal lead stearate, and this is attributed mainly to the high quantity used. Its fluorescence and DIC micrographs also show that the grain structure has completely disappeared, and that a new structure (sub-grains) has been revealed. These sub-grains are devoid of stabilizer and, thus, fluoresce brightly in the matrix (Figure 7.16c). Figure 7.16c also reveals another point of interest, that a melt pool and not sintered powder bed is formed by using a higher concentration of internal lubricant. In other words, the addition of higher concentrations of internal lubricant reduces the surface strength of the grains and on compression moulding results in significant structural modification. However, this leads to lower impact strength (Table 7.5) and solvent absorption due to lower melt elasticity and lower heat of fusion compared with formulation j. Similar features were also obtained by using DIC microscopy (Figure 7.17b).

It was not totally unexpected to find that compression moulding which contains an impact modifier has the lowest impact strength

FIGURE 7.16: Fluorescence micrographs of formulations containing different 'secondary' additives

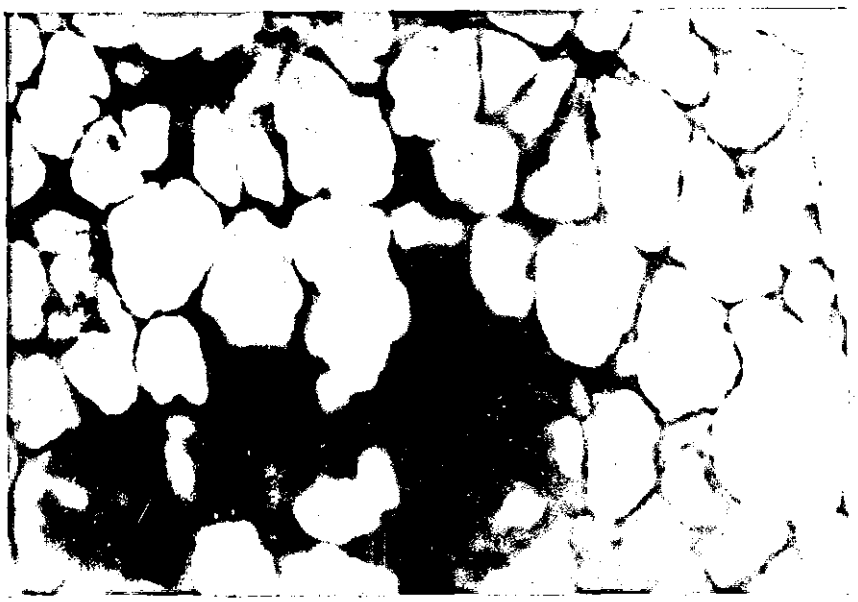

(a) Contains glycerol monostearate.
Loss of some grain boundaries is clearly evident

(b) Contains impact modifier.
No appreciable loss of grain identity

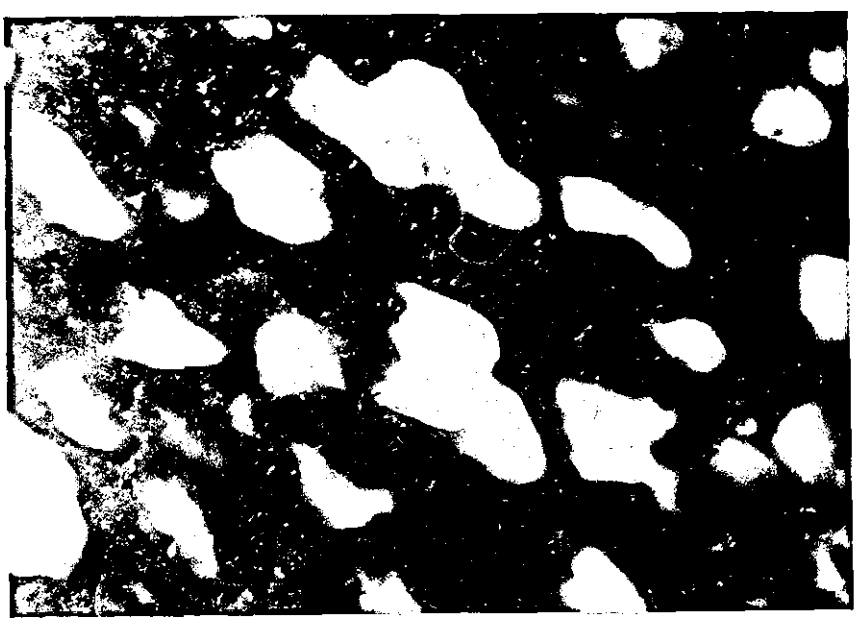

(c) Contains normal lead stearate.
Complete loss of grain identity, exposing the sub-grains

50μm

FIGURE 7.17: DIC micrographs of two vastly different formulations

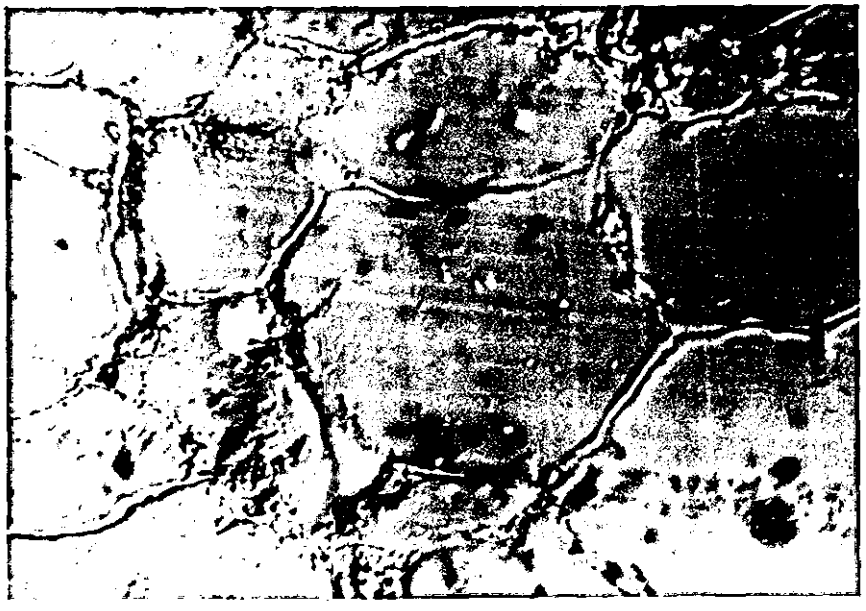

(a) Contains impact modifier (K120N)
Grain boundaries are very much in evidence

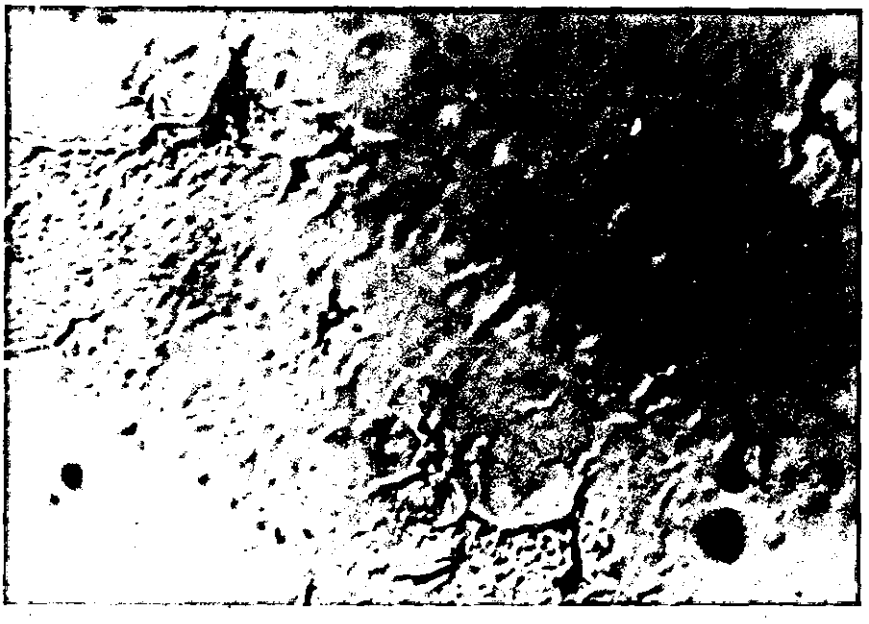

(b) Contains normal lead stearate
No evidence of grain boundaries or identity

50 µm

compared with other formulations (Table 7.5). Fluorescence and TEM micrographs (Figures 7.16 and 7.15) revealed that particles of both stabilizer and impact modifier remained mainly on the grain boundaries. They are high melting point particles (see Appendix 2), and since they remain on the grain periphery, a high level of grain fusion will be difficult to achieve. It is also evident from DIC micrographs that the PVC grains were barely fused (Figure 7.17a). This is confirmed by the fact that when the moulding was left in acetone for 15 minutes it almost completely disintegrated.

The SEM examination of fracture surfaces shows not only some element of ductility but also the presence of sub-grains and primary particles in samples containing normal lead stearate stabilizer. These features were completely absent in the samples containing impact modifier, and at a minimum in GMS containing mouldings. This SEM observation strongly confirmed those made with UV fluorescence and DIC microscopy methods.

## 7.4 Conclusion

Earlier work has largely been concerned with structural modification at low shear mouldings - almost entirely based on liquid stabilizer[1,148,180]. Here the relationship between distribution of stabilizer and changes in morphological features, as a function of temperature, concentration of stabilizer and lubricants and certain additives, have been investigated using chiefly UV fluorescence and differential interference contrast (DIC) microscopy. From the observations made the following conclusions can be drawn:

1. At low processing temperatures the features of the original grains are largely unchanged, and the stabilizer which coated these grains during blending remained as coating at the periphery of the grains in moulded samples. However, at 170$^{o}$C

the shape of the grains was found to change significantly due to compaction effects.

2. Sub-grains and primary particles were still very much in evidence in mouldings produced at higher temperatures. It was found that temperature alone, without shearing and fluxing, cannot cause enough grains destruction which should lead to a uniform distribution of stabilizer particles in the moulding. Instead, higher than the normal processing temperature led to poor particle flow, and intense degradation which produced a 'honeycomb' matrix from hydrogen chloride evolution.

3. It was also found that high melting point additives reduce the degree of fusion and, hence, impact strength because they remain mainly on the grains periphery. That is why the incorporation of impact modifier K120N into the standard formulation gave mouldings of low level of fusion and impact strength.

4. High concentration of external lubricant provides an increased resistance to interparticle fusion (that is, loss of grain identity) which, in turn, affects distribution of stabilizer. Higher structural modification and better distribution of stabilizer was obtained by lowering the concentration of external lubricant and increasing that of internal lubricant. However, this led to the reduction of impact strength due to lower melt elasticity.

5. Micro-voids in the moulding appeared to be found mostly near agglomerated stabilizer particles. Therefore the occurrence of micro-voids is not wholly associated with the evolution of HCl - at least not in samples produced under the conditions such as those used here.

6. The mechanism of gelation (fusion model) observed in other processes does not wholly apply in the compression moulding

process. This is because obliteration of the grains' structure is 'never achieved', for solid stabilizer blends, without catastrophic degradation, so that the formation of substantial quantities of molecular chain entanglement network as a result of primary particle fusion is dependent on temperature and formulation.

Fold this label along the dotted line. Affix it to the envelope so as to seal it and cover the old address (or address panel) and postmarks.

BUSINESS REPLY SERVICE
Licence No. PHQ10

Department of Employment
Employment Service
Jobcentre
10 South Street (off Woodgate)
LOUGHBOROUGH
LE11 1YY

# CHAPTER 8

# SUMMARY OF THE EVALUATION AND PROCESSING METHODS

## 8.0 Correlation and Effectiveness of the Processes and Microscopical Methods Exploited

Two specific areas of study could be identified in this programme. The first part has involved the exploitation of a UV fluorescence microscopy and development of some effective sample preparation techniques. The second part of this work has been based on a close study of morphological changes and additive distribution in three areas of UPVC processing - blending, extrusion and compression moulding - using the developed techniques.

The mechanism of changes in morphological features (generally referred to as gelation mechanism) during UPVC processing, despite numerous publications, is still open to question. By using these developed microscopical techniques to study three vastly, but interrelated, areas of unplasticised polyvinylchloride (UPVC) fabrications some useful contributions have been made to this concept. This chapter will be discussed under two headings based on evaluation and fabrication methods used in this project.

## 8.1 Correlation of the Microscopical Techniques Used

The UV fluorescence microscopy has been used in conjunction with differential interference contrast (DIC) and electron microscopical methods to supplement the existing knowledge on the morphological changes in UPVC processing. There were substantial agreements between the results obtained with UV fluorescence and the differential interference contrast microscopy methods regardless of their specific areas of application. The UV fluorescence microscope has been used mainly in the biomedical field, and little if any extensive application has been made of it in polymer studies.

The pioneering work of Allsopp[50] revealed that the method is best suited to degradation analysis. However, it has been used here to obtain a correlation with powder bulk density, flow rate and particle size and size distribution which strongly support the primary concept that the 'breakdown' of grains is a dominant feature in a high-attrition blending. The measurement of relative fluorescence intensity of heat-treated grains (semi-quantitative fluorescence analysis) also shows good correlation with differential interference microscopical observations. For instance, both methods showed clear and related evidence that higher stabilizer loading implies more layers of stabilizer particles on the PVC grains. With the UV fluorescence analysis, grains containing higher concentration of stabilizer were seen to exhibit low fluorescence intensity on heating to 190°C. In other words, the PVC grains were protected from catastrophic degradation by the stabilizer particles. However, increase in image contrast in the DIC - indicating high stabilizer concentration up to a saturation level - is in good correlation with a systematic decrease in relative fluorescence intensity (see Figures 5.7 and 5.9 in Chapter 5). Preliminary study of stabilizer distribution on UPVC grains with a transmission electron microscope clearly showed that the stabilizer is not absorbed into the grains - which confirmed the sensitivity of the fluorescence and DIC microscopy methods (the TEM results were not shown here because this work was strictly designed to avoid the use of embedding techniques, which is a primary feature in TEM examination of powder grains).

Since the stabilizer particles 'protect' the PVC grains from thermal degradation, a fuller experiment was carried out to determine how much thermal protection a single stabilizer particle can offer in terms of the area it is occupying. Solvent-cast film containing large-size stabilizer particles 'A' (as schematically represented in Figure 8.1) was prepared as described in Chapter 4, and degraded in an oven (temperature range 170°C to 210°C). Fluorescence analysis showed that the suggestion that stabilizer

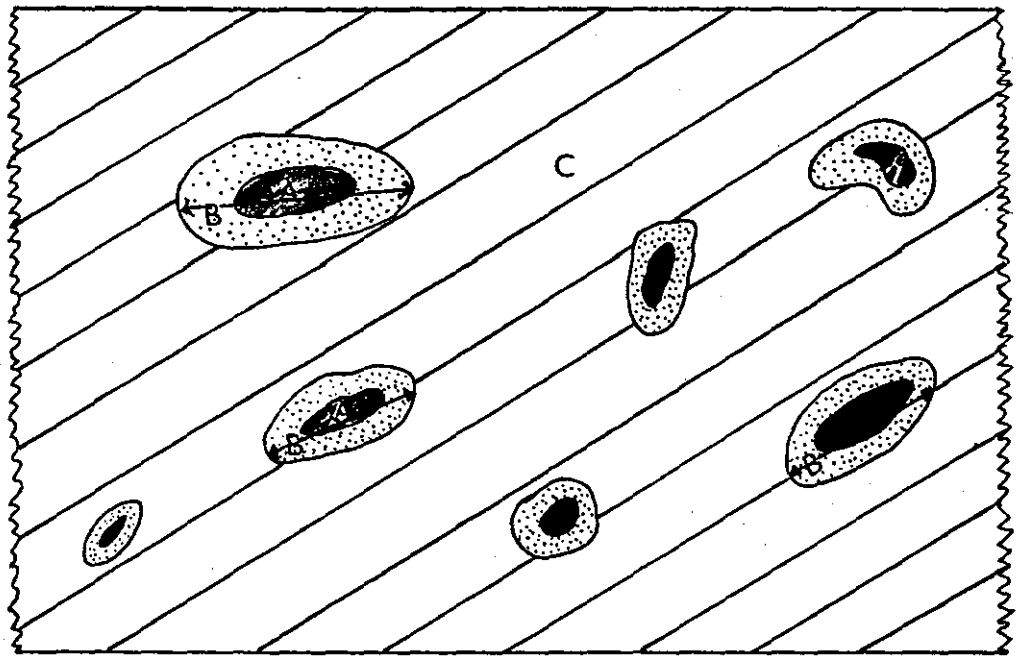


FIGURE 8.1: Schematic illustration of the suggested effectiveness of stabilizer particle against thermal degradation.
A = actual size of stabilizer particle;
B = anticipated magnitude of effective protection that can be offered by A; and
C = solvent-cast film

particles of size 'A' will be capable of protecting an area larger than its size (e.g. an area of size 'B' in Figure 8.1) appears to be superficial. From the experiment, it can be stated that each stabilizer particle can only 'protect' the area it is occupying from thermal degradation. It can be argued that this is, presumably, not an explicit technique for the proper evaluation of the hypothesis. However, its findings broadly agree with the fact that at high discharge temperature ($\sim 140^{o}C$) local degradation is common with grains of poor quality blends - due to stabilizer devoid areas.

In the evaluation of morphology of processed blends, again both the UV fluorescence and differential interference contrast microscopy (DIC) techniques showed results in broad agreement with conventional methods. By the use of UV fluorescence microscopy alone, a qualitative relationship was obtained between

discolouration and gelation mechanism, which was also found to correlate with the result obtained with differential scanning calorimeter. The loss of sub-grains along the extruder screws observed with DIC microscopy was also shown to be closely related to the loss of fluorescence intensity. Because of the limitation of small refractive index difference in DIC, it was a little difficult to make a systematic study of stabilizer distribution and morphological changes along the screws. This was more clearly evaluated with fluorescence microscopy. However, for a closer study of the role of additive in the fusion of grains and distribution in the superficially gelled matrix, the transmission electron microscope was found to be the most promising method. This is due to the advantages of using not only a higher magnification but also ultrathin specimens. This method also revealed the presence of micro-voids which was seen to be mainly associated with agglomeration of stabilizer particles. The migration of stabilizer particles into the UPVC sub-grains as a function of processing parameter - in compression moulding for instance - was observed to be strongly related to the areas of very low fluorescence. The scanning electron microscope apart from showing similar features (i.e. presence of primary particles etc) with the rest of the microscopy methods, was also found to be very useful in the assessment of large-size voids caused by evolution of hydrogen chloride. It was employed effectively in studying the mode of sample failure. The fracture surfaces observed correlated with the graphical traces of the Fractoscope Impact Tester.

In general terms, the microscopical methods exploited complement each other fairly well. It has been shown that each method explicitly explains what could have been otherwise difficult to interpret with a single technique.

## 8.2 Correlation and Effectiveness of Processing Methods

The two methods used in this programme for the fabrication of dry blends are not only related to industrial interest but also they provide suitable conditions (low and high shear) for the study of gelation mechanisms in UPVC. The use of compression moulding provides a better insight into the mechanism of morphological changes at relatively low shear, perhaps, similar to the gelation mechanism observed along extruder screws.

The morphological aspects of PVC have been shown in the introductory chapter to be classified into several phases. These different phases are built-up during polymerisation and are destroyed to an entanglement network during fabrication. Consider the direct processing of powder resin, the first stage involves blending - where it has been shown that most of the grains (120 μm average size) are broken down into smaller size grains. This has been shown by many workers to improve the output rate and fusion level of the subsequent fabrication stage[53,131]. (This work was not designed to evaluate these relationships, even though the dry blend quality has been shown to meet the standard requirements). High-speed blending thus modifies the structure of the PVC grains - resulting in an increase in the bulk density of the blend. Since the bulk density is correlated with the ability to efficiently feed the extruder screws, its direct influence on the output rate of the extruder is apparent. This agrees with the fact that inconsistency in the property of blends from different batches nearly always leads to erratic extrusion.

The subsequent extrusion of the dry blend at high shear of $10\text{-}10^3$ $sec^{-1}$ has been shown to result in a significant structural modification. Although many publications expressed different opinions as to the mechanism of gelation of UPVC, they have always agreed on one point: that the fusion mechanism is largely governed by the processing conditions. In this study UV fluorescence microscopy method has been employed to study structural modification at different processing parameters, and at the

same time highlighting the sensitivity and usefulness of this method in the study of polymer morphology and degradation. The correlations obtained exhibit a relationship of structural modification to physical properties for high and low shear processing. Along the extruder screws a good relationship exists between the fluorescence microscopical observations and physical property results (solvent absorption and heat of fusion). The degree of fusion - as calculated from the endothermic peak of DSC thermograms - increases as the melt is fluxed and moved towards the tips of the screws. In other words as the blend is fluxed, sheared and moved through each screw zone, it is compacted and melted. Then the adjacent grains fused into a high-energy state of physical cohesion. At the latter screw zones (vent and metering zones) elongation of the sub-grains occur, leading to subsequent formation of superficially homogeneous melt. This concept of particles modification along the extruder screws is in good correlation with those observed in compression moulding at different temperatures. However, along the screws a sub-grain is 'destroyed' after the length-wise diameter is about twice the diameter of its original size. Another common feature is that particle elongation occurs when about 60% melt-pool is formed. These features somehow were not observed by Allsopp and the other workers on mechanism of UPVC gelation. In compression moulding process, at low temperature the level of compaction and fusion of adjacent particles results nearly always in a low energy state of physical cohesion. This means that the product is usually very brittle. At higher temperature, a melt pool of high physical strength is formed which sometimes lead to a product with high ductility. However, unlike extruder screw samples, particle elongation is rare in compression mouldings of the type used in this project.

In the final extrudate the degree of particle fusion (sometimes referred to as gelation level) has been shown earlier on (Chapter 6) to be dependent upon the thermo-mechanical history of the material.

FIGURE 8.2: The micrographs of Brabender samples prepared at different temperatures

A: Prepared at 160°C

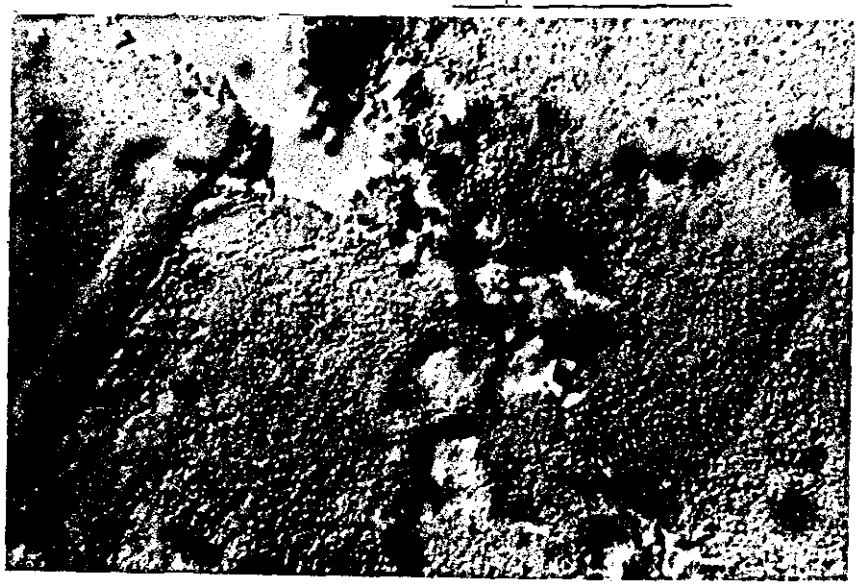

(i) DIC micrograph showing highly homogeneous mel

30 μm

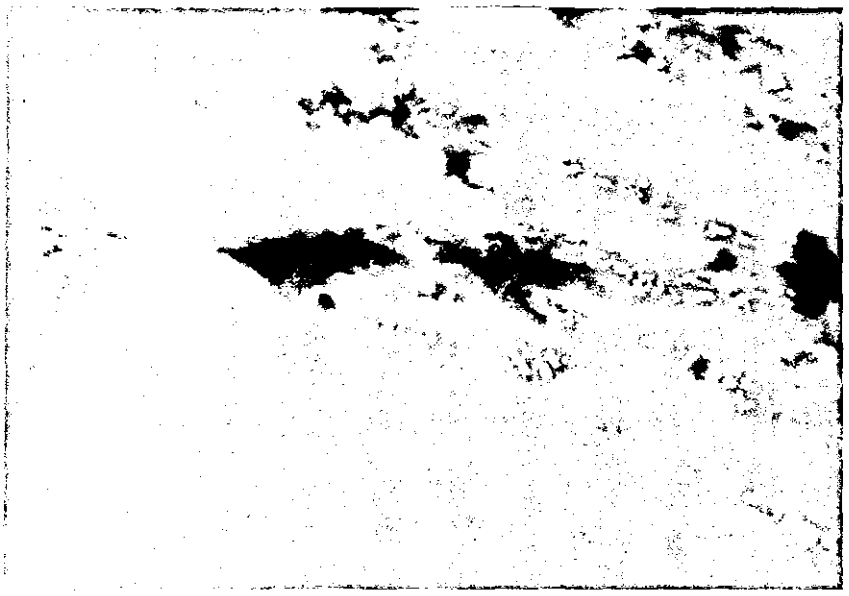

(ii) Fluorescence micrograph showing stabilizer particles. Again no evidence of sub-grains

50 μm

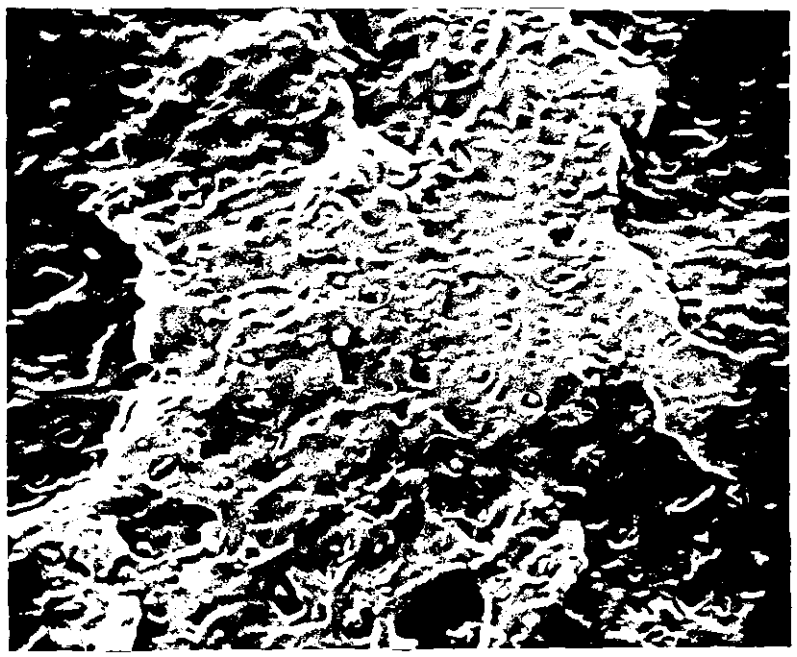

(iii) SEM micrograph of fracture surface showing large quantity of primary particles. Mag. x6K.

Compare with Fig 8.2b (iii) and Fig 6.24

B: Prepared at 205°C

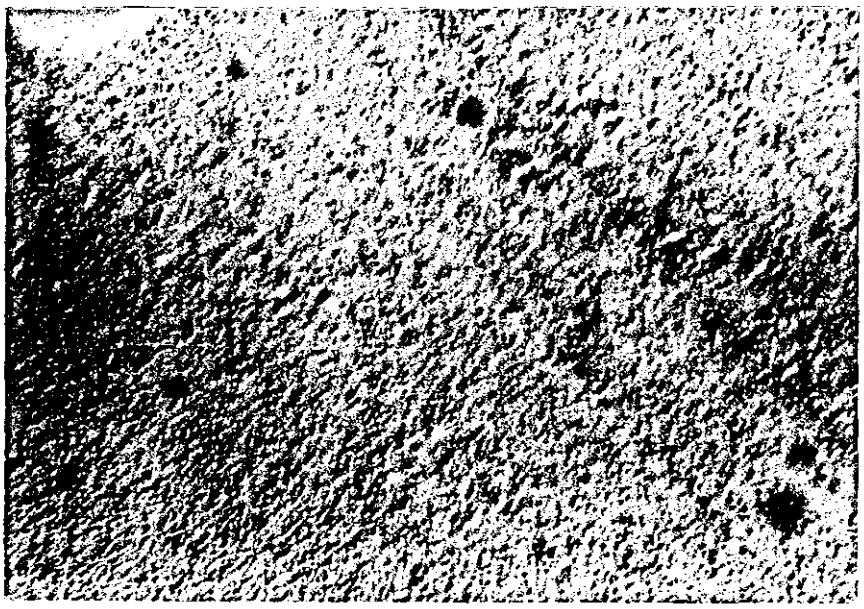

(i) DIC micrograph showing highly homogeneous melt

30 μm

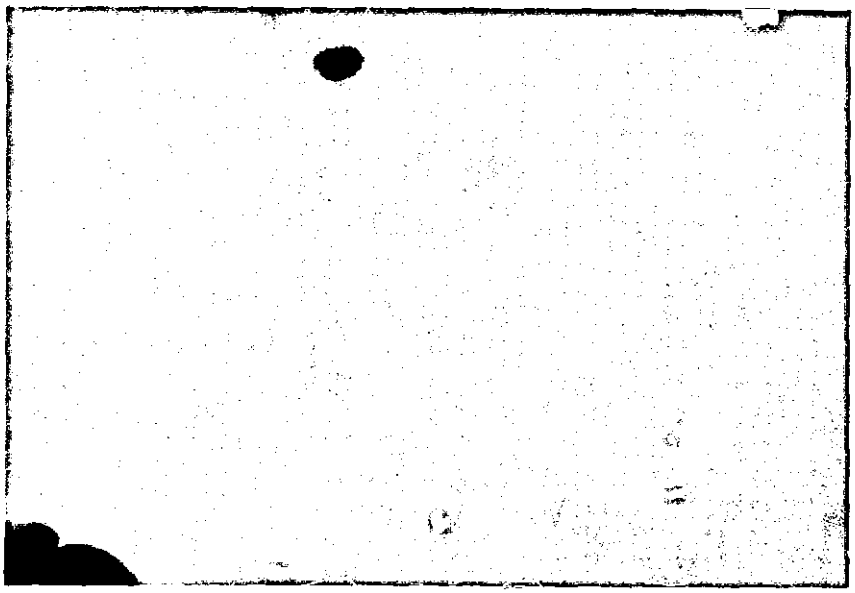

(ii) Fluorescence micrograph. Size of stabilizer has been reduced due to prolonged shearing. Also no evidence of subgrains

50 μm

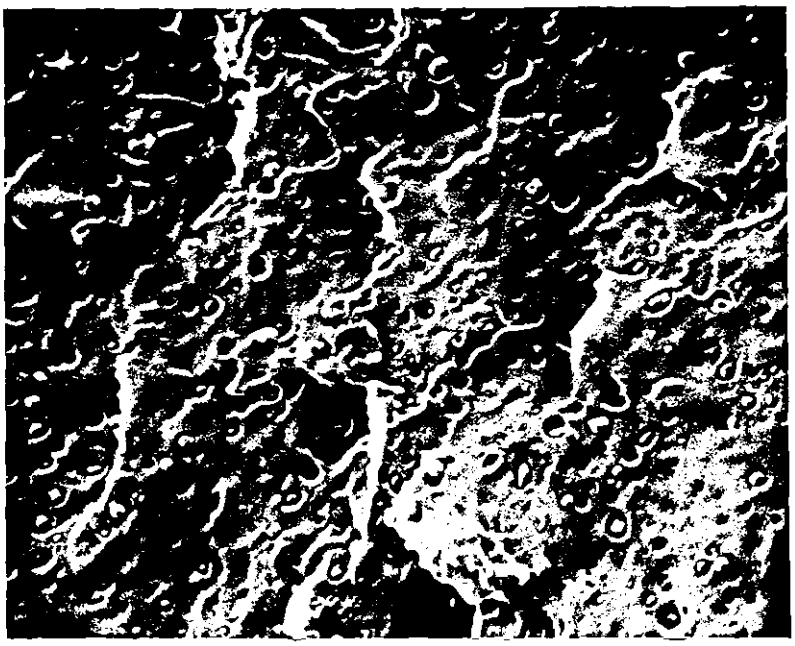

(iii) SEM micrograph of fracture surface. Still there exist large quantity of primary particles despite higher processing temperature.
Mag. x5K

Compare with Fig.8.2a (iii) and Fig.6.24

The morphological changes for extrudates of different extrusion temperatures and speeds observed with fluorescence microscopy, and the results of physical property measurements show good correlation. They indicate that the best mechanical property is obtained at optimum degree of homogeneity of the melt. An increase in solvent absorption with increase in the extrusion temperature was an evidence of the formation of chain entanglement network. In a further attempt to explain the gelation mechanism in the final extrudates, samples were prepared with a Brabender Plasticorder at a temperature range from 150 to 210°C (see Chapter 4, Section 4.2). Since the Brabender Plasticorder has higher shear compared with a twin-screw extrusion machine, extra mechanical history at longer residence time would result in lower residual grains in the samples - indicating higher secondary crystallites. The UV fluorescence and differential interference contrast microscopy show that, in fact, the products contain little if any sub-grains (Figure 8.2) - for temperatures from 160°C onwards. In contrast, the twin-screw extruder samples prepared at the same temperature range contain substantial amounts of residual grains. From the qualitative comparison (i.e. by UV fluorescence and DIC microscopy) of samples prepared with Brabender, extruder and compression moulding it can be concluded that shear rate contributes largely to the 'destruction' of sub-grains during processing. These samples were further evaluated with differential scanning calorimetry and solvent absorption tests. The results are compared in Figures 8.3 and 8.4 respectively, where it can be seen that the extrudate has the highest degree of fusion. This means that although highest degree of homogeneity of melt is observed with Brabender samples, there is no substantial destruction of primary crystallinity sites in the melt pool. (This is largely due to the effect of lubricants - which should be higher in a small size barrel of the Brabender mixer). This is supported by the fact that there is no significant difference in the solvent absorption values of the Brabender samples compared with those of the extrudates (Figure 8.4). The SEM micrographs (Figure 8.2) also confirm

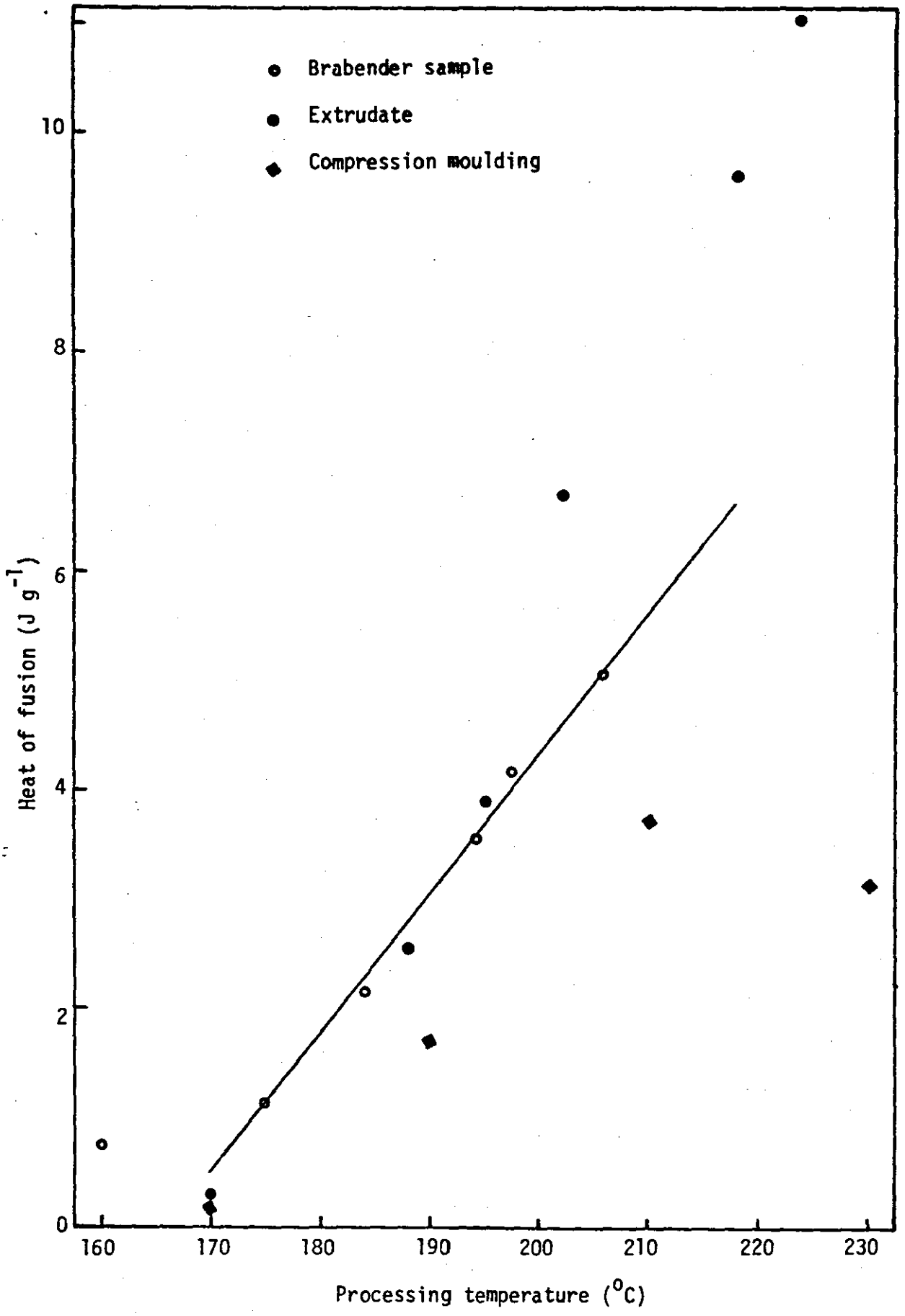


FIGURE 8.3 : Comparison of heat of fusion in different processes

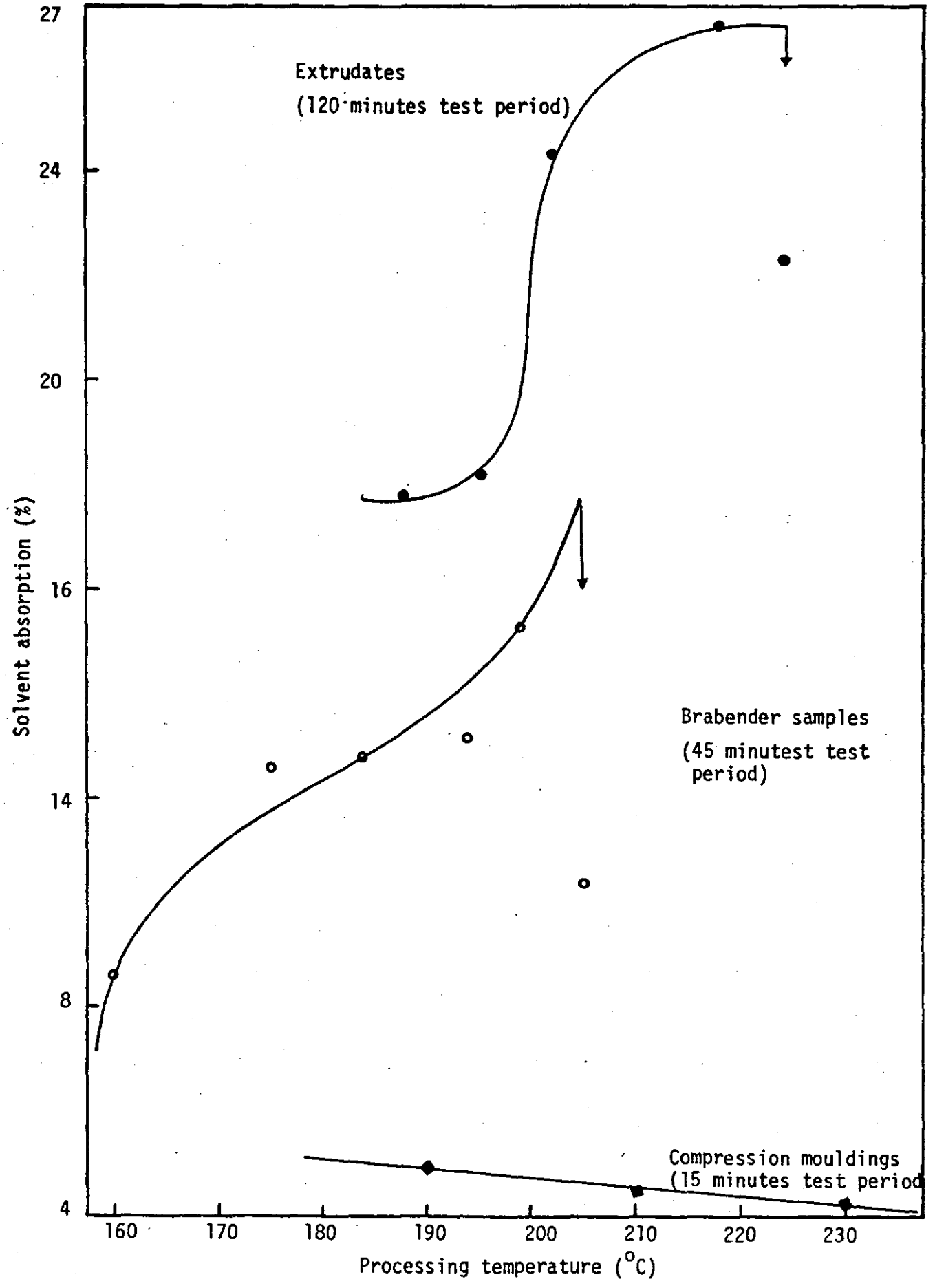


FIGURE 8.4. Solvent absorption for samples of different

that there are large numbers of primary particles present in the Brabender samples. Thus it has been shown that completely fused homogeneous melt precludes absence of sub-grains, but not total melting of the primary particles. A system where the primary particles are completely melted will lead to molecular chain disentanglement - resulting in poor mechanical property. This is common with overgelled materials as shown with samples extruded at 224$^{o}$C (see Chapter 6).

Based on the use of UV fluorescence and DIC microscopy techniques in conjunction with other 'conventional methods', the model for the mechanism of gelation (structural modification) in an extrusion process is as given in Figure 8.5. Captions illustrating the regions of high and low mechanical property etc have also been included.

FIGURE 8.5: Mechanism of morphological changes in UPVC melt processing

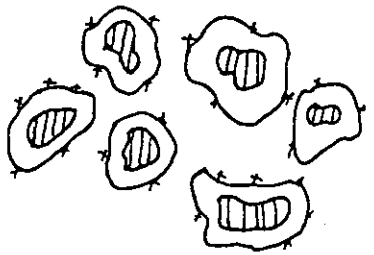

High-grain compaction
Heat melts grains to fuse highly compacted boundaries and exposes sub-grains. Fluxing disperses additives

Highly fused grain-boundaries, exposing sub-grains. High loss of grain-boundaries

Normal temperature (low shear)

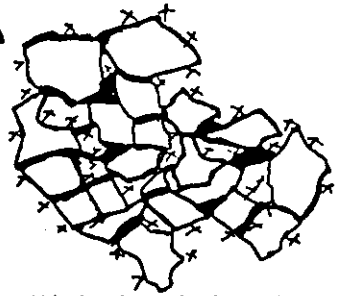

High densification of grains. (Additives still within grains)

Higher temperature

No sub-grains but quantity of primary particles and density of chain entanglement in the melt depend on processing temperature

Shearing elongates grains. High temperature melts elongated sub-grains

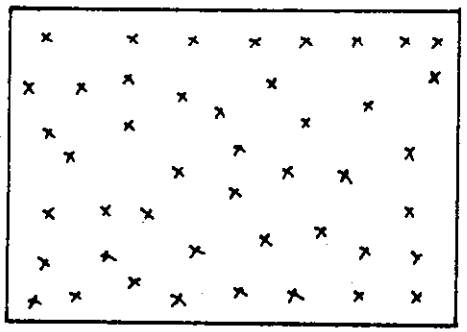

Second final melt (no sub-grains). (Obtainable mostly in higher shear processes. Optimum mechanical property and highest chain entanglement network are largely determined by thermal history. Very high temperature leads to chain disentanglement).

Higher temperature melting the remaining sub-grains. (Extrusion only)

First final melt. (The melt obtained in nearly all extrusion products. The quantity of sub-grains depends on formulation and extrusion temperature).

# CHAPTER 9

# GENERAL CONCLUSION AND FURTHER RESEARCH

As a result of the work a number of major conclusions can be drawn and these have already been given at the end of each discussion chapter. However, a summary of these conclusions will be given below based on highlighting the primary points. In addition, the extent to which the project objectives have been met are summarised and suggestions are made for future work which could be carried out to elucidate features which were highlighted by the present work.

## 9.1 General Conclusions

In this study of some morphological aspects of UPVC processing, the objectives have been considered under three chapters - which in the text represented also the three fabricating methods. The first and second project objectives (see Chapter 1, Section 1.2.2) were evaluated in Chapter 5, the third in Chapter 6 and finally the fourth in Chapter 7.

In Chapter 5, powder blends containing particle fractions which were heat-treated at 190$^{o}$C for 10 minutes were prepared and examined. No evidence was found for particle agglomeration, even at a relatively low blending speed. However, there was substantial evidence for breakdown of particles being the dominant feature in "high-speed" blending. It must be pointed out that no evidence of gross deformation or structural modification was observed. In other words, the grains are not being destroyed into sub-grains of small size particles by blending, rather the fines are being formed by the breakdown of agglomerates existing in the starting materials.

The distribution of additives in dry-blends was accounted for by the shape and not the size of the PVC grains. Thus, for suspension polymer grains more additive particles accumulate in the re-entrant area (valley) on the surface, for mass polymer

grains best distribution was obtained as a result of the strawberry-like appearance of their surfaces, and for emulsion polymer grains the 'glossy' rounded surface did not permit a proper adhesion of large amounts of additive. It does suggest, therefore, that particle shape is also a major factor when selecting the polymer type and/or condition for dryblending. In general terms, it was found that the best distribution of stabilizer is associated with early melting of the lubricant (i.e. about 5 minutes) prior to the end of blending cycles.

Having established that dry-blending leads solely to the formation of small size particles another important aspect of the study was to determine the effect of different blenders on dry-blend characteristics. Since each blender has specific rotor design and arrangement, the blends they produce should be expected to vary in characteristics. Indeed, the blade arrangements and charge weight were found to affect particle size and size distribution, powder densities, flow rate and additive distribution but not Brabender fusion time. This is a highly significant point for it has been reported by Guimon[131] that powder density affects extruder output rate. Thus, it clearly suggests an extruder output rate can be increased by the use of appropriate blender/proper blade arrangements.

There were broad agreements between differential interference contrast microscopical observation and results obtained with UV fluorescence microscopy. The latter method also confirmed, by qualitative analysis, that blends discharged at higher temperatures (e.g. 140$^{o}$C) were slightly degraded. It must be pointed out that such a level of degradation could neither be detected by conventional visual methods nor by normal light reflectance methods.

To meet the third and fourth project objectives, extrudates (Chapter 6) and compression mouldings (Chapter 7) were examined as examples of areas of highest dry-blending fabrication and lowest

shear rate process respectively. The fluorescence microscopy clearly revealed the mechanism of changes in morphological features associated with high and low shear processes. By studying the fusion of particles along the extruder screw, it has been established that the UPVC grains melt to reveal the sub-grains. The latter, in turn, melt after being elongated to a length which is about twice the size of their original diameter. The final product may contain sub-grains whose sizes and shapes largely depend on the products thermo-mechanical history. Hence, samples of compression moulding were found to contain disc-shaped sub-grains while elongated sub-grains were dominant in extrudates. This is an extension of Allsopp's CDEF mechanism which showed that elongation of grains occur in e.g. extrusion. This work also shows that complete melting/disappearance of sub-grains does not necessarily include the complete fusion of primary particles, but mostly exposing them to subsequent thermal treatment. It was found that extrudates with virtually no trace of sub-grains gave the best mechanical performance, but not the highest heat of fusion. On melting a large quantity of the primary particles by processing at higher temperature ($224^{o}C$ in this case) the extrudate mechanical properties were adversely affected. However, the heat of fusion was found to increase - which is due to the formation of more secondary crystallites.

By using different lubricant types and concentrations extrudates having different microstructures were produced. Their mechanical properties also varied with lubricant types and concentrations. Thus at high concentration of external lubricant it is found that the extrudates contain larger amounts of sub-grains, but when the external lubricant concentration was lowered the amount of sub-grains became smaller with corresponding change to better topography and mechanical properties. This resistance to fusion by the sub-grains, thus is enhanced by high concentration of the external lubricant which reduces the friction between sub-grains and surface of the extruder barrel.

The loss of fluorescence intensity in the final extrudates was found to depend not only on type of formulation but also on stabilizer distribution. A well stabilized product would have little if any fluorescence because of small amounts of degradation (double-bonds) in the sample. Also, where additives are distributed in a random manner, the fluorescence intensity of the extrudate was found to be highly 'submerged'.

To summarise, therefore, the application of UV fluorescence microscopy in the field of polymer technology has been highlighted. In effect, a technique has been developed which was used to evaluate the structural modification of unplasticised polyvinylchloride and distribution of solid additives during fabrication as a function of processing parameters, concentration of stabilizer and lubricants, and other 'secondary' additives. Hence, the work has been of necessity a broad-based investigation (in morphological changes in powder blend, extrudates and compression mouldings) which has led to the establishment of a model for UPVC melt processing. As much as it has paved the way for better understanding of morphological changes and degradation in PVC processing, it has shown also that the use of UV fluorescence microscopy will prove indispensable in the field of polymer technology for those studying additive distribution, morphology and degradation.

## 9.2 Suggestions for Further Research

In considering future work much more emphasis should be given to the following areas:

1. In some literature it has been suggested that high agglomeration of particles occurs at relatively low blending speeds, such as those obtained with ribbon mixer types. The blends prepared with these mixer types, thus should be studied with

fluorescence microscopy (semi-qualitative method) to conclude whether there exists the agglomeration of large-size grains in such a high quantity.

2. The influence of dry-blend properties on subsequent moulding is still very much an open question. Its study was partly started at the onset of this programme, but with little success. A more systematic study of the dependence of product qualities on blending conditions and blend properties will probably explain the erratic productions sometimes observed in extrusion.

3. The use of fluorescence microscopy to study the mechanism of gelation of PVC containing liquid stabilizer system will be worth investigating. Since liquid stabilizer is absorbed into the PVC grains during blending (unlike solid stabilizer), an investigation of samples prepared by low shear process might show the extent of the absorption - being that stabilizer devoid areas will fluoresce strongly. Thus, it will also be possible to follow more closely the appearance and subsequent elongation of sub-grains during processing.

4. Finally, a close study of the samples prepared with Brabender Plasticorder at different temperatures and rotor-speeds - possibly by comparing the effect of solid and liquid stabilizers on structural modification should be made. The loss of sub-grains observed with fluorescence microscopy can be related to the degree of fusion measured with differential scanning calorimetry - which was not fully carried out in this work.

## REFERENCES


1. WENIG, W: *'The microstructure of PVC as revealed by X-ray and light scattering'*, J. Polymer Science (Polymer Physics Ed), (1978), Vol. 16, pp. 1635-1649.

2. REGNAULT, H V: *'The discovery of vinylchloride monomer'*, Annales in Chemistry and Physics (1835), Vol. 58, pp. 301-320.

3. REGNAULT, H V: *'Organisch-Chemische Untersuchungen'*, Liebigs Annales in Chemistry, (1835), Vol. 15, pp. 60-74.

4. REGNAULT, H V: *'Researches in organic chemistry'*, Annales in Chemistry and Physics, (1835), Vol. 59, pp. 358-375.

5. HOFMANN, A W:
Liebigs Annales, (1860), Vol. 115, pp. 271.

6. BAUMANN, E: *'Polymerization of vinylchloride'*, Liebigs Annales in Chemistry, (1872), Vol. 162, pp. 308.

7. KLATTE, F:
German Patent 281,877 to Chemie Fabrik Griesheim Elektron, April 4, (1913).

8. OSTROMISLENSKY, I I:
British Patent 6299 to Society for Production and Sale of Resin Articles, Bogatyr, March 13, (1912).

9. _____ Austrian Patent 70,348 to Chemie Fabrik Griesheim Elektron, June 1, (1915).

10. SEMON, W L:
United States Patent 1,929,453 to B F Goodrich Co, Oct.10 (1933).

11. SUSICH, G V and FIKENTELERS, H:
German Patent 659,042 to I G Farbenindustrie A G, April 22, (1938).

12. AUCHTER, J F: *'PVC: outlook and opportunities'*, Rubber Age, (1971), pp.79-82.

13. HURARD, H: *'Where is PVC heading in Europe'*, Modern Plastic International, February, (1971), Vol. 1, No. 2, pp. 17-20.

14. KEANE, D P, STOBAUGH, R C and TOWNSEND, P L: *'Vinylchloride: How, where, who, future'*, Hydrocarbon Process, February 1973, Vol. 52: Pt. 1: No. 2, pp. 99-110.

15. FUJITA, T: *'General trends in the PVC industry'*, Japan Plastic Age, July 1971, Vol. 9, No. 7, pp. 25-28.

16. ———— *'Vinylchloride polymers'*, Encyclopaedia of Polymer Science and Technology, 1971, Vol. 14.

17. AUCHTER, J F: *'PVC: Outlook and opportunities'*, Rubber Age, 1971, Vol. pp. 80.

18. PENN, W: *'PVC technology'*, Applied Science Publishers, London, 1971.

19. WAKI, I: *'Current situation and problems of material development'*, Japan Plastic Age, 1971, Vol. 9, No. 7, pp. 29-32.

20. KOTLYAR, I B:
Plastic Massy, 1967, Nov. issue, pp. 17-20.

21. ———— *'Plastics supply and demand, highlighted discussion held in Budapest'*, Chemical and Engineering News, Oct. 19, 1970, Vol. 48, pp. 47.

22. KHVILIVITSKII, R . Ya, TOMASHCHUK, V I, TUMANN, Ya V and BUTAKOVA, T V: *'Influence of stirring on the quality of suspension PVC'*, Plastic Massy, 1969, No. 4, pp. 16-19.

23. Plastics World, Jan. 1971, Vol. 29, pp. 11.

24. Chemical Week, Aug. 22, 1964, pp. 93, *'Oxychlorination'*.

25. ————————, *'One step to vinylchloride from ethylene'*, European Chemical News, Aug. 21, 1964, pp. 27.

26. ————————, French Patent 1,330,367 issued to ICIANZ (Imperial Chemical Industries of Australia and New Zealand) June 6, 1962.

27. SELIKOFF, I J and HAMMOND, E C: *'Toxicity of vinylchloride -polyvinylchloride'*, Annales New York Acad. Science, 1973, Vol. 246, pp. 1-337.

28. ————————, *'Occupational safety and health administration (DSHA) Inaugurates temporary standard on vinylchloride'*, Rubber Age, 1974 June, Vol. 104, pp. 70.

29. ————————, *'PVC cancer deaths'*, Rubber Age, Sept. 1974, Vol. 106, pp. 78.

30. FARBER, E and KORAL, M: *'Suspension polymerization kinetics of vinylchloride'*, Polymer Engineering and Science, 1968, Vol. 8, pp. 11-18.

31. MATTHEWS, G A R: Vinyl and Allied Polymers, Vol. 2, Publ. Iliffe, London, 1972.

32. PENN, W: PVC Technology, 3rd Edition, Publ. Applied Science Publishers, London, 1971.

33. BRYDSON, J D: Plastics Materials, 3rd Edition, Publ. Newnes-Butterworths, London, 1975.

34. MARVEL, C S and HORNING, E C: *'Organic Chemistry'*, An Advanced Treatise (Ed), Gilman, H et al, 2nd Edition, Publ. Wiley, New York, Vol. 1 (Chapter 8), 1943, pp. 754.

35. GEDDES, W C: *'Thermal decomposition of polyvinylchloride III: An investigation of discolouration'*, European Polymer J, 1967, Vol. 3, pp. 747-765.

36. BRAUN, D and BENDER, R F: *'On the mechanism of thermal dehydrochlorination of polyvinylchloride'*, European Polymer J. Supplement, 1969, Vol. 5, pp. 269-283.

37. BRAUN, D and WARTMAN, L H: *'Structure and mechanism of dehydrochlorination of polyvinylchloride'*, J. Applied Polymer Science, 1958, Vol. 28, pp. 537-546.

38. GEDDES, W C: *'Thermal decomposition of polyvinylchloride II'*, European Polymer J, 1967, Vol. 3, pp. 733-744.

39. HENSON, J H L and HYBART, F J: *'The degradation of polyvinylchloride II: oxidative degradation in solution'*, J. Applied Polymer Science, 1973, Vol. 17, No. 1, pp. 129-138.

40. AYRE, G, HEAD, B C and POLLER, R C: *'Thermal degradation and stabilization of polyvinylchloride'*, J. Polymer Science - Macromolecular Reviews, 1974, Vol. 8, pp. 1-49.

41. FRYE, A H, HORST, R W and POLIOBAGIS, M A: *'The chemistry of polyvinylchloride stabilization III: Organotin stabilizers having radioactively tagged alkyl groups'*, J. Polymer Science 1964, A2, pp. 1765-1784.

42. KING, L P and NOEL, F: *'Characterization of lubricants for polyvinylchloride'*, Polymer Engineering and Science, 1972, Vol. 12.

43. HARTITZ, J E: *'The effect of lubricants on the fusion of rigid polyvinylchloride'*, Polymer Engineering and Science, 1974, Vol. 14, pp. 392-398.

44. STERNAGEL, H G: *'Effect of lubricants in PVC blends'*, Kunststoff Technik, Dec. 1970, Vol. 9, pp. 428-432.

45. WINKLER, D E: *'Mechanism of polyvinylchloride degradation and stabilization'*, J. Polymer Science, 1959, Vol. 35, pp. 3-14.

46. KENYON, A S: *'Polymer degradation mechanisms'*, National Bureau of Standards, Circular 25, Nov. 16, 1953, pp. 81.

47. DRUESEDOW, D and GIBBS, C F: *'Effect of heat and light on PVC'*, Modern Plastics, June 1953, Vol. 30, No. 10, pp. 216.

48. HEMSLEY, D A, KATCHY, E M, LINFORD, R J and MARSHALL, D E: *'The behaviour of PVC powder during blending and gelation'*, PVC Processing International Conference, April 1978, Egham Hill, Surrey, Paper 9.1.

49. GALE, G M: *'Dry blend extrusion of rigid PVC'*, Plastics and Polymers, June 1970, pp. 183-191.

50. ALLSOPP, M W: *'Mechanism of gelation of rigid PVC'*, Manufacture and Processing of PVC, Chapter 8, Burgess R H (Ed), Appl. Science Publ. London, 1982, pp. 183-213.

51. NISSEL, F R and SHAVER, L D: *'Finished product extrusion from rigid PVC dry blend'*, SPE J., Jan. 1966, Vol. 22, pp. 29-33.

52. ROLLS, J A and WEILL, P S: *'Properties of rigid pipe produced from PVC powder compound'*, SPE J., 1962, Vol. 16, pp. 1395.

53. JONES, D R and HAWKES, J C: *'Dry blend extrusion of unplasticised PVC'*, Transaction and Journal - Plastics Institute, 1967, Vol. 35, pp. 773-781.

54. FAULKNER, P G: *'The use of a temperature programmable Brabender mixing head for the evaluation of the processing characteristics of polyvinylchloride'*, J. Macromolecular Science - Physics, B11(2), 1975, pp. 251-279.

55. SINGLETON, C J, STEPHENSON, T, ISNER, J and GEIL, P H: *'Processing - morphology - property relationships of plasticised polyvinylchloride'*, J. Macromolecular Science, - Physics, B14(1), 1977, pp. 29-86.

56. BORT, D N, RYLOV, Y Y, OKLADNOV, N A, SHTARKMANN, B P and KARGIN, V A: *'Morphology of bulk polyvinylchloride'*, Polymer Science - USSR, 1965, Vol. 7, pp. 50-57.

57. TREGAN, R and BONNEMAYNE, A: *'The different types of PVC grains'*, Rev. Plast. Modern, 1970, Vol. 23 (3), pp. 244.

58. KRZEWKI, R J and SIEGLAFF, C L: *'Structural heterogeneity of suspension polyvinylchloride resin'*, Polymer Engineering and Science, Nov. 1978, Vol. 18, pp. 1174-1181.

59. GEIL, P H: *Polymer morphology'*, J. Macromolecular Science - Chemistry, A11(7), 1977, pp. 1271-1280.

60. ALLSOPP, M W: *'The development and importance of suspension PVC morphology'*, Pure and Applied Chemistry, 1981, Vol. 53, pp. 449-465.

61. HATTORI, T, TANAKA, K and MATSUA, M: *'Fusion of particulate structure in polyvinylchloride during powder extrusion'*, Polymer Engineering and Science, 1972, Vol. 12, pp. 199.

62. LANG, P W: *'Nomarski differential interference contrast'*, American Laboratory, April 1970, pp. 45-52.

63. WORK, J L: *'Solid-state structure of melt blended incompatible polymeric mixtures involving polyvinylchloride'*, Polymer Engineering and Science, 1973, Vol. 13, pp. 46-50.

64. HORI, Y: SPE Japan RETEC, Japan Plastics, 1969, Vol. 3(2), pp. 4-49 (page 48).

65. BERENS, A R and FOLT, V L: *'The significance of a particle-flow process in PVC melts'*, Polymer Engineering and Science, 1968, Vol. 8, pp. 5-10.

66. SINGLETON, C, ISNER, J, GEZOVICH, D M, GEIL, P H, TSOU, P K C and COLLINS, E A: *'Processing-morphology-property studies of polyvinylchloride'*, Polymer Engineering and Science, 1974, Vol. 14 (5), pp. 371-381.

67. GEIL, P H and GEZOVICH, D M: *'Morphology of plasticised polyvinylchloride'*, Inter. J. Polymeric Mats., 1971, Vol. 1, pp. 3-16.

68. MUNSTEDT, H: *'Relationship between rheological properties and structure of polyvinylchloride'*, J. Macromolecular Science - Physics, B14(2), 1977, pp. 195-213.

69. TERSELIUS, B and RANBY, B: *'Phase structure of polyvinyl-chloride and PVC/polymer blends'*, Pure and Applied Chemistry, 1981, Vol. 53, pp. 421-448.

70. SHINAGAWA, Y: *'Gelation of PVC'*, Plastic Indiana News, May 1973, pp. 65-73.

71. SUMMERS, J W, ISNER, J D and RABINOVITCH, E B: *'How the morphology of polyvinylchloride compounds affects toughness and weatherability'*, Polymer Engineering and Science, 1980, Vol. 20, pp. 155-159.

72. SINGLAFF, C L: *'Rheological properties of PVC: General flow properties and unstable flow'*, SPE Transactions, 1964, Vol. 4, pp. 129-136.

73. SCHNEIDER, A, Kunststoffe Rdsc, 1963, Vol. 7 (10), pp. 333.

74. MATTHEWS, G A R: Advances in PVC Compounding and Processing, (Ed) M Kaufman, Publ. Maclaren, London, 1962.

75. PILZ, P: Kunststoffe, 1957, Vol. 47, pp. 64.

76. WOOD, R: *'Continuous compounding equipment: Pt 2'*, Plastics and Rubber International, February 1980, Vol. 5(1), pp. 27.

77. SIMONDS, H R: Encyclopaedia of Plastics Equipments, Reinhold Publishing Corporation, New York, 1964.

78. STREET, L F: *'Plastifying extrusion'*, Inter. Plastics Engineering, July 1961, Vol. 1, pp. 289-298.

79. REINECKE, L K: *'Latest advances in compounding techniques for PVC blends'*, Progve. Plast., Nov. 1969, Vol. 42, pp. 28-31.

80. MITRA, S: *'Processing of polyvinylchloride with particular reference to bulk polymers'*, Ind. Plast. Rev., Oct. 1972, Vol. 18, No. 10, pp. 13-21.

81. KOSHIDA, T and MURAKAMI, K: *'Recent advances in PVC processing techniques'*, Japan Plast. Age, July 1971, Vol. 9, No. 7, pp. 39-44.

82. BORT, D N, GUZEEV, V V and PEREDEREEVA, S I: *'Electron microscope study of the dispersion PVC aerosil in plasticised PVC'*, Koll. Zh., May/June 1971, Vol. 33, No. 3, pp. 349-351.

83. GORSHKOV, V S and SIROTKINA, N L: *'Investigation of the grain structure of suspension PVC using a scanning electron microscope'*, Plast. Massy, 1969, No. 10, pp. 65-66.

84. NELSON, E M: *'A bibliography of works dealing with the microscope and other optical objects'*, J. Royal Microscopy Soc., 1902, Vol. 22, pp. 20-22.

85. BARTER, E F: Dictionary of Inventions and Discoveries, 3rd edition (Ed. Carter, E F), Publ. Robin Clark Ltd, England, 1978.

86. FELDMAN, A and FORD, P: Scientists and Inventors, Publ. Aldus Books Ltd, London, 1979.

87. PEACOCK, H A: Elementary microtechniques, 3rd edition, Edward Arnold (Publ) Ltd, New York, 1966.

88. HEMSLEY, D A: *'Microscopy of polymer surfaces'*, Development in Polymer Characterization I, (Ed. J V Dawkins), Publ. Applied Science Pub. Ltd, London, 1978, pp. 245-275.

89. ROCHOW, E G and ROCHOW, T G: An Introduction to Microscopy by means of light, electrons, X-rays or ultrasound, Publ. Plenum Pub. Co., New York, 1978.

90. LANG, W: Series of papers available from Carl Zeiss of Oberkochem, West Germany (Instruction Manual for Zeiss III R.S. fluorescence attachment).

91. Instruction manual for Differential Interference Microscope, Model T, supplied by Nikkon, Tokyo 100, Japan.

92. PRIMSELAAR, W J: *'The commercial future of PVC'*, International Conference, PVC Processing II, Brighton, April 1983, paper 1.1.

93. CLAYTON, H M: *'Health and safety aspects of PVC processing'*, International Conference, PVC Processing II, Brighton, April 1983, paper 35.1.

94. WREDDEN, J H: *'The microscopic examination of plastics materials'*, A series of articles in Plastics, London, Vols. 9-13, 1945, pp. 341-388.

95. MOREHEAD, F F: *'Modern microscopy of films and fibres'*, Bull. Amer. Soc. Test. Mat., No. 165, January 1950, pp. 54.

96. LANGTON, N H and STEPHENS, M: *'The microscopic examination of rubbers, plastics and fillers'*, Plastics, London, August, 1960, Vol. 25, No. 274, pp. 329.

97. MATTHEWS, G A R: Private communication.

98. BRADBURY, S: The evolution of the Microscope, Publ. Pergamon Oxford, 1967.

99. Practical Methods in Electron Microscopy, 3rd edition (Ed. Glanert, A M), Vol. 2, Publ. North-Holland Pub. Co., New York, 1979.

100. HEIMENDAHL, M Von: Electron Microscopy of Materials: An introduction, Publ. Academic, New York, 1980.

101. CROSSLETT, V E: *'The future of the electron microscope'*, J. Royal Microscopy, 1967, Vol. 87, pp. 53-76.

102. HAINE, M E: The Electron Microscope, Publ.Interscience Pub. Inc, New York, 1961.

103. HALL, C E: Introduction to Electron Microscopy', Publ. McGraw-Hill, New York, 1953.

104. *'Particle Identification'*, The Particle Atlas, 2nd edition, (Ed. McCrone, W C and Delly, J G), Vol. 1, Publ. Ann Arbor Science Publishers Inc., Michigan, USA, 1973, pp. 275.

105. Technigram B262, Technical data for suspension PVC Breon S110/11, B P Chemicals Ltd, Devonshire House, Mayfair Place, London, W1X 6AY.

106. WALSH, D J, HIGGINS, J S, DOUBE, C P and McKEOWN, J G: *'Small angle scattering studies of PVC and PVC blends'*, Polymer, 1981, Vol. 22, pp. 168-174.

107. SULLIVAN, P and WUNDERLICH, B: *'The interference microscopy of crystalline linear high polymers'*, SPE Transactions, April 1964, pp. 113-116.

108. HALE, A J: The Interference Microscope in Biological Research, Publ. E and S Livingstone Ltd, London, 1958.

109. PRICE, G R and SCHWARTZ, S: *'Review of fluorescence microscopy'*, Physical Techniques in Biological Research, (Ed. G Oster and A W Pollister), 1956, Vol. 3, Publ. Academic Press, New York.

110. UDENFRIEND, S: Fluorescence Assay in Biology and Medicine, Publ. Academic Press, New York, 1970, Vol. II.

111. GRANT, J and RADLEY, J A: *'Review of potential industrial applications of fluorescence microscopy'*, Fluorescence Analysis in UV Light, 4th Edition, Publ. Chapman and Hall, London, 1954.

112. JONES, R N: *'Fluorophotometry and phosphorimetry: fluorescence'*, Encyclopaedia of Spectroscopy (Ed. G L Clark), Publ. Reinhold Publishing Corp., New York, 1960, pp. 373.

113. DUNSTON, J M and JONES, R N: *'Fluorescence'*, Encyclopaedia of Chemistry (3rd edition), Publ. Reinhold Publishing Corp., New York, 1957, pp. 407.

114. BENFORD, J B: *'Ultraviolet microscopy'*, The Encyclopaedia of Microscopy, (Ed. G L Clark), Publ. Reinhold Corp., New York, 1961, pp. 548-550.

115. STOWARD, P J: *'Fluorescence microscopy and histochemistry'*, Luminescence in Chemistry (Ed. E J Brown), Publ. Van Nostrand Co. Ltd., London, 1968, pp. 222-250.

116. BIRKS, J B: Photophysics of Aromatic Molecules, Publ. Wiley, New York, 1970.

117. CLAR, E: The Aromatic Sextet, Publ. Wiley, London, 1972.

118. ARGANER, R and WHITE, C E: Fluorescence Analysis: A Practical Approach, Publ. Dekker, New York, 1970.

119. ROGERS, L B and WEHRY, E L: *'Fluorescence and phosphorescence of organic molecules'*, Fluorescence and Phosphorescence Analysis, (Ed. D M Hercules), Publ. Interscience, USA, 1966, pp. 81-98.

120. WILLIAMS, R T: *'Effects of chemical structure on fluorescence'*, Fluorescence News, 1970, Vol. 5, No. 3, pp. 3-5.

121. BRIDGES, J W: *'Fluorescence of organic compounds'*, Luminescence in Chemistry (Ed. E J Bowen), Publ. Van Nostrand Co. Ltd., London, 1968, pp. 77-106.

122. GERRARD, D L and MADDAMS, W F: *'The resonance Raman spectrum of thermally degraded polyvinylchloride'*, Macromolecules, Feb. 1975, Vol. 8, pp. 54-58.

123. De COSTE, J B: *'Thermal processing stability of vinyl-chloride plastics'*, SPE J., Aug. 1965, pp. 764-769.

124. AHLSTRON, D J, GEIGLEY, A G, LIEBMAN, S A, MELUSKEY, J T and QUINN, E J, *'Thermal decomposition of polyvinylchloride and chlorinated polyvinylchloride II - organic analysis'*, J. Polymer Science, 1971, Pt. A-1, Vol. 9, pp. 1921-1935.

125. GALE, G M: *'Twin screw extrusion of PVC dry-blends 2'*, RAPRA Members Journal, April 1974, pp. 105-107.

126. ERNST, L: Wetzlar of West Germany. Leitz MPU Compact-microscopy photometer Instruction Handbook.

127. BRIGGS, R D, CHAN, R K S and LEE, C W M: *'Transient behaviour of viscoelastic fluid in an extruder'*, J. Applied Polymer Science, 1968, Vol. 12, pp. 115-122.

128. KLINE, M: *'Macroscopic particle size and shape of polymers and their relationship to processing'*, VIPAG Newsletter, Vol. 1, No. 3, 1965, pp. 14-26.

129. CORRY, A, RENNER, D and SHIFFER, A: *'Dry-blending of free-flowing elastomeric PVC powders'*, SPE J., Feb. 1966, pp. 107-111.

130. GALE, G M: *'High speed mixing of unplasticised PVC powder'* RAPRA Research Report No. 172.

131. GUIMON, C: *'Improvement in the extrusion of rigid-PVC powder blends'*, SPE-ANTEC, Detroit, Vol. 13, 1967, pp. 1085-1092.

132. MOROHASHI, H: *'Dry-blend compound manufacturing technique and extrusion technique for rigid-PVC pipe'*, Japan Plastics, 1968, Vol. 2, pp. 27-35.

133. ALLEN, T: Particle Size Measurement, (Publisher), Chapman and Hall, London, 1968.

134. ————: *'Classification of methods for determining particle size'*, Analyst, 1963, Vol. 88, No. 1044, pp. 156.

135. Particle Atlas (Publ.) McCrone Associates, 2820 South Michigan Avenue, Chicago, Illinois, 60616.

136. KAYE, B H and MURPHY, R: *'Some aspects of the efficiency of statistical methods of particle size analysis'*, Powder Technol., 1968-69, Vol. 2, pp. 97-110.

137. HEYWOOD, H: *'A comparison of methods of measuring microscopical particles'*, Transact. AIME, 1945, Vol. 4, pp. 391.

138. Zeiss T G 23 Particle Size Analyser-Manuals, Commercial information made available by Carl Zeiss Corporation, Oberkochen, Wurt, West Germany.

139. SCHRAMM, G: *'Measuring the fusion rate of rigid PVC dry-blend'*, International Plastics Engineering, 1965, Vol. 5, pp. 420-425.

140. DARBY, J R, SEPPALA, H J and TOUCHETT, N W: *'Fusion rates of plasticizers'*, Plastics Technology, July 1964. Vol. 10, pp. 33-35.

141. KARASZ, F E, BAIR, H E and O'REILLY, J M: *'Thermodynamic properties of poly (2,6-dimethyl-1,4-phenylene ether'*, J. Polymer Science (Polymer Physics), 1968, Vol. 6, pp. 1141

142. MILLER, G W: *'The thermal characterization of polymers'*, Appl. Polymer Symp. No. 10, Analysis and Characterization of Coatings and Plastics, Vol. 35, Interscience Publishers, New York, 1969.

143. LAMBERT, A: *'Glass-transition measurements on polystyrene by differential scanning calorimetry'*, Polymer, Vol. 10, No. 5, 1969, pp. 319.

144. ————————: *'Differential scanning calorimeter'*, Industrial Equipment News, New York, Jan. 1969, Vol. 18, No. 1, pp. 1.

145. Du Pont 990 Thermal Analyser; laboratory manual.

146. GILBERT, M and VYVODA, J C: *'X-ray diffraction of processed PVC'*, Polymer, 1978, Vol. 19, pp. 862-863.

147. BAKIR, M A: *'Effects of some injection moulding variables on the properties of injection moulded rigid PVC'*, PhD Thesis 1980, Loughborough University of Technology.

148. GILBERT, M and VYVODA, J C: *'Thermal analysis technique for investigating gelation of rigid PVC compounds'*, Polymer, 1981, Vol. 22, pp. 1134-1136.

149. COPSEY, C J, GILBERT, M, MARSHALL, D E and VYVODA, J C: *'The dependence of PVC structure and properties on injection moulding variables'*, Inter. Conference, PVC Processing, April 6-7, 1978, paper A1.1-3.

150. ROCHOW, T G and ROCHOW, E G: Resinography, Publ. Plenum Press, New York, 1976.

151. HARTSHORNE, N H and STUART, A: Crystals and the Polarizing Microscope, 4th edition, Publ. American Elsevier, New York, 1970, pp. 275-288.

152. BORN, M and WOLF, E: Principles of Optics, Publ. Pergamon Press, 1964, pp. 705-708.

153. ROCHOW, T G and ROCHOW, E G: An Introduction to Microscopy by means of Light, Electrons, X-rays or Ultrasound, Chapter 5, Publ. Plenum, New York, 1978.

154. ALLSOPP, M W: *'Mechanism of gelation of rigid PVC'*, International Conference - PVC Processing II, Brighton, April 26-28, 1983, Paper 4.

155. KATCHY, E M: *'Effect of blending and subsequent processing on morphology of PVC powder'*, PhD Thesis, Loughborough University of Technology, 1979.

156. RENKIS, A I: *'How to dry blend PVC for fluidized bed'*, Plastics Technology, Oct. 1962, Vol. 8, pp. 33-36.

157. VYVODA, J C: Private communication, formerly with Institute of Polymer Technology, Loughborough University of Technology.

158. HEMSLEY, D A, HIGGS, R P and MIADONYE, A: *'UV fluorescence microscopy in the study of polyvinylchloride powders and extrudates'*, Polymer Comm., 1983, April, Vol. 24, pp. 103-106.

159. BOULTON, A J: Developments in PVC Technology, (Ed. J Henson and A Whelan), p. 90.

160. CARLETON, L T and MISHUCK, H: *'Dry blending behaviour of commercial PVC'*, J. Applied Polymer Science, Vol. 8, 1964, pp. 1221-1255.

161. GILBERT, M, HEMSLEY, D A and MIADONYE, A: *'Assessment of fusion in PVC compounds'*, Inter. Conf., PVC Processing II, April 1983, Preprint, Paper 5, pp. 1-10.

162. KULAS, F R and THORSHANG, N P: *'The influence of stabilizers on the fusion of rigid PVC'*, Polymer Eng. and Science, 1974, Vol. 14, pp. 366-369.

163. CHANG, I C and LOGAN, S M: *'Effects of lubricants on second fusion behaviour of rigid PVC'*, Polymer Eng. and Science, 1979, Vol. 19, pp. 1110-1116.

164. TOUCHETTE, N W, SEPPALA, H J and DARBY, J R: *'Fusion characteristics of plasticised PVC'*, Plastics Technology, July 1964, Vol. 10, pp. 33-35.

165. GALE, G M: *'Twin screw extrusion of PVC dry blends I'*, RAPRA Members Journal, 1974, March, pp. 68-72.

166. ANDREWS, K E, BUTTERS, C and WAIN, B J: *'Some characteristics of lubricants in rigid PVC I'*, British Plastics, Oct. 1970, Vol. 43, pp. 97-101.

167. NATURMAN, L I: *'Rigid PVC - a survey of material, processing and markets'*, SPE J., June, 1964, pp. 510.

168. MARSHALL, B I: *'Lubrication of PVC'*, British Plastics, Aug. 1969, Vol. 42, pp. 70-78.

169. BEHRENS, H: *'Description of the relationship between structure and properties'*, Plaste. U. Kaut., Jan. 1973, Vol. 20, No. 1, pp. 2-6.

170. GALE, G M and HINDMARCH, R S: *'How to achieve quality polymer blends by a new extrusion technique'*, Paper presented at a meeting of the Rubber Division American Chemical Society, Chicago, Oct. 5-8, 1982, Contribution No. 73.

171. GALE, G M: *'Distributive mixing in single screw extruders'*, Plastics and Rubber Processing and Applications, 1982, Vol. 2, No. 4, pp.347-352.

172. BAJAJ, P and VARSHEY, S K: *'Morphology and mechanical properties of poly(dimethyl-siloxane-6-styrene-6-dimethyl siloxane) block copolymer'*, Polymer, 1980, Vol. 21, pp. 201-206.

173. MENGES, G and BERNDSTEN, N: *'Extrusion of PVC - the consequences of particle structure'*, International Conference, PVC Processing, April 1978, Egham Hill, Surrey, Paper 12.

174. MARSHALL, D E, HIGGS, R P and OBANDE, O P: *'The effect of extrusion conditions on the fusion, structure and properties of rigid PVC'*, International Conference, PVC Processing II, April 1982, paper 13.

175. TERSELIUS, B: *'Effect of processing on the structure and properties of PVC'*, PhD Thesis, Department of Polymer Technology, Royal Institute of Technology, Stockholm, Sweden, 1983.

176. BENJAMIN, P: *'The influence of processing on the properties of PVC pipe'*, International Conference, PVC Processing, April 1978, Egham Hill, paper B5.

177. COLLINS, E A and KRZEWKI, R J: *'Rheology of PVC Compound, III; effects of modifying resins'*, J. Vinyl Technology, June 1981, Vol. 3, pp. 116.

178. TERSELIUS, B and JANSEN, J F: *'Effect of internal pressure resistance - gelation of PVC II'*, Dept. of Polymer Technology, Stockholm (unpublished).

179. HEMSLEY, D A, GILBERT, M and VYVODA, J C: *'Structural order in oriented PVC mouldings'*, Polymer, Vol. 21, 1980, pp. 109-115.

180. BLUNDELL, D J: *'Small-angle X-ray study of microdomains in rigid PVC'*, Polymer, 1979, Vol. 20, pp. 934-938.

181. TADMER, Z, LIPSHITZ, S D and LAVIC, R: *'Dynamic model of a plasticating extruder'*, Polymer Engineering and Science, 1974, Vol. 14, pp. 112-119.

182. FENNER, R T: *'Computer modelling of quality in screw extrusion'*, Plastics and Rubber International, 1979, Vol. 4, No. 5, pp. 219-222.

# APPENDIX 1

## DETAILED RESULTS OF FLUORESCENCE INTENSITY MEASUREMENTS

TABLE 1:

The detailed results of relative fluorescence intensity of powder resin heat treated at different temperatures and times

I: 5 minute heating time

| Heat treated Temp (°C) | Relative fluorescence intensity (%) | | | | | | |
|---|---|---|---|---|---|---|---|
| | 1 | 2 | 3 | 4 | 5 | 6 | Average |
| 150 | 13.6 | 14.4 | 14.6 | 13.9 | 13.9 | 14.7 | 14.18 |
| 160 | 22.9 | 23.1 | 23.3 | 22.6 | 20.6 | 21.6 | 22.35 |
| 170 | 30.2 | 30.5 | 30.0 | 31.9 | 33.9 | 31.1 | 26.77 |
| 180 | 42.1 | 48.9 | 44.7 | 41.9 | 44.8 | 42.8 | 44.20 |
| 190 | 75.1 | 72.9 | 72.1 | 78.9 | 73.4 | 79.5 | 75.32 |
| 200 | 98.5 | 92.0 | 100.4 | 90.9 | 99.7 | 100.1 | 97.27 |
| 210 | 85.2 | 89.5 | 90.6 | 85.5 | 84.7 | 94.8 | 88.38 |

II: 10 minutes heating time

| Heat treated Temp (°C) | Relative fluorescence intensity (%) | | | | | | |
|---|---|---|---|---|---|---|---|
| | 1 | 2 | 3 | 4 | 5 | 6 | Average |
| 150 | 14.5 | 15.2 | 16.4 | 16.6 | 16.3 | 14.0 | 15.50 |
| 160 | 23.5 | 23.4 | 23.9 | 28.2 | 26.4 | 23.4 | 24.80 |
| 170 | 42.3 | 36.6 | 43.3 | 36.2 | 38.9 | 40.0 | 39.55 |
| 180 | 63.4 | 69.1 | 64.2 | 57.8 | 67.0 | 60.0 | 63.55 |
| 190 | 103.2 | 96.5 | 98.4 | 110.2 | 100.2 | 119.4 | 104.64 |
| 200 | 83.4 | 74.2 | 76.9 | 86.7 | 84.1 | 85.4 | 81.78 |
| 210 | 61.5 | 64.9 | 59.1 | 61.9 | 58.8 | 68.2 | 62.40 |

III: 15 minutes heating time

| Heat treated Temp (°C) | Relative fluorescence intensity (%) | | | | | | |
|---|---|---|---|---|---|---|---|
| | 1 | 2 | 3 | 4 | 5 | 6 | Average |
| 150 | 17.6 | 16.3 | 17.0 | 21.7 | 20.1 | 20.8 | 18.92 |
| 160 | 35.3 | 35.9 | 33.0 | 28.5 | 33.8 | 28.9 | 32.57 |
| 170 | 39.7 | 47.4 | 50.0 | 45.3 | 39.8 | 43.2 | 44.23 |
| 180 | 69.7 | 67.8 | 64.0 | 60.1 | 65.3 | 68.2 | 65.85 |
| 190 | 98.2 | 102.0 | 91.1 | 90.4 | 96.8 | 98.4 | 96.15 |
| 200 | 80.0 | 76.4 | 78.1 | 71.8 | 82.6 | 75.5 | 77.40 |
| 210 | 36.6 | 44.3 | 44.9 | 42.5 | 40.9 | 39.9 | 41.52 |

TABLE 2:

A detailed result of relative fluorescence intensity of extruder screw samples of different temperatures ('core' region)

A: Screw sample of 170°C

| Screw Channel | Relative fluorescence intensity (%) | | | | | | |
|---|---|---|---|---|---|---|---|
| | 1 | 2 | 3 | 4 | 5 | 6 | Average |
| 1st | 37.0 | 34.5 | 33.2 | 37.0 | 38.5 | 40.2 | 36.73 |
| 6th | 36.3 | 44.5 | 36.8 | 40.2 | 46.9 | 46.0 | 41.78 |
| 12th | 42.5 | 43.5 | 42.4 | 42.8 | 52.1 | 46.8 | 45.02 |
| 24th | 54.0 | 58.2 | 43.6 | 43.2 | 47.0 | 46.5 | 48.75 |
| 29th | 53.2 | 58.0 | 55.7 | 49.9 | 56.2 | 57.1 | 55.02 |
| 33rd | 91.2 | 96.5 | 104.9 | 95.2 | 88.9 | 90.9 | 94.60 |
| 36th | 56.9 | 71.4 | 65.2 | 58.2 | 57.1 | 66.4 | 62.37 |
| 38th | - | - | - | - | - | - | - |

B: Screw sample of 194°C

| Screw Channel | Relative fluorescence intensity (%) | | | | | | |
|---|---|---|---|---|---|---|---|
| | 1 | 2 | 3 | 4 | 5 | 6 | Average |
| 1st | 40.8 | 39.5 | 46.2 | 40.9 | 39.8 | 42.5 | 41.62 |
| 6th | 62.0 | 60.2 | 54.0 | 60.2 | 59.3 | 59.1 | 59.13 |
| 12th | 60.9 | 62.2 | 57.9 | 63.5 | 67.3 | 67.0 | 63.13 |
| 24th | 70.1 | 64.2 | 71.9 | 64.3 | 65.5 | 66.8 | 67.48 |
| 29th | 67.2 | 74.6 | 72.8 | 73.1 | 69.0 | 68.4 | 70.85 |
| 33rd | 74.2 | 76.0 | 67.5 | 69.8 | 75.5 | 70.9 | 74.83 |
| 36th | 110.1 | 111.0 | 105.8 | 110.6 | 110.4 | 109.9 | 109.63 |
| 38th | 73.6 | 72.4 | 69.7 | 72.0 | 69.2 | 71.7 | 72.05 |

C: Screw sample of 210°C

| Screw Channel | Relative fluorescence intensity (%) | | | | | | |
|---|---|---|---|---|---|---|---|
| | 1 | 2 | 3 | 4 | 5 | 6 | Average |
| 1st | 48.1 | 51.6 | 51.8 | 50.6 | 50.3 | 49.8 | 50.37 |
| 6th | 47.8 | 50.5 | 55.2 | 57.0 | 55.1 | 54.7 | 53.38 |
| 12th | 54.4 | 58.7 | 57.0 | 60.1 | 62.0 | 59.4 | 58.60 |
| 24th | 61.6 | 54.9 | 61.0 | 61.2 | 58.2 | 62.2 | 59.85 |
| 29th | 64.9 | 61.0 | 64.6 | 61.2 | 63.2 | 62.2 | 62.75 |
| 33rd | 63.5 | 70.8 | 66.6 | 63.1 | 67.3 | 65.1 | 66.07 |
| 36th | 99.2 | 95.8 | 100.6 | 93.6 | 92.6 | 95.4 | 96.20 |
| 38th | 65.9 | 72.3 | 70.2 | 69.7 | 69.4 | 72.1 | 69.93 |

## APPENDIX 2:

## MELTING TEMPERATURES OF ADDITIVES (DETERMINED BY DSC)

TABLE 3:

The table given below shows the melting points or temperatures of the additives used in the project. This clarifies which additives melt during blending and those that melt during extrusion.

| Additives | Melting temperatures °C (DSC peaks) | Comments |
|---|---|---|
| Dibasic lead stearate (DBLS)<br>2 PbO. Pb $(OOC.C_{17}H_{35})_2$ | 95<br>166<br>188 | Large peak<br>"<br>" |
| Calcium stearate<br>$Ca(OOc.C_{17}H_{35})_2$ | 120<br>161<br>196 | Large peak<br>Very small peak<br>" " "<br>(179-180-p-Ref. CRC Handbook) |
| G.S. 2411P Wax | 84-101 | Broad peak - may be doublet |
| Oxidised polyethylene wax | 75- 98 | Broad peak - may be doublet |
| Glycerol monostearate (GMS) | 120-135 | Broad peak |
| Palaroid K120N | 80<br>126<br>182<br>220 | Very small peak<br>" " "<br>" " "<br>Broad peak |
| Normal lead stearate | 97<br>112 | Sharp peak<br>" " |
| Mixed additives | | |
| DBLS + Ca.St.+ Wax 2411P (equal amounts) | 80-108<br>124<br>169 | Broad peak - triplet<br>Sharp peak<br>Broad peak |
| DBLS + Calcium stearate (equal amounts | 116<br>173<br>198 | Broad peak |

N.B. As all these are all industrial grade materials, the small peaks probably result from impurities

# APPENDIX 3

## SCHEMATIC REPRESENTATION OF HIGH-SPEED MIXERS BLADE ARRANGEMENTS USED

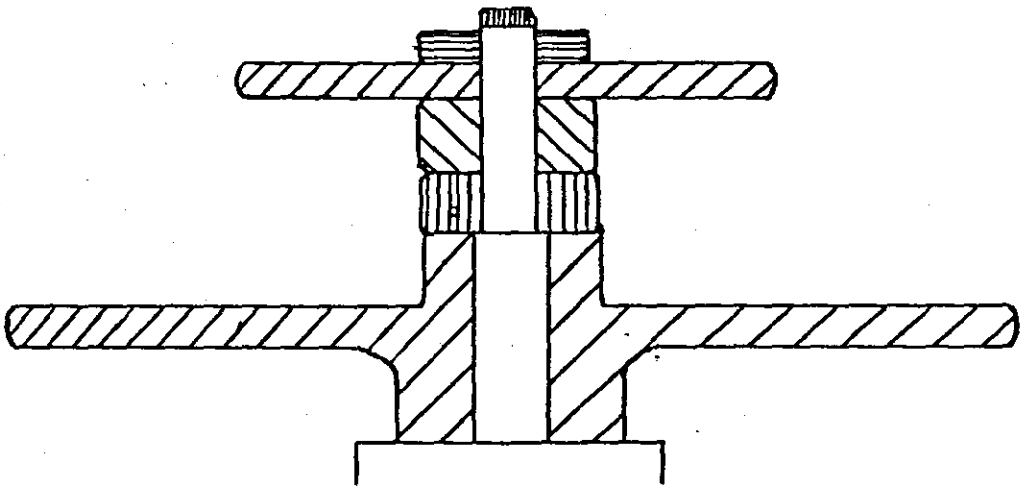

(a) Typical blade arrangement of the Fielder blender (double-layer blade arrangement)

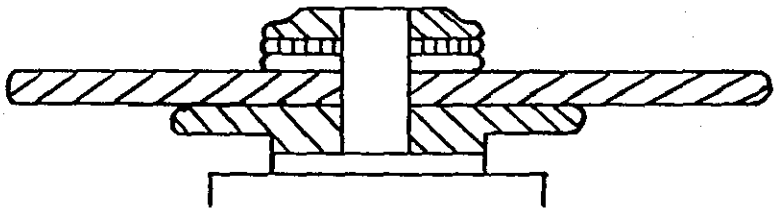

(b) Typical blade arrangement of the Henschel blender (single-layer blade)

APPENDIX 4: Thermograms and Graphs for Blending Parameters

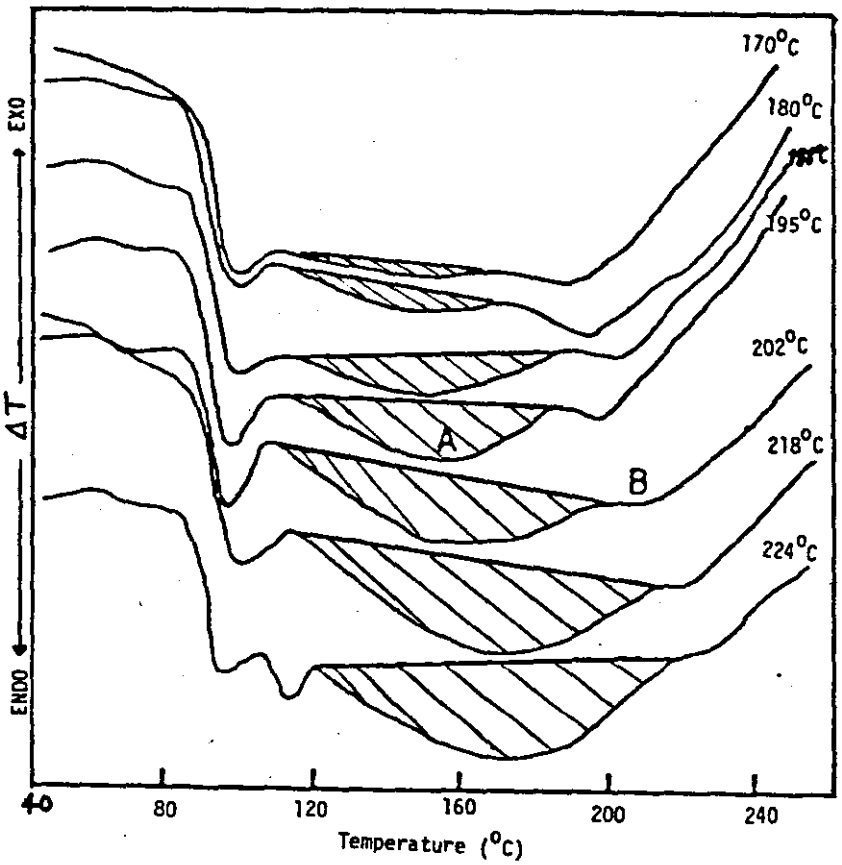


FIGURE 1 : Thermograms for extruded PVC

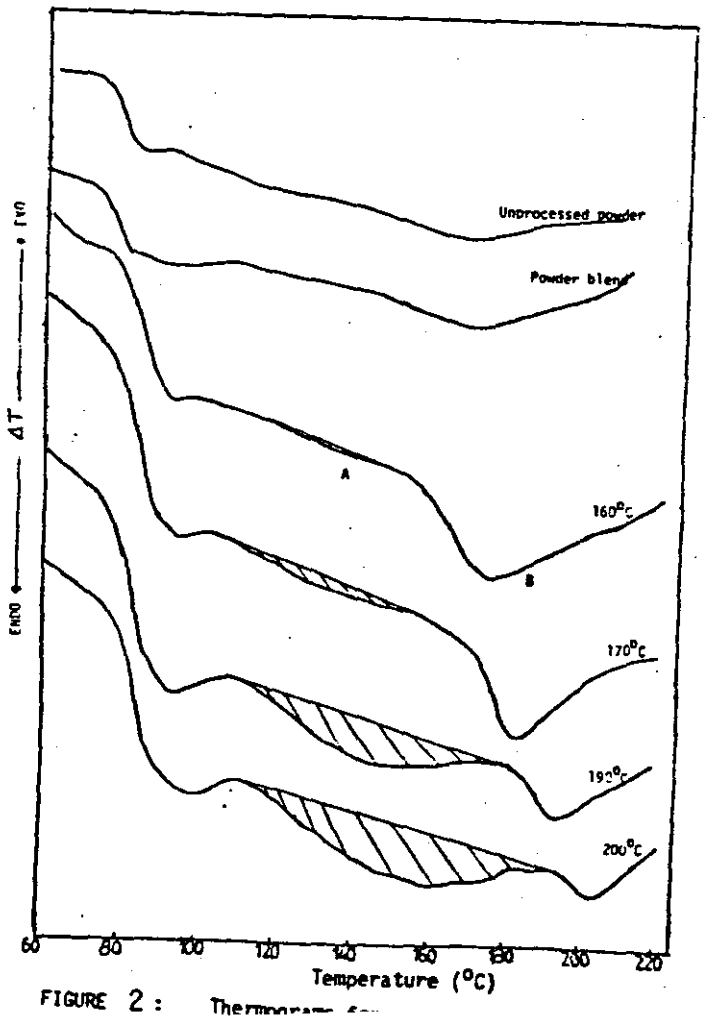


FIGURE 2 : Thermograms for

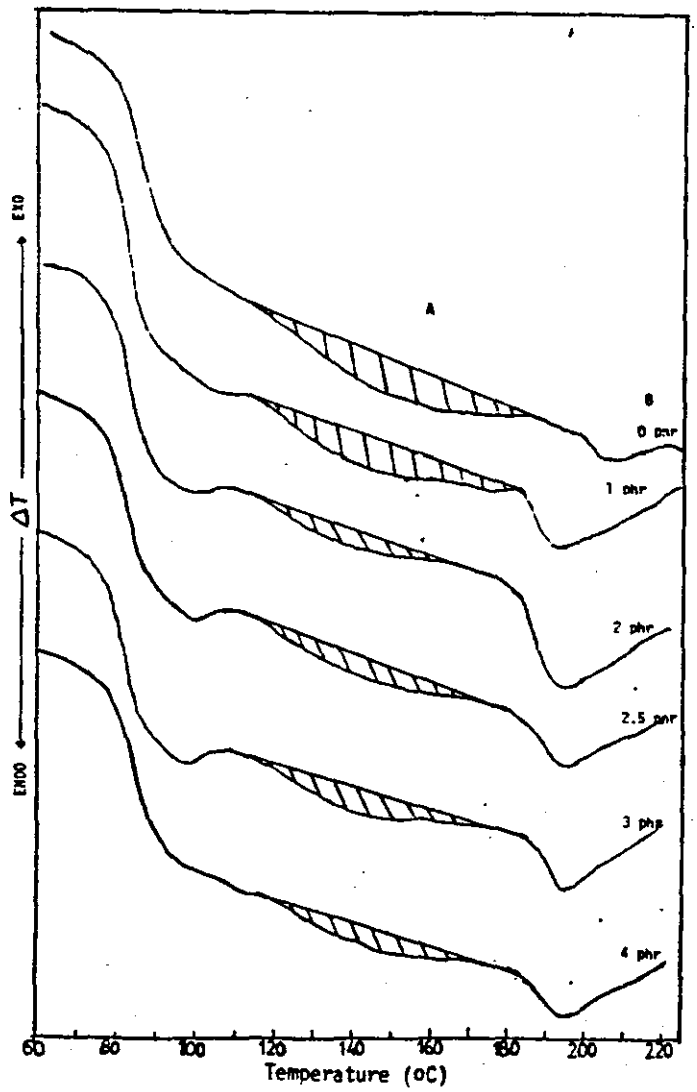


FIGURE 3 : Thermograms for compression mouldings containing different concentrations of DBLS stabilizer

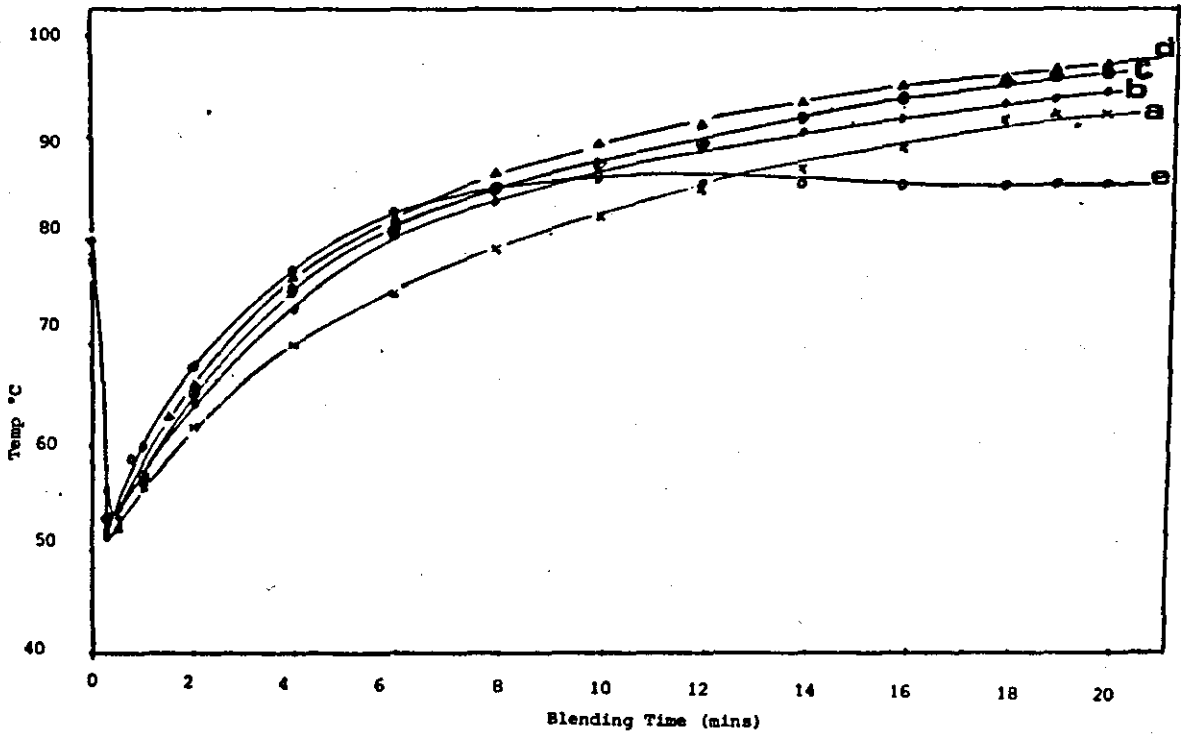


Figure 4: Variation of temperature with blending time as a function of DBLS concentration. a, 0phr; b, 1phr; c, 2phr; d, 3phr; e, 4phr.

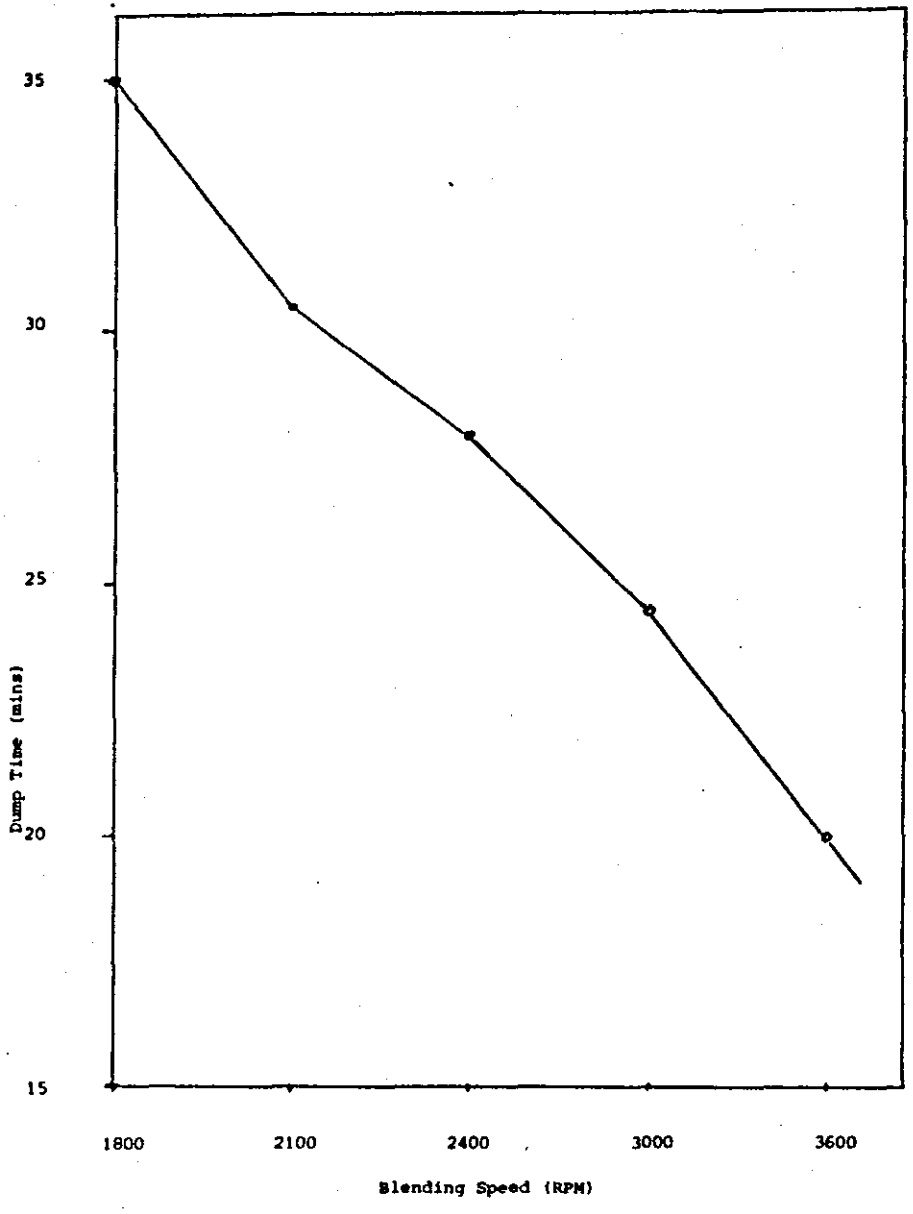


Figure 6 Variation of Blending Speed with Dump Time in a Fielder Blender at a Blending Temperature of 120°C.

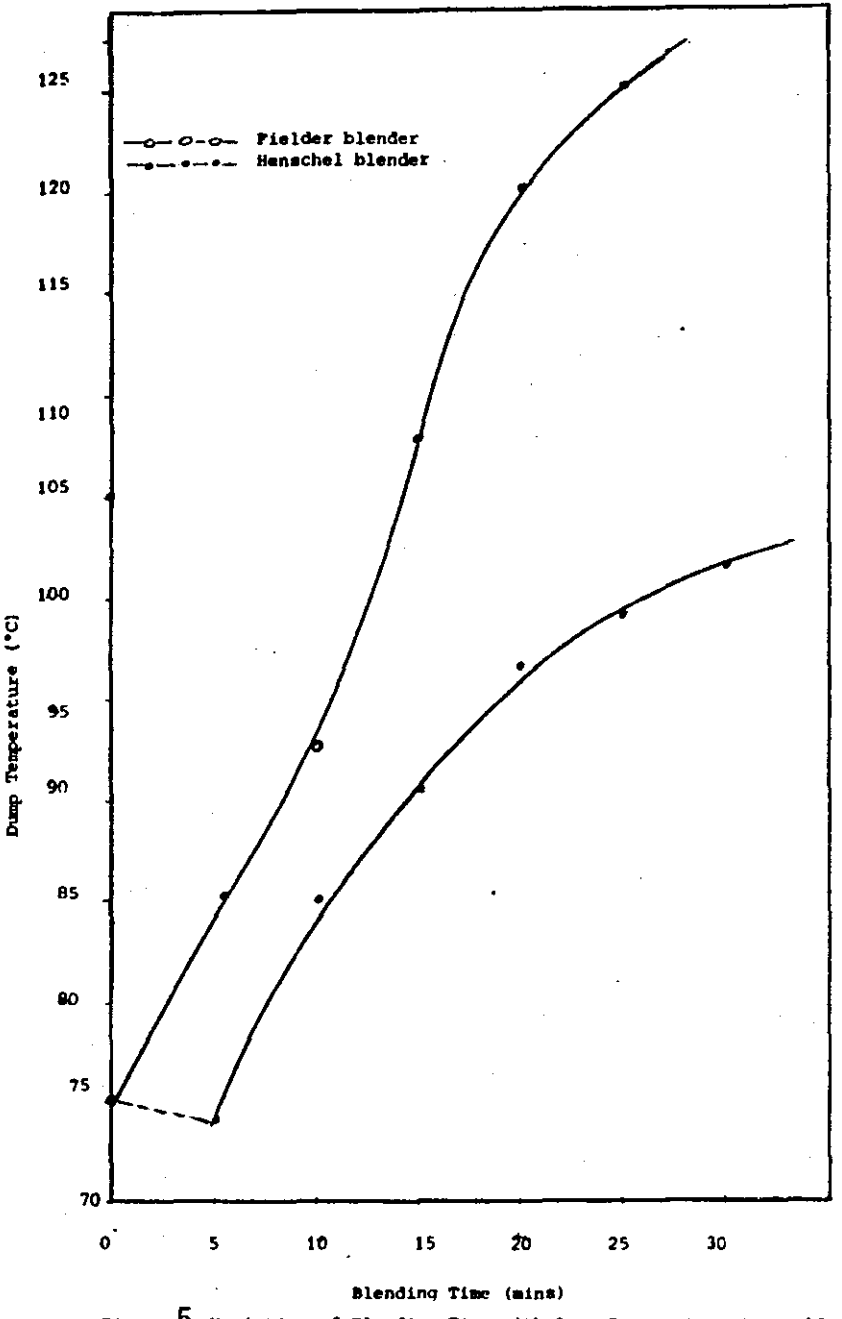


Figure 5 Variation of Blending Time with Dump Temperature in Fielder and Henschel Blenders for the Standard Formulation.